



University of
Stavanger

FACULTY OF SCIENCE AND TECHNOLOGY

MASTER'S THESIS

Study programme/specialisation: Environmental Technology	Spring semester 2017 Open
Author: Maria Elisabeth B. Råken Signature of author
Programme coordinator: Roald Kommedal Supervisor: Kåre Bredeli Jørgensen	
Title of master's thesis: <i>Synthesis of tubastrine analogues as potential antifouling agents</i>	
Credits: 30	
Keywords: tubastrine, antifouling, guanidine, Arbuzov, Horner-Wadsworth- Emmons, Ullmann, Wittig, alkylation	Number of pages: 80 + Supplemental material: 54 Stavanger, 12.07.2017

Acknowledgements

I would first like to express my sincere gratitude to my supervisor, associate professor Kåre Bredeli Jørgensen at the University of Stavanger. His door was always open whenever I had questions about my research or needed laboratory advisement. I am truly grateful for the opportunity to challenge and improve my knowledge and laboratory skills with this project.

I would also like to thank PhD student Sindhu Kancherla and post doctor Emil Lindbäck for guidance with laboratory work whenever needed and for creating an enjoyable lab environment.

Finally, I would like to thank my family and partner for the support and continuous encouragement throughout my years of study. This accomplishment would not have been possible without them.

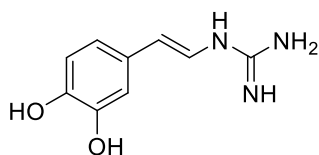
Thank you.

Maria Elisabeth B. Råken

Stavanger, 2017.

Abstract

In recent years, several isolated natural products containing a guanidine group have proven to have antibacterial effects. Preparation of such molecules synthetically is therefore highly relevant for mitigation and control of biofouling. With reference to the guanidine natural product tubastrine, several pathways for syntheses of analogues was outlined and tested in this research project. The microwave assisted C-N cross coupling reaction reported by Lorentzen et al. (2015)[1] was studied in detail and optimized from 49 to 67 %. Research was conducted on preparing *para*-alkylated starting materials for the same reaction and suitable conditions for selective *para*-alkylation was determined. A maximum of 73 % selective *para*-alkylation was observed.

*Structure of tubastrine*

In addition, syntheses of analogues with differences in the main molecular structure was tested. Attempts were made to synthesize an analogue with one additional carbon between the aromatic ring and the guanidine group via amide to amine reduction. Reduction of the amide was not successful. Furthermore, reactions utilizing the natural product dopamine was tested for synthesis of an analogue without the olefinic chain found in tubastrine. Dopamine reacted with the required solvent DMF and produced the corresponding amide. Finally, synthesis of an amidine analogue of tubastrine was tested using Meerwein's reagent. The amidine analogue was produced in 58 % yield.

Contents	
Abbreviations	1
Overview of synthesized molecules	2
1. Introduction	4
2. Theory	
2.1 Introduction to fouling	5
2.2 Development of chemical antifoulants	6
2.3 Natural products as antifoulants	9
2.4 Guanidine natural products	10
2.5 Retrosynthetic routes for tubastrine analogues	13
2.5.1 Retrosynthetic routes A and B ₁	14
2.5.2 Retrosynthetic route B ₂	15
2.5.3 Retrosynthetic route C ₁ and C ₂	16
2.5.4 Retrosynthetic route D	17
2.5.5 Retrosynthetic route E	18
2.6 Reactions for the synthesis of tubastrine analogues	
2.6.1 Arbuzov reaction	19
2.6.2 Horner-Wadsworth-Emmons (HWE) reaction	20
2.6.3 Wittig reaction	21
2.6.4 Modified Ullmann reaction	22
2.6.5 Heck reaction	25
2.6.6 Guanylation by 1 <i>H</i> -pyrazole carboxamide hydrochloride	26
3. Results and discussion	
3.1 Results for routes A and B ₁ /B ₂	
3.1.1 Results for route A	27
3.1.2 Results for route B ₁	28
3.1.3 Results for selective <i>para</i> -alkylation in route B ₂	31
3.1.4 Results for reactions of <i>para</i> -alkylated products in route B ₂	34
3.2 Results for route C	
3.2.1 Result for routes C ₁ and C ₂	36
3.2.2 Alternative reactions for reduction/chain degradation of vinyl amide	39
3.3 Results for route D	40
3.4 Results for route E	41
4. Conclusion	42
5. Scope for further research	44
6. Experimental	45
Synthesis of allyl guandine (2)	45
Synthesis of diethyl (2-amino-2-oxoethyl)phosphonate (3)	46
Synthesis of 3,4-bis((<i>tert</i> -butyldimethylsilyl)oxy)benzaldehyde (4a)	47
Synthesis of 4-(benzyloxy)-3-hydroxybenzaldehyde (4b)	48
Synthesis of 4-(hexyloxy)-3-hydroxybenzaldehyde (4c)	49
Synthesis of 4-(dodecyloxy)-3-hydroxybenzaldehyde (4d)	50
Synthesis of 3,4-bis(dodecyloxy) benzaldehyde (4e)	50
Synthesis of 3-((<i>tert</i> -butyldimethylsilyl)oxy)-4-(dodecyloxy)benzaldehyde (4f)	51

Synthesis of (<i>E</i>)-3-(3,4-dihydroxyphenyl)acrylamide (5a)	52
Synthesis of (<i>E</i>)-3-(3,4-bis(<i>tert</i> -butyldimethylsilyloxy)phenyl)acrylamide (5b)	53
Synthesis of (<i>E</i>)-3-(3,4-dimethoxyphenyl)acrylamide (5c)	55
Synthesis of (<i>E</i>)-3-(3,4-bis(<i>tert</i> -butyldimethylsilyloxy)phenyl)prop-2-en-1-amine (6a)	56
Synthesis of (<i>E</i>)-3-(3,4-dimethoxyphenyl)prop-2-en-1-amine (6b)	57
Synthesis of (<i>E</i>)-1-(3-(3,4-dimethoxyphenyl)allyl)guanidine (7a)	58
Synthesis of methyl (<i>E</i>)-3-(4-(hexyloxy)-3-hydroxyphenyl)acrylate (8a)	59
Synthesis of (<i>E</i>)-3-(4-(dodecyloxy)-3-hydroxyphenyl)acrylate (8b)	60
Synthesis of methyl (<i>E</i>)-3-(3-((<i>tert</i> -butyldimethylsilyloxy)-4-(dodecyloxy)phenyl)acrylate (8c)	61
Synthesis of methyl (<i>E</i>)-3-(3,4-bis(dodecyloxy)phenyl)acrylate (8d)	62
Synthesis of (<i>E</i>)-3-(3,4-bis(<i>tert</i> -butyldimethylsilyloxy)phenyl)acrylic acid (9a)	63
Synthesis of (<i>E</i>)-3-(4-(benzyloxy)-3-hydroxyphenyl)acrylic acid (9b)	64
Synthesis of (<i>E</i>)-3-(4-(dodecyloxy)-3-hydroxyphenyl)acrylic acid (9c)	65
Synthesis of (<i>E</i>)-3-(3-((<i>tert</i> -butyldimethylsilyloxy)-4-(dodecyloxy)phenyl)acrylic acid (9d)	67
Synthesis of (<i>E</i>)-3-(3,4-bis(dodecyloxy)phenyl)acrylic acid (9e)	68
Synthesis of (<i>E</i>)-3-(3,4-bis(<i>tert</i> -butyldimethylsilyloxy)phenyl)acryloyl chloride (10)	69
Synthesis of (<i>E</i>)-3-(3,4-bis(<i>tert</i> -butyldimethylsilyloxy)phenyl)acrylamide (5b)	69
Synthesis of (<i>E</i>)-3-(3,4-bis(<i>tert</i> -butyldimethylsilyloxy)phenyl)- <i>N</i> -carbamimidoyl acrylamide	70
Synthesis of (<i>E</i>)-4-(2-iodovinyl)-1,2-dimethoxybenzene (11a)	71
Synthesis of (<i>E</i>)-((4-(2-iodovinyl)-1,2-phenylene)bis(oxy))bis(<i>tert</i> -butyldimethylsilane) (11b)	72
Synthesis of (<i>E</i>)-1,2-bis(dodecyloxy)-4-(2-iodovinyl)benzene (11c)	73
Synthesis of (<i>Z</i>)-1-(<i>E</i>)-3,4-dimethoxystyryl)-2,3-bis(<i>tert</i> -butoxycarbonyl)guanidine (12a)	74
Synthesis of 2-(3,4-bis(<i>tert</i> -butyldimethylsilyloxy)phenyl)ethan-1-amine (14)	75
Synthesis of 1-(3,4-dihydroxyphenethyl)guanidine (16)	76
Synthesis of (<i>E</i>)-3-(3,4-dimethoxyphenyl)acrylimidamide (17)	77
7. References	78

Appendix A – ¹H NMR and ¹³C NMR spectra

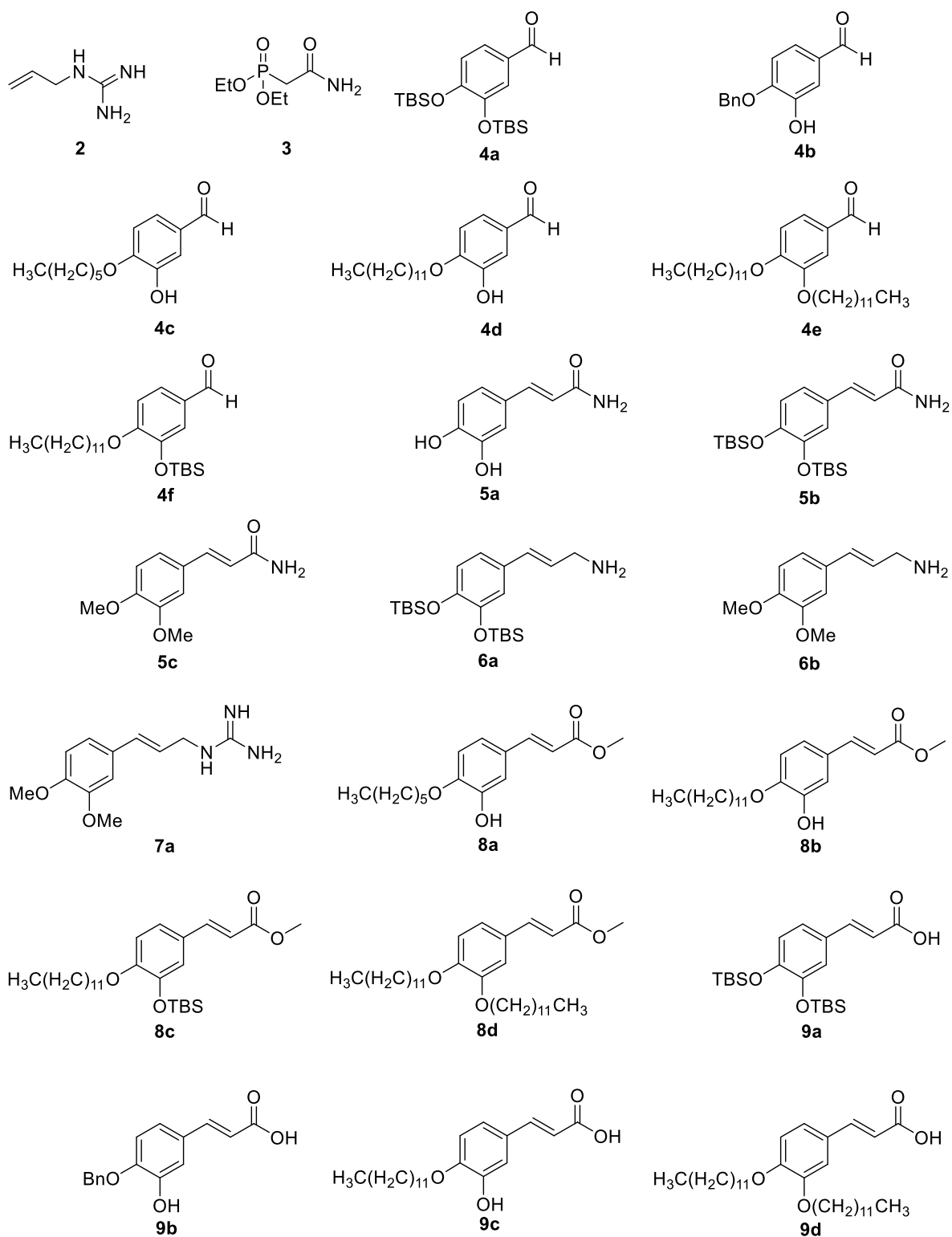
Appendix B – MS spectra

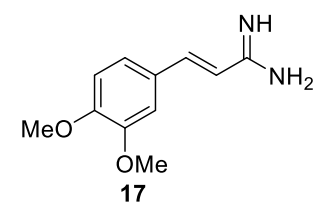
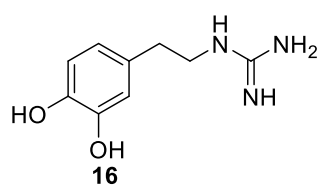
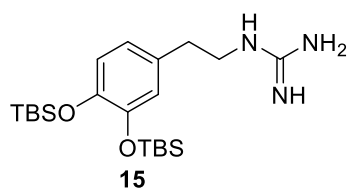
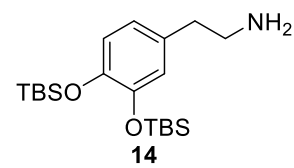
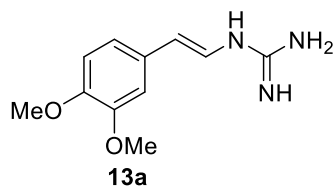
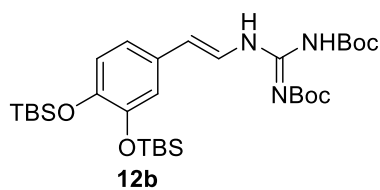
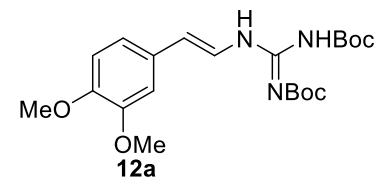
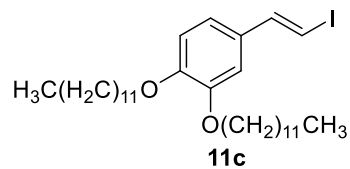
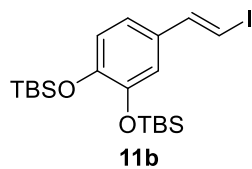
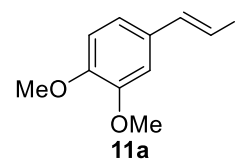
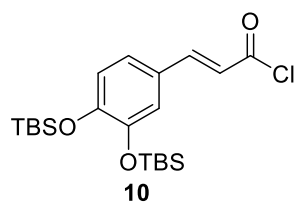
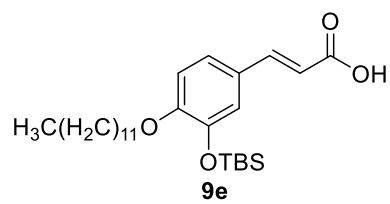
Abbreviations

AF	Antifouling
bp	Boiling point
d	Doublet
DCM	Dichloro methane
DMF	Dimethyl formamide
Et ₂ O	Diethyl ether
EtOAc	Ethyl Acetate
IR	Infrared
LAH	Lithium Aluminium Hydride
m	Multiplet
MeCN	Acetonitrile
mp	Melting point
MS	Mass spectroscopy
NMP	Natural Marine Products
NMR	Nuclear magnetic resonance
PE	Petroleum ether
q	Quartet
r.t.	Room temperature
s	Singlet
S. M.	Starting material
t	Triplet
TBT	Tributyl tin
THF	Tetrahydrofurane
TLC	Thin-Layer Chromatography
δ	Chemical shift (ppm) downfield from TMS

Overview of molecules

1*H*-pyrazole carboxamide hydrochloride was assigned compound number 1.





1. Introduction

Fouling is generally defined as the settlement and accumulation of undesired deposits on internal or external surfaces. The extent, severity and costs of fouling can be significant, as it often deteriorates protective coatings and alter the physical and mechanical properties of surfaces. Fouling is not an unknown phenomenon, and a broad range of chemical solutions have been developed to mitigate, control and remove unwanted deposits. However, the majority of these solutions have proven to be of great ecotoxicological concern. For that reason, natural products with antifouling properties is now a prevailing research area for the development of environmentally benign chemicals for surface control.

In recent years, natural products containing a guanidine group have been reported to demonstrate excellent antibacterial properties. Due to the extreme polar behaviour of guanidine compounds, isolation from nature have proven to be a challenging issue. Consequently, the development of methods for synthesising guanidine natural products in the laboratory is important for future applications of such products within the antifouling industry.

In this project, synthesis of the guanidine bearing natural product tubastrine and analogues are studied. The described work is partly based on previous results from the study performed by Lorentzen et al. (2015) at the University of Stavanger. In addition, several new routes for synthesis of analogues are outlined and tested.

The new routes for synthesis of tubastrine analogues are developed with the aim of producing pathways that can easily be used to synthesize analogues with different substituents and properties in later projects. As several new reactions were tested in a limited amount of time, a scope for further research and optimization of the described chemistry is also included.

2. Theory

2.1 Introduction to fouling

Settlement and deposition of unwanted material on immersed surfaces is a serious concern in a broad range of industries. Over the last decades, several chemicals have been developed to meet the demand for clean and smooth process surfaces. However, many chemicals efficient for this purpose have also raised ecotoxicological concern. This introduction will cover important advances in antifouling chemicals with a particular focus on research of the antifouling properties of guanidine natural products.

Fouling is the settlement, deposition and accumulation of an unwanted phase on the surface of submerged objects. The term fouling refers to accumulation on a system or component surface and is often associated with the deterioration of a process function. The deposited material may be either inorganic, organic or biologic and one can distinguish between macro- and microfouling based on the size of the deposited material. Typical microfoulants include bacteria and diatomic biofilms, while macrofouling is usually associated with macroalgae, barnacles, mussels and bryozoans.[2]. Common types of fouling include chemical reaction fouling, corrosion fouling, biofouling and composite fouling[3].

Biofouling is the accrual of a biological community on an interface usually associated with the formation of biofilms. Biofouling poses operational risk to most industries where operations are carried out in water, for instance paper manufacturing, underwater constructions, aquaculture and desalination plants[4]. When an object is immersed, organic material will adsorb to the surface within seconds and form a conditioning layer. Following the formation of the conditioning layer, primary colonizers such as bacteria, yeast and diatoms will establish within the protective biofilm structures. Roughly one week after immersion, secondary colonizers settle, followed by invertebrate larvae in the last step of the biofilm formation. Secondary colonizers comprise the spores of fungi, protozoa and macro algae[2]. Globally, more than 4000 marine species have been reported to cause biofouling[5].

In general, there is little variation in the groups of organisms responsible for fouling worldwide although the dominant specie may vary. The biofouling intensity is however greatly influenced by differences in seasonal temperatures at different latitudes. Tropical and sub-tropical regions have the most stable biofouling communities due to more consistent water temperature and light intensity than in temperate and polar regions. In

addition, factors such as salinity, nutrient levels and flow rates greatly affect the biofouling intensity[2].

Biofouling on process equipment surfaces is a challenging issue in a broad range of industries and may cause large economical and operational losses. The main consequences include impaired heat transfer, flow instabilities, flow blockages and corrosion in addition to hull roughness in the shipping industry. Biofouling on ship hulls greatly increases the frictional resistance and decreases the drag. Thus, additional shaft power is needed which greatly rises fuel costs. In addition, hundreds of millions additional tons of CO₂ and other contaminants may be added to the environmental budget. It is estimated that by protecting ships from fouling, 150 billion USD will be saved by the global shipping industry each year.[6]

Although fouling is often related to such detrimental effects on industrial man-made structures, biofouling can also occur on the surface of living organisms through epibiotic relationships. Adsorption onto a host (basibiont) will modify its surface properties and modulate several surface-bound regulations such as chemical, optical or tactile detections.[7] This may lead to costly consequences in the aquaculture.

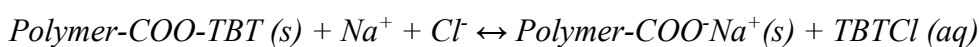
Due to the range of possible consequences and costs related to fouling, the development of chemical countermeasures is highly relevant. The application of antifoulants to prevent settling organisms dates all the way back to ancient Greece, where lead sheeting was used to protect ships[7]. Today, antifouling (AF) techniques to control fouling can be divided into three main categories: chemical, physical and biological methods. Chemical methods are the focus point in this thesis and chemical properties of antifouling compounds will be discussed further.

2.2. Development of chemical antifoulants

Chemicals designed for antifouling purposes must possess certain basic properties, most importantly toxicity towards the target organisms only, compatibility with the delivery system (e.g. paint), low bioaccumulation and non-persistence of residual material[8]. Since the late 20th century, organotin derivatives (TBT) have been widely used in antifouling coatings, including tributyltin oxide (TBTO) and tributyltin fluoride(TBTF)[4]. These compounds are powerful fungicides able to inhibit the growth of a large range of fouling species at low concentrations by releasing toxic persistent substances to the local environment[9]. Due to the self-polishing effect of TBT

antifouling paints which causes TBT paints to become more hydraulically efficient over time, the application expanded rapidly between 1950 and 1980[7].

The main binder in TBT-based paint is a copolymer with a number of pendant tributyltin carboxylate ester functional groups. The self-polishing effect is caused by the hydrolysis and ion-exchange reactions between sea water and the TBT carboxylate ester groups, which solubilizes as the substance soap[7]. Thus, as each copolymer layer of TBT reacts, a soluble acid polymer is formed which is easily eroded by water. This action exposes new layers of the TBT polymers to react. The mechanism is illustrated in the reaction below[10]:



However, TBT derivatives have shown endocrine disrupting effects and have been found to be present in a wide range of animals and plants with adverse effects. Due to the intrinsic properties, TBT is now considered a substance of very high concern by the EU and the chemical is banned by many countries in addition to the International Maritime Organization (IMO)[11].

The banning of TBT induced a strong demand for less toxic and less persistent antifouling agents. New types of AF paint were developed with copper compounds such as cuprous oxide (Cu_2O) and metallic copper added singly or in mixtures as biocides to TBT-based coatings. However, as several algal species showed physiological affection from the copper formulations[12], booster biocides for AF control were developed for a complete replacement of TBT. The booster biocides were developed to be present at the coat/paint-water interface and prevent settling of fouling organisms. Examples of booster biocides used or promoted for use included Diuron, Irgarol 1051TM, zinc pyrithione, Sea-Nine 211TM, dichlofluanid, TCMBT and TCMS pyridine[13, 14]. Several of these agents previously permitted are now strongly regulated, including Diuron and Irgarol 1051TM, due to severe contamination of coastal and marine environments worldwide (figure 2.1). Irgarol 1051TM was detected in Australia, despite not being applied as an antifoulant in Australian industries and was found to have high toxicity towards periphytic communities[13].

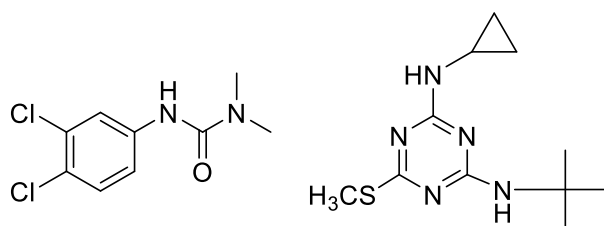


Figure 2.1: Structure of Diuron (left) and Irgarol 1051TM

The effective antifouling properties of the triazine herbicide Irgarol 1051TM ((2-[*tert*-butylamino]-4-[cyclopropylamino]-6-[methylthio]-1,3,5-triazine) emerges from the mode of action as an inhibitor for photosystem II[15]. The substance is able to readily penetrate tissues and impair the electron transport within the chloroplast at concentrations down to ng/l, by replacing plastoquinone B (Q_B). Thus, Irgarol 1051TM and its degradation product M1 (also known as GS26575) is found to be significantly more toxic than other triazines such as atrazine and simazine. Irgarol 1051TM is considered to be non-biodegradable, with half-lives up to 100 and 200 days in seawater and freshwater respectively[16]. In addition to reduced metabolism, studies on exposure of Irgarol 1051TM and Diuron towards pacific oysters recorded adverse effects on fertilization success and offspring development[17].

Diuron ((1-(3,4-dichlorophenyl)-1,1-dimethylurea)) is a substituted urea and classified as an herbicide for broad spectrum uses. Despite the differences in the chemical structures of Diuron and Irgarol 1051TM, the disruption effects of the photosynthetic process in PSII are similar[18]. The purpose of both chemicals in antifouling coatings is the leaching and exposure towards targeted fouling organisms. However, these substances may also leach unintentionally from treated surfaces and contaminate non-targeted aquatic environments. Diuron is classified as less toxic than many common biocides but is on the other side one of the most persistent. The substance is reported to show no signs of degradation when associated with paint particles in sediments under anaerobic conditions[19].

2.3 Natural products as antifoulants

High reported concentrations and adverse effects from tin- and biocide booster based antifouling agents have caused a demand for environmentally benign and low-toxicity alternatives to control surface colonization. Newer strategies now aim at developing natural products based on the chemical defences of sessile marine organisms that are able to maintain the body fouling free[20]. These natural marine products (NMPs) occur naturally in nature and it is therefore believed that the environmental issues reported from the synthetic biocides can be avoided.

Many sessile marine organisms are able to resist overgrowth without carrying out any physical or mechanical means of defence. Such marine organisms have during their course of evolution developed chemical defence systems, as they lack the ability to physically escape attacks. The chemical weapons can thus ensure the ability to ward off natural enemies, competitors and epibionts[2] and several are reported to carry excellent non-toxic antifouling properties[21]. The defence system is primarily associated with the production of secondary metabolites. Such bioactive metabolites have been reported to have antimicrobial, antiviral and antifouling activities[22]. It has been shown that for instance 2,5,6-tribromo-1-methylgramine obtained from the sea moss *Zoobotryon pellusidium* has high antifouling activity towards barnacles without killing the fouling species[23]. The same effect have been seen with the natural product Homarine (N-methyl-4-picolinic acid) obtained from the corals *Dendronephthya sp.*

Alkaloids are natural nitrogen-containing secondary metabolites produced by a variety of organisms. Alkaloid metabolites display a broad spectrum of biological activities including antimicrobial actions[24]. A class of the alkaloids is the guanidine alkaloids which will be further elaborated in chapter 2.4.

2.4 Guanidine natural products

Guanidines are biologically active substances with a broad range of activities including antibacterial, antiviral, anticancer, antiprotozoal, antibiotic and antihistaminic activities[25]. Guanidines are very strong bases, and the diverse range of chemical behaviour can be attributed to the ability of electron-donating nitrogen atoms to participate in directional hydrogen bonds.

Electrostatic interactions at the cell membrane of the organism is believed to be the proceeding antimicrobial mechanism of guanidine compounds. The attraction between a positively charged ion of the guanine group and the negatively charged cell surface disrupt the cellular charge balance. Thus, breakdown of the cell membrane is triggered, which leads to leakage of intracellular contents[26]. Due to the polar behaviour of guanidine alkaloids originating from the strong basicity, isolation from complex mixtures may be challenging[27]. Yet, a number of guanidine bearing substances have been isolated and characterized from marine invertebrates, especially from sponges. Among them are bromotryrosine guanidine derivatives such as Aplysinamisine II illustrated in figure 2.2, from the sponge *Aplysina cauliformis*[28].

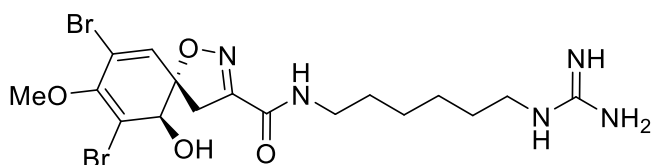


Figure 2.2: Structure of Aplysinamisine II

Marine sponges are considered to be the biological species which constitutes the most prolific source of guanidine metabolites. This is likely due to the sponge tissues comprising a complex assembly of microorganisms resulting in multiple metabolite sources[29].

Marine bromo-indole guanidines derived from tryptophan and arginine have also been shown to carry antifouling properties[30]. Baretin is a bromo-indole antifouling agent isolated from the sponge *Geodia baretii* which has been reported to show a strong settlement inhibition of barnacle larvae. Interestingly, studies on baretin analogues revealed that removing the bromine atom from the molecule resulted in a total loss of the inhibitory antifouling effect[22].

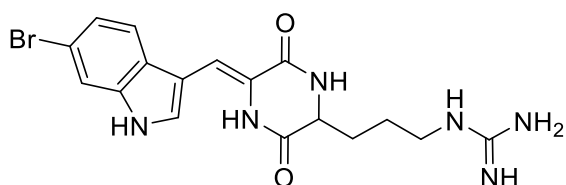


Figure 2.3: Structure of baretin

Several other natural products with similar chemical properties as baretin have been found to demonstrate antifouling activities. A reported example is synoxazolidinones, secondary metabolites originating from the tunicate *S. Pulmonaria* which has been shown to be both antibacterial and antitumoral[31]. Comparison studies between synoxazolidinones and the natural product pulmonarin from the same tunicate revealed that the latter displays a lower bioactivity towards microalgae and barnacles[31]. The structural difference between these two metabolites is significant, with the former having a guanidine group similar to the structure of baretin.

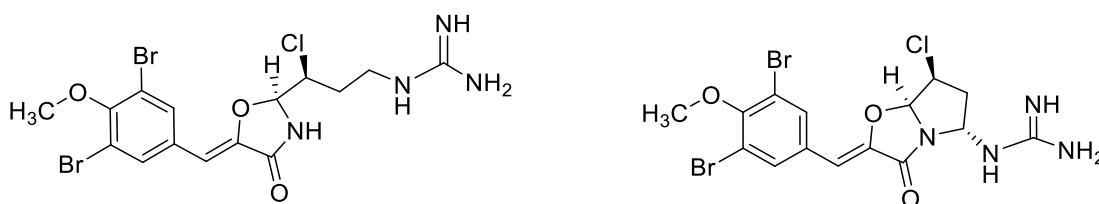


Figure 2.4: Structures of synoxazolidinones

Igumnova et al. reported that the common structure of the cationic amphipatic marine antimicrobials can be described as following; one lipophilic group, one linear or cyclic spacer group and one cationic group (e.g. guanidine)[32]. The same study reported that larger lipophilic groups in general enhances the antimicrobial activity. A comparison between the antimicrobial activity of amine and guanidine groups revealed that guanidines are more potent against bacteria and displays lower haemolytic activity compared to the amine derivatives.

Based on the reported activities of substances with guanidine components from several different studies, the molecule 1-[(*E*)-2-(3,4-dihydroxyphenyl)vinyl] guanidine (tubastrine) and its analogues are interesting for further SAR studies. Tubastrine is a guanidino dihydroxystyrene natural product, previously isolated from the coral *Tubastrea aurea*[33], the ascidian *Ascidiella scabra*, the dendrodoa specie *Dendrodoa Grossularia*[34] and the ascidian *Aplidium orthium*[35]. The substance was identified as being the active substance from several ascidians responsible for the inhibition of

epidermal growth factor receptors including *Ascidella scabra*[34]. Tubastrine has also been reported to show antiviral[33], antimicrobial[35] and anticancer[34] effects and may thus possess similar antifouling properties as the previously described guanidines. The structures of tubastrine and 3-dehydroxytubastrine are illustrated in figure 2.5.

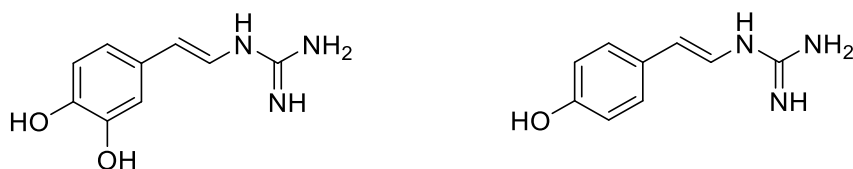


Figure 2.5: Structure of tubastrine and 3-dehydroxy-tubastrine

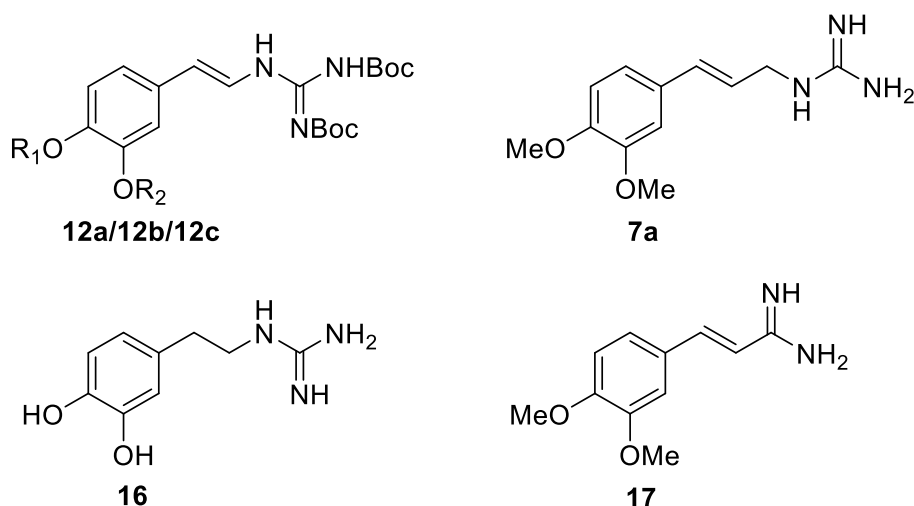
Tubastrine is believed to be a product of the metabolism of the amino acid tyrosine, which involves the formation of the guanidine group. A further hydroxylation leads to the formation of the tubastrine catechol. However, there is no evidence for the second hydroxyl group being essential for the antimicrobial activity[36]. This master thesis will cover the synthesis of tubastrine analogues, with the purpose of testing the chemicals' antifouling properties.

2.5 Retrosynthetic routes for tubastrine analogues

Previous attempts to synthesize tubastrine and 3-dehydroxy tubastrine have been conducted with the aim of developing methods that can easily be used to synthesize analogues. The first reported attempt on synthesis of tubastrine and analogues was conducted by Santos et al. in 2007 [37]. This synthesis failed in the final step in the attempt to dehydrate 1-(2-hydroxy-2-(4-methoxyphenyl)ethyl)guanidine and no further research has been reported from the authors.

In the following subchapters, different retrosynthetic routes for synthesis of tubastrine analogues are outlined. Route A and B₁ display retrosynthetic work developed by Lorentzen et al[1]. In the process of optimising the latter route, B₁ was extended to include *para*-selective alkylation reactions as illustrated in the retrosynthetic route B₂. In addition, route C₁ and C₂ were developed with the aim of producing an analogue containing one additional carbon between the benzene ring and the hydrophilic guanidine group.

Route D illustrates the synthesis of a tubastrine analogue without the characteristic double bond found between the benzene ring and the guanidine group in tubastrine. In Route E, the characteristic guanidine group has been replaced by an amidine group to produce an amidine analogue. An overview of the purposed end products for this project is displayed in figure 2.6.



12a: R₁=R₂= Me, **12b:** R₁=R₂=TBS, **12c:** R₁=Dodecyl, R₂=H

Figure 2.6: Overview of possible analogues

2.5.1 Retrosynthetic routes A and B₁

In 2015, Lorentzen et al.[1] outlined the two disconnection approaches seen in Figure 2.7 for the synthesis of tubastrine. Disconnection A illustrates a Heck cross-coupling reaction between an aryl halide and a protected vinyl guanidine, whereas disconnection B₁ illustrates a C-N cross-coupling between the aryl vinyl halide and a protected guanidine. The latter is also known as the modified Ullmann reaction. The aryl vinyl halide compounds are synthesized by a Hunsdiecker-Borodin type decarboxylation reaction using NIS and LiOAc.

As it became clear for the authors that the vinyl guanidine required in route A was not obtainable for the study, route B₁ was applied by Lorentzen with overall yields of 15.5 % and 7.3 % for tubastrine and 3-dehydroxy tubastrine, respectively.

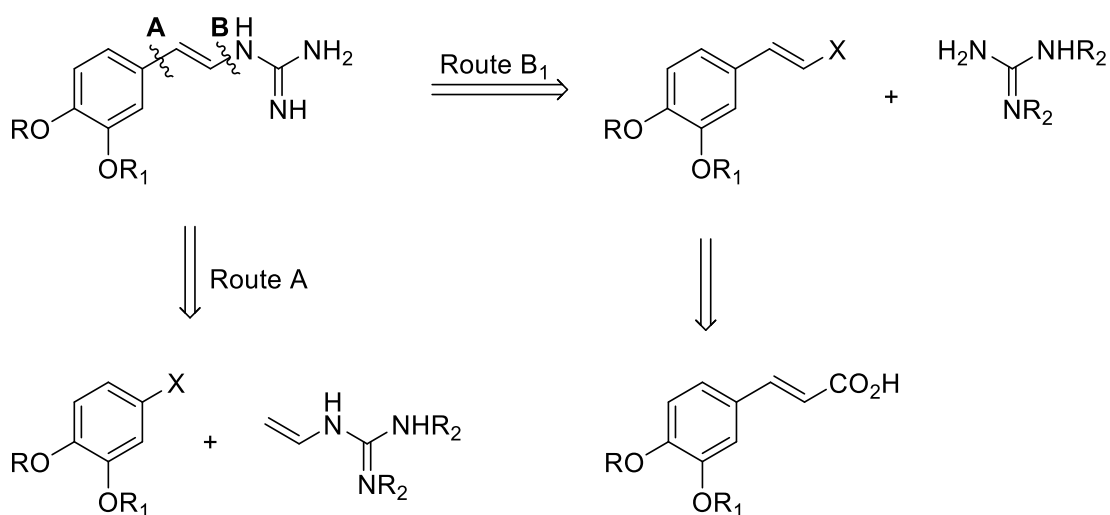


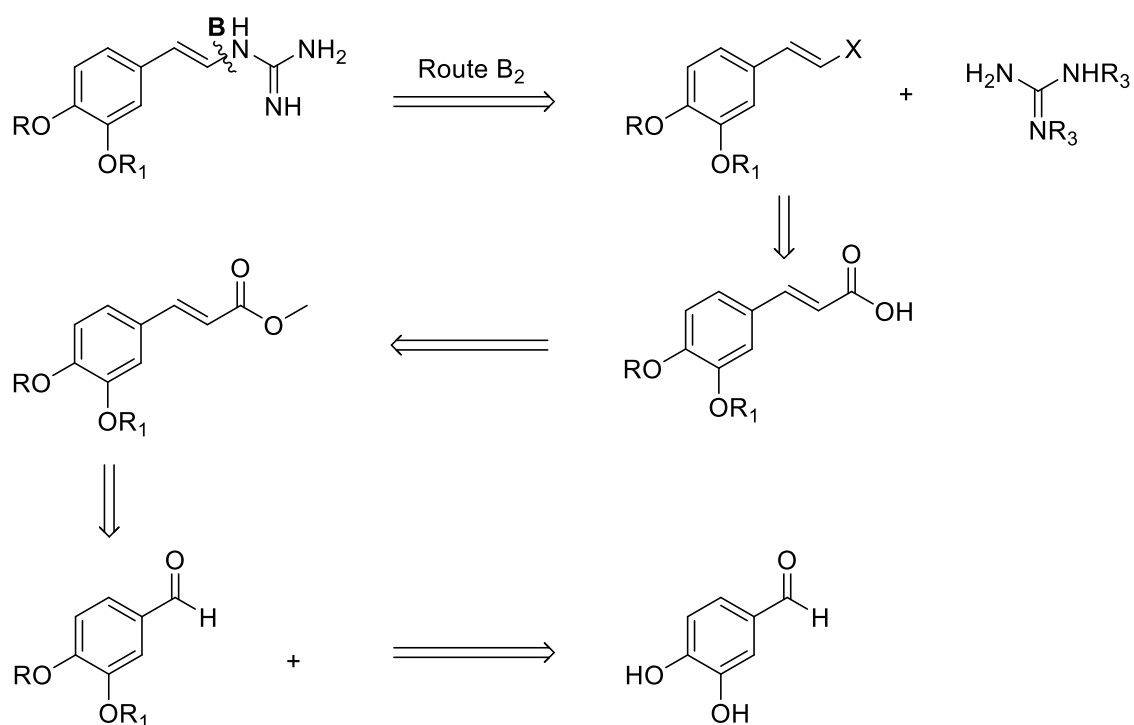
Figure 2.7: Retrosynthetic routes A and B₁ for tubastrine synthesis by Lorentzen et al.

The two outlined routes A and B₁ are the starting points for this research project. As vinyl guanidine is still inaccessible, allyl guanidine is to be synthesized and utilized in the Heck reaction in route A. The aim of this reaction is to produce an analogue with a three-carbon chain compared to the two-carbon chain found in tubastrine.

Attempts to optimize the B₁ pathway was conducted by adjusting a selection of the parameters in the microwave assisted C-N cross coupling reaction. Starting materials for the B₁ reactions are acrylic acids with various substituents on the aromatic ring. A particular focus was given to the synthesis of *para*-alkylated compounds as further described for the retrosynthetic route B₂.

2.5.2 Retrosynthetic route B₂

As it has been reported that larger lipophilic groups generally enhance antibacterial activity, attempts were made to produce analogues containing substituents with greater lipophilicity. Alkylation of the *para*-positioned hydroxyl group in the commercially available caffeic acid was therefore investigated. The lower pK_a of the *para*-positioned hydrogen atom in caffeic acid can be explained by the possibility of a resonance structure ranging from the aromatic ring through the double bond to the carboxylic acid functional group (pK_a = 8.6 versus 11.2 for the *meta*-position). This feature was utilized to study the possibility of selective alkylation of the *para*-position prior to the steps described in route B₁[38]. In addition, alkylations of the commercially available 3,4-dehydroxy benzaldehyde was tested for selective *para*-alkylation. Further synthesis from this product involved a general Wittig reaction to produce the acrylate and conversion to of the acrylate to the acid in route B₁. For illustrative purposes the alkylation process and subsequent Wittig reaction is found in retrosynthetic route B₂ below, where the starting materials differ from route B₁.



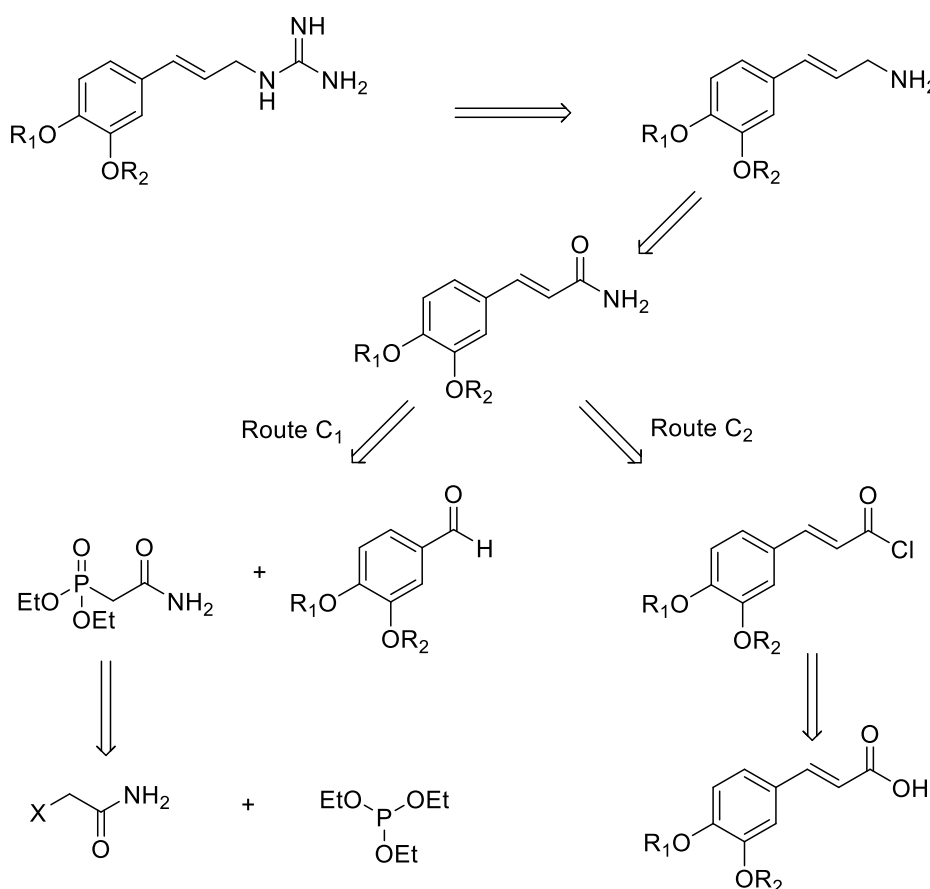
R₃=Boc and R₁= Bn, R₂=H or R₁=Hexyl, R₂=H or R₁=Dodceyl, R₂=H or R₁=Dodceyl, R₂=TBS or R₁=R₂=dodecyl

Figure 2.8: Retrosynthesis for route B₂

2.5.3 Retrosynthetic routes C₁ and C₂

The retrosynthesis for routes C₁ and C₂ are illustrated in figure 2.9. This route does not allow for synthesis of tubastrine itself, but rather analogues containing one additional carbon between the double bond and the guanidine group. The 3-carbon chain can also be found in antifoulants such as baretin and selected synoxazolidinones.

The illustrated retrosynthetic route C₁ corresponds to an Arbuzov reaction producing the amide phosphonate. Subsequently, the phosphonate reacts with a substituted benzaldehyde in a Horner-Wadsworth-Emmons reaction to give the α,β -unsaturated amide. A reduction of the amide will give the corresponding amine which can be further transformed into a guanidine group by reacting with 1*H*-pyrazole-1-carboxamide hydrochloride. Route C₂ illustrates the same end products with different starting materials. Starting with the commercially available caffeic acid, the amide can be synthesised from acylation and direct amidification of the carboxylic acid. One advantage of route C₁/C₂ is the avoidance of metal coupling reactions in the synthesis of the three-carbon chain.



R₁ = R₂ = H or R₁ = R₂ = TBS or or R₁ = R₂ = Me

Figure 2.9: Retrosynthesis for route C₁ and C₂

2.5.4 Retrosynthetic route D

The starting material for Route D is the natural catecholamine dopamine. In contrast to tubastrine, dopamine does not contain a double bond between the benzene ring and the hydrophilic group. The motive behind this approach is therefore to test the significance of the double bond on the antifouling properties of the compound.

The biogenic amine dopamine is formed in both vertebrates and invertebrates during decarboxylation of L-DOPA by DOPA decarboxylase. Dopamine is involved in a wide range of physiological functions in invertebrates and has been tested exogenously in settlement studies on *B. Amphitrite*[39],[40]. L-DOPA and dopamine were shown to significantly inhibit settlement in concentration ranges from 30 to 500 μM [41] and is therefore an interesting starting point for synthesis of antifouling products.

The retrosynthesis for route D is illustrated in figure 2.10.

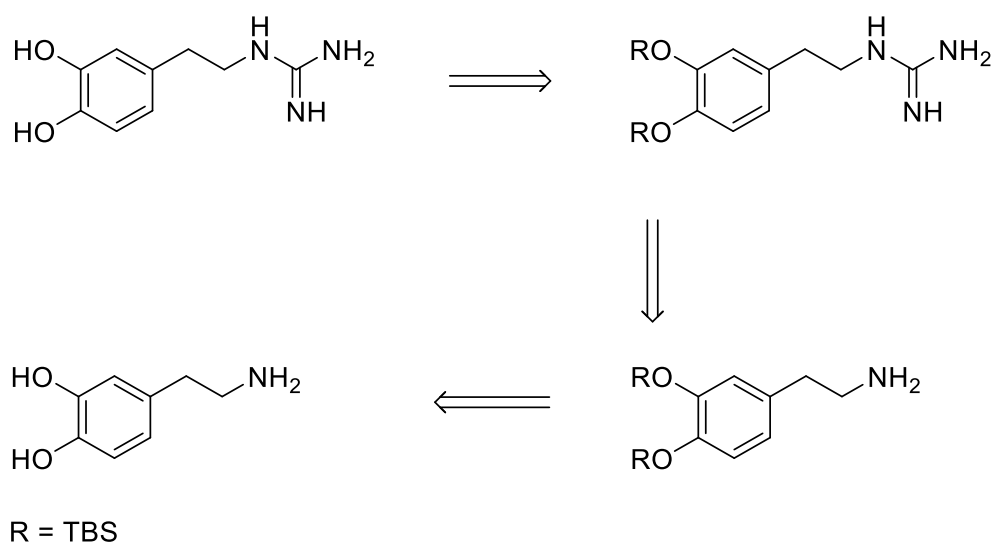


Figure 2.10: Retrosynthesis for route D

2.5.5 Retrosynthetic route E

In addition to the described routes for guanidine analogues, research was conducted on developing an amidine analogue, where an amidine group replaces the known antibacterial guanidine group. Amidine compounds represented by the formula below are known to have anti complement activity[42] and the guanidine resemblance raises an interesting question to whether the structural similarity may be reflected in the antimicrobial activity of such molecules.

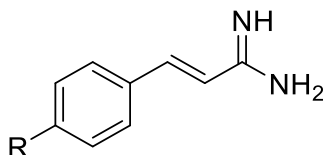


Figure 2.11: General structure for an amidine analogue

The retrosynthetic route E below illustrates the synthesis of amidine analogues. The first step in the reaction corresponds to the described Horner Wadsworth Emmons reaction between an Arbuzov salt and the disubstituted benzaldehyde found in route C₁. In the second step, the amide group is converted to an amidine functional group by reaction with Meerwein's reagent ((C₂H₅)₃O(BF₄)) and gaseous ammonia.

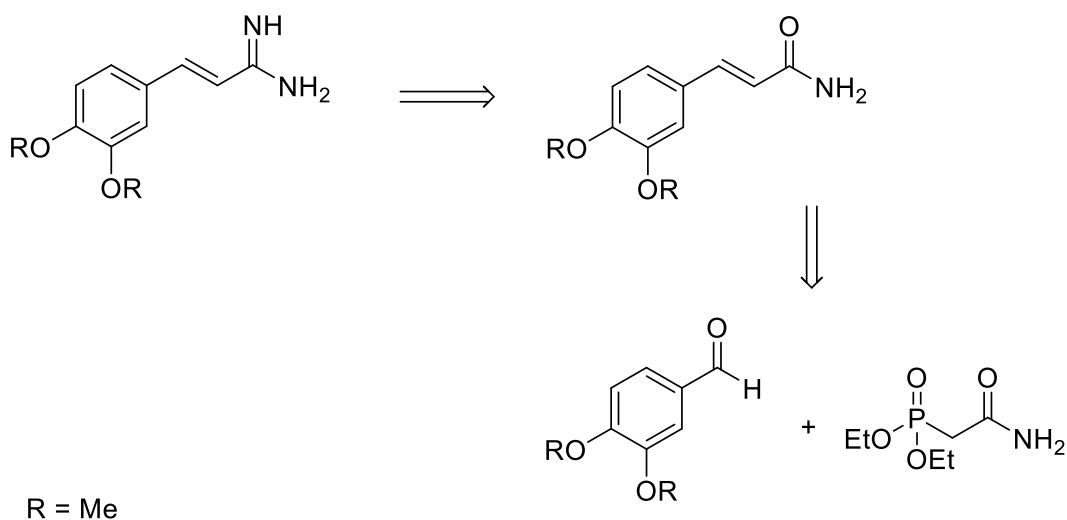


Figure 2.12: Retrosynthesis for route E

2.6 Reactions for synthesis of tubastrine analogues

2.6.1 Arbuzov reaction

The Arbuzov reaction, also known as the Michaelis-Arbuzov rearrangement, is a reaction for production of an alkyl phosphonate from a trialkyl phosphite and an alkyl halide[43]. The Arbuzov reaction is one of the most versatile mechanisms for formation of carbon-phosphorus bonds.

The first step in the Arbuzov reaction involves a nucleophilic attack by the phosphite on the electrophilic alkyl halide to produce a phosphonium intermediate in a S_N2 reaction. The intermediate product is unstable under reaction conditions and the halide ion reacts readily with the phosphonium intermediate to give the alkyl phosphonate as illustrated in figure 2.13.

Acyl halides constitutes the most reactive halides in the Arbuzov reaction. For alkyl halides the reactivity generally decreases going from primary to tertiary alkyl halides. Reactivity also decreases with decreasing atom radius of the halide.[44]

The phosphonates produced in the Arbuzov reaction are starting materials for the Horner-Wadsworth-Emmons reaction described in chapter 2.6.2.

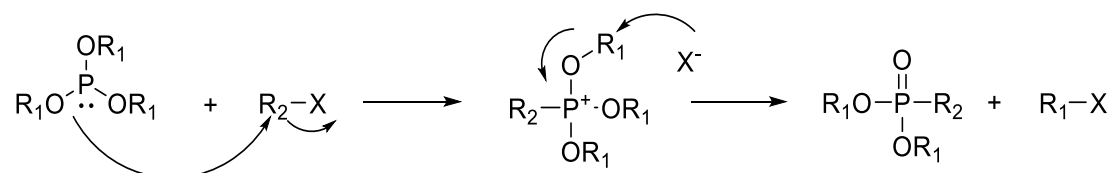


Figure 2.13: Overview of the Arbuzov reaction.

2.6.2 Horner-Wadsworth-Emmons reaction

The Horner-Wadsworth-Emmons (HWE) reaction is close in nature to the Wittig reaction and a valuable tool for synthesizing α,β -unsaturated carbonyl compounds.[45] Since first reported by Wadsworth and co-workers, a number of developments has resulted in a broad range of possible products in high yields. This includes the synthesis of both esters, amides, carboxylic acids, ketones and aldehydes. An important feature of the HWE reaction is the thermodynamically favoured formation of the *trans*-alkene.

In contrast to the phosphonium ylides used in the Wittig reaction, the phosphonate stabilized carbanions used in HWE reactions are more nucleophilic and less basic. The first step in the HWE reaction involves deprotonation of the phosphonate to give the phosphonate carbanion. According to studies performed by Thompson and Heatcock on the HWE reaction with various aldehydes, lithium salts gave the greater (*E*)-stereoselectivity for disubstituted olefins[46].

The second step of the reaction is a nucleophilic addition of the carbanion onto the aldehyde or ketone. If $R_2=H$, the intermediates can interconvert as illustrated in figure 2.14. Another observation made by Thompson and Heatcock revealed that increasing the bulkiness of the aldehyde will also increase the (*E*)-stereoselectivity.

The final step in the HWE-reaction is the elimination of the phosphate. The phosphate salt produced is readily removed by aqueous extraction.

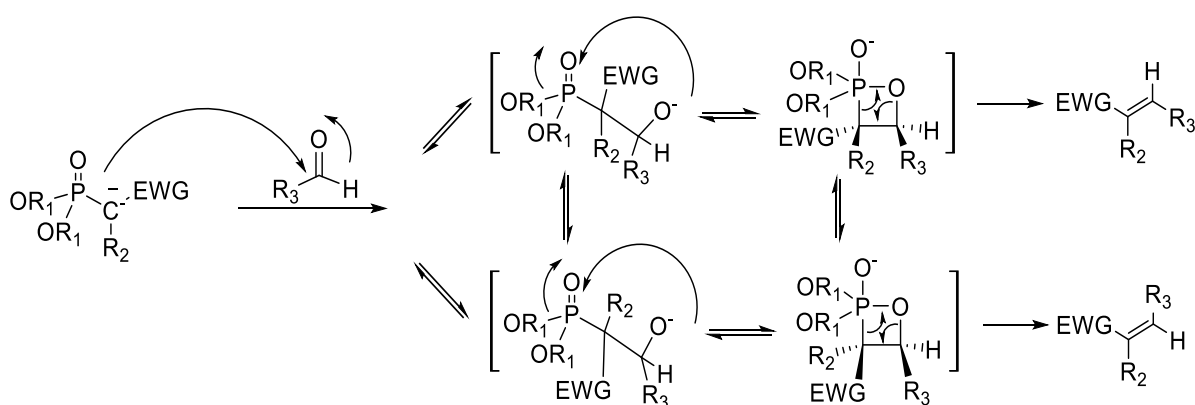


Figure 2.14: Overview of the Wadsworth-Horner-Emmons reaction[47]

2.6.3 Wittig reaction

The Wittig reaction is a common reaction for synthesis of alkenes from aldehydes or ketones, where the carbonyl group reacts with an ylide produced from a phosphonium salt[48].

The first step in the Wittig reaction is the production of a negatively charged polarized ylide carbon center by a strong base. The reactivity of the ylide is strongly dependent upon its substituents. In situations where the substituents are electron withdrawing, the negative charge may be delocalized over several carbon centres and the reactivity is thus reduced. Due to the instability of ylides in the presence of water and oxygen, Wittig reactions are carried out under inert atmospheres.

The negatively charged ylide will bind to the carbonyl via a nucleophilic addition to produce a zwitterion (betaine) as illustrated in figure 2.15. In this step, the reactivity of the carbonyl group increases with the electrophilic character of the carbon-oxygen double bond. From research using ^{31}P -NMR it is proven that the betaine generates a ring structured oxaphosphetane intermediate. Due to the energetically favoured formation of a phosphorus-oxygen double bond, the ring structure will decompose in the final step to produce an alkene and phosphine oxide[48].

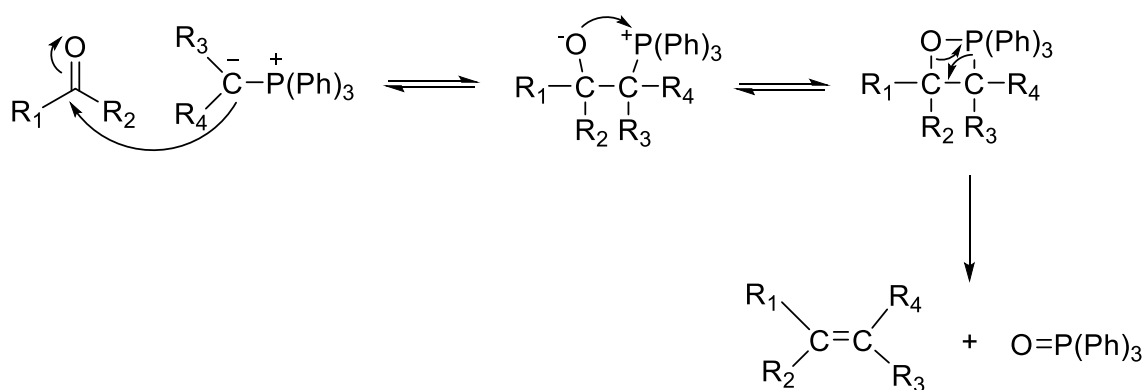


Figure 2.15: Wittig reaction mechanism

2.6.4 Modified Ullmann reaction

The Ullmann reaction is a copper-mediated aromatic nucleophilic substitution reaction developed by Fritz Ullmann and Irma Goldberg. Since first reported in the early 1900's, the reaction mechanism of the Ullmann reaction has been widely studied and several proposed mechanisms are still discussed today.

Due to the harsh reaction conditions in the original proposed reaction, milder catalytic versions known as the “modified Ullmann reaction” have been developed. The main difference between the old and improved reactions are the presence of ligands which enhances the solubility of the copper precursors. However, despite thorough research on the improved reaction, there exists no consensus on the mechanism of the modified Ullmann reaction. Copper exists in a wide range of oxidation states and many solvents and ligands show excellent coordination effects with this element. As copper may be present in different oxidation states in the reaction, different mechanisms are proposed. These mechanisms can be divided into two main categories: those in which the oxidation state remains constant (1 and 2) and those where the oxidation state changes throughout the cyclic reaction (3 and 4) [49]:

- 1) σ -bond metathesis through a four-centre intermediate
- 2) π -complexation of copper(I) on ArX
- 3) Oxidative addition of ArX on copper(I) giving a Cu(III) intermediate
- 4) Aryl radical intermediates via either halide atom transfer (AT) or single electron transfer (SET)

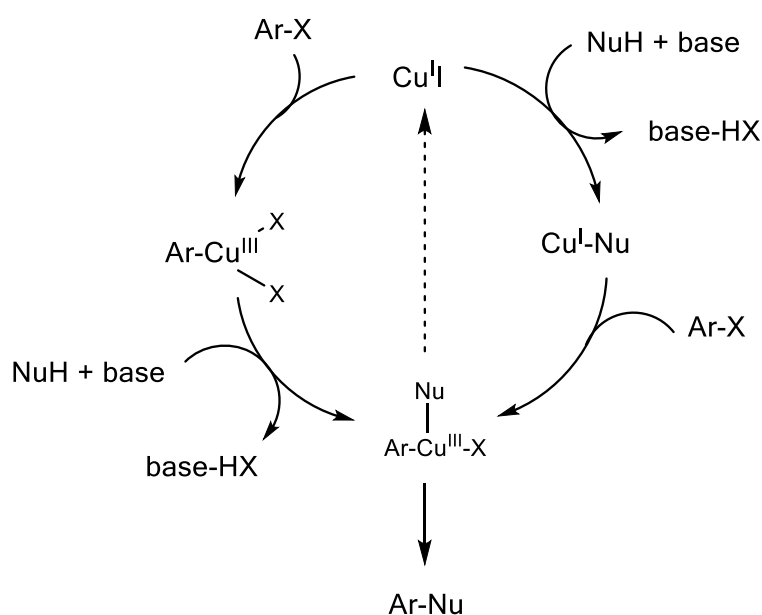


Figure 2.16: Proposed orders of oxidative addition in the Cu(I)/Cu(III) mechanisms

Figure 2.16 illustrates the two possible oxidative addition/reductive elimination pathways suggested for the modified Ullmann reaction. The left hand side of the cycle shows an oxidative addition of the aryl halide to copper, resulting in a copper(III) complex. Following, the halogen in the complex is exchanged for the nucleophile via reductive elimination, the coupling product is released and the Cu(I) is regenerated. In the right hand side mechanism the nucleophile reacts with the copper halide before the oxidative addition takes place. Although the latter mechanism has been favoured in most recent reports, the relative order is still uncertain.

The mechanistic pathway involving a σ -bond metathesis is illustrated in figure 2.17. In the first step, the halide is displaced by the nucleophile to form a copper-nucleophile complex. This intermediate complex acts as the catalyst for the upcoming coupling. The copper catalyst coordinates with the aryl halide in a new four-centred intermediate where the coordination is oriented by the charges on Cu^+ and the electronegative halide. Thus, the partial positive charge on the carbon atom will support the substitution of the nucleophile resulting in the coupling product and free Cu(I).

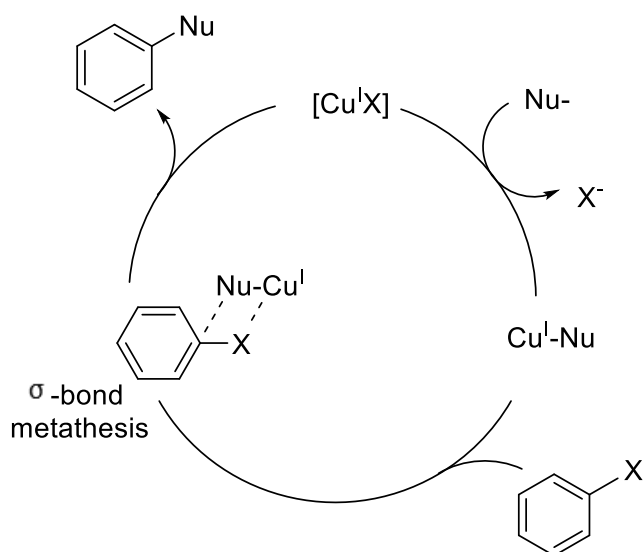


Figure 2.17: σ -bond metathesis through a four-centre intermediate[49]

The π -complexation of copper(I) on ArX where copper maintains its oxidation state is illustrated in figure 2.18. This proposed mechanism starts with a coordination of the copper catalyst to the aryl halide. Following, the copper-aryl halide complex undergoes a polarisation where the halide is substituted for the nucleophile and the halide is released. The final release of the coupling product regenerates the copper (I) catalyst.

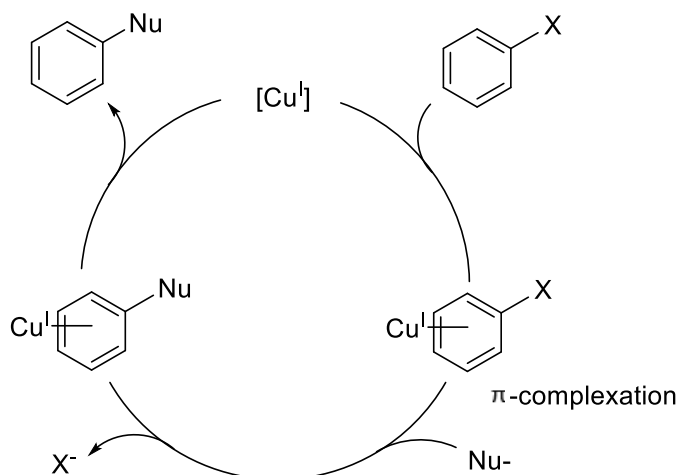


Figure 2.18: π -complexation of copper(I) on ArX[49]

Some researchers have also reported mechanisms involving aryl radical intermediates from either single electron transfer (SET) from the aryl halide or halide atom transfer (IAT). In the SET mechanism, the copper(I) catalyst is oxidized to copper(II) by a single electron from the aryl halide, resulting in an aryl halide radical anion. The aryl halide radical then couples with the nucleophile to give the coupling product and the copper(II) is reduced back to copper(I)[50]. However, with the exception of the results reported from van Koten and coworkers, the IAT and SET mechanisms generally lacks experimental support. In conclusion, the oxidative addition/reductive elimination mechanistic pathways are in most cases favoured although no definite consensus on the mechanism of the modified Ullmann reaction exists.

2.6.6 Heck reaction

The Heck reaction is an important reaction in organic synthesis. The reaction involves a C-C bond formation of an alkene with an alkyl, aryl or vinyl group by the use of a palladium catalyst[51]. R_1 is used for the alkyl/aryl/vinyl group as illustrated in figure 2.19. The R_1 -palladium complex is generated from the reaction between the R_1 -halide and a palladium-(0) complex. A ligand is employed in the Heck reaction for stabilizing effects, e.g. triphenylphosphine.

The R_1 -palladium complex then adds to the alkene by olefin insertion, followed by a β -elimination reaction to release the substituted alkene. A stoichiometric amount of base, e.g. trimethylamine (Et_3N) is necessary for regeneration of the palladium-(0) complex.

The regioselectivity in the olefin insertion is largely determined by steric factors and the substitution of the hydrogen atom tends to occur at the carbon center with the larger number of hydrogens. Electron withdrawing groups on the alkene may improve the regioselectivity while electron donating groups may result in a greater mixture of regioisomers[44].

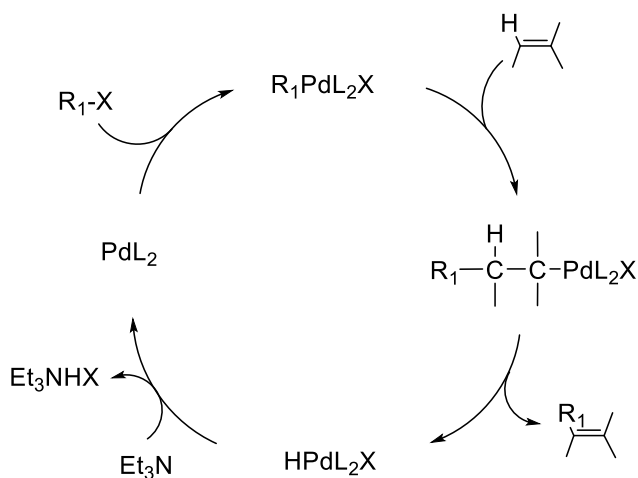


Figure 2.19. Overview of the Heck reaction

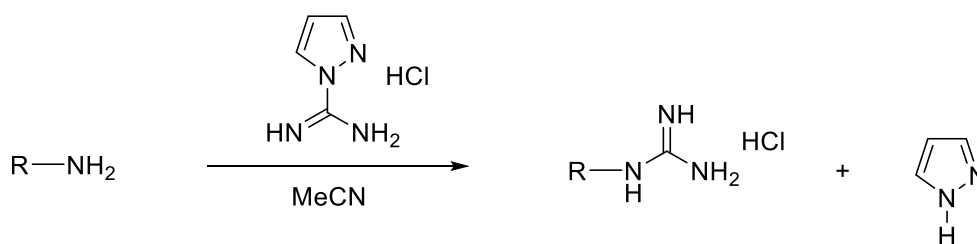
2.6.5 Guanylation by 1*H*-pyrazole carboxamide hydrochloride

Guanidine compounds are biologically active substances with strong polar activity as described in chapter 2.4 Their basic and polar behaviour have caused a demand for preparing such compounds synthetically, as isolation from nature may be challenging.

A common method for preparation of guanidines is the reaction between a primary amine and 1*H*-pyrazole carboxamide hydrochloride. The method was first described by Bernatowicz et al. in 1992[52], in relation to applications in peptide synthesis. In 2017, Bakka et al. reported a simplified synthesis with the same guanylation agent, which eliminated the need for chromatographic purification[53]. By running the reaction in acetonitrile (MeCN) instead of the commonly employed solvent DMF, chromatographically pure compounds were achieved in high yield (59 – 93 %).

In addition, the authors demonstrated that for a variety of amines, basic conditions did not necessarily increase the yield nor decrease the reaction time.

The reaction of a primary amine with 1*H*-pyrazole carboxamide hydrochloride is illustrated in figure 2.20.



R = lipophilic group

Figure 2.20: Guanylation of primary amines by 1*H*-pyrazole carboxamide hydrochloride

3. Results and discussion

3.1 Results for routes A and B₁/B₂

3.1.1 Results for route A

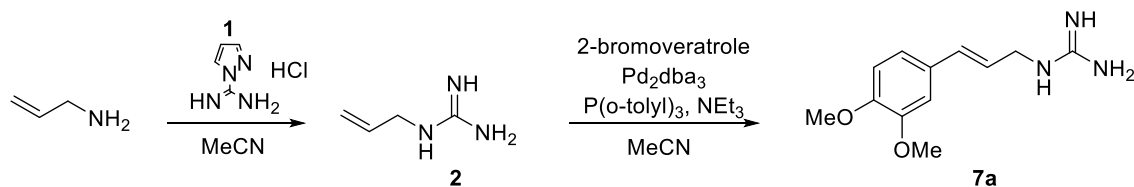
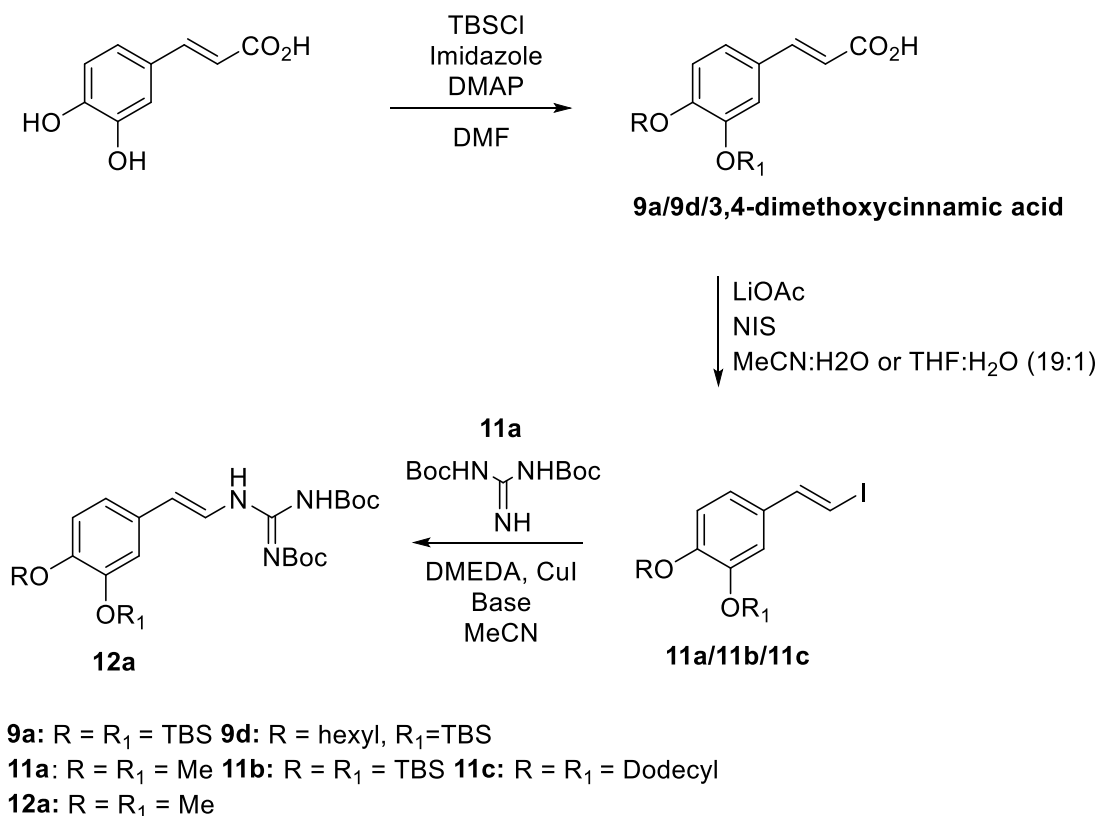


Figure 3.1: Overview of route A

Based on the work of Lorentzen et al.[1], route A and B₁ were studied and tested in greater depth. For route A, several attempts have previously been made to synthesize the required starting material vinyl amine. However, this molecule has proven not to be obtainable and thus allyl amine was utilized as illustrated in figure 3.1. Allyl amine was converted to allyl guanidine (2) in high yield (98%), by reaction with 1*H*-Pyrazole-1-carboxamide hydrochloride. The palladium catalysed Heck coupling between allyl guanidine and 3,4-dimethoxybenzyl bromide were tested twice.

The strong polarity of compound 7a ensued a particularly challenging work up. Attempts were made to purify the product by reverse flash column chromatography. However, the isolation of compound 7a was not accomplished. According to NMR analyses, the major constituents of the product mixture were the starting materials along with significant impurities. The minor appearance of product was identified by the double bond signals in ¹H-NMR. From NMR integration, the product yield of 7a was determined to be approximately 7.9 %.

Due to the low yield, challenging work-up and unavailability of vinyl amine in route A, other routes were investigated for more efficient syntheses of tubastrine analogues.

3.1.2 Results for route B₁Figure 3.2: Overview of route B₁

Based on the reported success of Route B₁ with a maximum yield of 49 % in the final step[1], attempts were made to improve the reaction conditions and yield of this reaction. The first step in route B₁ involved a protection of the free -OH groups in the commercially available caffeic acid. In this project, silyl protection was utilized (**9a**, 90 %) or 3,4-dimethoxy cinnamic acid was applied as the starting material. The acid was further converted to a halogen by reaction with lithium acetate (LiOAc) and N-bromosuccinimide (NIS)[54] in a Hunsdiecker-Borodin decarboxylation reaction. This reaction produced the methoxy- and silyl protected products **11a** and **11b** in 80 % and 90 % yield respectively.

The microwave assisted C-N cross coupling reaction between vinyl iodide and 1,3-bis(*tert*-butoxycarbonyl)guanidine have been studied in great detail by Lorentzen et al.[1]. Ligands, bases, solvents, heating sources and reaction times have been investigated to find the optimal reaction conditions. The maximum yield (49 %) was reported in a microwave assisted reaction with K₃PO₄ (2.05 eq.) as base, DMEDA (2.30 eq.) as ligand, CuI (1.15 eq.) as catalyst, MeCN as solvent, reacting at 65 °C, 50 W for 35 minutes. As the microwave assisted coupling improved the yields compared to traditional heating, the

microwave was utilized to improve the reaction in this project. A variety of ligands were also tested, with *N,N*-dimethylethylenediamine (DMEDA) as the most promising. Different bases tested by Lorentzen included K_3PO_4 , K_2CO_3 , Cs_2CO_3 and Et_3N , with K_3PO_4 giving the highest yield. However, in this project it became clear that K_3PO_4 has poor solubility in acetonitrile which was confirmed to be the most suitable solvent for this reaction.

Due to the poor solubility of K_3PO_4 ($pK_a = 12.4$), other bases with similar pK_a values were tested in this project as displayed in table 3.1. Before applying the bases in the reaction, the general solubility in acetonitrile was evaluated. $Ba(OH)_2$ ($pK_a = 13.85$) showed poor solubility in MeCN, while the 1,5-Diazabicyclo[4.3.0]non-5-ene ($pK_a = 12.7$) and $(CH_3)_3COK$ ($pK_a = 17$) showed promising solubility. 1,5-Diazabicyclo[4.3.0]non-5-ene was tested twice, while keeping the remaining microwave conditions as previously reported. Analysis by NMR showed no reaction despite the similar basicity. The greater steric hindrance of this base may have been the decisive factor in the reaction.

Table 3.1: Overview of MW C-N cross coupling reactions for compound 11a

Entry	Base	11a (mg)	MW	Yield
1	Potassium phosphate (K_3PO_4)	58	65 °C, 50 W	49 %
2	1,5-diazabicyclo[4.3.0]non-5-ene	58	65 °C, 50 W	Nr
3	1,5-diazabicyclo[4.3.0]non-5-ene	58	65 °C, 50 W	Nr
4	Potassium <i>tert</i> -butoxide ($(CH_3)_3COK$)	58	65 °C, 50 W	- ^a
5	Potassium <i>tert</i> -butoxide ($(CH_3)_3COK$)	58	65 °C, 50 W	59 %
6	Potassium <i>tert</i> -butoxide ($(CH_3)_3COK$)	58	85 °C, 50 W	67 %
7	Potassium <i>tert</i> -butoxide ($(CH_3)_3COK$)	58	85 °C, 50 W	66 %
8	Potassium <i>tert</i> -butoxide ($(CH_3)_3COK$)	58	100 °C, 50 W	- ^b
9	Potassium <i>tert</i> -butoxide ($(CH_3)_3COK$)	150	85 °C, 100 W	≈ 20 % ^c
10	Potassium <i>tert</i> -butoxide ($(CH_3)_3COK$)	150	85 °C. 90 W	≈ 10 % ^c

a: Compound decomposed over night

b: Chemicals decomposed during reaction

c: Not isolated

Potassium *tert*-butoxide ((CH₃)₃COK) showed slightly greater solubility in acetonitrile compared to potassium phosphate. The lower steric hindrance as well as the higher pKa favoured this base for the C-N cross coupling reaction. Utilizing this base while keeping the other reaction conditions intact gave product **12a** in 59 % yield as a yellow oil.

As there was no reported testing on the effect of temperature change in the reaction, different temperatures were tested at 50 W. An increase in the temperature from 65 °C to 85 °C proved to have a positive effect, giving product **12a** in 67 % yield. A further increase in the temperature to 100 °C gave decomposition of the starting materials and no reaction. A temperature of 85 °C with potassium *tert*-butoxide as base is therefore proposed as the new optimum reaction conditions for the C-N cross coupling.

Attempts were made to scale up the microwave reaction by running the experiment with 2.59 times the amount of starting material in the same size MW vials (10 ml) and increased effect. The scaled up reactions were tested at 100 W and 90 W. At 100 W, ¹H-NMR analysis after flash chromatography purification indicated a starting material/product mixture with an approximate production of ≈ 20 % **12a**. Significant amounts of impurities were also present. At 90 W, the product conversion was only 10-15 %. Consequently, the remaining microwave experiments in this project were performed at the original scale (58 mg, 0.2 mmol of **11a**).

3.1.3 Results for selective *para*-alkylation reactions in route B₂

Reported studies have shown that an increased size of the lipophilic part of the molecule may enhance the antimicrobial activity[32]. For that reason, attempts were made to alkylate the *para*-positioned -OH group in route B₂ prior to the microwave assisted C-N coupling in route B₁. Alkylation of both caffeic acid and 3,4-dihydroxybenzaldehyde were tested as displayed in table 3.2. Alkylation of the aldehyde was followed by a general Wittig reaction and the ester produced was further hydrolysed into the acid as displayed in figure 3.4. From this point, the final paths of route B₁ and B₂ were equal.

The first alkylation reaction conducted was between caffeic acid and benzyl bromide with two equivalents of sodium carbonate (Na₂CO₃) in acetone under reflux. The reaction did not proceed as the base was likely to weak. The reaction was therefore repeated using potassium carbonate (K₂CO₃) base as illustrated in figure 3.3. This reaction produced 50 % of a *para/meta*-alkylated product mixture and 50 % starting material was recovered.

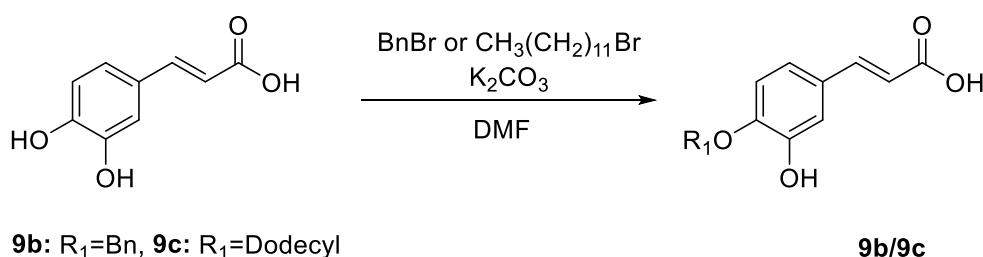
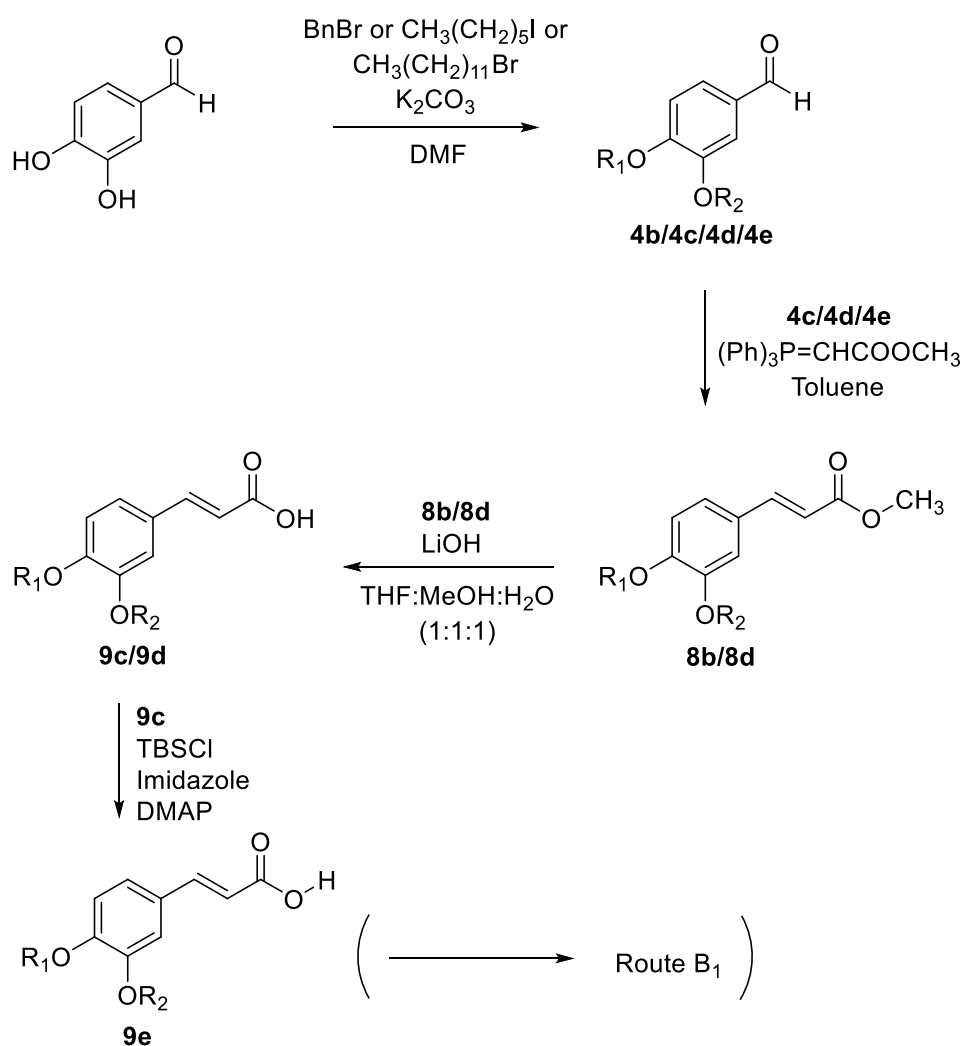


Figure 3.3: Alkylation of caffeic acid

Because the lower pK_a of the *para*-positioned hydrogen can be explained by the extended resonance structure, it is likely to believe that a resonance structure involving a shorter π -electron transfer distance will increase the reactivity of the compound. For that reason, the *para*-selective alkylation with BnBr was repeated using 3,4-dihydroxybenzaldehyde and one equivalent K₂CO₃ in DMF as illustrated in figure 3.4. The reaction was heated to 60 °C for four hours and then stirred at room temperature for an additional 18 hours. The reaction produced only 11 % of the pure *para*-alkylated product **4b**. Following this result, other alkylation reagents were tested for selective *para*-alkylation.

Couladouros et al. reported that 0.88 equivalents of base gives the highest fraction of the pure *para*-product[55], although this reaction can only yield 100 % if the bicarbonate is able to deprotonate the hydroxyl groups. Thus, a new alkylation was tested using 0.88 equivalents K_2CO_3 and 1-iodohexane as the alkylation reagent with 3,4-dihydroxybenzaldehyde in DMF as the starting material. Unlike the previous alkylations, the reaction was stirred at 90 °C throughout the entire reaction time. With a 73 % yield of the pure *para*-alkylated product **4c**, the reaction conditions were suitable for making further alkylated starting materials.



4b: $R_1=\text{Bn}$, $R_2=\text{H}$ **4c:** $R_1=\text{hexyl}$, $R_2=\text{H}$ **4d:** $R_1=\text{dodecyl}$, $R_2=\text{H}$ **4e:** $R_1=R_2=\text{dodecyl}$
8b: $R_1=\text{dodecyl}$ $R_2=\text{H}$ **8d:** $R_1=R_2=\text{dodecyl}$
9c: $R_1=\text{dodecyl}$ $R_2=\text{H}$ **9d:** $R_1=R_2=\text{dodecyl}$

Figure 3.4: Route B₂: Alkylation of 3,4-dihydroxybenzaldehyde

To increase the lipophilicity of the starting material even further, 3,4-dihydroxybenzaldehyde was also alkylated by 1-bromodecane using the same conditions as previously described. In the first entry, the reaction produced 51 % of the pure *para*-alkylated product **4d**, 25.3 % of a *para*-/*meta*-alkylated mixture and 18.4 % of the double substituted product **4e**. In the second entry, the reaction produced 63 % of the pure *para*-substituted product **4d** and 24 % of the double substituted product **4e**.

Due to the successful alkylations using 1-bromodecane, direct alkylation of caffeic acid was tested in one last attempt (Figure 3.3). As the carboxylic acid proton has a pKa of 4.8, the base equivalency was increased to 1.5. However, in this alkylation process a selective *para*-alkylation was not possible, and the reaction produced 67 % of the double substituted product. The reason for the non-selective alkylation of caffeic acid is likely the formation of the unfavourable resonance form illustrated in figure 3.5.

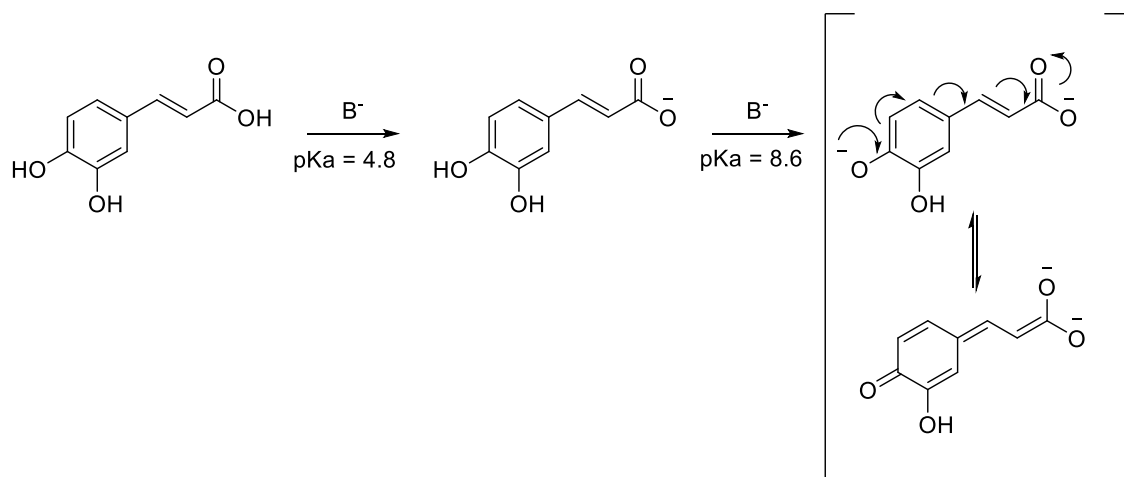
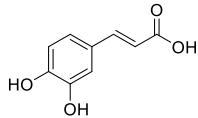
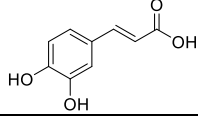
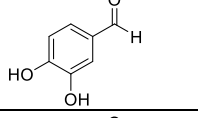
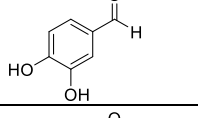
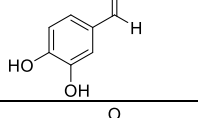
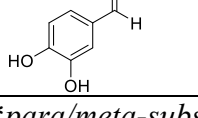


Figure 3.5: Deprotonation of caffeic acid

The results tabulated in table 3.2 show no clear consistency in the products produced by the alkylation reactions and both pure *para*-alkylated products, *meta*-alkylated products and double-alkylated products may be produced. However, 0.88 equivalents of K₂CO₃ in DMF at 90 °C for a minimum of 24 hours gave the highest yield for the alkylated products **4c** and **4d**.

In the synthesis of **4d**, the double alkylated by-product was assigned the product number **4e**, as this compound was utilized in the further reactions in route B₂.

Table 3.2: Overview of alkylation reactions

Starting material (S.M.)	Alkyl reagent	Desired product	<i>para</i> -subst.	<i>meta</i> -subst.	Double subst.	Recovery of S.M.
	BnBr	9b*	50 %		-	50 %
	Br(CH ₂) ₁₁ CH ₃	9c	-	-	67 %	-
	BnBr	4b	11 %	-	-	25 %
	I(CH ₂) ₅ CH ₃	4c	73 %	6 %		-
	Br(CH ₂) ₁₁ CH ₃	4d	51 %		18 % (4e)	-
	Br(CH ₂) ₁₁ CH ₃	4d	63 %	-	24 % (4e)	-

**para/meta*-substituted products and starting material not separated.

3.1.4 Results for reactions of *para*-alkylated products in route B₂

The next step in route B₂ involved a general Wittig reaction between the alkylated benzaldehyde and methyl (triphenyl-phosphoranylidene)acetate to produce the vinyl ester as illustrated in figure 3.4. Using 1.5 equivalents of sodium hydride (NaH) as a base in the reaction between the hexylalkylated benzaldehyde **4d** and the Wittig salt produced 56 % of the product **8b** and 44 % starting material (**4d**) in a mixture inseparable by flash column chromatography. As protection of the second hydroxyl group is required in the final steps, the dodecylalkylated benzaldehyde was silyl protected prior to the Wittig reaction (**4f**), in an attempt to increase the chromatographic separation. However, due to unknown reasons, the silyl protecting group did not withstand the Wittig reaction conditions and the NMR spectra clearly illustrated that the silyl group was not present on the product molecule.

For that reason, the reaction was repeated without protecting groups and rather additional equivalents of base for deprotonation of the free -OH group. Using 2.5 equivalents did however only produce traces of the product and the same result was seen when the base equivalency was increased to 3. As the most promising result was produced with only 1.5

equivalents of base, the reaction was repeated without base and heating. This Wittig reaction produced 100 % of the pure product **8b**, and only the (*E*)-isomer was identified by NMR analysis. The double alkylated aldehyde **4e** was converted to the vinyl ester by the same conditions to produce the more lipophilic product **8d**.

The vinyl esters **8b** and **8d** produced from the Wittig reactions were then further hydrolysed to the corresponding carboxylic acids **9c** and **9d** by reaction with LiOH in THF:MeOH:H₂O 1:1:1. The first hydrolysis reaction of **8b** was completed in 19 hours, by stirring the reaction at room temperature. This reaction produced the product in 100 % yield after purification. In the second entry, the reaction was scaled up and heated to 50 °C. Heating the reaction decreased the reaction time to 7 hours and gave product **9c** in 99 % yield after purification. Compound **8d** was hydrolysed in 15 hours and gave compound **9d** in 100 % yield.

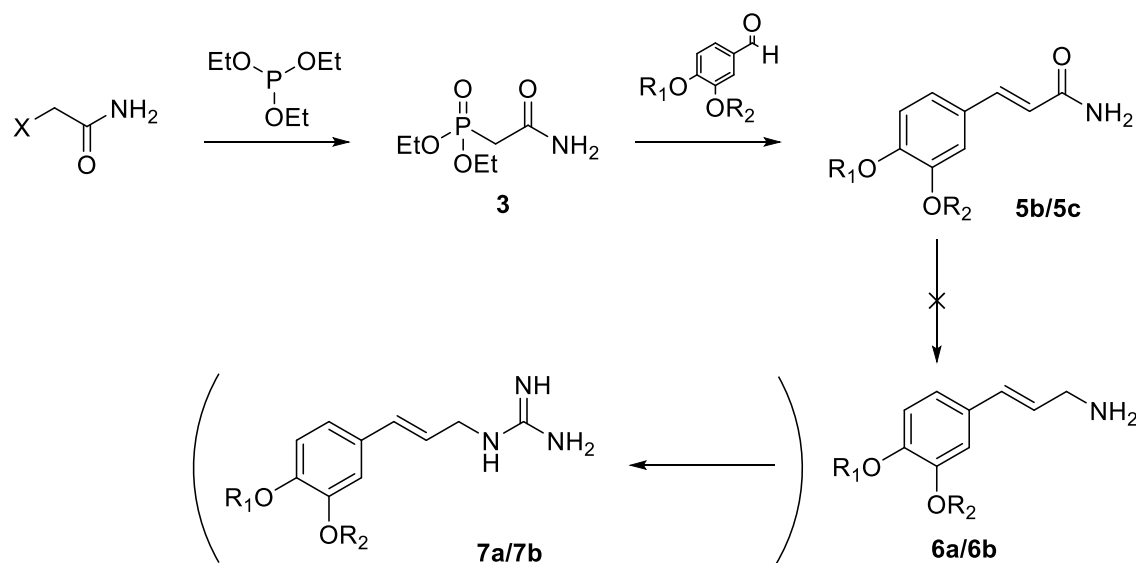
The final step before the Hunsdiecker-Borodin halogenation reaction was the temporary silyl protection of the free hydroxyl group in compound **9c**. In contradiction to earlier experiments this reaction did not proceed despite several attempts. Only traces of **9d** was identified by NMR. As silylation of caffeic acid and compound **4d** (alkylated benzaldehyde) gave positive results, no definitive explanation to the low reactivity can be given. However, one reason may be the greater steric hindrance in molecule **9c**, where both the 12-carbon alkyl chain and the opposite 3-carbon carboxyl acid give rise to steric challenges. In addition, it is worth mentioning that TBSCl purchased from Sigma Aldrich were applied in the successful silylation reactions, whereas TBSCl from VWR were utilized in the attempts to silylate compound **9c**.

As protection of **9c** was not accomplished, **9d** was the only alkylated compound converted to the vinyl halide. Conversion of double alkylated **9d** gave the product **11c** in 65 % yield. Due to shortage of time, the remaining C-N cross coupling (route B₁) was not tested for the alkylated products. However, with the exception of the remaining protection of the hydroxyl group in compound **9c**, a solid pathway for production of alkylated starting materials for the microwave assisted cross coupling reaction was established.

3.2 Results for route C

3.2.1 Results for route C₁ and C₂

Route C, including C₁ and C₂, was developed with the aim of producing a tubastrine analogue containing one additional carbon between the benzene ring and the guanidine group. The first steps of route C were split into two different pathways (C₁/C₂), as the amide can be synthesized from different starting materials. Route C₁ is illustrated in figure 3.6.



5b: R₁ =

Figure 3.6: Overview of route C₁

Route C₁ corresponds to an Arbuzov reaction followed by a general Horner Wadsworth Emmons (HWE) reaction. The Arbuzov reagent was synthesized from triethyl phosphite and 2-bromoacetamide in a dry media reaction, and gave the expected product **3** in high yield (98 %). Subsequently, the Arbuzov reagent served as the starting material for a HWE reaction to produce the vinyl amide. The first attempt to synthesize the vinyl amide was a reaction between the Arbuzov reagent and 3,4-dihydroxybenzaldehyde in diethyl ether (Et₂O) using four equivalents of potassium hydroxide (KOH) as base to produce the unprotected compound **5a**. However, due to low solubility of the starting materials in Et₂O, no reaction proceeded. A new attempt was made using the same conditions with THF as a solvent, but the solubility was still an issue. The solubility problems in this reaction were likely to be caused by the deprotonation of the free -OH groups and thus protection of these groups were necessary.

3,4-dihydroxybenzaldehyde was protected by *tert*-butyldimethylsilyl chloride in DMF using imidazole and DMAP as catalyst, which produced the protected benzaldehyde **4a** in high yield (98 %). A new attempt was then made to synthesize the vinyl amide **5b** from the protected benzaldehyde and the Arbuzov reagent in THF with two equivalents of KOH as base. During workup, water was added to dissolve the Arbuzov salt by-product. However, the product also dissolved in the water phase and was not possible to dissolve in EtOAc during extraction. The reaction gave **5b** in 25 % yield after purification. In the second attempt, extraction with water was excluded and silica was added for direct purification with flash column chromatography. The alternative work up increased the yield of **5b** to 36 %.

To further increase the yield for the HWE reaction in route C₁, the stronger base NaH was applied. The reaction between the Arbuzov reagent and the protected benzaldehyde in THF with two equivalents NaH as base increased the yield of **5b** to 51 % after purification. In addition to synthesizing the silyl protected vinyl amide, the dimethyl protected product **5c** was synthesized using the same conditions. This reaction produced the product in 99 % yield after purification. The difference in yield for the two different starting materials is significant and may be explained by the greater solubility of 3,4-dimethoxy benaldehyde in THF.

In route C₂ an alternative procedure for the synthesis of vinyl amide is tested, as illustrated in figure 3.7. The starting material for this route is the commercially available caffeic acid. The free -OH groups of caffeic acid was protected by *tert*-butyldimethylsilyl chloride to produce **9a** in high yield (90 %). The protected caffeic acid was acylated to compound **10** by thionyl chloride under reflux. Due to the instability of acyl chlorides, direct amidification was conducted using MeOH/NH₃. This pathway produced the vinyl amide **5b** in 42 % yield, with a higher fraction of impurities than **5b** produced from the HWE reaction. Consequently, the HWE reaction between the Arbuzov salt and the substituted benzaldehyde using NaH as base is the favoured reaction for the synthesis of the vinyl amide.

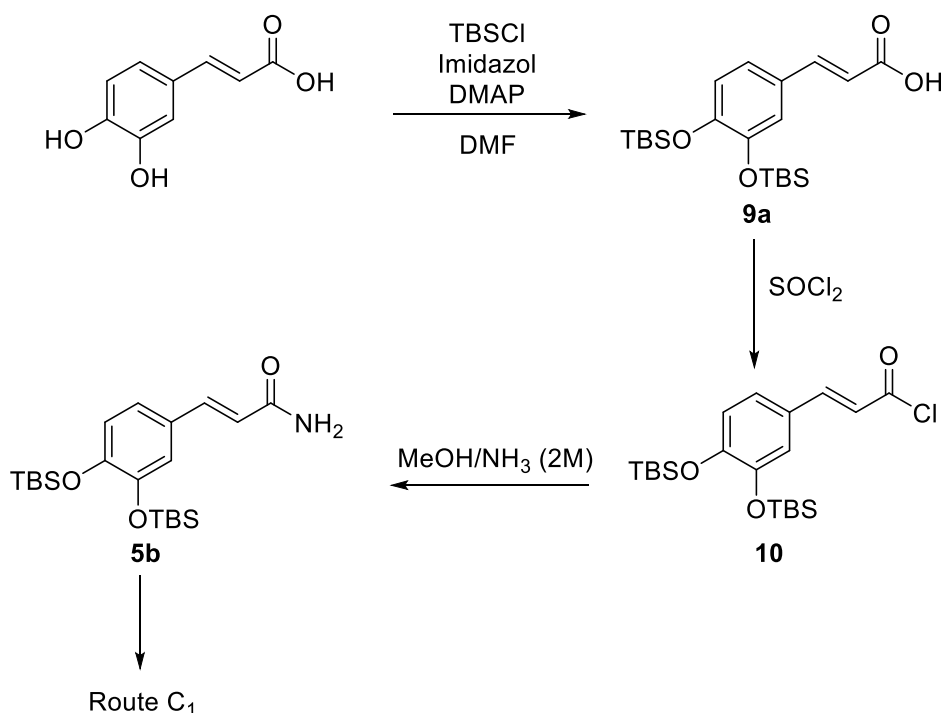


Figure 3.7: Overview of route C₂

The next step in route C (both C₁ and C₂) was a reduction of the amide to the corresponding amine. Lithium Aluminium Hydride (LAH) was tested for the reduction of **5b**, however the double bond was attacked during the reaction. Most likely, the LAH 1,2-attack involved an intermediate complex with the double bond. A new attempt at reducing the amide **5c** was tested using a 1M boron tetrahydrofurane complex solution[56]. This reaction did not proceed. As the amide reduction proved to be too challenging with the available chemicals, no further reduction reactions were tested. However, theoretical research on possible reduction or chain degradation reactions was carried out, as described in chapter 3.2.2.

A final attempt was made to synthesize the an amido-guanidine analogue, by simply doing a guanylation of the vinyl amide with 1*H*-pyrazole-1-carboxamide HCl. This reaction did not proceed.

3.2.2 Alternative reactions for reduction/chain degradation of vinyl amide

Recently, Volkov et al. reported the use of $\text{Mo}(\text{CO})_6$ catalysed chemoselective hydrosilylation of α,β -unsaturated amides for the formation of the corresponding allylamines[57]. As selective hydrogenation of amides is not applicable for compounds containing double bonds, the hydrosilylation method with different transition metals as catalysts is favoured. The authors reported full conversion of tertiary amides to tertiary amines using TMDS as silane source. However, as the general reactivity of the reaction decreased significantly going from tertiary to primary amides, this reduction was not tested in this project.

In addition of reduction of amides to amines giving a tubastrine analogue with one additional carbon, reactions involving chain degradation were studied. A chain degradation by one carbon results in the two carbon olefinic chain found in tubastrine. These reactions include the Hoffmann rearrangement, Schmidt reaction, and the Curtius rearrangement. Although the reactions were not tested due to the uncertainty of the imine-enamine equilibrium and limited time, they are highly relevant for the synthesis of both tubastrine and analogues.

The Hoffmann rearrangement reduces amides to amines with concomitant chain degradation by one carbon. Thus, the inexpensive and commercially available caffeic acid can be converted to an amide and reduced to an amine giving the two-carbon olefin chain found in tubastrine. Although using different reagents, the Schmidt reaction and the Curtius rearrangement works by the same principle. The uncertainty of these methods is however the equilibrium between the enamine produced and formation of the imine.

3.3 Results for route D

The aim of route D was to produce an analogue without the characteristic double bond found in tubastrine. The natural product dopamine was considered to be an excellent starting point as the resemblance between the two compounds is strong. An overview of route D is illustrated in figure 3.8.

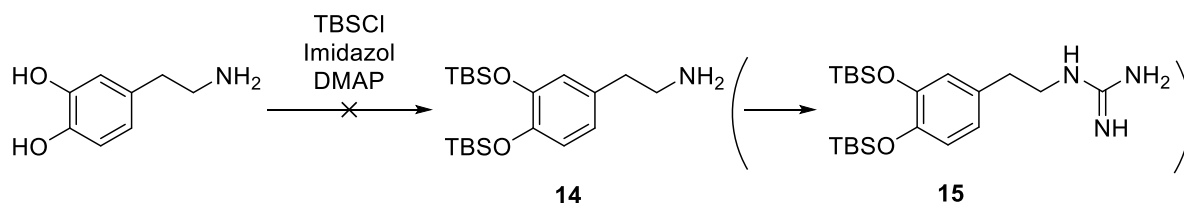


Figure 3.8: Overview of route D

The first step in route D involved a general silyl protection of dopamine hydrochloride. As for the previous reported silyl protections, the reaction was carried out in DMF with imidazole and DMAP. After purification, HR-MS and NMR analysis could confirm that the silylated amine **14** was only produced as the minor by product. According to HR-MS, the major compound was *N*-(3,4-bis((*tert*-butyldimethylsilyloxy)phenethyl)formamide, which indicates a reaction between the amine and DMF in addition to the silylation. ^1H -NMR showed a signal for the amide hydrogen at 8.12 ppm and ^{13}C -NMR showed the amide carbon signal at 161 ppm. These values match the predicted signals for the amide product. The molecular structure is illustrated in figure 3.9. To avoid the undesired amide formation, several other solvents were tested for the synthesis of compound **14** (DCM, MeCN, THF). However, none were able to solubilise the polar dopamine hydrochloride.

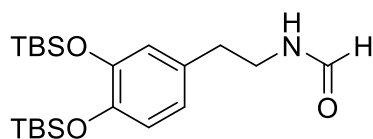


Figure 3.9: Structure of *N*-(3,4-dihydroxy phenethyl)formamide

Because of the great activity of the electron lone pair on the amine group in dopamine, other mechanisms for protection of the -OH groups may also be problematic. For instance, a simple methylation using MeI and a suitable base will favour methylation of the amine over the desired ether synthesis.

One final attempt was therefore made to directly guanylate dopamine without protection of the -OH groups. This reaction did not proceed.

3.4 Results for route E

Attempts were made to synthesize an amidine analogue of tubastrine. Several reactions have been reported for the synthesis of amidines, and conversion from amides is a common approach. In this project, an amidine analogue was prepared by the reaction of compound **5c** with triethyloxonium fluoroborate (Meerwein's reagent) and gaseous ammonia at ambient temperature. The reaction is illustrated in figure 3.10.

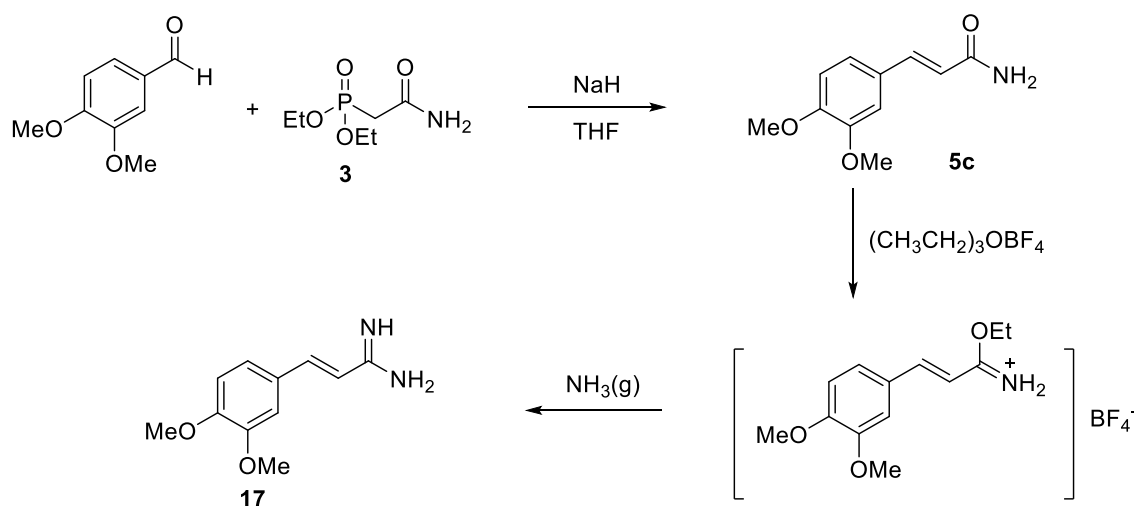


Figure 3.10: Overview of route E

The amide reactant **5c** was synthesized by the same method as the amides in route C₁. In the first attempt to synthesize the amidine, gaseous ammonia was not available. Therefore, a 2 M MeOH/NH₃ solution was utilized as the ammonia source in the reaction. From TLC analysis it was clear that the intermediate was formed, however the ammonia solution was not able to convert the imidic ester fluoroborate to the corresponding amidine.

As ammonia gas became available, the reaction was repeated. A set up for continuous flow of ammonia was however not attainable due to the lack of a needle valve in the armature. After 2/3rd of the expected reaction time, an overpressure in the supply tube caused the tube to blow off and continuation of the reaction was not possible. As TLC and NMR analysis indicated product, the unfinished reaction mixture was purified by aqueous flash column chromatography in small quantities (< 30 mg/column). NMR integration indicated a 1:0.5 product:starting material ratio before purification.

The Meerwein reaction produced the product **17** in 58 % yield after purification. A higher product yield is expected with proper equipment and a complete reaction time.

4. Conclusion

The purpose of this research project was to develop new synthetic routes for various syntheses of tubastrine analogues. The motive behind the production of tubastrine analogues was the potential antibacterial effect and applications in the antifouling industry.

Route A and B₁, developed by Lorentzen et al.[1], were included in this research. Allyl guanidine was applied in route A, in an attempt to synthesize the analogue **7a**. The reaction proved to give poor yield and challenging work up procedures, with only ≈ 7.9 % product conversion. As the purpose of this project was to develop new routes, route A was not further investigated.

The microwave assisted C-N cross coupling reaction in route B₁ were optimized in this project. By changing the base from K₃PO₄ to *t*-BuOK and increasing the temperature from 65 °C to 85 °C, the yield for the final step and product **12a** was increased from 49 to 67 %.

Selective alkylation of the *para*-positioned hydroxyl group in tubastrine analogues was studied extensively in route B₂. Attempts were made to alkylate both caffeic acid and 3,4-dihydroxybenzaldehyde prior to the steps of route B₁. The optimal conditions for selective *para*-alkylation proved to be alkylation of 3,4-dihydroxybenzaldehyde by 0.88 equivalents of K₂CO₃ and 1.0 equivalent of the alkyl reagent in DMF at 90 °C for a minimum of 24 hours. By applying these criteria, a maximum of 73 % selective *para*-alkylation was observed (**4c**). Selective *para*-alkylation of caffeic acid was not accomplished, as the reaction produced the double alkylated product under the same conditions.

In route C (C₁ and C₂), synthesis of an analogue with one additional carbon was tested. The reactions in route C involved synthesis of an amide with a 3-carbon chain, followed by reduction to the corresponding amine and conversion to guanidine. In route C₁, the Arbuzov and Horner-Wadsworth-Emmons reactions for synthesis of compound **3** (98 %), and the amide **5c** (99 %) were successful and gave the compounds in excellent yields. Amide **5b** were obtained in a 51 % yield by the same reactions. In route C₂, an attempt was made to synthesize the same amide (**5b**) by acylation and direct amidification of caffeic acid. This pathway produced **5b** in a lower yield (42 %), and thus Arbuzov/HWE proved to be the better method for synthesis of the required vinyl amide.

Reduction of the amide to the amine were tested twice by applying LAH and BH₃-THF as reducing agents to **5b** and **5c**, respectively. LAH attacked the double bond, while BH₃-THF showed no reaction.

Synthesis of an analogue without the double bond in route D failed in the first step. A side reaction between the amine in dopamine and the DMF solvent produced the corresponding amide. Other solvents were not able to solubilise dopamine hydrochloride.

In route E, synthesis of an amidine analogue of tubastrine was tested using Meerwein's reagent and gaseous ammonia. Despite technical difficulties with the ammonia supply and an incomplete reaction time, product **17** was obtained and isolated in 58 % yield.

In conclusion, the results from this research project have laid a solid foundation for more extensive studies on tubastrine analogues. Both the successful and unsuccessful reactions are important indications on what pathways to follow next, and hopefully this work will contribute to a complete synthesis of tubastrine analogues in the future.

5. Scope for further research

The chemistry and work performed in this research project have been extensive in terms of the number of routes and reactions. Consequently, several of the outlined routes for analogues requires additional work and further optimization.

In the synthesis of alkylated tubastrine analogues, it was confirmed that alkylation of 3,4-dihydroxybenzaldehyde followed by a general Wittig reaction gave the most selective *para*-alkylation. However, silylation of the second hydroxyl group proved to be challenging and thus alternative protection reactions should be further studied. By using the described alkylation mechanism followed by the MW C-N cross coupling, a number of alkylated products may be produced and tested for antimicrobial activity. Scale up of the MW assisted coupling should be further explored in terms of the conditions required for conversion of more than 58 mg starting material in each run.

Amides were synthesized by the HWE reaction in high yields in route C₁, however the amide to amine reduction was not successful. As described in chapter 3.2.2, several other mechanisms for amide reduction exists and can be tested. In addition, a number of chain degrading mechanisms for synthesis of the enamine were described. An enamine synthesis may give an enamine/imine equilibrium and it is unknown whether this equilibrium will affect the conversion of the amine to a guanidine functional group. Thus, these reactions require additional research on the stability of the enamine for such compounds.

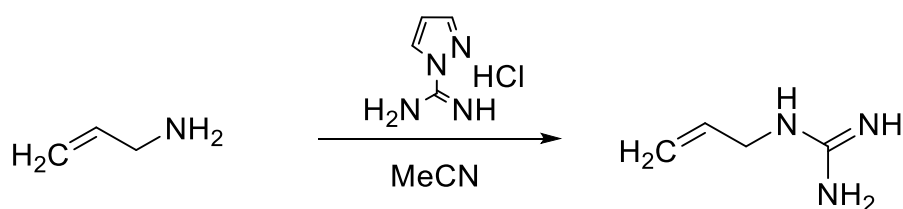
Reactions for protection of dopamine in other solvents than DMF is required for the synthesis of an analogue without the double bond in the pathway described in route D. If dopamine protection by other reagents is accomplished, the amine may be further converted to guanidine by the guanylation mechanism described in chapter 2.6.5.

Finally, an increased yield of the amidine analogue described in route E may be obtained by adequate equipment and reaction times. As the starting material to product conversion was approximately 2/3 in 2/3rd of the expected reaction time, a further optimization of the yield is likely possible.

6. Experimental

Proton nuclear magnetic resonance spectra (^1H NMR) and carbon nuclear magnetic resonance spectra (^{13}C NMR) were recorded with Bruker Ascend 400 MHz. Recorded shifts for protons are reported in parts per million (ppm, δ scale) downfield from tetramethylsilane. TLC-analyses were performed using Silica gel 60 F₂₅₄ and studied with a UVi tec limited 230V 50Hz UV-lamp. MS analyses were obtained using HR-MS with ESI, performed by the University of Tromsø. Kugelröhr distillation was carried out in a BÜCHI Glass oven B-585. For flash chromatography, silica gel normasil 60 40-63 μm (VWR) or Celite[®] 545 (VWR) were applied.

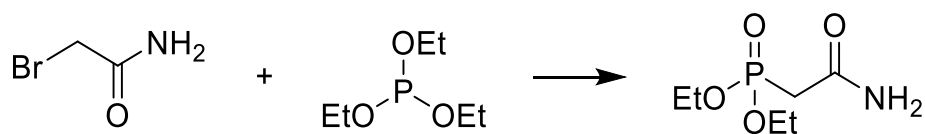
Synthesis of allyl guandine (2)



Allyl amine (0.76 ml) and 1*H*-pyrazole-1-carboxamide hydrochloride (**1**) (1.464 g) were added to MeCN (5.8 ml) and refluxed for 3 hours. During workup, Et₂O was added to induce precipitation and the substance was dried under reduced pressure. As the substance did not precipitate, recrystallization was carried out with MeOH:H₂O in a 5:1 ratio. The product did not recrystallize. The reaction produced compound **2** in 98 % as a thin brown oil.

^1H -NMR (400 MHz, D₂O) δ : 7.65 (s, 1 H), 6.36 (t, J = 2.14 Hz, 2H), 5.77-5.85 (m, 1 H), 5.17-5.24 (m, 2 H), 4.70 (s, 2H), 3.76-3.78 (m, 1 H) ppm

^{13}C -NMR (100 MHz, D₂O) δ : 43.0, 104.9, 116.3, 132.2 ppm

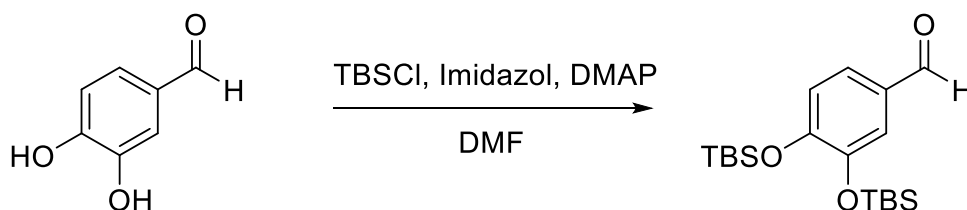
Synthesis of diethyl (2-amino-2-oxoethyl)phosphonate (3)

Triethyl phosphite (7.5 ml, 43.49 mmol) was added to 2-bromoacetamide (2.0 g, 14.49 mmol) and stirred at 110 °C for 12 hours to produce a yellow solution. Precipitation was induced by distillation of the residual triethyl phosphite. The solid precipitate was washed with hexane (3x10 ml). Hexane was evaporated under reduced pressure and the product was dried under vacuum for 7 hours. The reaction produced 2.77 g (98 %) of **3** as a white solid.

¹H-NMR (400 MHz, CDCl₃)δ: 6.84(s, 1H), 5.84(s, 1H), 4.10-4.19(m, 4H), 2.87(d, J = 20.7 Hz, 2H), 1.34(t, 6H) ppm

¹³C-NMR (100 MHz, CDCl₃)δ: 166.4, 62.8, 35.6, 16.3(2C) ppm

HRMS (ESI) m/z: [M + H]⁺ calculated for C₆H₁₅NO₄P: 196.0694 found 196.0733

Synthesis of 3,4-bis((*tert*-butyldimethylsilyl)oxy)benzaldehyde (4a)

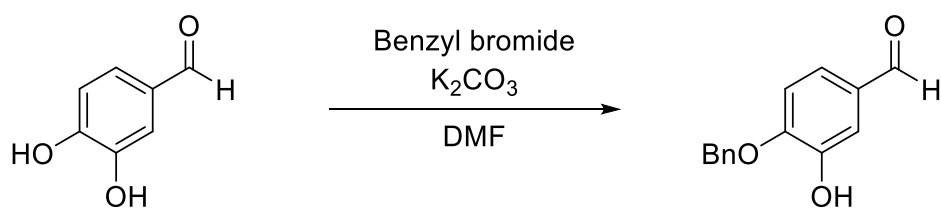
Entry	3,4-dihydroxybenzaldehyde (g)	Time (h)	Yield (%)
1	0.2	1	-*
2	0.5	1.5	98

*product oxidation and extraction difficulties

To a solution of 3,4-dihydroxybenzaldehyde (3.62 mmol, 0.5 g) in 6.0 ml DMF, imidazole (10.86 mmol, 0.74 g), DMAP (0.36 mmol, 0.044 g), and TBSCl (10.86 mmol, 1.64 g) were added. The solution was stirred at room temperature for 1.5 hour. DMF (10 ml) was added prior the extraction. The reaction mixture was extracted with PE (3x15 ml) and the combined organic phase was dried over anhydrous magnesium sulphate. The remaining solvent was removed under reduced pressure. The final product was vacuum dried for 7 hours to produce 1.305 g (98 %) of **4a** as a pale yellow oil.

¹H-NMR (400 MHz, CDCl₃)δ: 9.83 (s, 1 H), 7.38 (s, 1 H), 7.28 (s, 1 H), 6.96 (d, J = 8.3 Hz, 1 H), 0.86-1.27 (m, 18 H), 0.02-0.35 (m, 12 H) ppm

¹³C-NMR (100 MHz, CDCl₃)δ: 190.9, 153.4, 147.8, 130.7, 125.3, 120.8, 120.6, 25.8 (6C), 18.5 (2C), -0.4 (4C) ppm

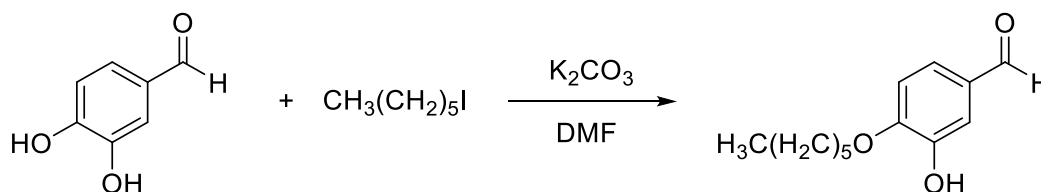
Synthesis of 4-(benzyloxy)-3-hydroxybenzaldehyde (4b)

A solution of 3,4-dihydroxybenzaldehyde (2.5 g, 18.1 mmol) and K₂CO₃ in DMF (30 ml) was stirred at 60 °C for 4 hours. Afterwards, the reaction was cooled to room temperature, BnBr (2.15 ml, 18.1 mmol) was added and the reaction was stirred for 15 hours. The product was extracted with water and EtOAc (3x30 ml) and the combined organic phase was washed with NH₄Cl and brine. The product was dried over MgSO₄ and concentrated under reduced pressure. After purification by flash column chromatography (heptane:EtOAc 3:1) the reaction yielded 0.42 g (11 %) of the *para*-positioned product **4b** as a white solid. In addition, 0.96 g (25 %) starting material was recovered from the reaction.

¹H NMR(400 MHz, CDCl₃)δ: 9.81(s, 1H), 7.45(d, J = 2.1 Hz, 1H), 7.38-7.42(m, 6H), 7.02(d, J = 8.27 Hz, 1H), 5.19(s, 2H) ppm

¹³C NMR(100 MHz, CDCl₃)δ: 191.0, 151.0, 146.4, 135.3, 130.8, 127.9(2C), 124.4, 114.5, 111.6, 77.4, 77.1, 76.8, 71.3 ppm

HRMS (ESI) m/z: [M + H]⁺ calculated for C₁₄H₁₃O₃: 229.0820, found 229.0859

Synthesis of 4-(hexyloxy)-3-hydroxybenzaldehyde (4c)

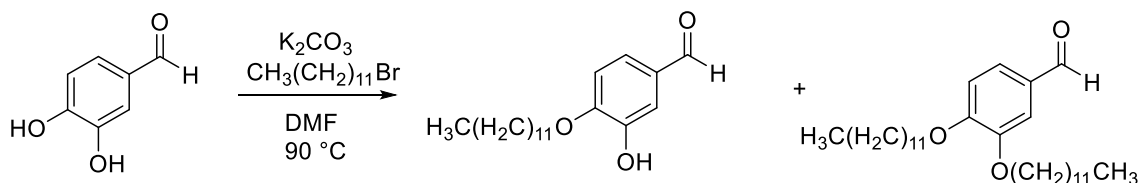
To a suspension of 3,4-dihydroxybenzaldehyde (1.00 g, 7.24 mmol) in DMF (10 ml), K_2CO_3 (0.88 g, 6.37 mmol) and 1-iodohexane (1.07 ml, 7.24 mmol) was added. The reaction mixture was stirred at 90 °C for 24 hours. Upon reaction completion, water (60 ml) was added to the DMF and decanted off the solid carbonate. The water phase was extracted with EtOAc (4x40 ml) and the combined organic phase was extracted with brine, dried over MgSO_4 and concentrated under reduced pressure. Purification by flash column chromatography (Heptane:EtOAc 7:1) yielded 1.166 g (73 %) of the pure *para*-positioned product **4c** as white crystals.

^1H NMR(400 MHz, CDCl_3) δ : 9.83(s, 1H), 7.40-7.44(m, 2H), 6.95(d, $J = 8.04$ Hz, 1H), 5.87(s, 1H), 4.13(t, 2H), 1.86(p, 2H), 1.33-1.49(m, 6H), 0.86-0.93(m, 3H) ppm

^{13}C NMR(100 MHz, CDCl_3) δ : 191.0, 151.3, 146.2, 130.4, 124.5, 114.0, 110.9, 69.3, 31.5, 29.0, 25.6, 22.6, 14.1 ppm

HRMS (ESI) m/z : $[\text{M} + \text{H}]^+$ calculated for $\text{C}_{13}\text{H}_{19}\text{O}_3$: 223.1289, found 223.1329

Synthesis of 4-(dodecyloxy)-3-hydroxybenzaldehyde (**4d**)/ 3,4-bis(dodecyloxy)benzaldehyde (**4e**)



Entry	Base (eq)	Time (h)	Total yield	Yield 4d	Yield 4e
1	1	26	95 %	51 %	18 %
2	0.88	30	87 %	63 %	24 %

To a suspension of 3,4-dihydroxybenzaldehyde (2.00 g, 14.48 mmol) in DMF (25 ml), K_2CO_3 (2.00 g, 14.48 mmol) and 1-bromododecane (3.48 ml, 14.48 mmol) was added. The reaction mixture was stirred at 90 °C for 26 hours. Upon reaction completion, water (125 ml) was added to the DMF and the residues were dissolved in Et_2O . The water phase was extracted with $EtOAc$ (4x50 ml) and the combined organic phases were extracted with brine, dried over $MgSO_4$ and concentrated under reduced pressure. Purification by flash column chromatography (5 % to 10 % $EtOAc$ /heptane) yielded 2.259 g (51 %) of the pure *para*-positioned product **4d** as white crystals. In addition 0.817 g (18.4 %) of the pure double substituted product **4e** was isolated and 1.121 g (25.3 %) of a *para*-/*meta*-substituted product mixture.

NMR values for the pure para-substituted product:

1H NMR(400 MHz, $CDCl_3$) δ : 9.83(s, 1H), 7.40-7.44(m, 2H), 6.95(d, $J = 8.16$ Hz, 1H), 5.82(s, 1H), 4.13(t, 2H), 1.86(p, 2H), 1.47(p, 2H), 1.27(s, 16H), 0.88(t, 3H) ppm

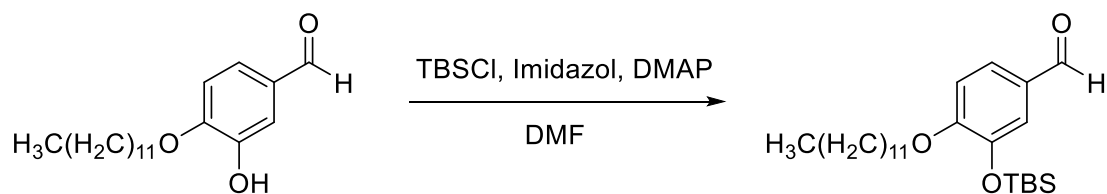
^{13}C NMR(100 MHz, $CDCl_3$) δ : 191.0, 151.3, 146.2, 130.5, 124.5, 114.1, 110.9, 69.2, 31.9, 29.6 (4C), 29.3 (2C), 29.0, 25.9, 22.4, 14.1 ppm

NMR values for the pure double substituted product:

1H NMR(400 MHz, $CDCl_3$) δ : 9.83(s, 1H), 7.38-7.42(m, 2H), 6.94(d, $J = 8.2$ Hz, 1H), 4.02-4.09(m, 4H), 1.81-1.88(m, 4H), 1.43-1.52(m, 4H), 1.26(s, 32H), 0.88(t, 6H) ppm

^{13}C NMR(100 MHz, $CDCl_3$) δ : 190.9, 154.7, 149.5, 129.9, 126.6, 111.8, 111.0, 69.1(2C), 31.9(2C), 29.7(10C), 29.4(2C), 29.1, 29.0, 26.0(2C), 22.7(2C), 14.1(2C) ppm

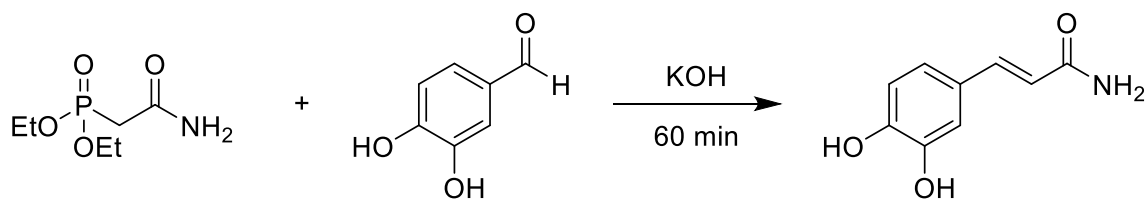
HRMS (ESI) m/z : $[M + H]^+$ calculated for $C_{19}H_{31}O_3$ (**4d**): 307.2228, found 307.2268 (**4e** is submitted for MS-analysis)

Synthesis of 3-((*tert*-butyldimethylsilyl)oxy)-4-(dodecyloxy)benzaldehyde (4f)

To a solution of compound **4d** (1.2 g, 3.92 mmol) in DMF(15.0 ml), imidazole (0.67 g, 9.79 mmol), DMAP (0.05 g, 0.39 mmol), and TBSCl (0.89 g, 5.88 mmol) were added. The solution was stirred at room temperature for 2 hours. Upon reaction completion the reaction mixture was extracted with heptane (3x30 ml) and the combined organic phase was washed with brine and dried over MgSO₄. The remaining solvent was removed under reduced pressure. The reaction produced 1.562 g (95 %) of **4f** as a yellow oil.

¹H NMR(400 MHz, CDCl₃)δ: 7.44(d, J = 9.05 Hz, 1 H), 7.35(t, 1H), 6.93(d, J = 9.05 Hz, 1H), 4.02(t, 2H), 1.84(p, 2H), 1.48(p, 2H), 1.26(s, 16H), 1.02(s, 9H), 0.86-0.91(m, 3H), 0.18(s, 6H) ppm

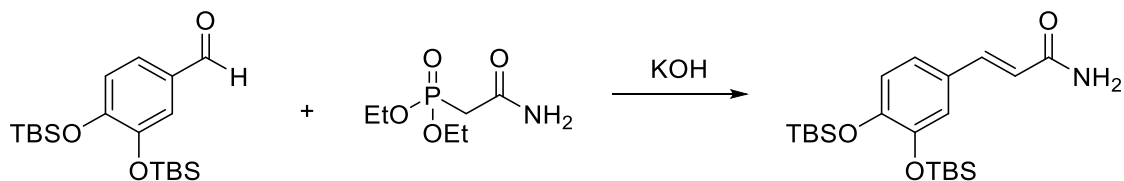
¹³C NMR(100 MHz, CDCl₃)δ: 190.1, 162.5, 156.4, 145.5, 129.9, 126.4, 120.0, 111.8, 68.8, 31.9, 29.6(4C), 29.3(2C), 29.2, 26.0, 25.6(4C), 22.7, 14.1, -4.6(2C) ppm

Synthesis of (*E*)-3-(3,4-dihydroxyphenyl)acrylamide (5a)

Entry	3 (g)	Solvent	KOH (g)	Time (min)	Yield
1	0.071	Et ₂ O	0.082	60	Nr
2	0.071	THF	0.082	60	Nr

Diethyl (2-amino-2-oxoethyl)phosphonate (**3**) (0.071 g, 0.362 mmol) and 3,4-dihydroxy benzaldehyde (0.05 g, 0.362 mmol) were dissolved in THF (1.5 ml) and added to a solution of powdered KOH (0.082 g, 1.448 mmol) dissolved in THF (0.5 ml). The reaction was stirred for 60 min at room temperature. No reaction according to TLC.

Synthesis of (*E*)-3-(3,4-bis(*tert*-butyldimethylsilyloxy)phenyl)acrylamide (**5b**)



Entry	4a	Experimental procedure	Base	Time (min)	Yield (%)
1	0.2	1 [58]	KOH	60	25
2	0.5	2	KOH	90	36
3	0.5	3	NaH	60	51

Experimental procedure 1

Diethyl (2-amino-2-oxoethyl)phosphonate (**3**) (0.107 g, 0.546 mmol) and 3,4-bis(*tert*-butyldimethylsilyloxy)benzaldehyde (**4a**) (0.2 g, 0.546 mmol) were dissolved in THF (1.5 ml) and added to a solution of powdered KOH (0.061 g, 1.091 mmol) dissolved in THF (0.5 ml). The reaction was stirred for 60 min at room temperature. The solvent was evaporated under reduced pressure and the crude product was washed with cold water (3x2 ml). The water was decanted and the product was purified using flash chromatography and vacuum dried for 5 hours. The reaction gave 0.055 g (25 %) of **5b**.

Experimental procedure 2

Diethyl (2-amino-2-oxoethyl)phosphonate (**3**) (0.27 g, 1.364 mmol) and 3,4-bis(*tert*-butyldimethylsilyloxy)benzaldehyde (**4a**) (0.5 g, 1.364 mmol) were dissolved in THF (4.5 ml) and added to a solution of powdered KOH (0.153 g, 2.73 mmol) dissolved in THF (1.5 ml). The reaction was stirred for 90 min at room temperature. The solvent was evaporated under reduced pressure and the product dissolved in acetone. Silica gel was added and the product was purified using flash chromatography. The reaction gave 0.203 g (36 %) of **5b**.

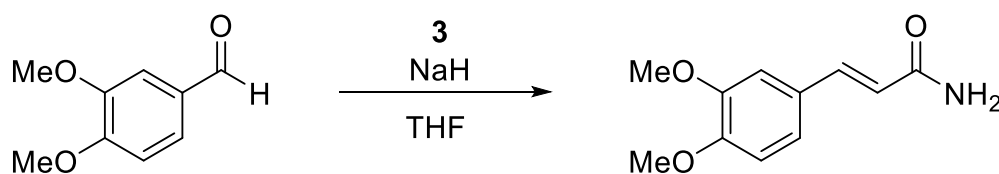
Experimental procedure 3

Diethyl (2-amino-2-oxoethyl)phosphonate (**3**) (0.319 g, 1.63 mmol) was dissolved in THF (4 ml) and stirred at room temperature for 2 min. NaH (65 mg, 2.70 mmol) was added and the solution was stirred for 15 min. 3,4-bis((*tert*-butyldimethylsilyl)oxy)benzaldehyde (**4a**) (0.45 g, 1.23 mmol) was dissolved in THF (4 ml) and added slowly. The reaction was stirred at room temperature for 60 min. After reaction completion the solvent was removed under reduced pressure. The residue was dissolved in EtOAc and extracted with water (3x30 ml). The combined organic solution was dried over MgSO₄ and the remaining solvent removed under reduced pressure. The reaction gave 0.254 g (51 %) of **5b**.

¹H-NMR (400 MHz, DMSO-d₆)δ: 7.45 (s, 2 H), 7.28 (d, J = 15.7 Hz, 1 H), 6.75-7.05 (m, 3 H), 6.38 (d, J = 15.7 Hz, 1 H), 0.82-0.94 (m, 18 H), -0.11-0.19 (m, 12 H) ppm

¹³C-NMR (100 MHz, DMSO-d₆)δ: 167.3, 148.1, 146.9, 139.3, 129.2, 122.3, 121.5, 120.8, 119.9, 26.1(6C), 18.6(2C), -3.8(4C) ppm

HRMS (ESI) m/z: [M + H]⁺ calculated for C₂₁H₃₈NO₃Si₂: 408.2346, found 408.2387

Synthesis of (*E*)-3-(3,4-dimethoxyphenyl)acrylamide (5c**)**

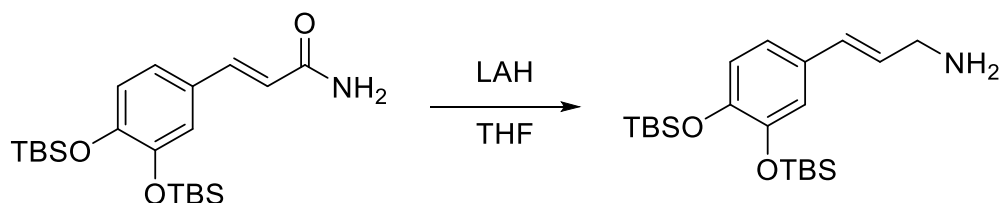
Entry	Compound 3 (g)	Time (min)	Yield
1	0.94	60	99 %
2	0.76	20	99 %

3,4-dimethoxybenzaldehyde (0.60 g, 3.61 mmol) was dissolved in THF (5 ml) and stirred at room temperature for 5 min. Diethyl (2-amino-2-oxoethyl)phosphonate (**3**) (0.94 g, 4.8 mmol) was dissolved in THF (6 ml) and added to the aldehyde solution. NaH (0.32 g, 7.9 mmol) was added slowly and the reaction was stirred at room temperature for 1 h. After reaction completion the solvent was removed under reduced pressure. The product was dissolved in EtOAc and residues dissolve in water. The solution was extracted with EtOAc (3x35ml). The combined organic solution was dried over MgSO₄ and the remaining solvent removed under reduced pressure. The reaction gave 0.741 g (99 %) of **5c** as a white solid.

¹H NMR(400 MHz, CDCl₃)δ: 7.58(d, J = 15.8 Hz, 1H), 7.08-7.11(m, 1H), 7.04(s, 1H), 6.85(d, J = 9.4 Hz, 1H), 6.34(d, J = 15.8 Hz, 1H), 5.67(s, 2H), 3.91 (s, 6H) ppm

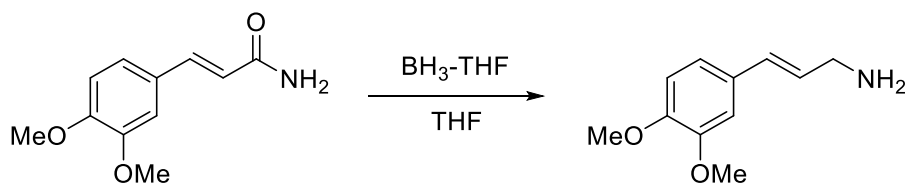
¹³C NMR(100 MHz, CDCl₃)δ: 168.1, 150.9, 149.2, 142.4, 127.5, 122.3, 117.3, 111.1, 109.7, 55.9(2C) ppm

HRMS (ESI) m/z: [M + H]⁺ calculated for C₁₁H₁₄NO₃: 208.0929, found 208.0967

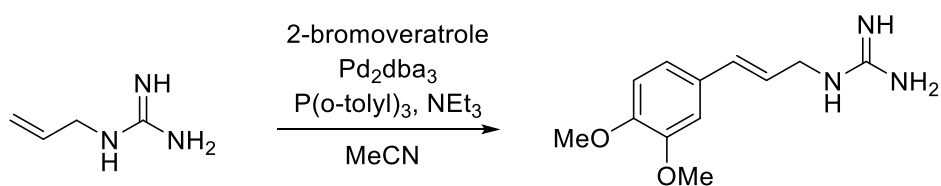
Synthesis of (*E*)-3-(3,4-bis(*tert*-butyldimethylsilyloxy)phenyl)prop-2-en-1-amine (6a)

(*E*)-3-(3,4-bis(*tert*-butyldimethylsilyloxy)phenyl)acrylamide (**5b**) (0.203 g, 0.50 mmol) was added to THF (5 ml), stirred for 2 minutes and added to a solution of LAH (0.057 g, 1.49 mmol) in THF (12 ml) at 0 °C. The solution was warmed to room temperature and stirred for 20 hours. Upon reaction completion, the reaction was cooled to 0 °C and quenched with water. The solution was filtered over celite and washed with hot THF. THF was removed under reduced pressure and the product was dissolved in EtOAc (15 ml) and washed with HCl (1 M, 3x10 ml) at 0 °C. The water phase was basified with NaOH (6 M) to a pH of 12. The solution was extracted with EtOAc (3x15 ml) and the combined organic phase was washed with brine, dried over MgSO₄ and concentrated.

No reaction according to NMR.

Synthesis of (*E*)-3-(3,4-dimethoxyphenyl)prop-2-en-1-amine (6b)

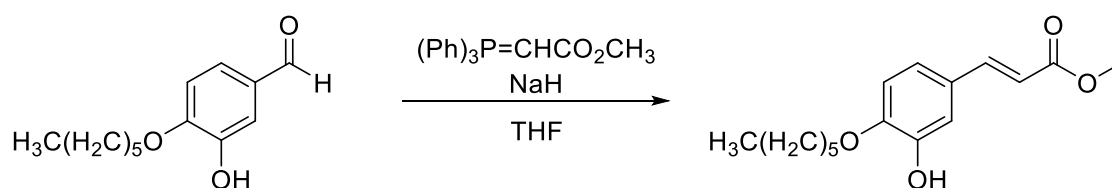
To a solution of compound 5c (0.2 g, 0.97 mmol) dissolved in THF (2.5 ml) was added BH₃-THF 1 M solution (1.93 ml, 1.93 mmol). The reaction was stirred at reflux under N₂ atmosphere for 3 hours and then cooled to room temperature. Anhydrous MeOH (1 ml) was added and reflux was resumed for 20 minutes. The solvents were evaporated under reduced pressure and the residues dissolved in DCM and washed with water (3x5 ml). The organic phase was dried over MgSO₄ and concentrated. No reaction according to NMR.

Synthesis of (*E*)-1-(3-(3,4-dimethoxyphenyl)allyl)guanidine (7a**)**

NEt₃ (5 ml) and MeCN (5 ml) were degassed individually two times (vacuum/N₂) and cooled with liquid nitrogen. Allylguanidine was degassed on vacuum. MeCN (0.8 ml) was added to Pd₂dba₃ (60 mg, 65.6 μmole) and *p*-(*o*-tolyl)₃ (40 mg, 0.13 mmol) and stirred for 5 min. 4-bromoveratrole (0.09 ml, 0.65 mmol) was added and stirred for 2 min. Allyl guanidine (100 mg, 0.74 mmol) and MeCN (1.2 ml) were added and stirred for 2 min. NEt₃ (0.18 ml, 1.29 mmol) was added and the solution was stirred at 80 °C under N₂-atmosphere for 18 hours.

EtOAc (20 ml) was added and the solution was filtered under vacuum. The EtOAc phase was removed and the solids were filtered with water (40 ml). The water phase was purified with reverse flash column chromatography (5 % to 100 % MeOH in H₂O).

*NMR analysis indicated a mixture of starting material, impurities and product after flash column chromatography. Calculated yield of product from ¹H-NMR integrals corresponds to approximately 7.9 % of product **7a**.*

Synthesis of methyl (*E*)-3-(4-(hexyloxy)-3-hydroxyphenyl)acrylate (8a**)**

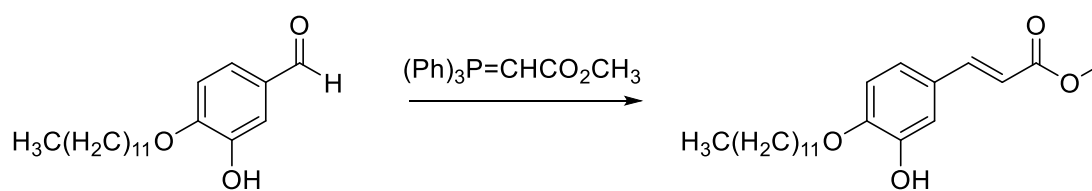
To a suspension of 4-(hexyloxy)-3-hydroxybenzaldehyde (**4c**) (0.90 g, 4.05 mmol) in THF (35 ml), methyl (triphenylphosphoranylidene)acetate (1.63 g, 4.86 mmol) was added. NaH (0.15 g, 6.08 mmol) was added at 0 °C and the reaction was stirred at 65 °C for 60 h. Upon reaction completion, water (40 ml) was added and the product was extracted with Et₂O (3x40 ml). The combined organic phase was washed with brine, dried over MgSO₄ and concentrated under reduced pressure. The product was purified with flash column chromatography (heptane:EtOAc, 7:1). The reaction produced 56.5 % of the product and 43.5 % starting material in a mixture not separable by flash chromatography. Yields are calculated from NMR integrals.

H_P = Proton signal from product, H_R = Proton signal from reactant

¹H NMR(400 MHz, CDCl₃)δ: 9.84 (s, 1H, 1H_R), 7.60(d, J = 15.8 Hz, 1H, 1H_P), 7.39-7.44(m, 2H, 2H_R), 7.13(s, 1H, 1H_P), 6.99-7.02(m, 1H, 1H_P), 6.94(d, J = 8.04 Hz, 1H, 1H_R), 6.82(d, J = 8.04 Hz, 1H, 1H_P), 6.28(d, J = 15.8 Hz, 1H, 1H_P), 5.78(s, 1H, 1H_R), 5.69(s, 1H, 1H_P), 4.13(t, 2H, 2H_R), 4.07(t, 2H, 2H_P), 3.79(s, 3H, 3H_P), 1.81-1.87(m, 4H, 2H_P + 2H_R), 1.34-1.48(m, 12H, 6H_P + 6H_R), 0.91(s, 6H, 3H_P + 3H_R) ppm

C_P = Carbon signal from product, C_R = Carbon signal from reactant

¹³C NMR(100 MHz, CDCl₃)δ: 191.0(C_R), 167.7(C_P), 151.3(C_R), 147.9(C_R), 146.2(C_P), 146.0(C_P), 144.7(C_P), 130.5(C_R), 127.8(C_P), 124.5(C_R), 121.8(C_P), 115.7(C_R), 114.1(C_P), 112.9(C_R), 111.3(C_P), 110.8(C_P), 69.3(C_R), 69.1(C_P), 51.6(C_P), 31.5(1C_P+1C_R), 29.0(1C_P+1C_R), 25.6(1C_P+1C_R), 22.6(1C_P+1C_R), 14.0(1C_P+1C_R) ppm

Synthesis of methyl (*E*)-3-(4-(dodecyloxy)-3-hydroxyphenyl)acrylate (8b**)**

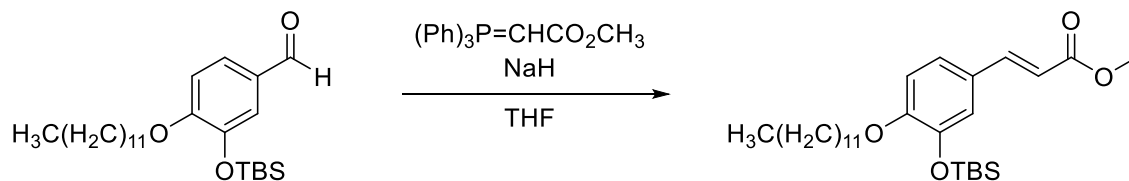
Entry	Base (eq)	Solvent	Time	Yield
1	NaH (2.5)	THF	40	Traces
2	NaH (3.0)	THF	30	Traces
3	-	Toluene	44	100 %

To a suspension of 4-(dodecyl)-3-hydroxybenzaldehyde (**4d**) (1.00 g, 3.27 mmol) in toluene (15 ml), methyl (triphenylphosphoranylidene)acetate (1.31 g, 3.92 mmol) was added. The reaction was stirred at room temperature under N₂ atmosphere for 44 h. Upon reaction completion, toluene was removed under reduced pressure. The product was purified with flash column chromatography (11 % to 20 % EtOAc:heptane). The reaction produced 1.18 g (100 %) of **8b** as a white solid.

¹H NMR(400 MHz, CDCl₃)δ: 7.59(d, J = 15.9 Hz, 1H), 7.13(s, 1H), 7.00(d, J = 9.9 Hz, 1H), 6.82(d, J = 8.5 Hz, 1H), 6.28(d, J = 15.9 Hz, 1H), 5.67(s, 1H), 4.07(t, 2H), 3.79(s, 3H), 1.83(p, 2H), 1.45(p, 2H), 1.26(s, 16H), 0.88 (t, 3H) ppm

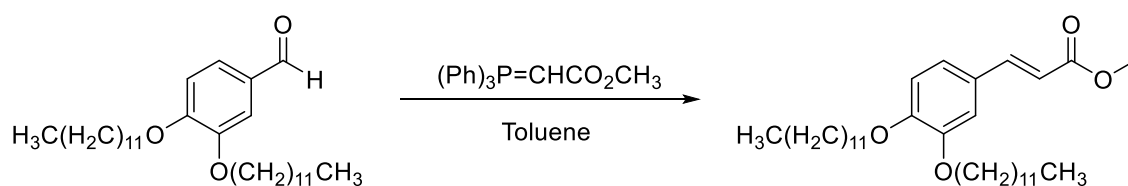
¹³C NMR(100 MHz, CDCl₃)δ: 167.7, 148.0, 146.0, 144.7, 127.8, 121.8, 115.7, 112.9, 111.3, 69.0, 51.6, 31.9, 29.64(2C), 29.57(2C), 29.5, 29.3, 29.1, 26.0, 22.7, 14.1 ppm

HRMS (ESI) m/z: [M + Na]⁺ calculated for C₂₂H₃₄NaO₄: 385.2355, found 385.2349

Synthesis of methyl (*E*)-3-(3-((*tert*-butyldimethylsilyl)oxy)-4-(dodecyloxy)phenyl)acrylate (8c**)**

To a suspension of 4-(hexyloxy)-3-hydroxybenzaldehyde (**4e**) (1.50 g, 3.57 mmol) in THF (50 ml), methyl (triphenylphosphoranylidene)acetate (1.43 g, 4.28 mmol) was added. NaH (0.13 g, 4.90 mmol) was added at 0 °C and the reaction was stirred at 65 °C for 40 h. Upon reaction completion, water (50 ml) was added and the product was extracted with Et₂O (3x50 ml). The combined organic phase was washed with brine, dried over MgSO₄ and concentrated under reduced pressure.

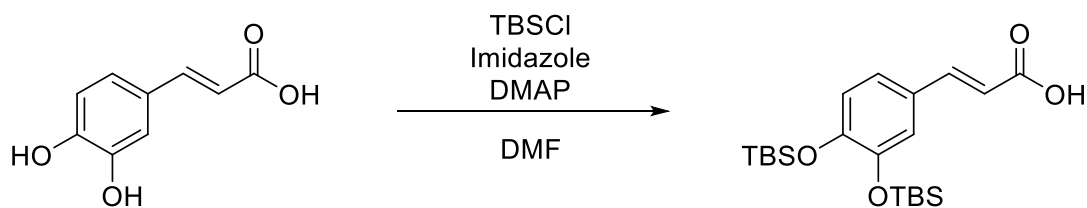
The product was purified with flash column chromatography (heptane:EtOAc, 8:1). The reaction produced 0.847 g (50 %) of **8b** as a white solid. *From NMR it was clear that the protecting silyl group was not present in the product. Thus, the reaction produced 50 % of 8c.*

Synthesis of methyl (*E*)-3-(3,4-bis(dodecyloxy)phenyl)acrylate (8d**)**

To a suspension of compound **4e** (0.55 g, 1.16 mmol) in toluene (10 ml), methyl (triphenylphosphoranylidene)acetate (0.47 g, 1.39 mmol) was added. The reaction was stirred at room temperature under N₂ atmosphere for 100 h. Upon reaction completion, toluene was removed under reduced pressure. The product was purified with flash column chromatography (heptane:EtOAc 7:1). The reaction produced 0.61 g (100 %) of **8d** as a white solid.

¹H NMR(400 MHz, CDCl₃)δ: 7.62(d, J = 15.9 Hz, 1H), 7.08-7.03(m, 2H), 6.85(d, J = 8.3 Hz, 1H), 6.29(d, J = 15.9 Hz, 1H), 4.04-3.98(m, 4H), 3.79(s, 3H), 1.82(p, 4H), 1.51-1.41(m, 4H), 1.26(s, br, 32H), 0.88(t, 6H) ppm

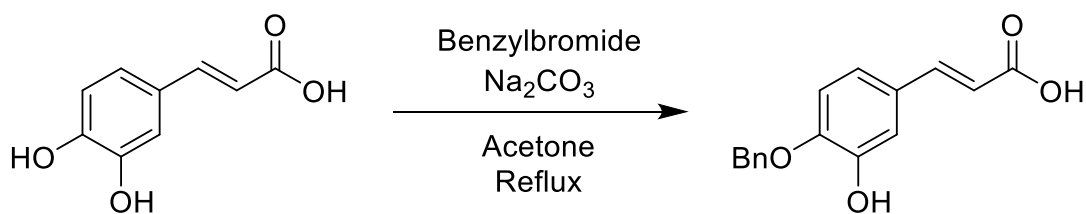
¹³C NMR(100 MHz, CDCl₃)δ: 167.8, 151.4, 149.2, 145.0, 127.2, 122.6, 115.2, 113.0, 112.3, 69.3, 69.1, 51.6, 31.9(2C), 29.6(6C), 29.3(4C), 29.2, 29.1, 26.0(2C), 22.7(2C), 14.1(2C) ppm

Synthesis of (*E*)-3-(3,4-bis(*tert*-butyldimethylsilyloxy)phenyl)acrylic acid (9a**)**

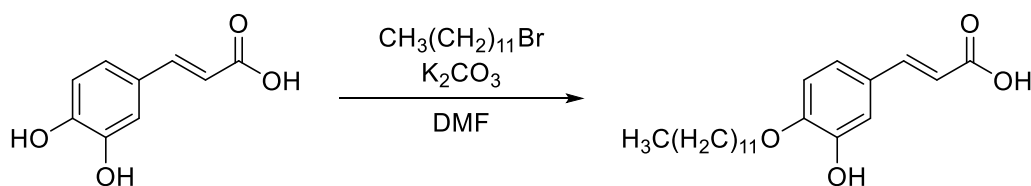
To a solution of caffeic acid (0.996 g, 5.53 mmol) in 12.0 ml DMF, imidazole (1.13 g, 16.59 mmol), DMAP (0.068 g, 0.53 mmol), and TBSCl (2.5 g, 16.59 mmol) were added. The solution was stirred at room temperature for 20 hours. The reaction mixture was extracted with PE (3x15 ml) and the combined organic solution was dried over MgSO₄. The remaining solvent was removed under reduced pressure. The final product was vacuum dried for 8 hours to produce 2.03 g (90 %) of **9a** as a pale oil.

¹H NMR(400 MHz, CDCl₃)δ: 7.65(d, J = 15.8 Hz, 1H), 7.03(s, 2H), 6.79-6.86(m, 1H), 6.24(d, J = 15.8 Hz, 1H), 0.98(s, 18H), 0.21(s, 12H) ppm

¹³C-NMR (100 MHz, CDCl₃)δ: 172.8, 149.9, 147.3, 147.1, 127.7, 122.7, 121.2, 120.6, 114.8, 25.9(6C), 18.5(2C), -4.0 (4C) ppm

Synthesis of (*E*)-3-(4-(benzyloxy)-3-hydroxyphenyl)acrylic acid (9b)

Caffeic acid (2.00 g, 11.1 mmol) was dissolved in acetone (40 ml) and stirred at room temperature for 1 min. Benzylbromide (1.45 ml, 12.2 mmol), sodium carbonate (2.36 g, 22.2 mmol) and catalytic amounts of I_2 were added to the solution. The reaction was refluxed for 30 h. Upon reaction completion the solvent was removed under reduced pressure and the product dissolved in EtOAc (40 ml). The EtOAc was washed with 0.5 M HCl (3x40 ml) and concentrated. The product was purified using flash chromatography (PE:EtOAc 4:1). No reaction according to NMR. Benzylbromide recovered.

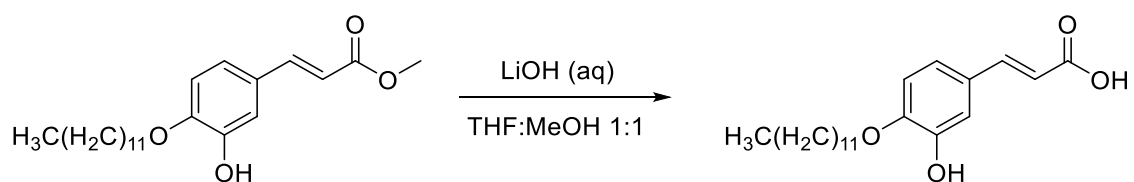
Synthesis of (*E*)-3-(4-(dodecyloxy)-3-hydroxyphenyl)acrylic acid (9c**)**

Caffeic acid (1.5 g, 8.33 mmol) and potassium carbonate (1.73 g, 12.49 mmol) was dissolved in DMF (20 ml) and stirred for 10 minutes. 1-Bromododecane (1.8 ml, 7.33 mmol) was added and the solution was stirred at 90 °C for 40 hours. Upon reaction completion the solution was acidified by 0.5 M HCl and extracted with heptane (3x30 ml). The product was purified by flash column chromatography (11 % to 25 % EtOAc in heptane) and produced 67 % of the pure double substituted product. Thus, the desired product **9c** was not produced in the reaction.

NMR for the pure double substituted product:

¹H NMR(400 MHz, CDCl₃)δ: 7.58 (d, J = 15.9 Hz, 1H), 7.13 (s, 1H), 7.00 (dd, J₁ = 2.1 Hz, J₂ = 8.4 Hz, 1H), 6.82(d, J = 8.4 Hz, 1H), 6.28(d, J = 15.9 Hz, 1H), 5.67(s, 1H), 4.18(t, 2H), 4.07 (t, 2H), 1.82(p, 2H), 1.69(p, 2H), 1.45 (p, 4H), 1.26 (s, 32H), 0.88(t, 6H) ppm

¹³C-NMR (100 MHz, CDCl₃)δ: 167.4, 147.9, 145.9, 144.4, 127.9, 121.7, 116.3, 112.9, 111.3, 69.0, 64.6, 31.9(2C), 29.6(12C), 29.3(2C), 26.0 (2C), 22.7(2C), 14.1 (2C) ppm

Synthesis of (*E*)-3-(4-(dodecyloxy)-3-hydroxyphenyl)acrylic acid (9c**)**

Entry	X (g)	Time (hours)	Yield (%)
1	0.200	21	100
2	0.925	7*	99

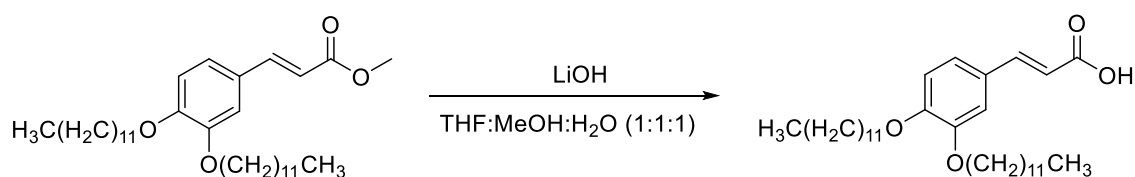
*50 °C throughout the entire reaction time

To a suspension of **8b** (0.2 g, 0.55 mmol) in THF:MeOH (10 ml, 1:1), a solution of LiOH (0.13 g, 5.5 mmol) in water (5 ml) was added. The yellow solution was stirred for 15 hours at room temperature and then an additional 4 hours at 50 °C. Upon reaction completion the product was acidified with 1 M HCl (40 ml), and extracted with EtOAc (3x40 ml). The combined organic phase was dried over MgSO₄, concentrated under reduced pressure and recrystallized from heptane. The reaction gave 192 mg (100 %) of **9c** as a white solid.

¹H NMR(400 MHz, CDCl₃)δ: 7.69(d, J = 15.8 Hz, 1H), 7.16(s, 1H), 7.04(dd, J₁ = 2.11 Hz, J₂ = 8.5 Hz, 1H), 6.84(d, J = 8.3 Hz, 1H), 6.29(d, J = 15.8 Hz, 1H), 5.68(s, br, 1H), 4.08(t, 2H), 1.83(p, 2H), 1.46(p, 2H), 1.26(s, 16H), 0.88(t, 3H) ppm

¹³C NMR(100 MHz, CDCl₃)δ: 148.3, 146.9, 146.0, 127.5, 122.2, 115.0, 113.2, 111.3, 69.1, 31.9, 29.6(6C), 29.3, 25.9, 22.7, 14.1 ppm

HRMS (ESI) m/z: [M + Na]⁺ calculated for C₂₁H₃₂NaO₄ 371.2198, found 371.2193

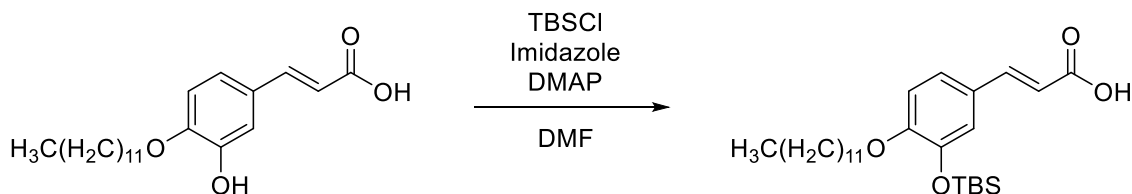
Synthesis of (*E*)-3-(3,4-bis(dodecyloxy)phenyl)acrylic acid (9d**)**

Compound **8d** (0.58 g, 1.09 mmol) was dissolved in THF:MeOH (1:1, 20 ml) and stirred for 2 min. LiOH (0.31 g, 13.12 mmol) in H₂O (10 ml) was added. The yellow solution was stirred at room temperature for 15 hours. Upon reaction completion, the solution was acidified by 1 M HCl (30 ml) and extracted with EtOAc (2x30 ml). The combined organic phase was concentrated under reduced pressure. The reaction produced 0.56 g (100 %) of **9d** as a white solid.

¹H NMR(400 MHz, CDCl₃)δ: 7.71(d, J = 15.9 Hz, 1H), 7.12-7.07(m, 2H), 6.86(d, J = 8.3 Hz, 1H), 6.29(d, J = 15.9 Hz, 1H), 4.04-3.99(m, 4H), 1.83(p, 4H), 1.52-1.42(m, 4H), 1.26(s, 32H), 0.88(t, 6H) ppm

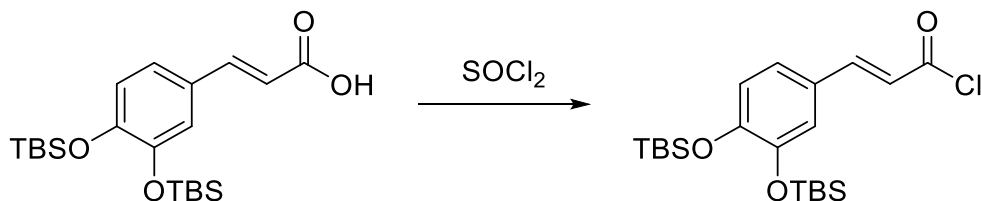
¹³C NMR(100 MHz, CDCl₃)δ: 171.5, 151.8, 149.2, 147.1, 126.9, 123.1, 114.3, 112.9, 112.4, 69.4, 69.0, 31.9(2C), 29.6(6C), 29.4(4C), 29.2, 29.1, 26.0, 25.9, 22.7(2C), 14.1(2C) ppm

Synthesis of (*E*)-3-(3-((*tert*-butyldimethylsilyl)oxy)-4-(dodecyloxy)phenyl)acrylic acid (**9e**)

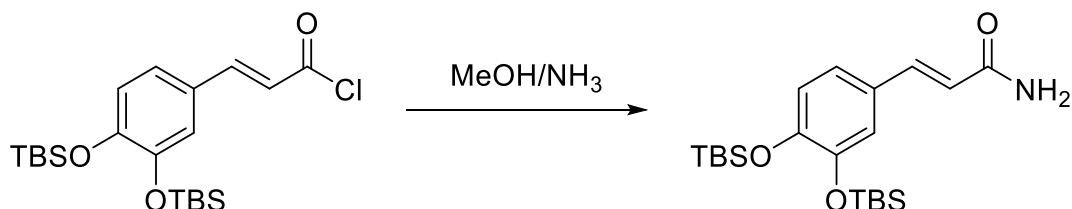


Entry	9c (g)	Time (h)	Yield
1	0.50	72	Traces
2	0.30	68	Traces

To a solution of compound **9c** (0.30 g, 0.98 mmol) in DMF (5 ml), imidazole (0.17 g, 2.45 mmol), DMAP (12 mg, 0.09 mmol), and TBSCl (0.22 g, 1.47 mmol) were added. The solution was stirred at room temperature for 68 hours. Water was added to the reaction (20 ml) and the reaction mixture was extracted with heptane (3x20 ml). The combined organic solution was dried over MgSO₄ and the solvent was removed under reduced pressure. According to TLC and NMR, the reaction produced only traces of the product.

Synthesis of (*E*)-3-(3,4-bis(*tert*-butyldimethylsilyloxy)phenyl) acryloyl chloride (10)

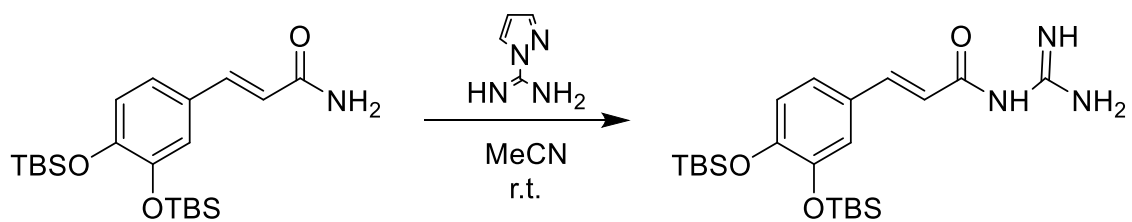
(*E*)-3-(3,4-bis(*tert*-butyldimethylsilyloxy)phenyl)acrylic acid **9a** (1.0 g, 2.45 mmol) was dissolved in SOCl₂ (10 ml) and stirred under reflux for 6.5 hours. The residue thionyl chloride was distilled off under reduced pressure and the product was utilized without any further purification.

Synthesis of (*E*)-3-(3,4-bis(*tert*-butyldimethylsilyloxy)phenyl) acrylamide (5b)

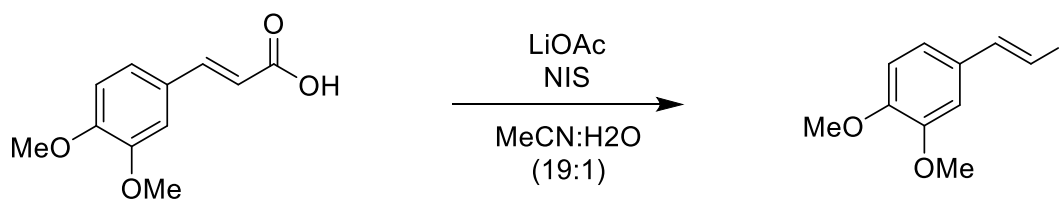
(*E*)-3-(3,4-bis(*tert*-butyldimethylsilyloxy)phenyl)acryloyl chloride (**10**) was dissolved in MeOH/NH₃ (2M, 10 ml) and stirred at room temperature over night. Volatiles were removed under reduced pressure and the residue was titrated with EtOAc. The product was purified with flash chromatography (PE:EtOAc 3:1). The reaction produced 0.423 g (42 %) of **5b**.

¹H NMR (400 MHz, CDCl₃) δ : 7.35(d, *J* = 15.8 Hz, 1H), 6.78(m, 2H), 6.60(d, *J* = 8.8 Hz, 1H), 6.02(d, *J* = 15.8 Hz, 1H), 0.77(s, 18H), 0.01(s, 12H) ppm

¹³C-NMR (100 MHz, CDCl₃) δ : 167.8, 149.5, 147.2, 144.9, 128.0, 122.3, 121.2, 120.4, 115.4, 38.7(2C), 25.9(6C), -4.1(4C) ppm

Synthesis of (*E*)-3-(3,4-bis(*tert*-butyldimethylsilyloxy)phenyl)-*N*-carbamimidoyl acrylamide

Compound **5b** (0.423 g, 1.039 mmol) and 1*H*-pyrazole-1-carboxamide hydrochloride (0.168 g, 1.143 mmol) were added to MeCN (5 ml) and stirred at room temperature for 48 h. The solvent was removed under reduced pressure and the precipitate was washed with MeCN and vacuum dried. No reaction according to NMR.

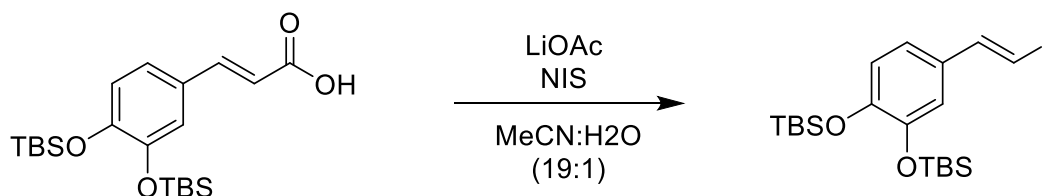
Synthesis of (*E*)-4-(2-iodovinyl)-1,2-dimethoxybenzene (11a)

To a solution of acrylic acid (1.5 g, 7.21 mmol) in MeCN:H₂O (19:1, 90 ml), LiOAc (95 mg, 1.44 mmol) and *N*-iodosuccinimide (1.62 g, 7.21 mmol) and were added. The solution was stirred at room temperature for 6 hours. Upon reaction completion the solvent was removed under reduced pressure. The product was purified with flash column chromatography (PE:EtOAc 5:1) and produced 1.88 g (90 %) of **11a** as a white solid. (The compound turned black after less than 24 hours).

¹H NMR(400 MHz, CDCl₃)δ: 7.35(d, J = 15.2 Hz, 1H), 6.79-6.86(m, 3H), 6.65(d, J = 15.2 Hz, 1H), 3.88(s, 6H) ppm

¹³C NMR(100 MHz, CDCl₃)δ: 149.5, 149.1, 144.6, 131.0, 119.4, 111.0, 108.4, 73.6, 55.9 (2C) ppm

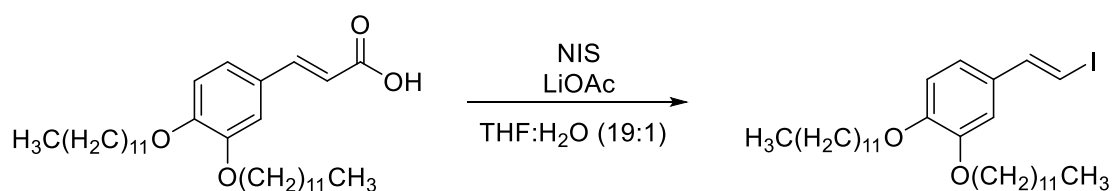
HRMS (ESI) m/z: [M + Na]⁺ calculated for C₁₀H₁₁INaO₂ 312.9701, found 312.9699

Synthesis of (*E*)-((4-(2-iodovinyl)-1,2-phenylene)bis(oxy))bis(*tert*-butyldimethyl silane) (11b**)**

To a solution of acrylic acid (**9a**) (0.88 g, 2.16 mmol) in MeCN:H₂O (19:1, 40 ml), LiOAc (284 mg, 0.43 mmol) and *N*-iodosuccinimide (485 mg, 2.16 mmol) were added. The solution was stirred at room temperature for 5 hours. Upon reaction completion, sodium thiosulphate was added (2 drops) and the solvent was removed under reduced pressure. The product was purified with flash column chromatography (2 % EtOAc in PE). The reaction gave 849 mg (80 %) of **11b** as a yellow oil.

¹H NMR(400 MHz, CDCl₃)δ: 7.30(d, J = 14.9 Hz, 1H), 6.75-6.80(m, 3H), 6.58(d, J = 14.9 Hz, 1H), 1.01(s, 18H), 0.22(s, 12H) ppm

¹³C NMR(100 MHz, CDCl₃)δ: 147.6, 147.0, 144.5, 131.5, 121.1, 119.6, 118.6, 73.7, 25.9(6C), 18.5(2C), -4.0 (4C) ppm

Synthesis of (*E*)-1,2-bis(dodecyloxy)-4-(2-iodovinyl)benzene (11c**)**

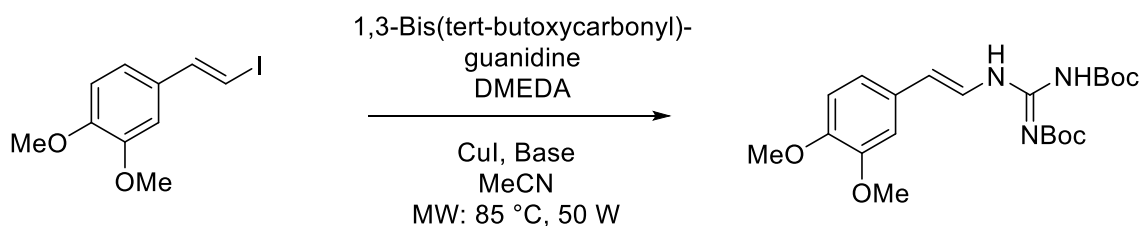
To a solution of compound **9e** (0.56 g, 1.09 mmol) in THF:H₂O (19:1, 40 ml), LiOAc (14 mg, 0.22 mmol) was added. The solution was stirred for 5 min before N-Iodosuccinimide (0.25 g, 1.09 mmol) was added. The reaction was stirred at room temperature for 14 hours. Upon reaction completion, saturated Na₂SO₃ (3 drops) was added and the solvent was removed under reduced pressure. The product was purified by flash column chromatography (heptane:EtOAc, 9:1) and gave 0.42 g (65 %) of **11c** as a yellow solid.

¹H NMR(400 MHz, CDCl₃)δ: 7.32(d, J = 14.9 Hz, 1H), 6.83(s, 1H), 6.80(s, 2H), 6.61(d, = 14.9 Hz, 1H), 3.98(t, 4H), 1.76-1.86(m, 4H), 1.41-1.50(m, 4H), 1.26(s, br, 32H), 0.88(t, 6H) ppm

¹³C NMR(100 MHz, CDCl₃)δ: 149.7, 149.2, 144.7, 130.9, 119.5, 113.4, 111.1, 73.6, 69.4, 69.2, 31.9(2C), 29.6(10C), 29.42, 29.37, 29.3, 29.2, 26.0(2C), 22.7(2C), 14.1(2C) ppm

(Sample is submitted for MS-analysis)

Synthesis of (Z)-1-((E)-3,4-dimethoxystyryl)-2,3-bis(tert-butoxycarbonyl)guanidine (12a)



A vial filled with 1,3-Bis(tert-butoxycarbonyl)guanidine (80 mg, 0.309 mmol), compound **11a** (58 mg, 0.2 mmol), potassium *tert*-butoxide (46 mg, 0.41 mmol), CuI (43 mg, 0.23 mmol), was evacuated and backfilled with nitrogen three times. DMEDA (50 μ l, 0.46 mmol) and MeCN (1.5 ml) were added and the blue mixture was heated in a microwave oven (85 °C, 50 W) for 35 min. The product was purified by flash column chromatography (heptane:EtOAc 5:1) and vacuum dried for 6 hours. The reaction produced 56 mg (67 %) of **12a** as a white oil.

Entry	Base	11a (mg)	MW	Yield
1	Potassium phosphate (K ₃ PO ₄)	58	65 °C, 50 W	49 %
2	1,5-diazabicyclo[4.3.0]non-5-ene	58	65 °C, 50 W	Nr
3	1,5-diazabicyclo[4.3.0]non-5-ene	58	65 °C, 50 W	Nr
4	Potassium <i>tert</i> -butoxide ((CH ₃) ₃ COK)	58	65 °C, 50 W	- ^a
5	Potassium <i>tert</i> -butoxide ((CH ₃) ₃ COK)	58	65 °C, 50 W	59 %
6	Potassium <i>tert</i> -butoxide ((CH ₃) ₃ COK)	58	85 °C, 50 W	67 %
7	Potassium <i>tert</i> -butoxide ((CH ₃) ₃ COK)	58	85 °C, 50 W	66 %
8	Potassium <i>tert</i> -butoxide ((CH ₃) ₃ COK)	58	100 °C, 50 W	- ^b
9	Potassium <i>tert</i> -butoxide ((CH ₃) ₃ COK)	150	85 °C, 100 W	≈ 20 % ^c
10	Potassium <i>tert</i> -butoxide ((CH ₃) ₃ COK)	150	85 °C, 90 W	≈ 10 % ^c

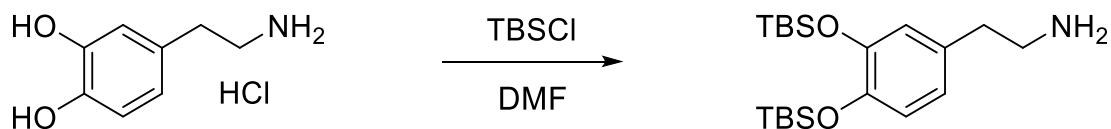
a: Compound decomposed over night b: Chemicals decomposed during reaction c: Not isolated

¹H NMR(400 MHz, CDCl₃) δ : 7.04(d, J = 14.6 Hz, 1H), 6.89-6.94(m, 2H), 6.83(d, J = 8.9 Hz, 1H), 6.35(d, J = 14.6 Hz, 1H), 3.90(s, 3H), 3.89(s, 3H) 1.55(s, 9H), 1.49(s, 9H) ppm

¹³C NMR(100 MHz, CDCl₃) δ :158.3, 152.3, 149.2, 148.4, 129.2, 124.8, 120.1, 118.7, 111.4, 108.6, 82.3, 56.0, 55.9, 28.3(2C), 28.1(4C) ppm

(Sample is submitted for MS-analysis)

Peaks at 0.88 and 1.26 in ¹H-NMR and 14.1, 22.7, 31.9 in ¹³C-NMR are due to minor oil impurities from alkane solvents.

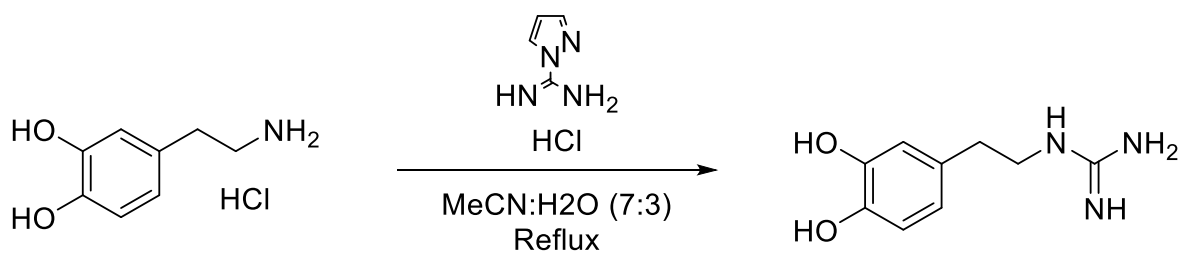
Synthesis of 2-(3,4-bis((*tert*-butyldimethylsilyl)oxy)phenyl)ethane-1-amine (14)

Dopamine hydrochloride (0.84 g, 4.42 mmol) was dissolved in DMF (11 ml) and stirred for 5 min. TBSCl (2.00 g, 13.27 mmol), imidazole (0.90 g, 13.27 mmol) and DMAP (0.054 g, 0.44 mmol) were added and the reaction was stirred at room temperature for 25 hours. After reaction completion, water (30 ml) was added and extracted with PE (3x30 ml). Solids were filtered from the oil and the product was dried over anhydrous MgSO₄, concentrated under reduced pressure and dried under vacuum for 16 hours.

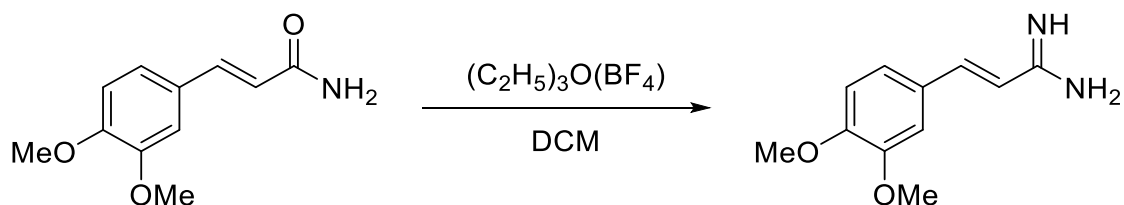
NMR and HR-MS indicated that compound 14 was not produced. Dopamine HCl was silylated according to the reaction, however a side reaction between Dopamine HCl and DMF gave the amide illustrated in figure 3.9. NMR-values for the produced amide is listed below:

¹H NMR(400 MHz, CDCl₃)δ: 8.13(s, 1H), 6.75(d, J = 7.9 Hz, 1H), 6.59-6.66(m, 2H), 5.50(s, br, 1H), 3.48-3.54(m, 2H), 2.70(t, 2H), 0.98(s, 18H), 0.18(s, 12H) ppm

¹³C NMR(100 MHz, CDCl₃)δ: 161.0, 146.9, 145.7, 131.4, 130.6, 121.6, 121.1, 39.3, 34.7, 25.9(6C), 18.4(2C), -4.0(4C) ppm

Synthesis of 1-(3,4-dihydroxyphenethyl)guanidine (16)

Dopamine hydrochloride (0.68 g, 3.59 mmol) was dissolved in MeCN:H₂O (7:3, 10 ml). 1*H*-pyrazole-1-carboxamide hydrochloride (0.53 g, 3.59 mmol) was added and the reaction was stirred at reflux for 48 hours. The dark product mixture was added Et₂O to induce precipitation. As the product did not precipitate, the solvent were removed under reduced pressure and the product was vacuum dried for 4 hours. No reaction according to NMR.

Synthesis of (*E*)-3-(3,4-dimethoxyphenyl)acrylimidamide (17**)**

Compound **5c** (0.30 g, 1.45 mmol) was dissolved in DCM (3 ml) and stirred at rt. for 5 min. Meerwein's reagent (0.36 g, 1.88 mmol) was dissolved in DCM (2 ml) and added to the suspension. The yellow solution was left stirring at room temperature over night under N₂-atmosphere. Anhydrous MeOH (1.5 ml) was added and gaseous ammonia bubbled through the solution for 2 hours. After disconnection from the ammonia supply, the reaction was stirred an additional 18 hours at room temperature.

The solvents were evaporated under reduced pressure and the product was purified by flash column chromatography (3 % 0.05 HCl in MeCN to 10 % 0.1 M HCl in MeCN) in small fractions (< 30 mg/column).

NMR integration indicated a ratio of 1:0.5 for **17:5c** (66 %). Purification of 30 mg crude product produced 58 % of the pure isolated **17**.

¹H NMR(400 MHz, CD₃OD)δ: 7.74(d, J = 16.3 Hz, 1H), 7.22-7.27(m, 2H), 7.03(d, J = 8.9 Hz, 1H), 6.61(d, J = 16.3 Hz, 1H), 3.89(s, 6H) ppm

¹³C NMR(100 MHz, CD₃OD)δ: 163.9, 152.4, 149.6, 144.6, 128.4, 123.5, 111.4, 111.3, 110.0, 55.2, 55.1 ppm

(Sample is submitted for MS-analysis)

References

1. Lorentzen, M., et al., *Total synthesis of tubastrine and 3-dehydroxy tubastrine by microwave-assisted cross-coupling reactions*. Tetrahedron, 2015. **71**(43): p. 8278-8284.
2. Yebra, D. and C. Hellio, *Advances in marine antifouling coatings and technologies 2009*: Woodhead Publishing Limited.
3. Speight, J.G., *Fouling in refineries*. 2015: Gulf Professional Publishing.
4. Vladkova, T., *Surface Modification Approach to Control Biofouling*, in *Marine and Industrial Biofouling*, H.-C. Flemming, et al., Editors. 2009, Springer Berlin Heidelberg: Berlin, Heidelberg. p. 135-163.
5. Cao, S., et al., *Progress of marine biofouling and antifouling technologies*. Chinese Science Bulletin, 2011. **56**(7): p. 598-612.
6. Schultz, M.P., *Effects of coating roughness and biofouling on ship resistance and powering*. Biofouling, 2007. **23**(5): p. 331-341.
7. Dürr, S. and J. Thomason, *Biofouling*. 2010: Blackwell Publishing Ltd.
8. Finlay, J.A. and M.E. Callow, *The potential of alkylamines as antifouling biocides I: Toxicity and structure activity relationships*. Biofouling, 1996. **9**(4): p. 257-268.
9. Omae, I. and Omae Research Laboratories, *Organotin antifouling paints and their alternatives*. Appl. Organometal. Chem. , 2003. **17**: p. 81-105.
10. Ng, K.M., R. Gani, and K. Dam-Johansen, *Chemical product design: towards a perspective through case studies*. Vol. 23. 2006: Elsevier.
11. (IMO), I.M.O., *Anti-fouling systems*. 2002: www.imo.org.
12. Voulvoulis, N., M.D. Schrimshaw, and J.N. Lester, *Comparative environmental assessment of biocides used in antifouling paints*. Chemosphere, 2002. **47**(7): p. 789-795.
13. Price, A.R., J., *Booster biocide antifoulants: is history repeating itself?*, in *Late lessons from early warnings: science, precaution, innovation*. 2013, Publications office of the European Union, Luxembourg.
14. Carbery, K., *A Case Study of Irgarol Contamination in Coastal Environments: the Case of Caribbean Waters*. 2006, Univeristy of Puerto Rico. p. 44.
15. Jones, R., *The ecotoxicological effects of Photosystem II herbicides on corals*. Mar. Pollut. Bull., 2005. **51**(5-7): p. 495-506.
16. Callow, M.E. and G.L. Willingham, *Degradation of antifouling biocides*. Biofouling, 1996. **10**: p. 239-249.
17. Mai, H., et al., *Environmental concentrations of irgarol, diuron and S-metolachlor induce deleterious effects on gametes and embryos of the Pacific oyster, Crassostrea gigas*. Marine Environmental Research, 2013. **89**: p. 1-8.
18. Kottuparambil, S., S. Lee, and T. Han, *Single and interactive effects of the antifouling booster herbicides diuron and Irgarol 1051 on photosynthesis in the marine cyanobacterium, Arthrospira maxima*. Toxicology and Environmental Health Sciences, 2013. **5**(2): p. 71-81.
19. Thomas, K.V., et al., *Increased persistence of antifouling paint biocides when associated with paint particles*. Environmental Pollution, 2003. **123**(1): p. 153-161.
20. Qian, P.-Y., Y. Xu, and N. Fusetani, *Natural products as antifouling compounds: recent progress and future perspectives*. Biofouling, 2009. **26**(2): p. 223-234.
21. Fusetani, N., *Biofouling and antifouling*. Natural Product Reports, 2004. **21**(1): p. 94-104.

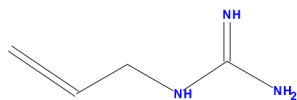
22. Sjögren, M., et al., *Antifouling activity of synthesized peptide analogs of the sponge metabolite baretin*. *Peptides*, 2006. **27**(9): p. 2058-2064.
23. Nakayama, H., Kagaku Kogyo, 1995. **46**(112).
24. Cushnie, T.P.T., B. Cushnie, and A.J. Lamb, *Alkaloids: An overview of their antibacterial, antibiotic-enhancing and antivirulence activities*. *International Journal of Antimicrobial Agents*, 2014. **44**(5): p. 377-386.
25. Said, M., et al., *Antitumor, Antioxidant and Antimicrobial Studies of Substituted Pyridylguanidines* *Molecules*, 2013. **18**: p. 10378-10396.
26. Yim, J.H., et al., *Development of Antimicrobial Coatings by Atmospheric Pressure Plasma Using a Guanidine-Based Precursor*. *ACS Applied materials & interfaces* 2013. **5**: p. 11836-11843.
27. Fattorusso, E. and O. Tagliatalata-Scafati, *Modern alkaloids: structure, isolation, synthesis, and biology*. 2008: John Wiley & Sons.
28. Rodriguez, A.D. and I.C. Pina, *Journal of Natural Products*, 1993. **56**: p. 907-914.
29. Berlinck, R. and S. Romminger, *The chemistry and biology of guanidine natural products*. *Natural Product Reports*, 2015. **33**(3): p. 367-524.
30. Sölter, S., et al., *Tetrahedron Lett*, 2002. **43**: p. 3385-3386.
31. Trepos, R., et al., *Antifouling compounds from the Sub-Arctic ascidian *Synoicum pulmonaria*: Synoxazolidinones A and C, Pulmonarins A and B, and synthetic analogues*. *Journal Of Natural Products*, 2014. **77**(9): p. 2105-2113.
32. Igumnova, E.M., et al., *Synthesis and antimicrobial activity of small cationic amphipathic aminobenzamide marine natural product mimics and evaluation of relevance against clinical isolates including ESBL-CARBA producing multi-resistant bacteria*. *Bioorganic & Medicinal Chemistry*, 2016. **24**: p. 5884-5894.
33. Ryuichi, S. and H. Tatsuo, *Tubastrine, a New Guanidinostyrene from the Coral *Tubastrea aurea**. *Chemistry Letters*, 1987. **16**(1): p. 127-128.
34. Barenbrock, J.S. and M. Köck, *Screening enzyme-inhibitory activity in several ascidian species from Orkney Islands using protein tyrosine kinase (PTK) bioassay-guided fractionation*. *Journal of Biotechnology*, 2005. **117**(3): p. 225-232.
35. Pearce, A.N., et al., *Orthidines A–E, tubastrine, 3,4-dimethoxyphenethyl- β -guanidine, and 1,14-sperminedihomovanillamide: potential anti-inflammatory alkaloids isolated from the New Zealand ascidian *Aplidium orthium* that act as inhibitors of neutrophil respiratory burst*. *Tetrahedron*, 2008. **64**(24): p. 5748-5755.
36. Tadesse, M., et al., *Isolation and biological activity of (E)-1-(4-hydroxystyryl)guanidine from the sub-Arctic ascidian, *Dendrodoa aggregata**. *Biochemical Systematics and Ecology*, 2010. **38**(4): p. 827-829.
37. Santos, K.O.C., M. V. and R.G.S. Berlinck, *Development of an approach for the synthesis of 3-dehydroxy-4-methoxy tubastrine*. *Quim. Nova*, 2007. **30**(8): p. 1892-1895.
38. Genaro-Mattos, T., Mauricio Q. A., and D.H.-L. Rettori, M., *Antioxidant Activity of Caffeic Acid against Iron-Induced Free Radical Generation—A Chemical Approach*. *PLoS ONE*, 2015. **10**(6): p. 1-12.
39. Blenau and Baumann, 2001.
40. Liebersat and Pflueger, 2004.
41. Kon-ya and Endo, 1995.
42. Setsuro, F., et al., *Amidine compound and anticomplement agent comprising same*. 1984, Torii & Co., Ltd., Tokyo: Japan. p. 20.

43. Bhattacharya, A. and G. Thyagarajan, *The Michaelis-Arbuzov rearrangement*. Chem. Rev., 1981(81): p. 415-430.
44. Laue, T. and A. Plagens, *Named Organic Reactions*. 1998, Baffins Lane, Chichester: John Wiley & Sons Ltd. .
45. Wadsworth, W.S.J., Org. React. (N.Y.), 1977. **25**(73).
46. Thompson, S.K.H., Clayton H., *Effect of cation, temperature, and solvent on the stereoselectivity of the Horner-Emmons reaction of trimethyl phosphonoacetate with aldehydes*. J. Org. Chem., 1990. **55**(10): p. 3386-3388.
47. Lefèbvre, G.S.-P., J., J. Chem. Soc., 1970: p. 1308-1309.
48. Laue, T. and A. Plagens, *Named Organic Reactions*. 1998, West Sussex, UK: John Wiley & Sons Ltd. 271-274.
49. Sperotto, E., et al., *The mechanism of the modified Ullmann reaction*. Dalton Transactions, 2010.
50. Evano, G.B., Nicolas *Copper-Mediated Cross-Coupling Reactions*. 2013: John Wiley & Sons. 840.
51. Heck, R.F. and H.A. Dieck, J. Am. Chem. Soc., 1974. **96**: p. 1133-1136.
52. Bernatowicz, M.S., Y. Wu, and G.R. Matsueda, *1H-Pyrazole-1-carboxamide hydrochloride an attractive reagent for guanylation of amines and its application to peptide synthesis*. The Journal of Organic Chemistry, 1992. **57**(8): p. 2497-2502.
53. Bakka, T.A.G., O. R., *Simple generalized reaction conditions for the conversion of primary aliphatic amines to surfactant-like guanidine salts with 1H-pyrazole carboxamide hydrochloride*. Synthetic Communications, 2017. **47**(2): p. 169-172.
54. Kuang, C., H. Senboku, and M. Tokuda, *Stereoselective synthesis of (E)- β -arylvinylic halides by microwave-induced Hunsdiecker reaction*. Synlett, 2000(10): p. 1439-1442.
55. Couladouros, E., *Total Synthesis of Combretastatins D*. Chem. Eur. J., 1998. **4**(1): p. 33-43.
56. Tamim F. Braish, L., Conn., *Preparation of intermediates in the synthesis of quinoline antibiotics*. 1992, Pfizer Inc. New York: United States. p. 6.
57. Volkov, A.T., F., et al., *MO(CO)₆ catalysed chemoselective hydrosilylation of α,β -unsaturated amides for the formation of allylamines*. Chem. Commun., 2014. **50**: p. 14508-14511.
58. Petrova, J., S. Momchilova, and N. Vassilev, *The HWE reaction in solid-liquid two phase system for the synthesis of α,β -unsaturated amides*. Phosphorus, Sulfur and Silicon and the related Elements, 2000. **164**(1): p. 87-94.

APPENDIX A

^1H -NMR and ^{13}C -NMR spectra

(2)

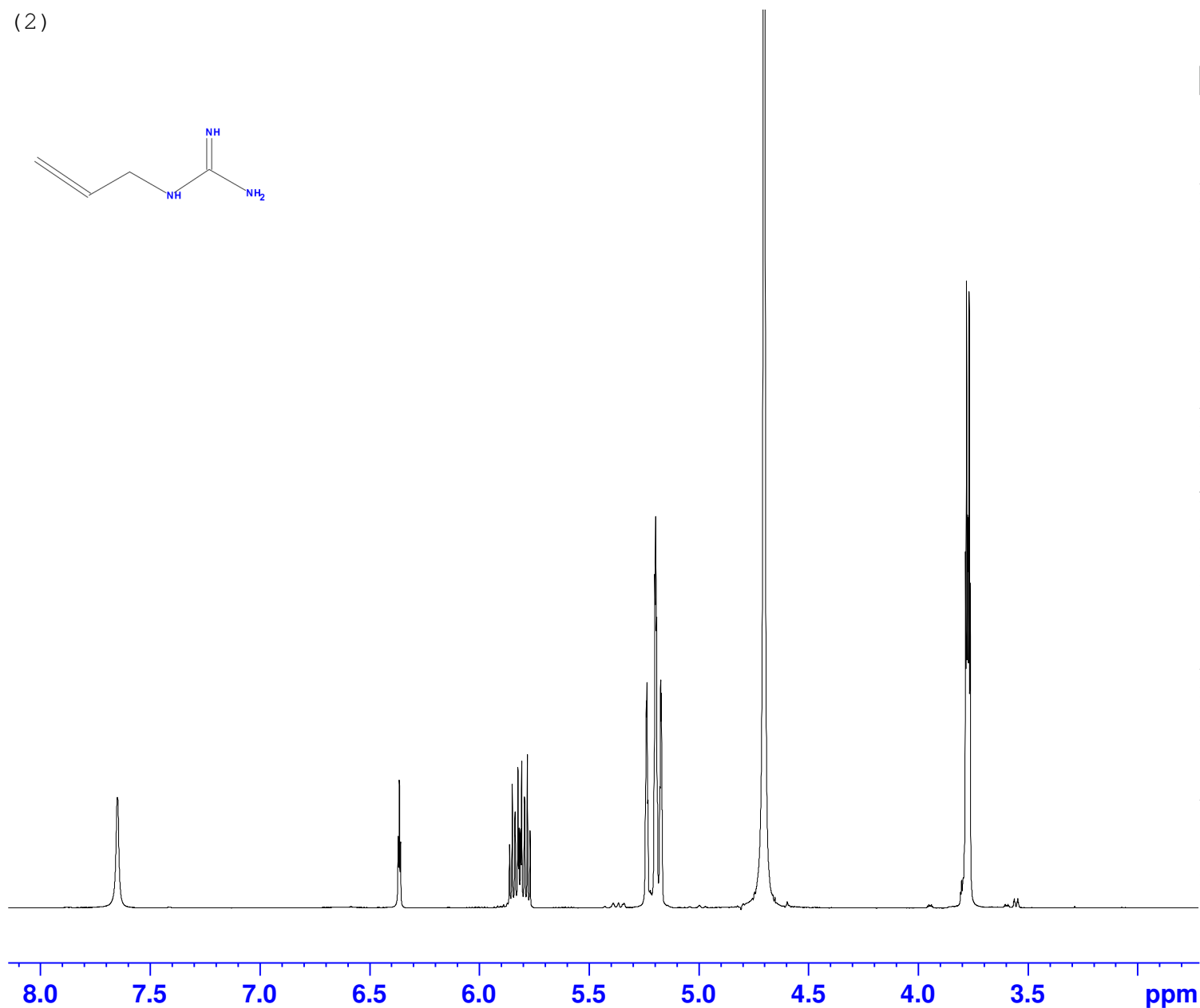


Current Data Parameters
NAME MBR16-1
EXPNO 1
PROCNO 1

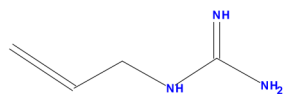
F2 - Acquisition Parameters
Date_ 20170222
Time 12.17
INSTRUM spect
PROBHD 5 mm PABBO BB/
PULPROG zg30
TD 65536
SOLVENT D2O
NS 16
DS 2
SWH 8012.820 Hz
FIDRES 0.122266 Hz
AQ 4.0894465 sec
RG 103.33
DW 62.400 usec
DE 6.50 usec
TE 300.0 K
D1 1.00000000 sec
TD0 1

==== CHANNEL f1 =====
SFO1 400.1324710 MHz
NUC1 1H
P1 8.60 usec
PLW1 18.10000038 W

F2 - Processing parameters
SI 65536
SF 400.1300000 MHz
WDW EM
SSB 0
LB 0.30 Hz
GB 0
PC 1.00



(2)

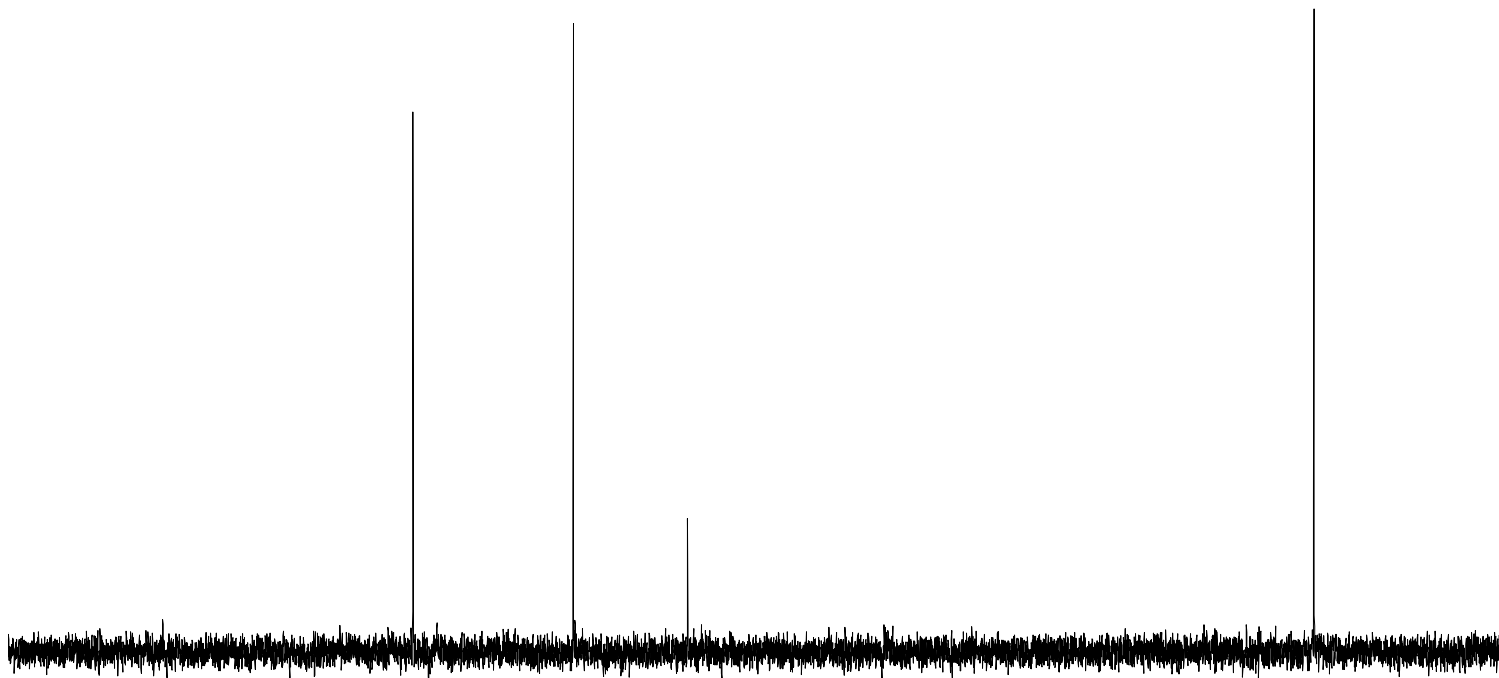


132.19

116.32

105.00

43.03



Current Data Parameters
NAME MBR16-1
EXPNO 2
PROCNO 1

F2 - Acquisition Parameters
Date_ 20170222
Time 12.33
INSTRUM spect
PROBHD 5 mm PABBO BB/
PULPROG zgpg30
TD 65536
SOLVENT D2O
NS 256
DS 2
SWH 24038.461 Hz
FIDRES 0.366798 Hz
AQ 1.3631488 sec
RG 200.88
DW 20.800 usec
DE 6.50 usec
TE 300.0 K
D1 2.0000000 sec
D11 0.0300000 sec
TD0 1

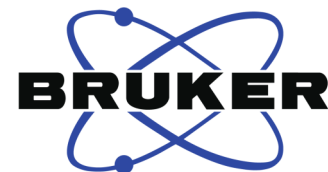
==== CHANNEL f1 =====
SFO1 100.6228298 MHz
NUC1 13C
P1 8.40 usec
PLW1 88.19999695 W

==== CHANNEL f2 =====
SFO2 400.1316005 MHz
NUC2 1H
CPDPRG[2] waltz16
PCPD2 90.00 usec
PLW2 18.10000038 W
PLW12 0.16527000 W
PLW13 0.13387001 W

F2 - Processing parameters
SI 32768
SF 100.6127685 MHz
WDW EM
SSB 0
LB 1.00 Hz
GB 0
PC 1.40

160 150 140 130 120 110 100 90 80 70 60 50 40 ppm

(3)

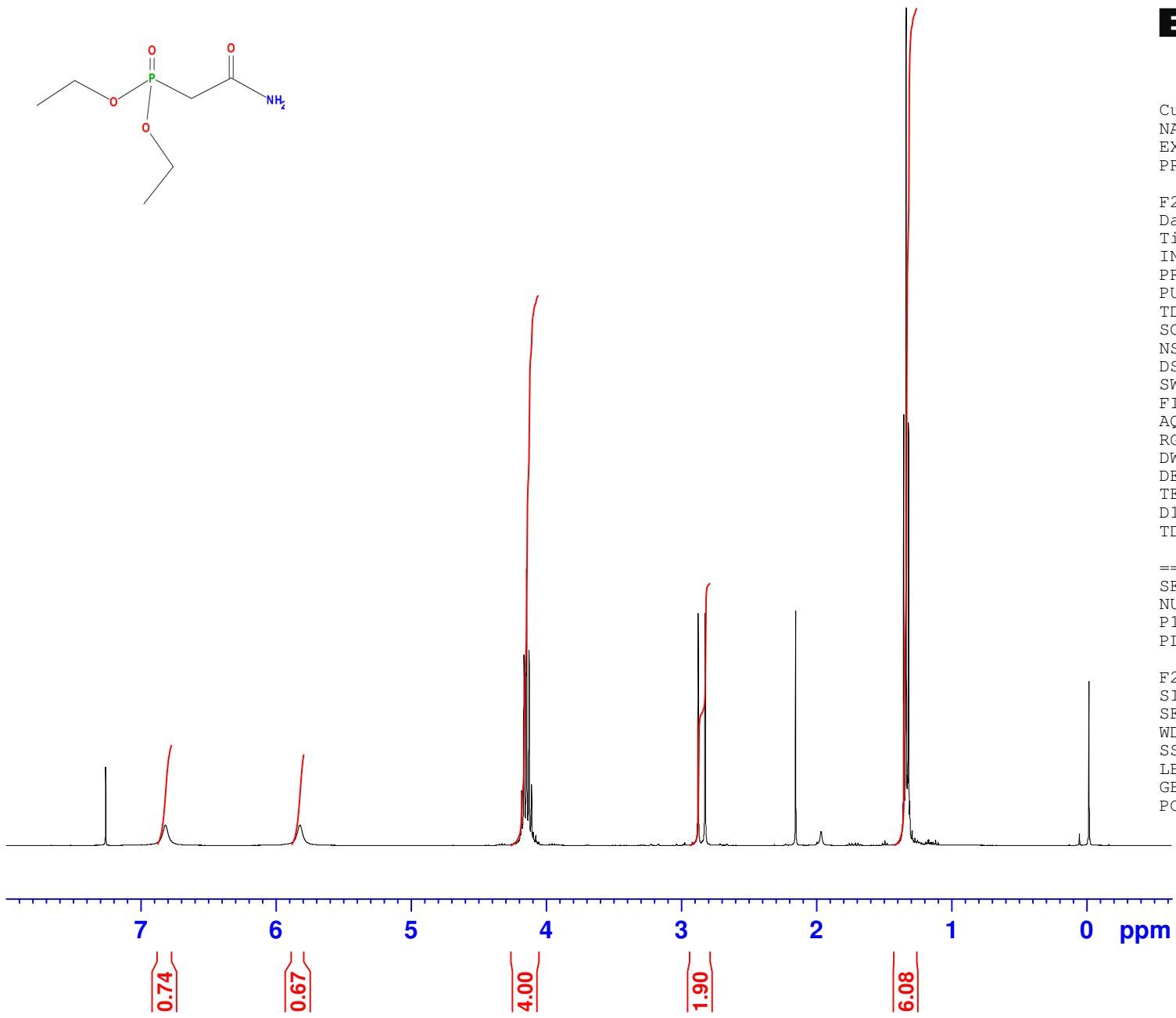


Current Data Parameters
NAME MBR17-5 new
EXPNO 1
PROCNO 1

F2 - Acquisition Parameters
Date_ 20170308
Time 15.50
INSTRUM spect
PROBHD 5 mm PABBO BB/
PULPROG zg30
TD 65536
SOLVENT CDC13
NS 16
DS 2
SWH 8012.820 Hz
FIDRES 0.122266 Hz
AQ 4.0894465 sec
RG 89.12
DW 62.400 usec
DE 6.50 usec
TE 300.0 K
D1 1.00000000 sec
TD0 1

==== CHANNEL f1 =====
SFO1 400.1324710 MHz
NUC1 1H
P1 8.60 usec
PLW1 18.10000038 W

F2 - Processing parameters
SI 65536
SF 400.1300097 MHz
WDW EM
SSB 0
LB 0.30 Hz
GB 0
PC 1.00



(3)



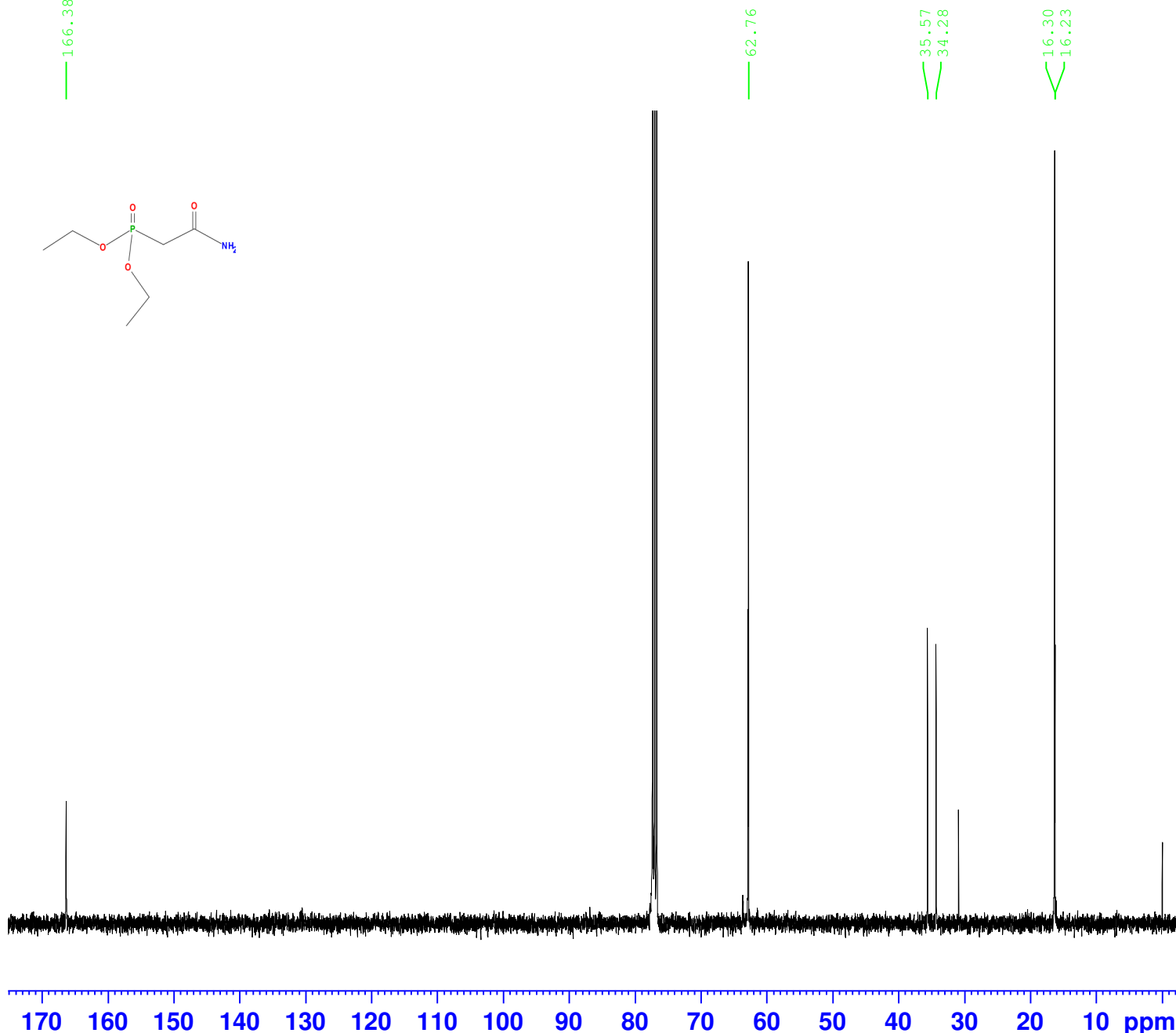
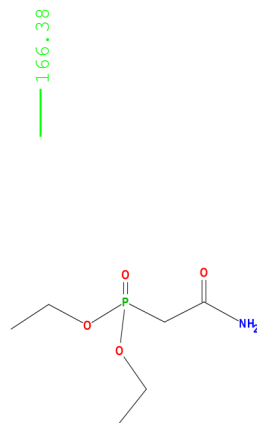
Current Data Parameters
NAME MBR17-5 new
EXPNO 2
PROCNO 1

F2 - Acquisition Parameters
Date_ 20170310
Time 5.05
INSTRUM spect
PROBHD 5 mm PABBO BB/
PULPROG zgpg30
TD 65536
SOLVENT CDC13
NS 1024
DS 4
SWH 24038.461 Hz
FIDRES 0.366798 Hz
AQ 1.3631488 sec
RG 200.88
DW 20.800 usec
DE 6.50 usec
TE 300.0 K
D1 2.0000000 sec
D11 0.0300000 sec
TD0 1

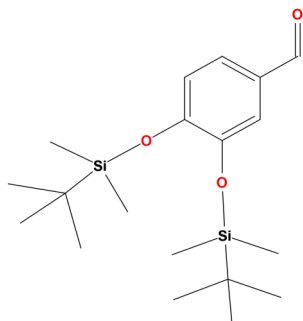
=====
CHANNEL f1
SFO1 100.6228293 MHz
NUC1 13C
P1 8.40 usec
PLW1 88.19999695 W

=====
CHANNEL f2
SFO2 400.1316005 MHz
NUC2 1H
CPDPRG[2] waltz16
PCPD2 90.00 usec
PLW2 18.10000038 W
PLW12 0.16527000 W
PLW13 0.13387001 W

F2 - Processing parameters
SI 32768
SF 100.6127735 MHz
WDW EM
SSB 0
LB 1.00 Hz
GB 0
PC 1.40



(4a)

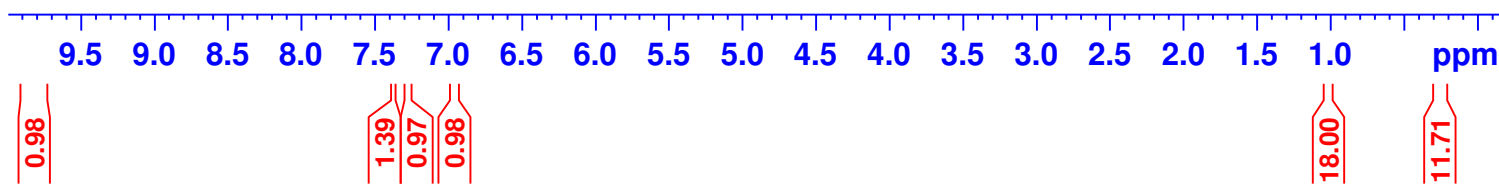
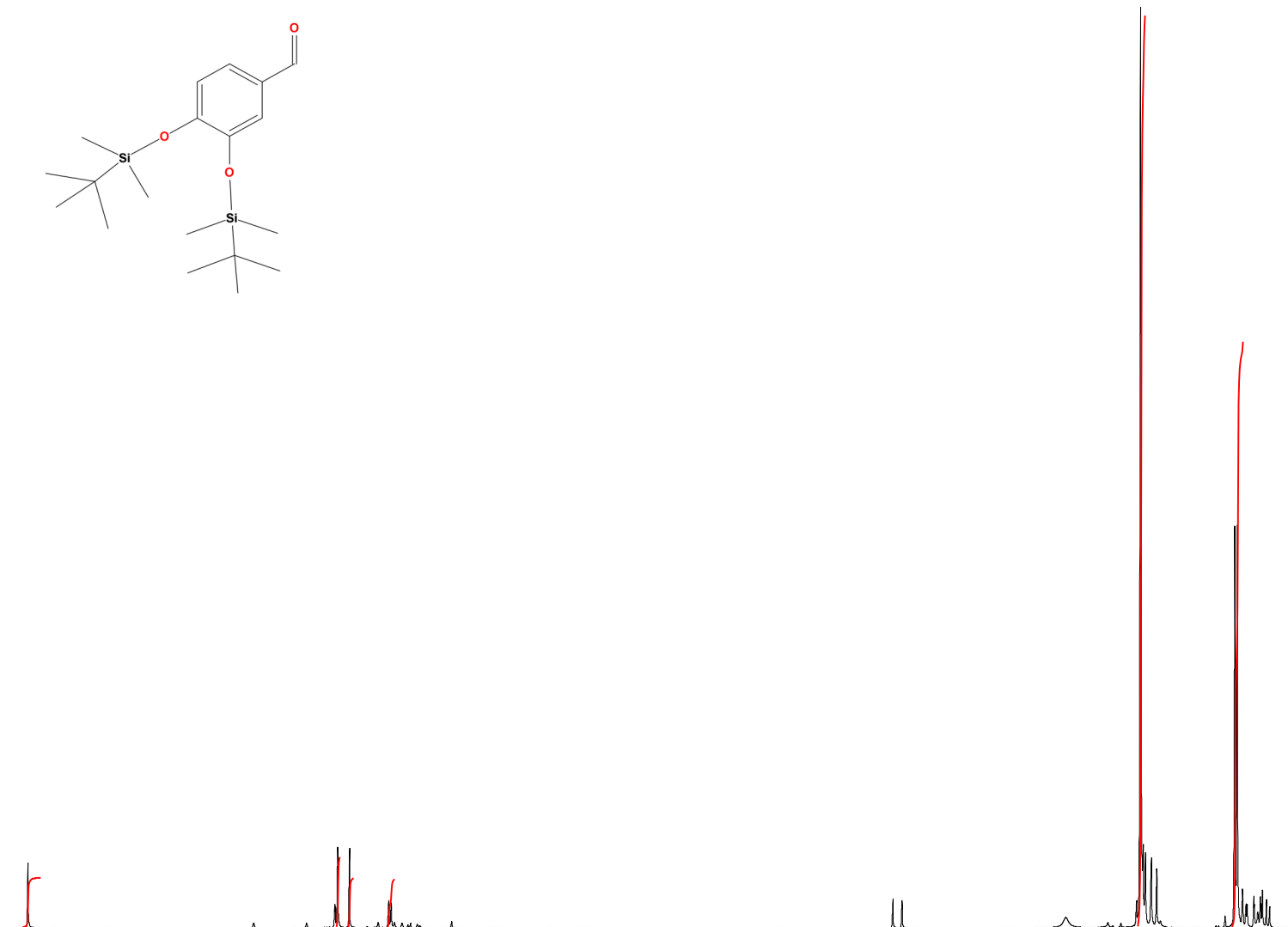


Current Data Parameters
NAME MBR17-9
EXPNO 1
PROCNO 1

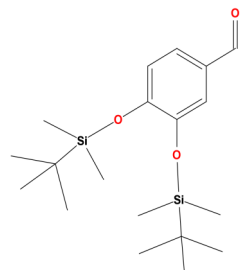
F2 - Acquisition Parameters
Date_ 20170201
Time 14.39
INSTRUM spect
PROBHD 5 mm PABBO BB/
PULPROG zg30
TD 65536
SOLVENT CDC13
NS 16
DS 2
SWH 8012.820 Hz
FIDRES 0.122266 Hz
AQ 4.0894465 sec
RG 128.29
DW 62.400 usec
DE 6.50 usec
TE 297.3 K
D1 1.00000000 sec
TD0 1

==== CHANNEL f1 =====
SFO1 400.1324710 MHz
NUC1 1H
P1 8.60 usec
PLW1 18.10000038 W

F2 - Processing parameters
SI 65536
SF 400.1300000 MHz
WDW EM
SSB 0
LB 0.30 Hz
GB 0
PC 1.00



(4a)



153.36

147.67

130.72

125.29

120.81

120.57

77.34

77.23

77.02

76.70

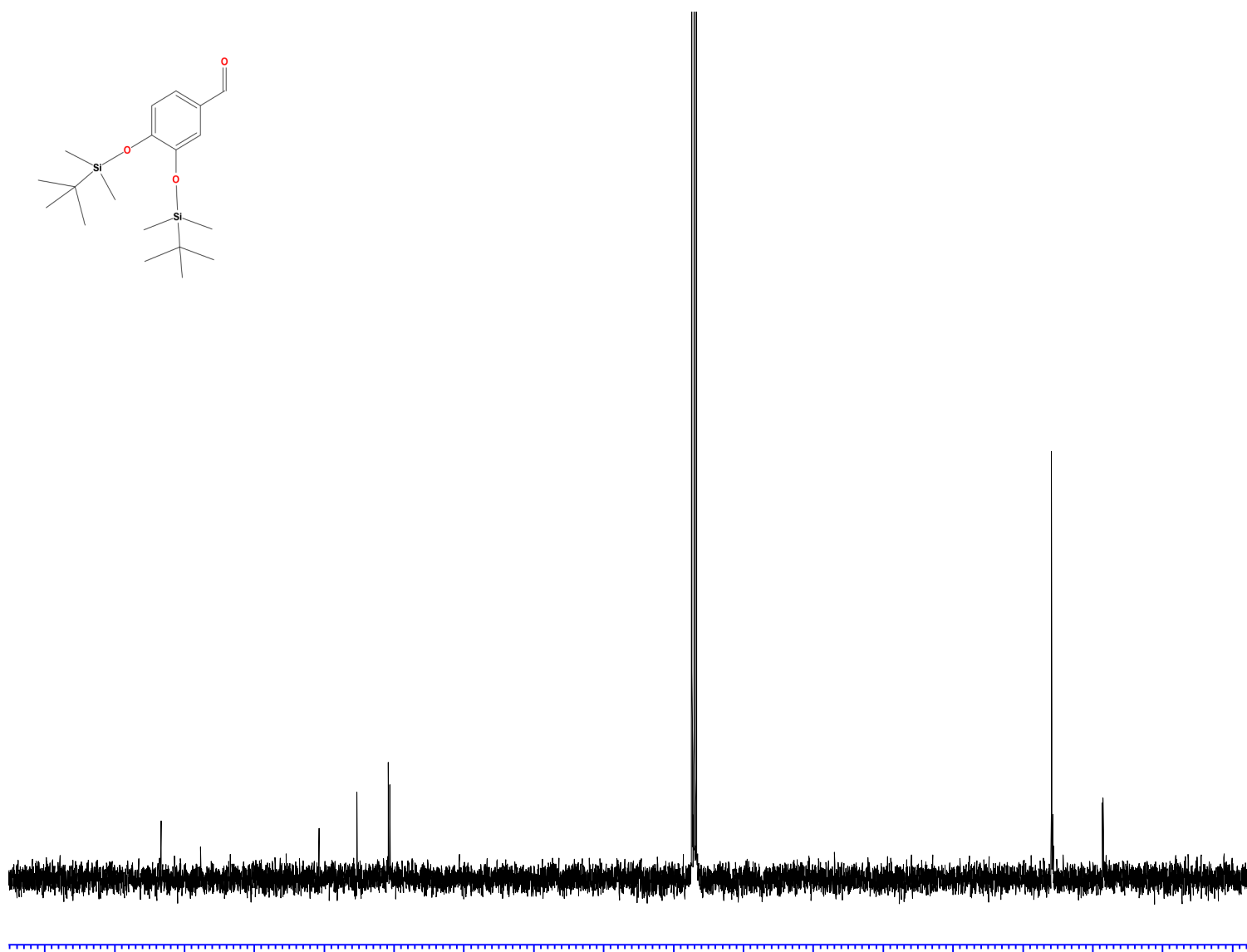
25.87

25.83

25.66

18.55

18.44



170 160 150 140 130 120 110 100 90 80 70 60 50 40 30 20 10 ppm



Current Data Parameters
NAME MBR17-9
EXPNO 2
PROCNO 1

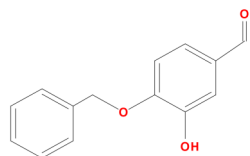
F2 - Acquisition Parameters
Date_ 20170201
Time 14.55
INSTRUM spect
PROBHD 5 mm PABBO BB/
PULPROG zgpg30
TD 65536
SOLVENT CDC13
NS 256
DS 2
SWH 24038.461 Hz
FIDRES 0.366798 Hz
AQ 1.3631488 sec
RG 200.88
DW 20.800 usec
DE 6.50 usec
TE 298.1 K
D1 2.00000000 sec
D11 0.03000000 sec
TD0 1

==== CHANNEL f1 =====
SFO1 100.6228298 MHz
NUC1 13C
P1 8.40 usec
PLW1 88.19999695 W

==== CHANNEL f2 =====
SFO2 400.1316005 MHz
NUC2 1H
CPDPRG[2] waltz16
PCPD2 90.00 usec
PLW2 18.10000038 W
PLW12 0.16527000 W
PLW13 0.13387001 W

F2 - Processing parameters
SI 32768
SF 100.6127685 MHz
WDW EM
SSB 0
LB 1.00 Hz
GB 0
PC 1.40

(4b)

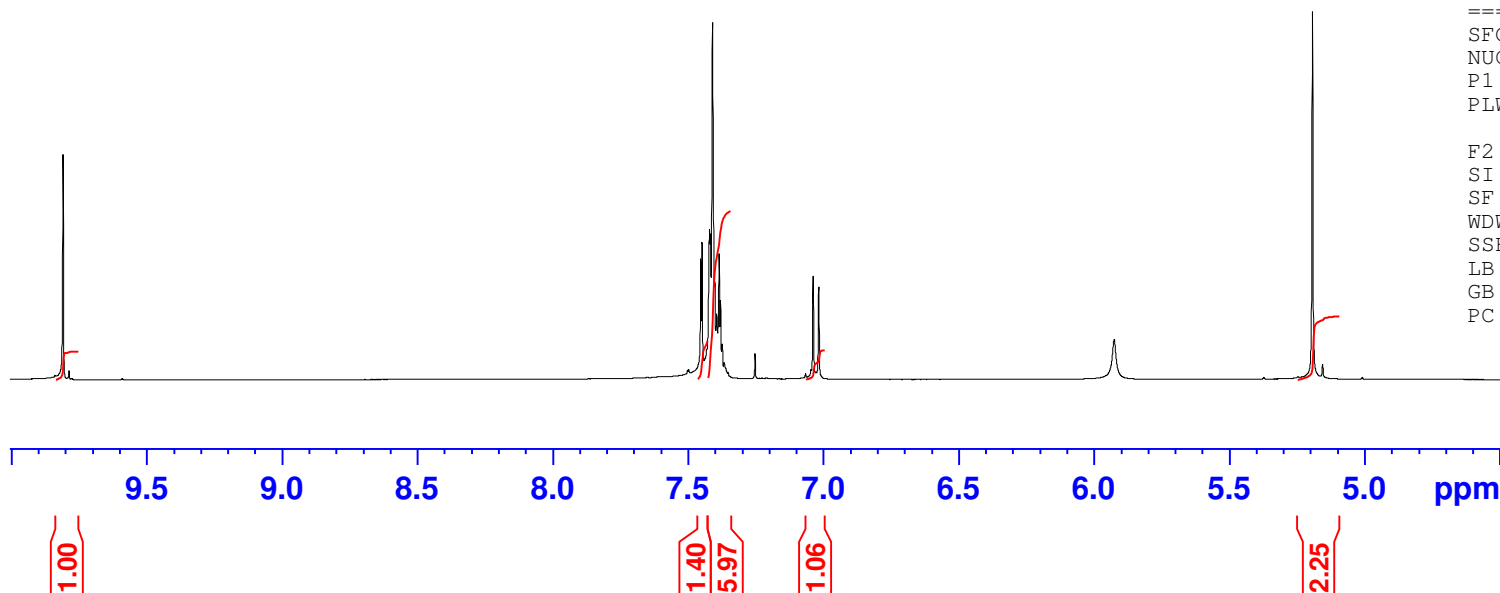


Current Data Parameters
NAME MBR17-29 pure
EXPNO 1
PROCNO 1

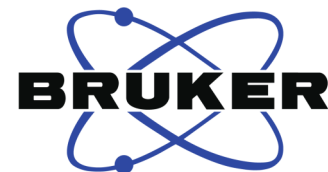
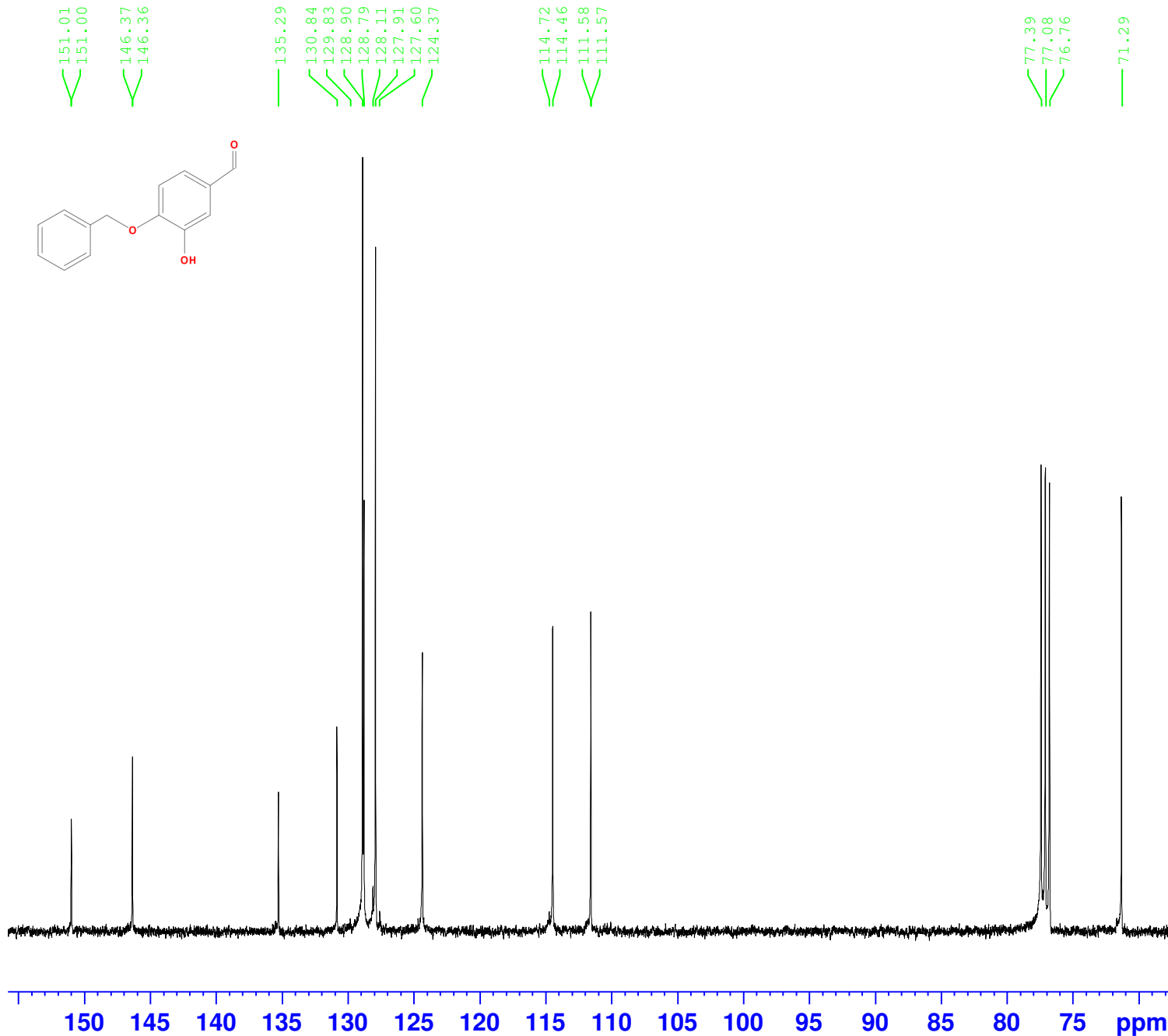
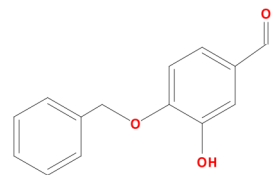
F2 - Acquisition Parameters
Date_ 20170427
Time 16.23
INSTRUM spect
PROBHD 5 mm PABBO BB/
PULPROG zg30
TD 65536
SOLVENT CDC13
NS 16
DS 2
SWH 8012.820 Hz
FIDRES 0.122266 Hz
AQ 4.0894465 sec
RG 71.31
DW 62.400 usec
DE 6.50 usec
TE 300.0 K
D1 1.00000000 sec
TD0 1

==== CHANNEL f1 =====
SFO1 400.1324710 MHz
NUC1 1H
P1 8.60 usec
PLW1 18.10000038 W

F2 - Processing parameters
SI 65536
SF 400.1300128 MHz
WDW EM
SSB 0
LB 0.30 Hz
GB 0
PC 1.00



(4b)



Current Data Parameters
NAME MBR17-29 pure
EXPNO 2
PROCNO 1

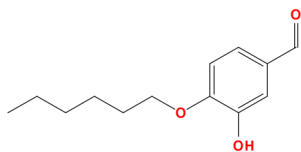
F2 - Acquisition Parameters
Date_ 20170429
Time 1.04
INSTRUM spect
PROBHD 5 mm PABBO BB/
PULPROG zgpg30
TD 65536
SOLVENT CDC13
NS 1024
DS 4
SWH 24038.461 Hz
FIDRES 0.366798 Hz
AQ 1.3631488 sec
RG 200.88
DW 20.800 usec
DE 6.50 usec
TE 300.0 K
D1 2.00000000 sec
D11 0.03000000 sec
TD0 1

=====
CHANNEL f1
SFO1 100.6228293 MHz
NUC1 13C
P1 8.40 usec
PLW1 88.19999695 W

=====
CHANNEL f2
SFO2 400.1316005 MHz
NUC2 1H
CPDPRG[2] waltz16
PCPD2 90.00 usec
PLW2 18.10000038 W
PLW12 0.16527000 W
PLW13 0.13387001 W

F2 - Processing parameters
SI 32768
SF 100.6127685 MHz
WDW EM
SSB 0
LB 1.00 Hz
GB 0
PC 1.40

(4c)

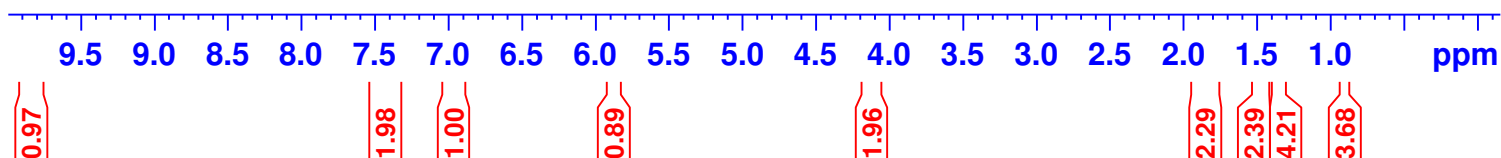
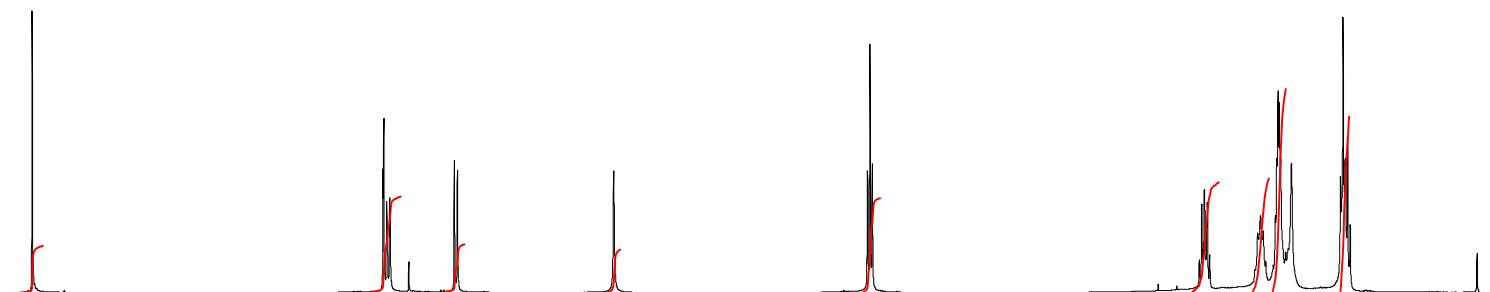


Current Data Parameters
NAME MBR17-43 14-20
EXPNO 1
PROCNO 1

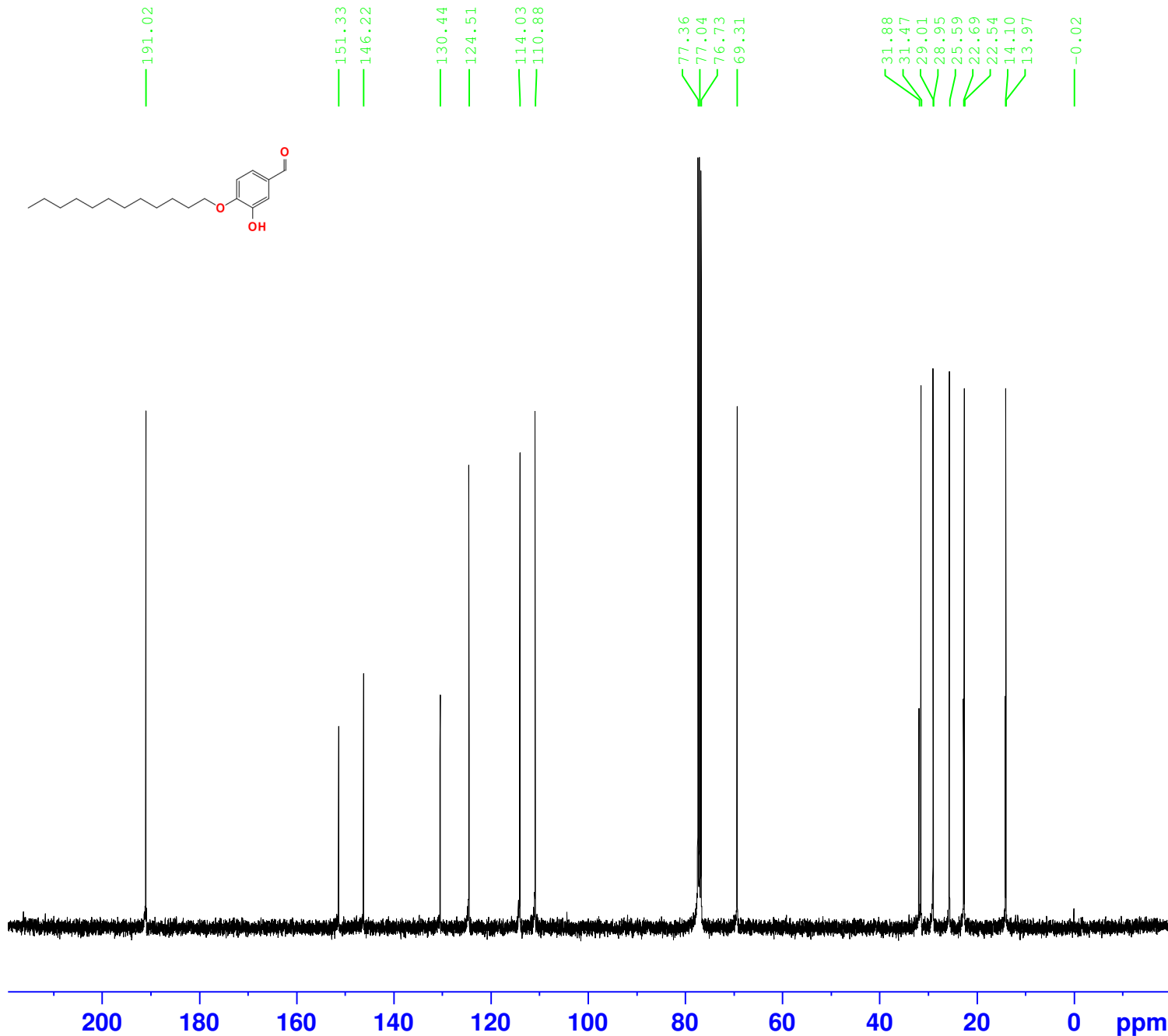
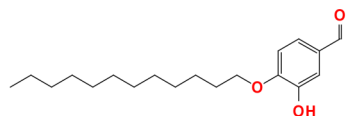
F2 - Acquisition Parameters
Date_ 20170427
Time 16.53
INSTRUM spect
PROBHD 5 mm PABBO BB/
PULPROG zg30
TD 65536
SOLVENT CDC13
NS 16
DS 2
SWH 8012.820 Hz
FIDRES 0.122266 Hz
AQ 4.0894465 sec
RG 31.74
DW 62.400 usec
DE 6.50 usec
TE 300.0 K
D1 1.00000000 sec
TD0 1

==== CHANNEL f1 =====
SFO1 400.1324710 MHz
NUC1 1H
P1 8.60 usec
PLW1 18.10000038 W

F2 - Processing parameters
SI 65536
SF 400.1300059 MHz
WDW EM
SSB 0
LB 0.30 Hz
GB 0
PC 1.00



(4c)



Current Data Parameters
NAME MBR17-43 14-20
EXPNO 2
PROCNO 1

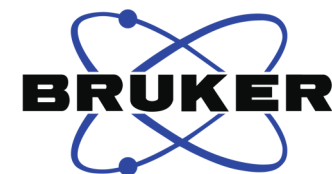
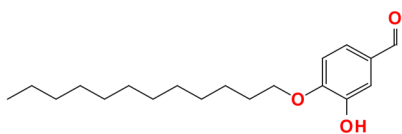
F2 - Acquisition Parameters
Date_ 20170427
Time 19.03
INSTRUM spect
PROBHD 5 mm PABBO BB/
PULPROG zgpg30
TD 65536
SOLVENT CDC13
NS 1024
DS 4
SWH 24038.461 Hz
FIDRES 0.366798 Hz
AQ 1.3631488 sec
RG 200.88
DW 20.800 usec
DE 6.50 usec
TE 300.0 K
D1 2.00000000 sec
D11 0.03000000 sec
TD0 1

==== CHANNEL f1 =====
SFO1 100.6228293 MHz
NUC1 13C
P1 8.40 usec
PLW1 88.19999695 W

==== CHANNEL f2 =====
SFO2 400.1316005 MHz
NUC2 1H
CPDPRG[2] waltz16
PCPD2 90.00 usec
PLW2 18.10000038 W
PLW12 0.16527000 W
PLW13 0.13387001 W

F2 - Processing parameters
SI 32768
SF 100.6127685 MHz
WDW EM
SSB 0
LB 1.00 Hz
GB 0
PC 1.40

(4d)

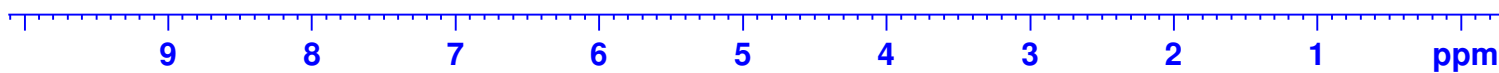
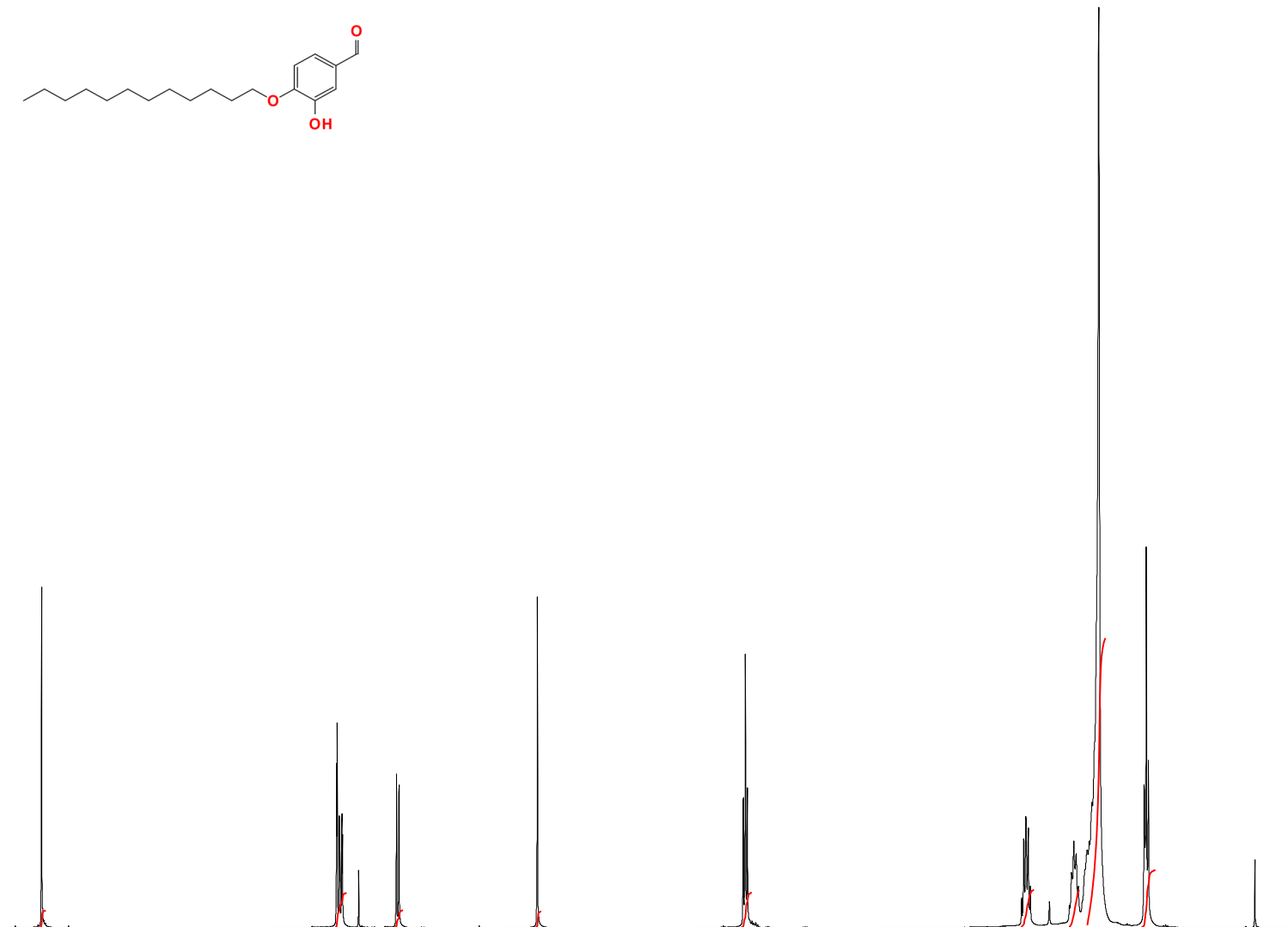


Current Data Parameters
NAME MBR17-45 29-45
EXPNO 3
PROCNO 1

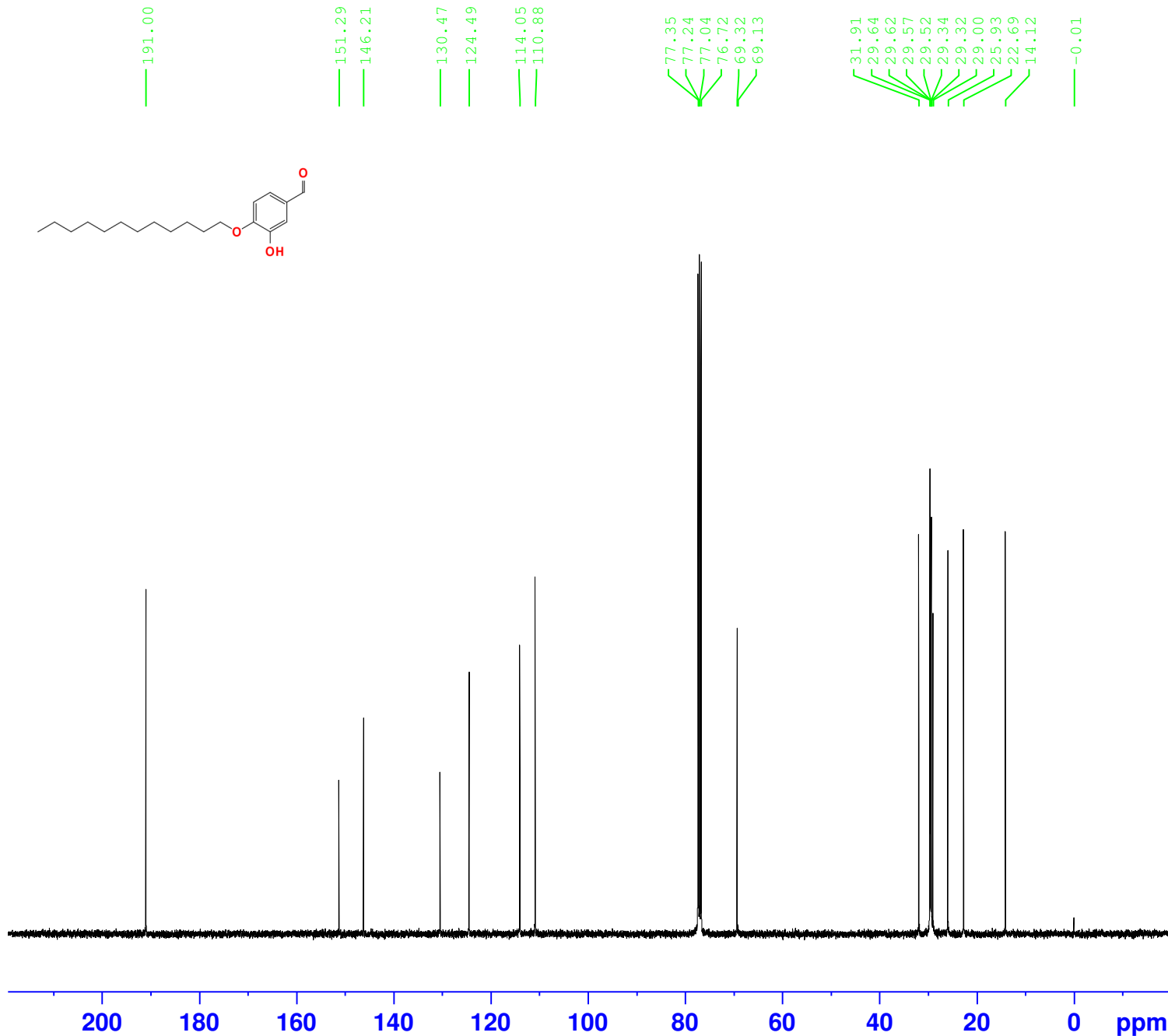
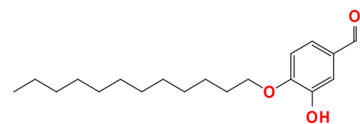
F2 - Acquisition Parameters
Date_ 20170503
Time 20.14
INSTRUM spect
PROBHD 5 mm PABBO BB/
PULPROG zg30
TD 65536
SOLVENT CDC13
NS 16
DS 2
SWH 8012.820 Hz
FIDRES 0.122266 Hz
AQ 4.0894465 sec
RG 31.74
DW 62.400 usec
DE 6.50 usec
TE 300.0 K
D1 1.00000000 sec
TD0 1

==== CHANNEL f1 =====
SFO1 400.1324710 MHz
NUC1 1H
P1 8.60 usec
PLW1 18.10000038 W

F2 - Processing parameters
SI 65536
SF 400.1300078 MHz
WDW EM
SSB 0
LB 0.30 Hz
GB 0
PC 1.00



(4d)



Current Data Parameters
NAME MBR17-45 29-45
EXPNO 2
PROCNO 1

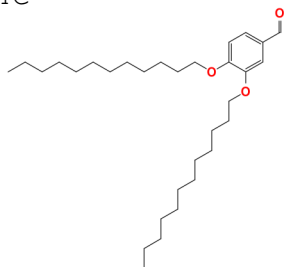
F2 - Acquisition Parameters
Date_ 20170503
Time 20.12
INSTRUM spect
PROBHD 5 mm PABBO BB/
PULPROG zgpg30
TD 65536
SOLVENT CDC13
NS 1024
DS 4
SWH 24038.461 Hz
FIDRES 0.366798 Hz
AQ 1.3631488 sec
RG 200.88
DW 20.800 usec
DE 6.50 usec
TE 300.0 K
D1 2.00000000 sec
D11 0.03000000 sec
TD0 1

=====
CHANNEL f1
SFO1 100.6228293 MHz
NUC1 13C
P1 8.40 usec
PLW1 88.19999695 W

=====
CHANNEL f2
SFO2 400.1316005 MHz
NUC2 1H
CPDPRG[2] waltz16
PCPD2 90.00 usec
PLW2 18.10000038 W
PLW12 0.16527000 W
PLW13 0.13387001 W

F2 - Processing parameters
SI 32768
SF 100.6127685 MHz
WDW EM
SSB 0
LB 1.00 Hz
GB 0
PC 1.40

4e

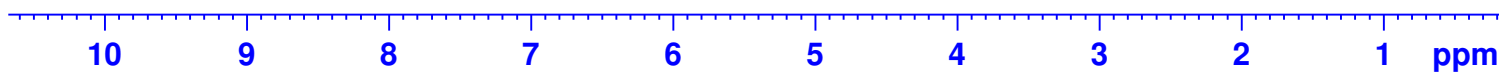
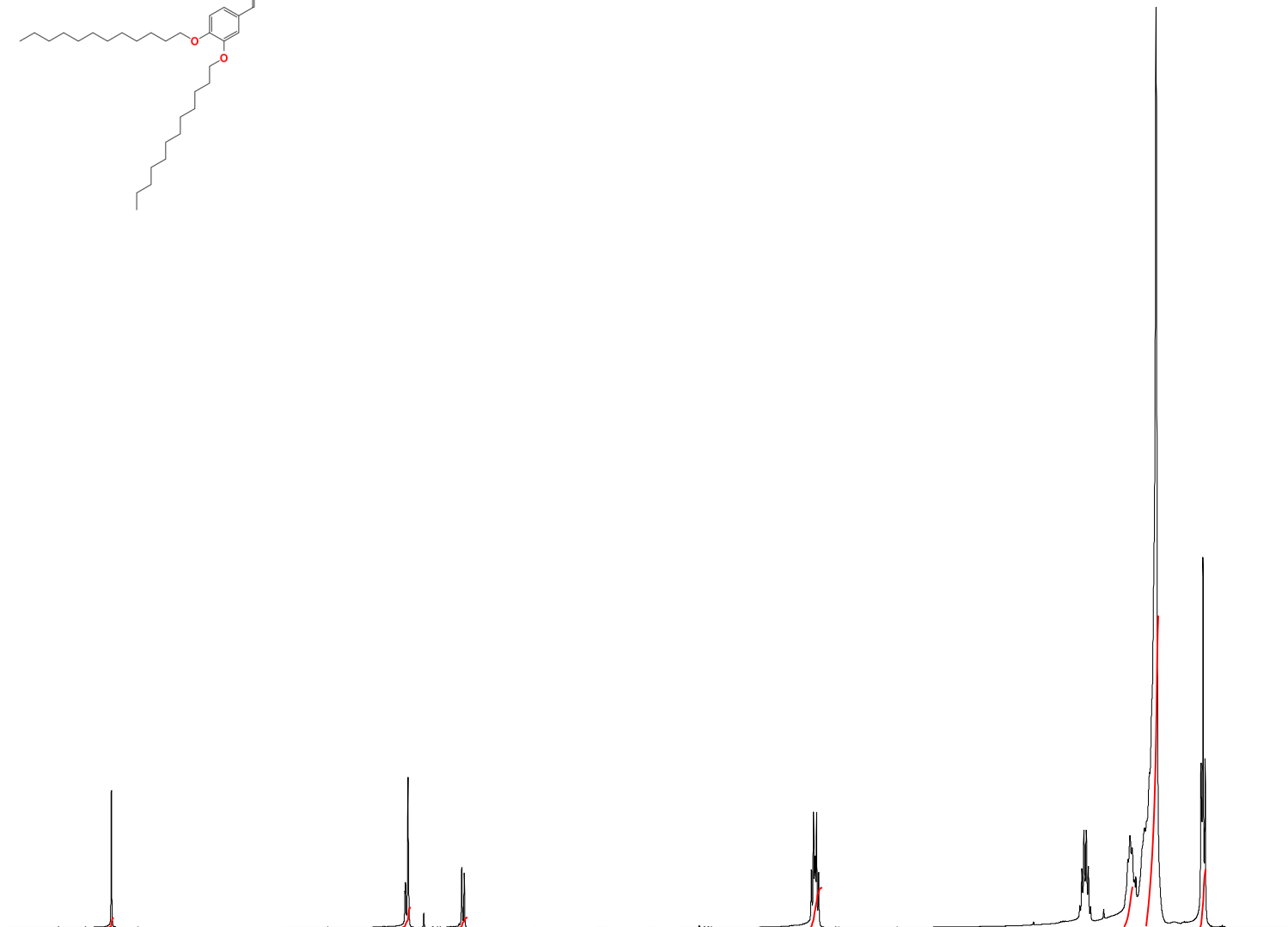


Current Data Parameters
NAME MBR17-45 13-23
EXPNO 1
PROCNO 1

F2 - Acquisition Parameters
Date_ 20170503
Time 22.06
INSTRUM spect
PROBHD 5 mm PABBO BB/
PULPROG zg30
TD 65536
SOLVENT CDC13
NS 16
DS 2
SWH 8012.820 Hz
FIDRES 0.122266 Hz
AQ 4.0894465 sec
RG 15.93
DW 62.400 usec
DE 6.50 usec
TE 300.0 K
D1 1.00000000 sec
TD0 1

==== CHANNEL f1 =====
SFO1 400.1324710 MHz
NUC1 1H
P1 8.60 usec
PLW1 18.10000038 W

F2 - Processing parameters
SI 65536
SF 400.1300075 MHz
WDW EM
SSB 0
LB 0.30 Hz
GB 0
PC 1.00



1.00

2.07

1.01

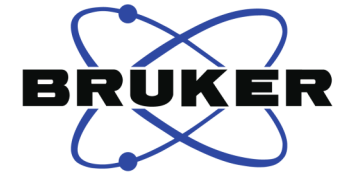
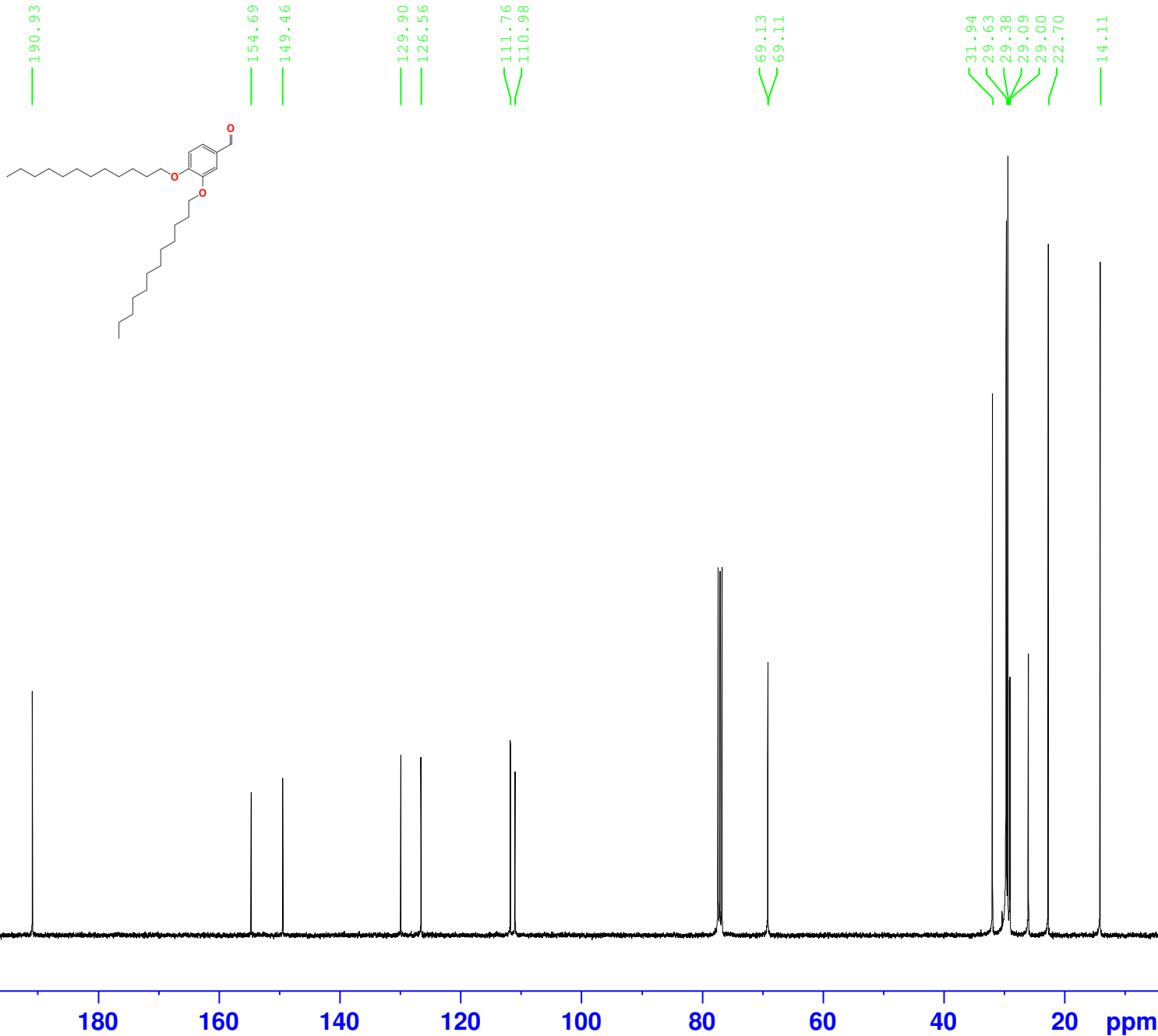
4.08

4.50

32.08

6.53

4e



Current Data Parameters
 NAME MBR17-45 13-23
 EXPNO 2
 PROCNO 1

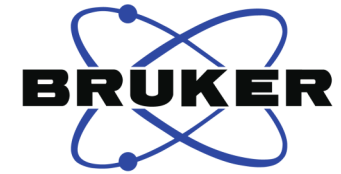
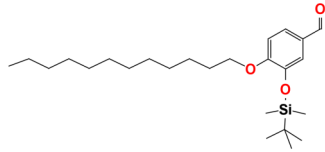
F2 - Acquisition Parameters
 Date_ 20170503
 Time 23.06
 INSTRUM spect
 PROBHD 5 mm PABBO BB/
 PULPROG zgpg30
 TD 65536
 SOLVENT CDC13
 NS 1024
 DS 4
 SWH 24038.461 Hz
 FIDRES 0.366798 Hz
 AQ 1.3631488 sec
 RG 200.88
 DW 20.800 usec
 DE 6.50 usec
 TE 300.0 K
 D1 2.00000000 sec
 D11 0.03000000 sec
 TD0 1

==== CHANNEL f1 =====
 SFO1 100.6228293 MHz
 NUC1 13C
 P1 8.40 usec
 PLW1 88.19999695 W

==== CHANNEL f2 =====
 SFO2 400.1316005 MHz
 NUC2 1H
 CPDPRG[2] waltz16
 PCPD2 90.00 usec
 PLW2 18.10000038 W
 PLW12 0.16527000 W
 PLW13 0.13387001 W

F2 - Processing parameters
 SI 32768
 SF 100.6127685 MHz
 WDW EM
 SSB 0
 LB 1.00 Hz
 GB 0
 PC 1.40

(4f)

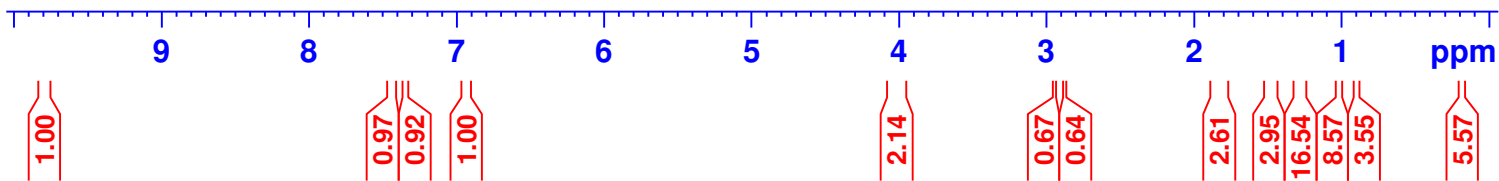
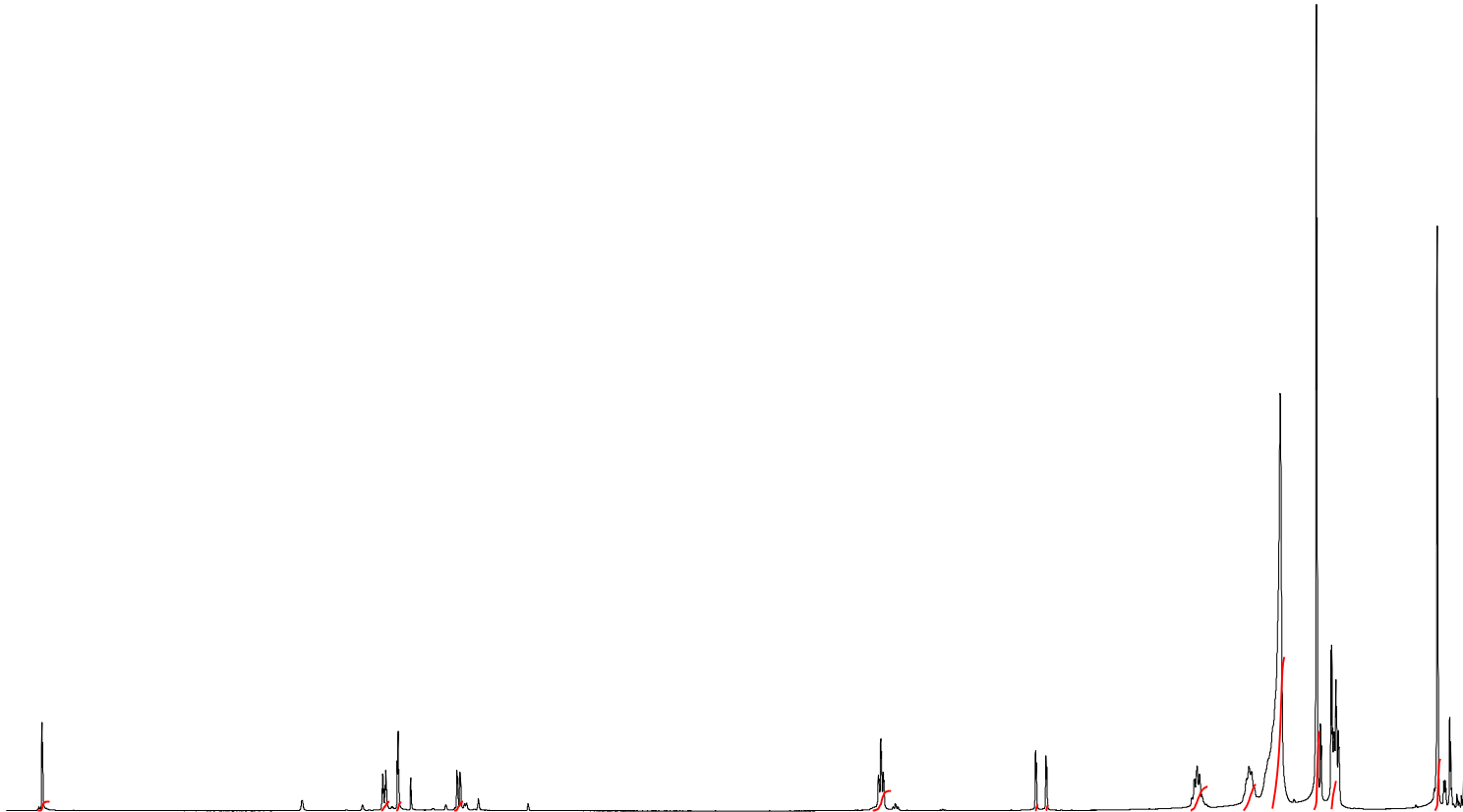


Current Data Parameters
NAME MBR17-46
EXPNO 1
PROCNO 1

F2 - Acquisition Parameters
Date_ 20170504
Time 17.20
INSTRUM spect
PROBHD 5 mm PABBO BB/
PULPROG zg30
TD 65536
SOLVENT CDC13
NS 16
DS 2
SWH 8012.820 Hz
FIDRES 0.122266 Hz
AQ 4.0894465 sec
RG 31.74
DW 62.400 usec
DE 6.50 usec
TE 300.0 K
D1 1.00000000 sec
TD0 1

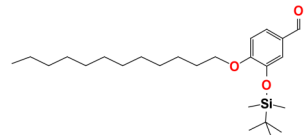
==== CHANNEL f1 =====
SFO1 400.1324710 MHz
NUC1 1H
P1 8.60 usec
PLW1 18.10000038 W

F2 - Processing parameters
SI 65536
SF 400.1300091 MHz
WDW EM
SSB 0
LB 0.30 Hz
GB 0
PC 1.00



(4f)

190.88
 156.42
 145.45
 129.89
 126.36
 120.01
 111.85



68.76

31.92
 29.63
 29.57
 29.38
 29.35
 29.19
 26.07
 25.64
 22.69
 18.36
 14.12



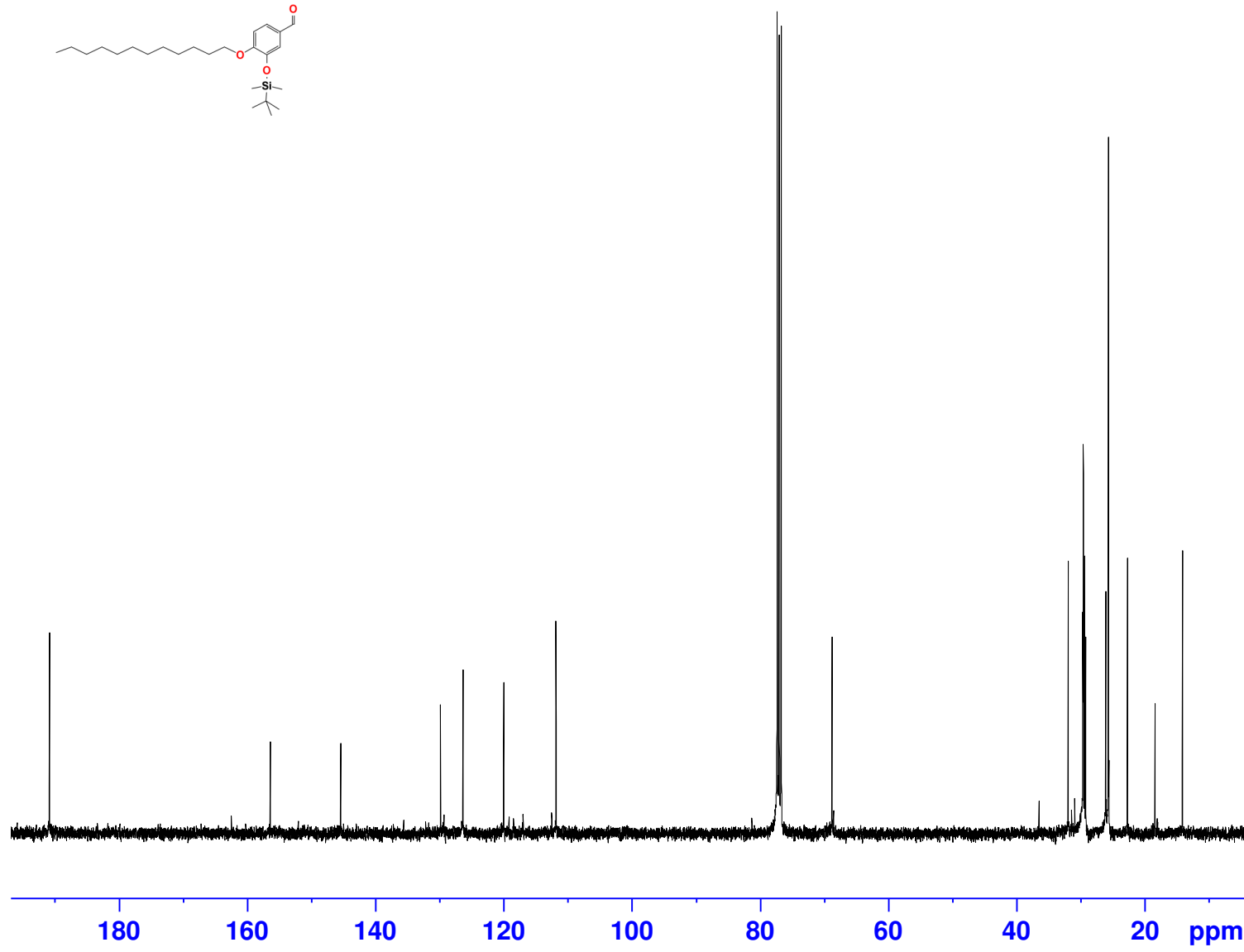
Current Data Parameters
 NAME MBR17-46
 EXPNO 2
 PROCNO 1

F2 - Acquisition Parameters
 Date_ 20170505
 Time 0.44
 INSTRUM spect
 PROBHD 5 mm PABBO BB/
 PULPROG zgpg30
 TD 65536
 SOLVENT CDC13
 NS 1024
 DS 4
 SWH 24038.461 Hz
 FIDRES 0.366798 Hz
 AQ 1.3631488 sec
 RG 200.88
 DW 20.800 usec
 DE 6.50 usec
 TE 300.0 K
 D1 2.00000000 sec
 D11 0.03000000 sec
 TD0 1

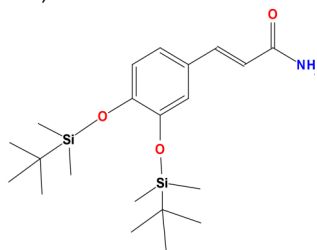
==== CHANNEL f1 =====
 SFO1 100.6228293 MHz
 NUC1 13C
 P1 8.40 usec
 PLW1 88.19999695 W

==== CHANNEL f2 =====
 SFO2 400.1316005 MHz
 NUC2 1H
 CPDPRG[2] waltz16
 PCPD2 90.00 usec
 PLW2 18.10000038 W
 PLW12 0.16527000 W
 PLW13 0.13387001 W

F2 - Processing parameters
 SI 32768
 SF 100.6127685 MHz
 WDW EM
 SSB 0
 LB 1.00 Hz
 GB 0
 PC 1.40



(5b)

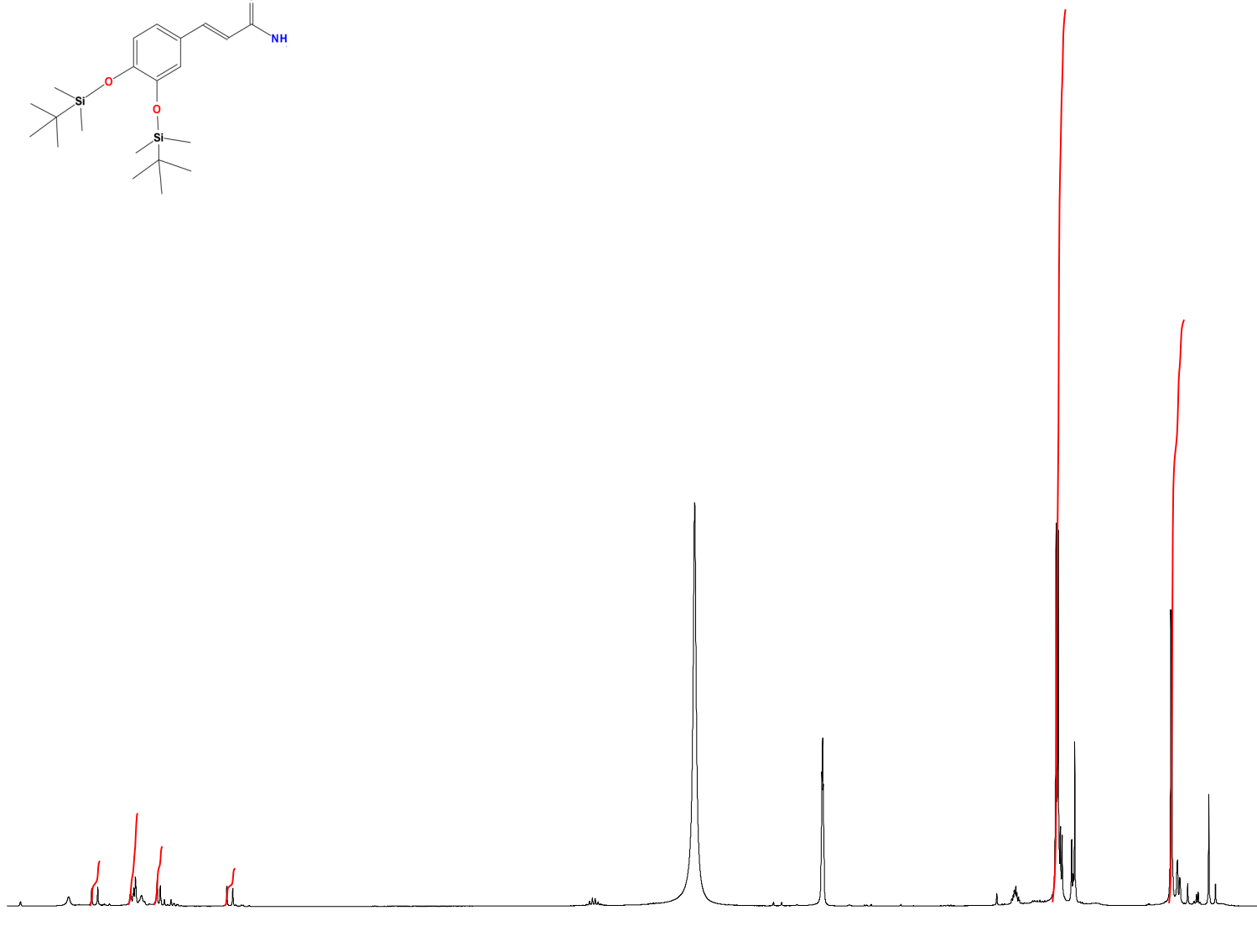


Current Data Parameters
NAME MBR17-22
EXPNO 1
PROCNO 1

F2 - Acquisition Parameters
Date_ 20170307
Time 12.47
INSTRUM spect
PROBHD 5 mm PABBO BB/
PULPROG zg30
TD 65536
SOLVENT DMSO
NS 16
DS 2
SWH 8012.820 Hz
FIDRES 0.122266 Hz
AQ 4.0894465 sec
RG 78.54
DW 62.400 usec
DE 6.50 usec
TE 300.0 K
D1 1.00000000 sec
TD0 1

==== CHANNEL f1 =====
SFO1 400.1324710 MHz
NUC1 1H
P1 8.60 usec
PLW1 18.10000038 W

F2 - Processing parameters
SI 65536
SF 400.1300089 MHz
WDW EM
SSB 0
LB 0.30 Hz
GB 0
PC 1.00

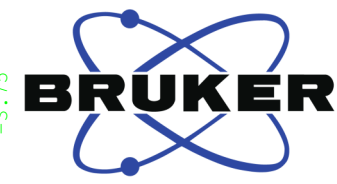
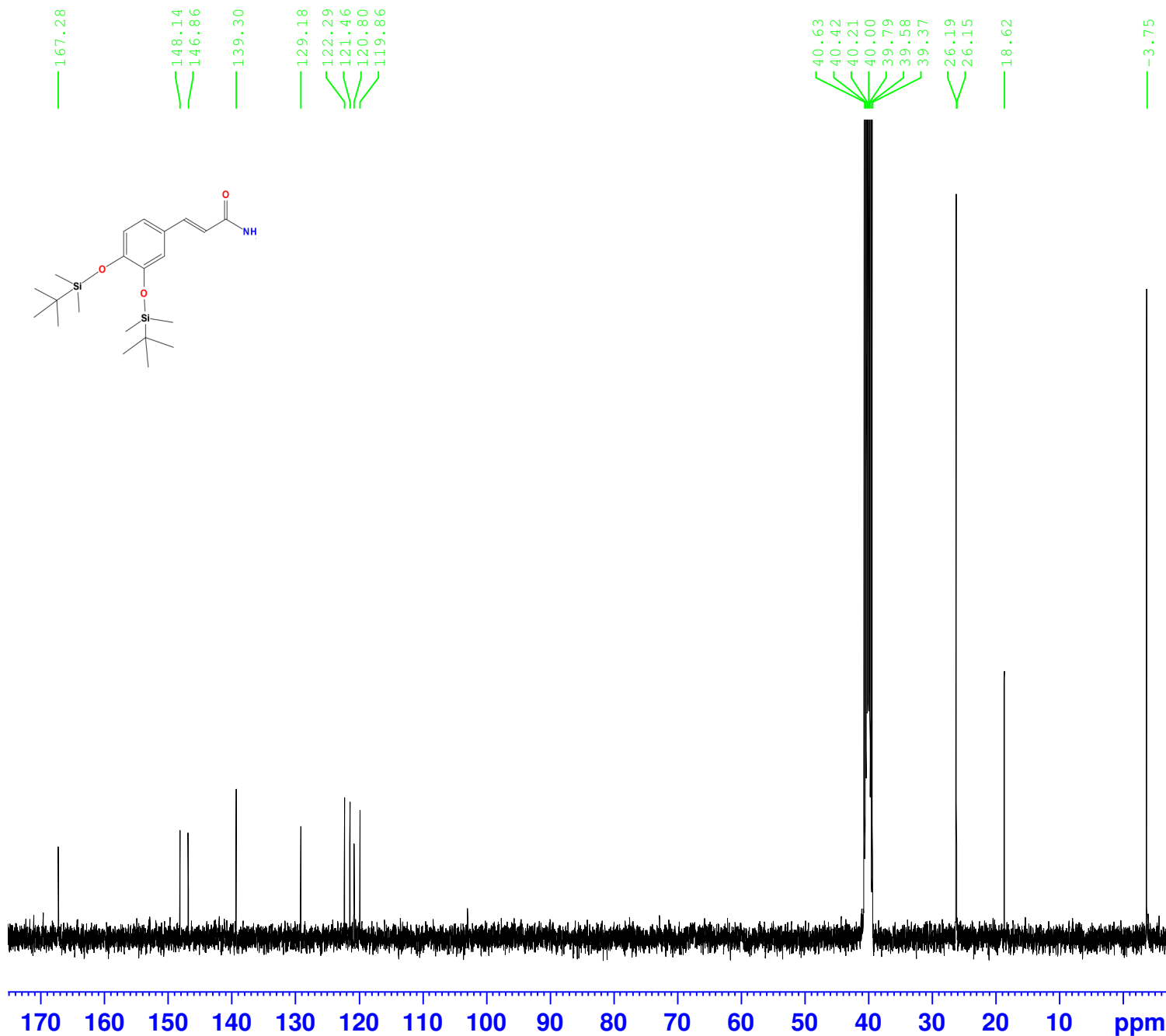


7.5 7.0 6.5 6.0 5.5 5.0 4.5 4.0 3.5 3.0 2.5 2.0 1.5 1.0 0.5 ppm

0.93
1.92
1.23
0.78

18.36
12.00

(5b)



Current Data Parameters
NAME MBR17-22
EXPNO 4
PROCNO 1

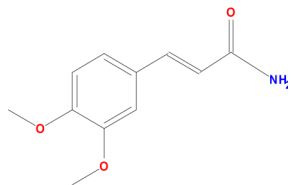
F2 - Acquisition Parameters
Date_ 20170329
Time 20.01
INSTRUM spect
PROBHD 5 mm PABBO BB/
PULPROG zgpg30
TD 65536
SOLVENT DMSO
NS 1024
DS 4
SWH 24038.461 Hz
FIDRES 0.366798 Hz
AQ 1.3631488 sec
RG 200.88
DW 20.800 usec
DE 6.50 usec
TE 300.0 K
D1 2.00000000 sec
D11 0.03000000 sec
TD0 1

==== CHANNEL f1 =====
SFO1 100.6228293 MHz
NUC1 13C
P1 8.40 usec
PLW1 88.19999695 W

==== CHANNEL f2 =====
SFO2 400.1316005 MHz
NUC2 1H
CPDPRG[2] waltz16
PCPD2 90.00 usec
PLW2 18.10000038 W
PLW12 0.16527000 W
PLW13 0.13387001 W

F2 - Processing parameters
SI 32768
SF 100.6127685 MHz
WDW EM
SSB 0
LB 1.00 Hz
GB 0
PC 1.40

(5c)

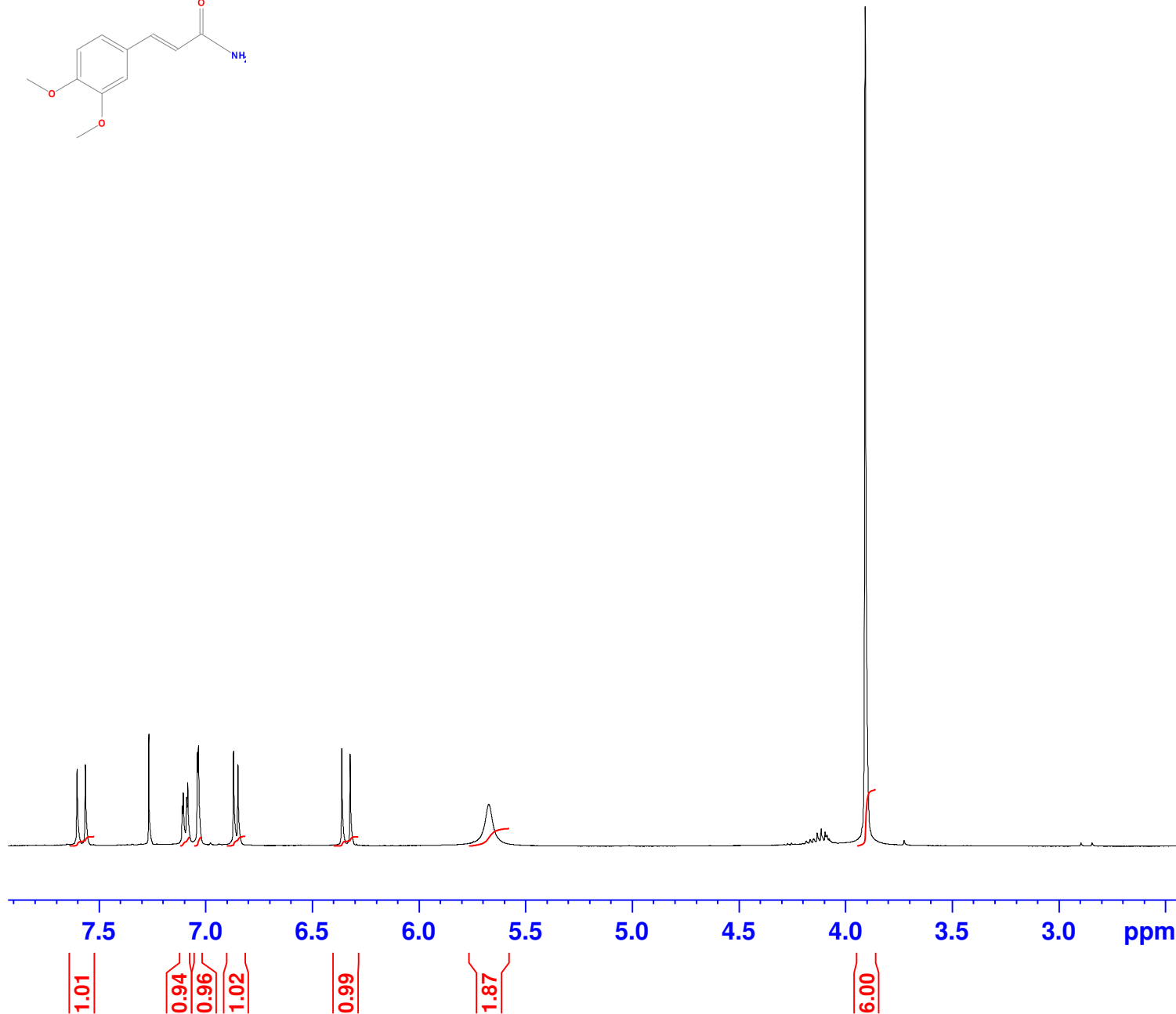


Current Data Parameters
NAME MBR17-36
EXPNO 1
PROCNO 1

F2 - Acquisition Parameters
Date_ 20170408
Time 14.04
INSTRUM spect
PROBHD 5 mm PABBO BB/
PULPROG zg30
TD 65536
SOLVENT CDC13
NS 16
DS 2
SWH 8012.820 Hz
FIDRES 0.122266 Hz
AQ 4.0894465 sec
RG 144
DW 62.400 usec
DE 6.50 usec
TE 300.0 K
D1 1.00000000 sec
TD0 1

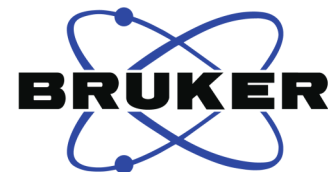
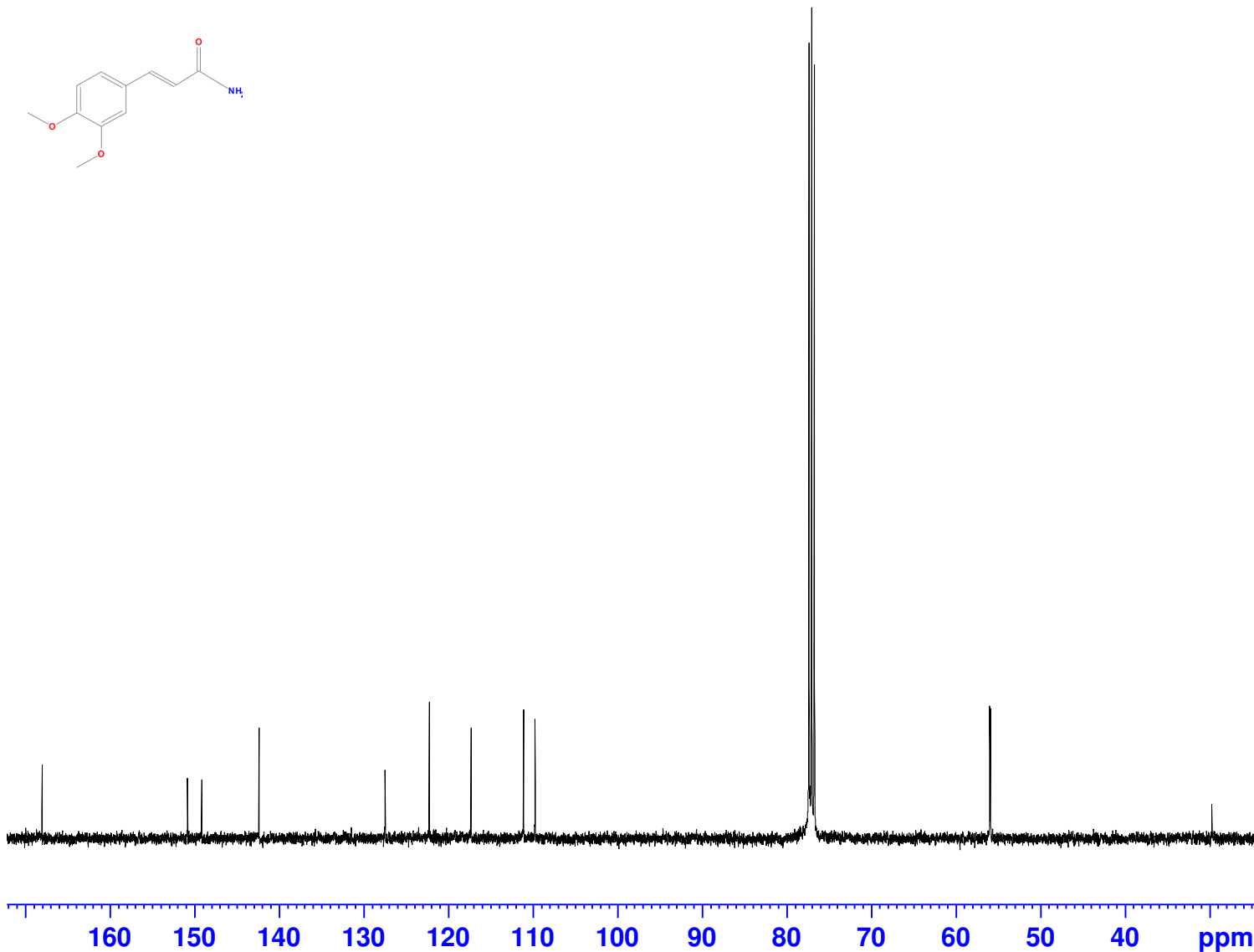
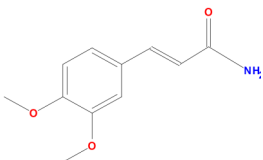
==== CHANNEL f1 =====
SFO1 400.1324710 MHz
NUC1 1H
P1 8.60 usec
PLW1 18.10000038 W

F2 - Processing parameters
SI 65536
SF 400.1300070 MHz
WDW EM
SSB 0
LB 0.30 Hz
GB 0
PC 1.00



(5c)

168.06
 150.86
 149.18
 142.39
 127.49
 122.27
 117.31
 111.10
 109.75
 77.35
 77.03
 76.71
 55.97
 55.89
 29.70



Current Data Parameters
 NAME MBR17-36
 EXPNO 3
 PROCNO 1

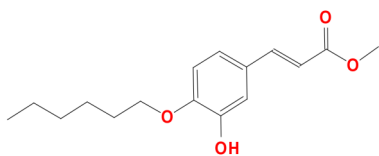
F2 - Acquisition Parameters
 Date_ 20170408
 Time 15.04
 INSTRUM spect
 PROBHD 5 mm PABBO BB/
 PULPROG zgpg30
 TD 65536
 SOLVENT CDC13
 NS 1024
 DS 4
 SWH 24038.461 Hz
 FIDRES 0.366798 Hz
 AQ 1.3631488 sec
 RG 200.88
 DW 20.800 usec
 DE 6.50 usec
 TE 300.0 K
 D1 2.00000000 sec
 D11 0.03000000 sec
 TD0 1

==== CHANNEL f1 =====
 SFO1 100.6228293 MHz
 NUC1 13C
 P1 8.40 usec
 PLW1 88.19999695 W

==== CHANNEL f2 =====
 SFO2 400.1316005 MHz
 NUC2 1H
 CPDPRG[2] waltz16
 PCPD2 90.00 usec
 PLW2 18.10000038 W
 PLW12 0.16527000 W
 PLW13 0.13387001 W

F2 - Processing parameters
 SI 32768
 SF 100.6127685 MHz
 WDW EM
 SSB 0
 LB 1.00 Hz
 GB 0
 PC 1.40

(8a)

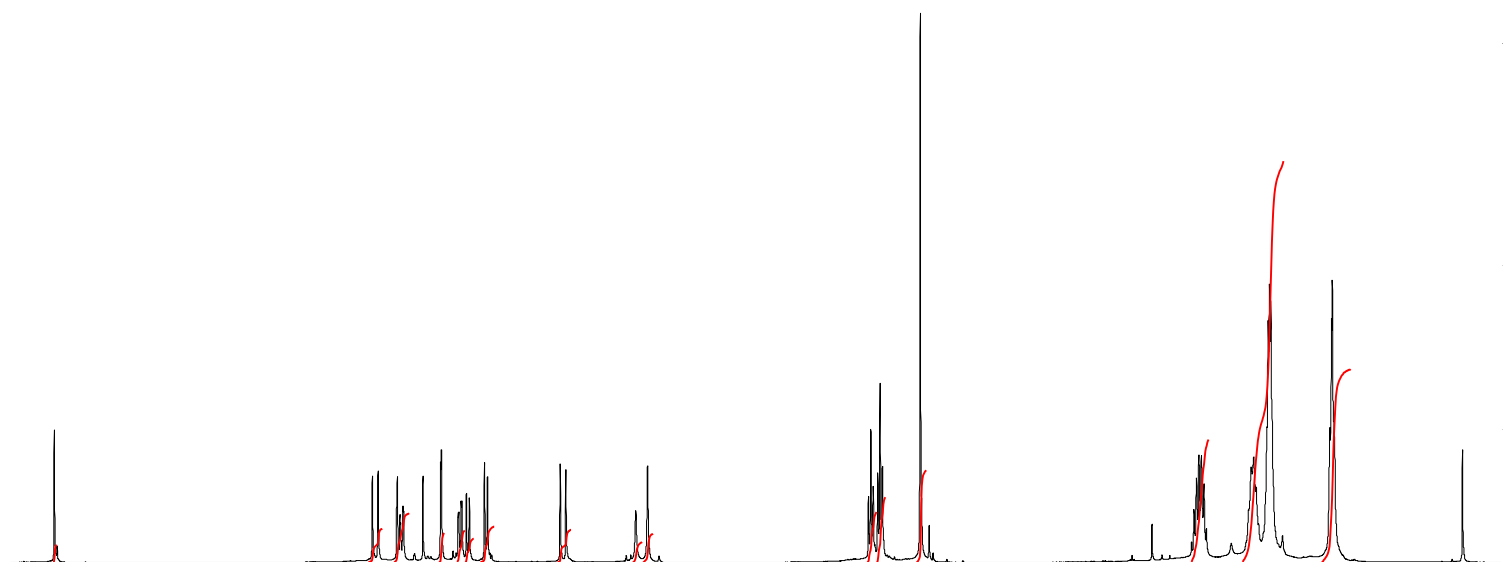


Current Data Parameters
NAME MBR17-44
EXPNO 1
PROCNO 1

F2 - Acquisition Parameters
Date_ 20170502
Time 11.23
INSTRUM spect
PROBHD 5 mm PABBO BB/
PULPROG zg30
TD 65536
SOLVENT CDC13
NS 16
DS 2
SWH 8012.820 Hz
FIDRES 0.122266 Hz
AQ 4.0894465 sec
RG 89.12
DW 62.400 usec
DE 6.50 usec
TE 300.0 K
D1 1.00000000 sec
TD0 1

==== CHANNEL f1 =====
SFO1 400.1324710 MHz
NUC1 1H
P1 8.60 usec
PLW1 18.10000038 W

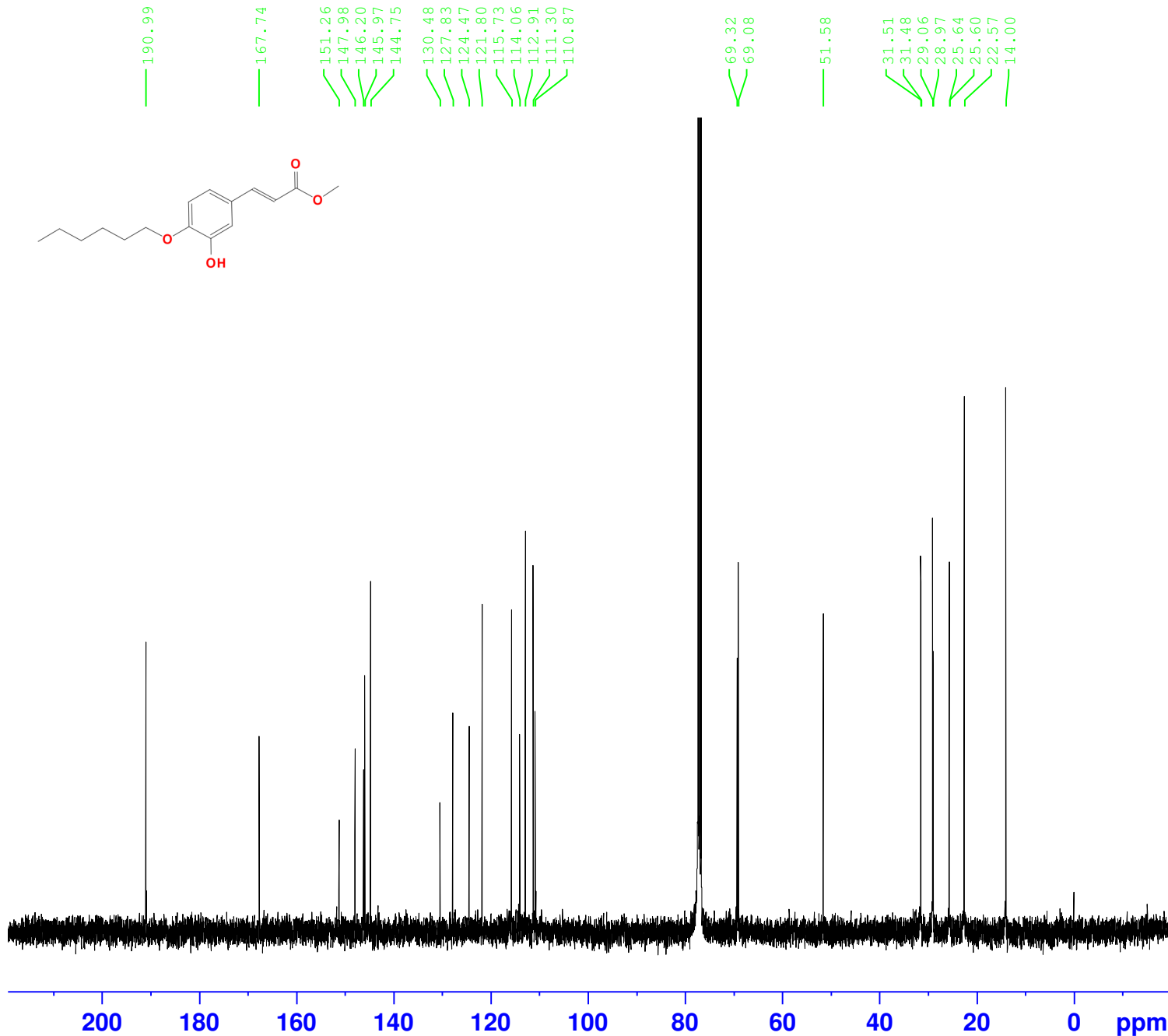
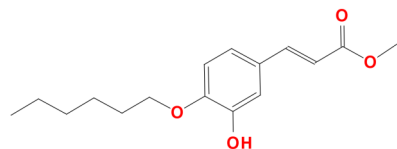
F2 - Processing parameters
SI 65536
SF 400.1300087 MHz
WDW EM
SSB 0
LB 0.30 Hz
GB 0
PC 1.00



10 9 8 7 6 5 4 3 2 1 ppm

0.56
1.07
1.53
0.92
1.01
0.74
1.12
1.02
0.65
0.90
1.58
2.05
2.86
3.84
12.44
5.99

(8a)



Current Data Parameters
NAME MBR17-44
EXPNO 2
PROCNO 1

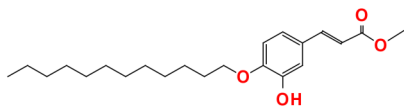
F2 - Acquisition Parameters
Date_ 20170502
Time 20.54
INSTRUM spect
PROBHD 5 mm PABBO BB/
PULPROG zgpg30
TD 65536
SOLVENT CDC13
NS 1024
DS 4
SWH 24038.461 Hz
FIDRES 0.366798 Hz
AQ 1.3631488 sec
RG 200.88
DW 20.800 usec
DE 6.50 usec
TE 300.0 K
D1 2.00000000 sec
D11 0.03000000 sec
TD0 1

==== CHANNEL f1 =====
SFO1 100.6228293 MHz
NUC1 13C
P1 8.40 usec
PLW1 88.19999695 W

==== CHANNEL f2 =====
SFO2 400.1316005 MHz
NUC2 1H
CPDPRG[2] waltz16
PCPD2 90.00 usec
PLW2 18.10000038 W
PLW12 0.16527000 W
PLW13 0.13387001 W

F2 - Processing parameters
SI 32768
SF 100.6127685 MHz
WDW EM
SSB 0
LB 1.00 Hz
GB 0
PC 1.40

(8b)

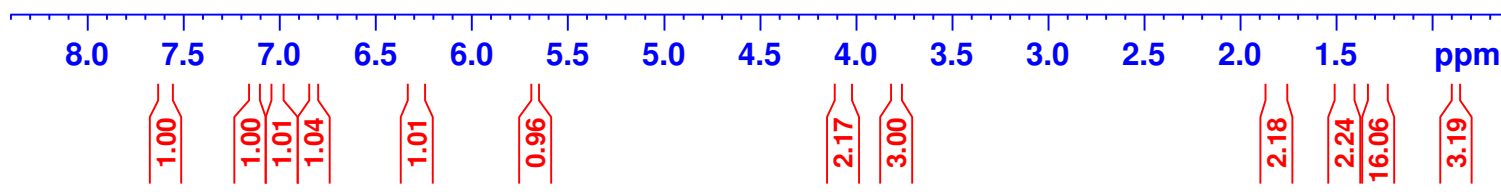
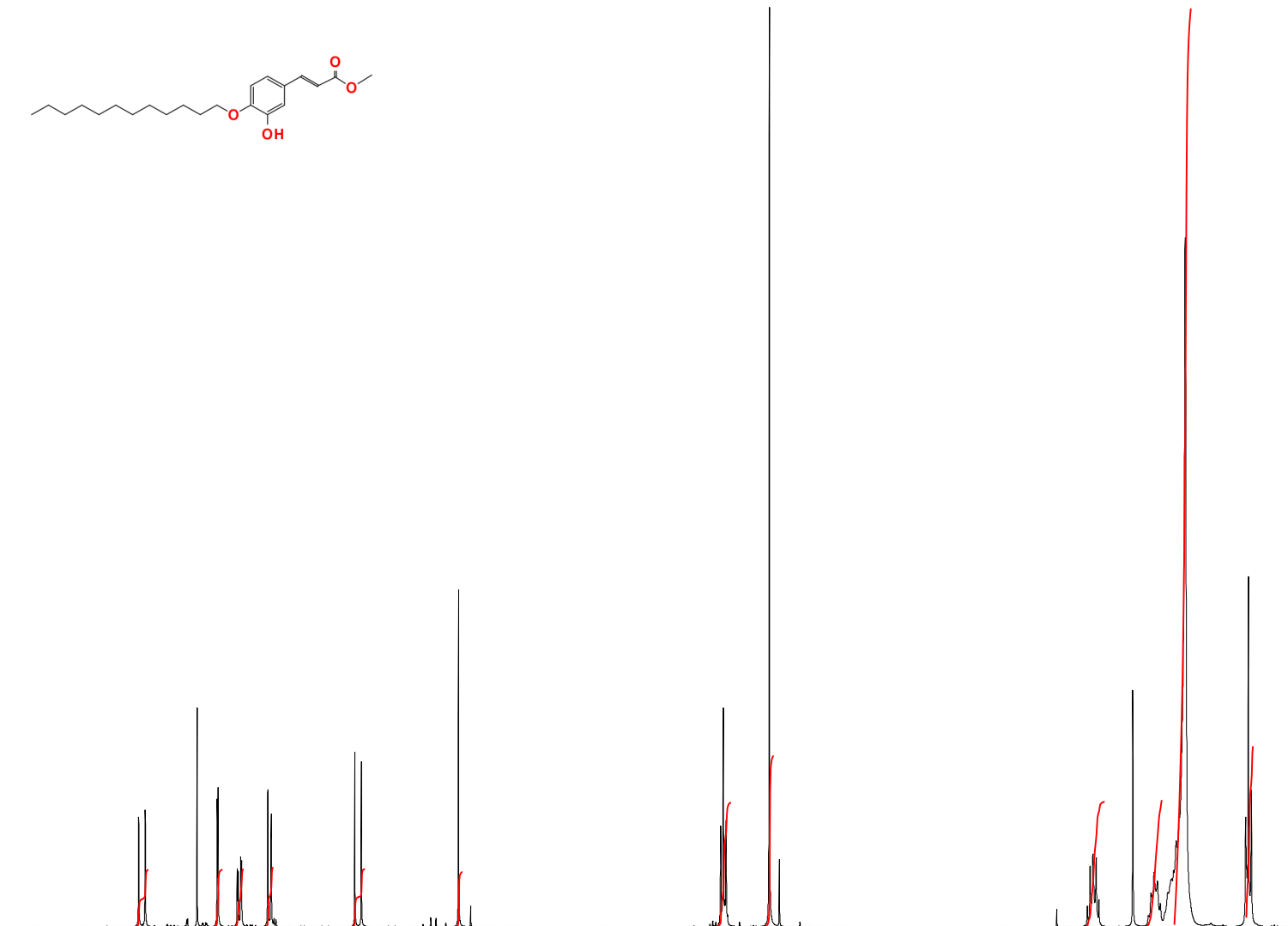


Current Data Parameters
NAME MBR17-53
EXPNO 1
PROCNO 1

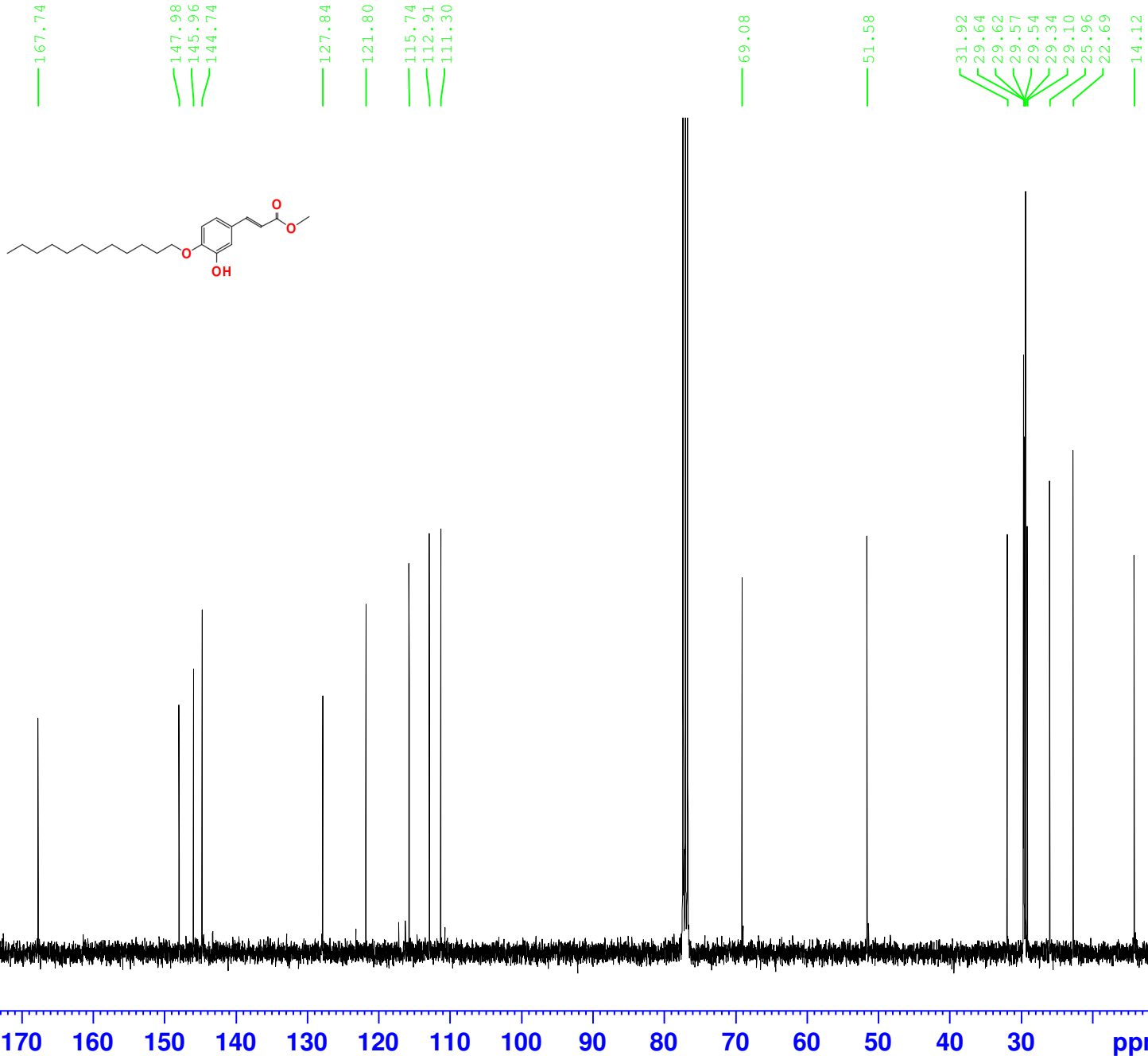
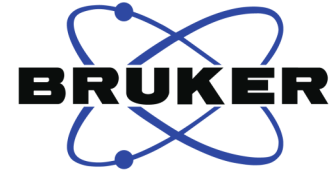
F2 - Acquisition Parameters
Date_ 20170530
Time 14.45
INSTRUM spect
PROBHD 5 mm PABBO BB/
PULPROG zg30
TD 65536
SOLVENT CDC13
NS 16
DS 2
SWH 8012.820 Hz
FIDRES 0.122266 Hz
AQ 4.0894465 sec
RG 103.33
DW 62.400 usec
DE 6.50 usec
TE 300.0 K
D1 1.00000000 sec
TD0 1

==== CHANNEL f1 =====
SFO1 400.1324710 MHz
NUC1 1H
P1 8.60 usec
PLW1 18.10000038 W

F2 - Processing parameters
SI 65536
SF 400.130097 MHz
WDW EM
SSB 0
LB 0.30 Hz
GB 0
PC 1.00



(8b)



Current Data Parameters
NAME MBR17-53
EXPNO 2
PROCNO 1

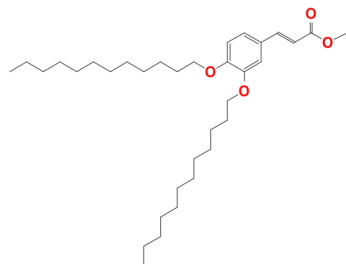
F2 - Acquisition Parameters
Date_ 20170530
Time 20.01
INSTRUM spect
PROBHD 5 mm PABBO BB/
PULPROG zgpg30
TD 65536
SOLVENT CDC13
NS 1024
DS 4
SWH 24038.461 Hz
FIDRES 0.366798 Hz
AQ 1.3631488 sec
RG 200.88
DW 20.800 usec
DE 6.50 usec
TE 300.0 K
D1 2.0000000 sec
D11 0.0300000 sec
TD0 1

==== CHANNEL f1 =====
SFO1 100.6228293 MHz
NUC1 13C
P1 8.40 usec
PLW1 88.19999695 W

==== CHANNEL f2 =====
SFO2 400.1316005 MHz
NUC2 1H
CPDPRG[2] waltz16
PCPD2 90.00 usec
PLW2 18.10000038 W
PLW12 0.16527000 W
PLW13 0.13387001 W

F2 - Processing parameters
SI 32768
SF 100.6127685 MHz
WDW EM
SSB 0
LB 1.00 Hz
GB 0
PC 1.40

8d

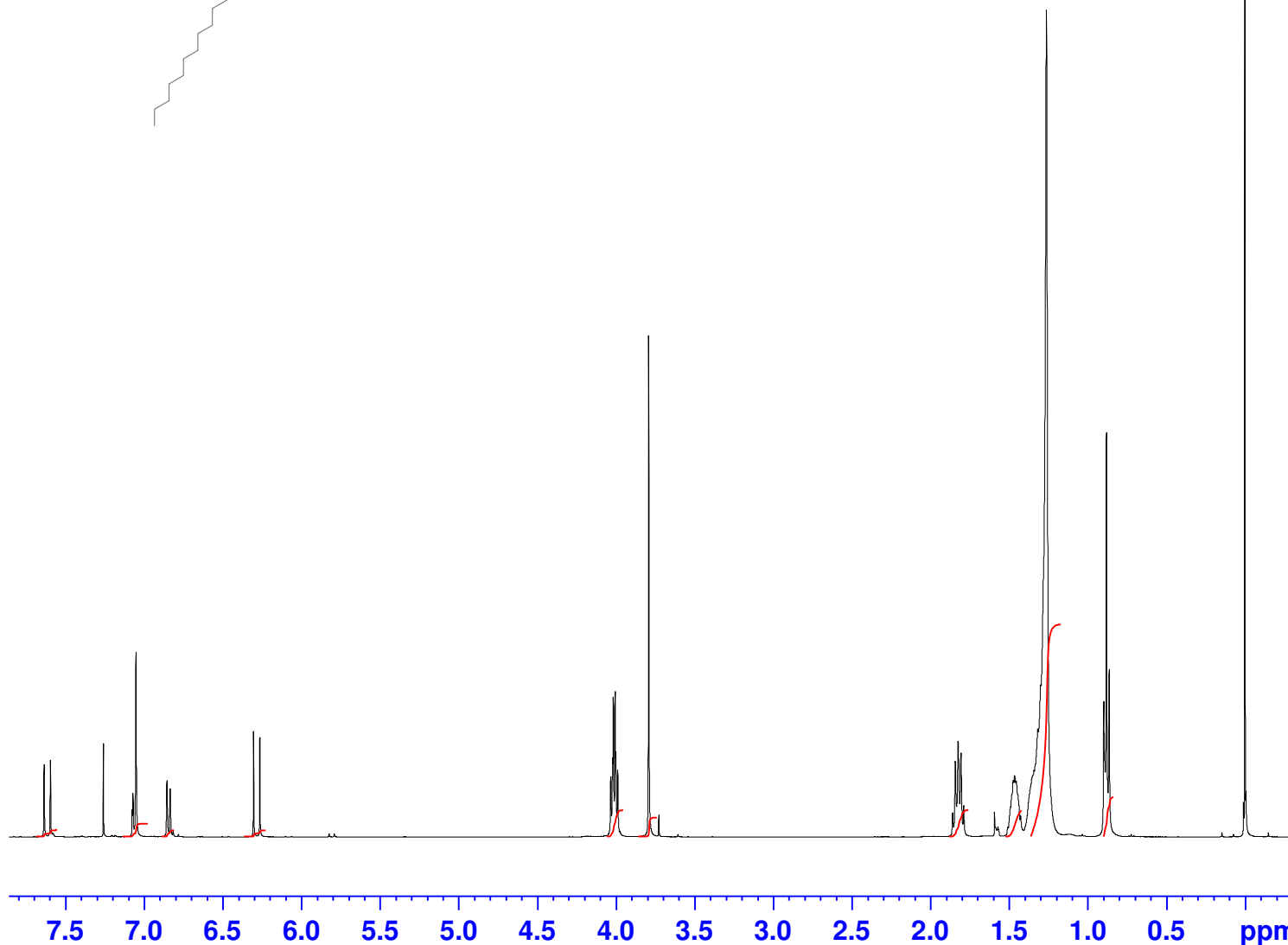


Current Data Parameters
NAME MBR17-64
EXPNO 1
PROCNO 1

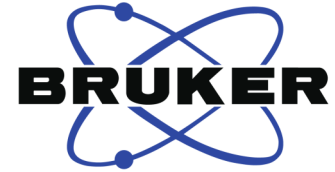
F2 - Acquisition Parameters
Date_ 20170702
Time 20.29
INSTRUM spect
PROBHD 5 mm PABBO BB/
PULPROG zg30
TD 65536
SOLVENT CDC13
NS 16
DS 2
SWH 8012.820 Hz
FIDRES 0.122266 Hz
AQ 4.0894465 sec
RG 58.75
DW 62.400 usec
DE 6.50 usec
TE 297.5 K
D1 1.00000000 sec
TD0 1

==== CHANNEL f1 =====
SFO1 400.1324710 MHz
NUC1 1H
P1 8.60 usec
PLW1 18.10000038 W

F2 - Processing parameters
SI 65536
SF 400.1300095 MHz
WDW EM
SSB 0
LB 0.30 Hz
GB 0
PC 1.00



1.00 1.97 1.01 0.97 4.03 2.92 4.04 3.99 32.18 6.02



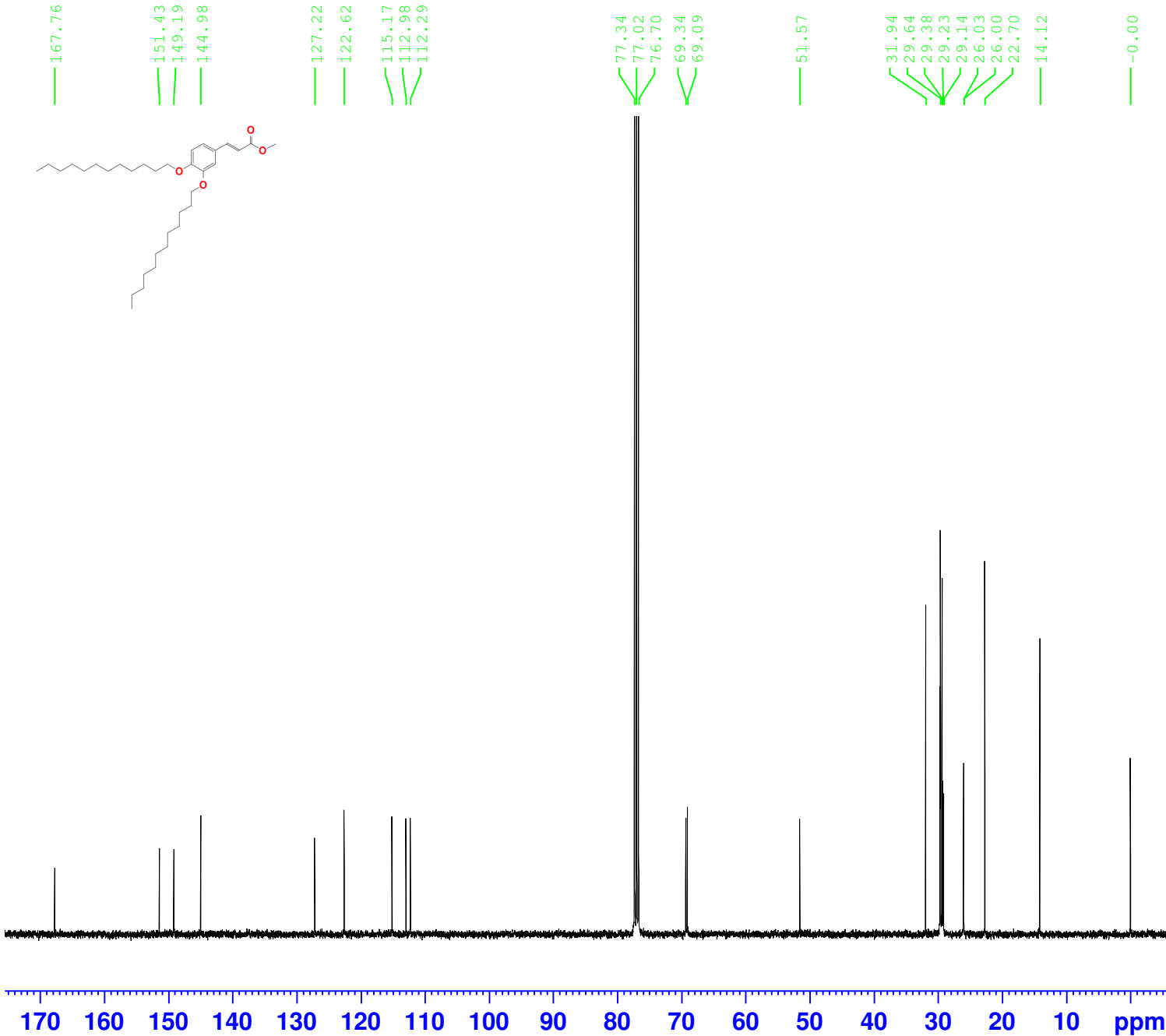
Current Data Parameters
NAME MBR17-64
EXPNO 2
PROCNO 1

F2 - Acquisition Parameters
Date_ 20170702
Time 21.29
INSTRUM spect
PROBHD 5 mm PABBO BB/
PULPROG zgpg30
TD 65536
SOLVENT CDC13
NS 1024
DS 4
SWH 24038.461 Hz
FIDRES 0.366798 Hz
AQ 1.3631488 sec
RG 200.88
DW 20.800 usec
DE 6.50 usec
TE 298.4 K
D1 2.0000000 sec
D11 0.0300000 sec
TD0 1

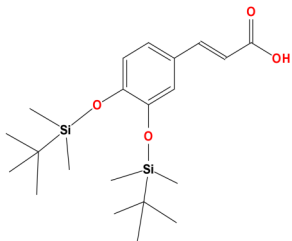
=====
CHANNEL f1
SFO1 100.6228293 MHz
NUC1 13C
P1 8.40 usec
PLW1 88.19999695 W

=====
CHANNEL f2
SFO2 400.1316005 MHz
NUC2 1H
CPDPRG[2] waltz16
PCPD2 90.00 usec
PLW2 18.10000038 W
PLW12 0.16527000 W
PLW13 0.13387001 W

F2 - Processing parameters
SI 32768
SF 100.6127688 MHz
WDW EM
SSB 0
LB 1.00 Hz
GB 0
PC 1.40



(9a)

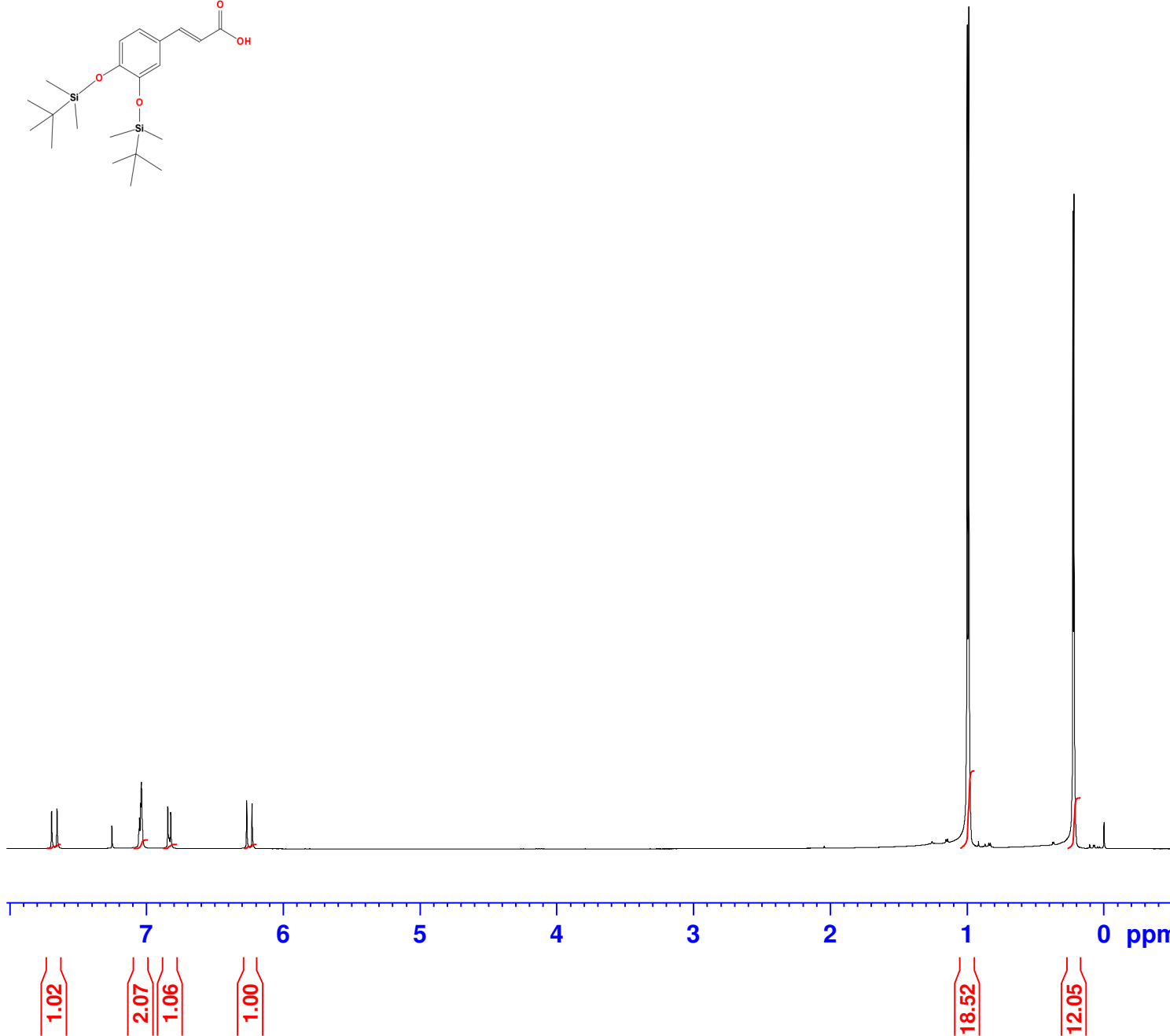


Current Data Parameters
NAME MBR17-13 1
EXPNO 1
PROCNO 1

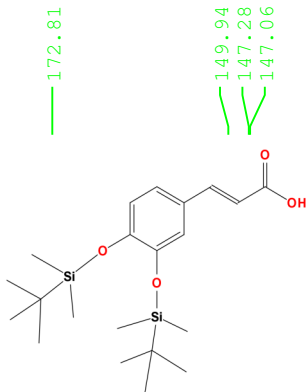
F2 - Acquisition Parameters
Date_ 20170506
Time 16.05
INSTRUM spect
PROBHD 5 mm PABBO BB/
PULPROG zg30
TD 65536
SOLVENT CDC13
NS 16
DS 2
SWH 8012.820 Hz
FIDRES 0.122266 Hz
AQ 4.0894465 sec
RG 58.75
DW 62.400 usec
DE 6.50 usec
TE 300.0 K
D1 1.00000000 sec
TD0 1

==== CHANNEL f1 =====
SFO1 400.1324710 MHz
NUC1 1H
P1 8.60 usec
PLW1 18.10000038 W

F2 - Processing parameters
SI 65536
SF 400.1300126 MHz
WDW EM
SSB 0
LB 0.30 Hz
GB 0
PC 1.00



(9a)



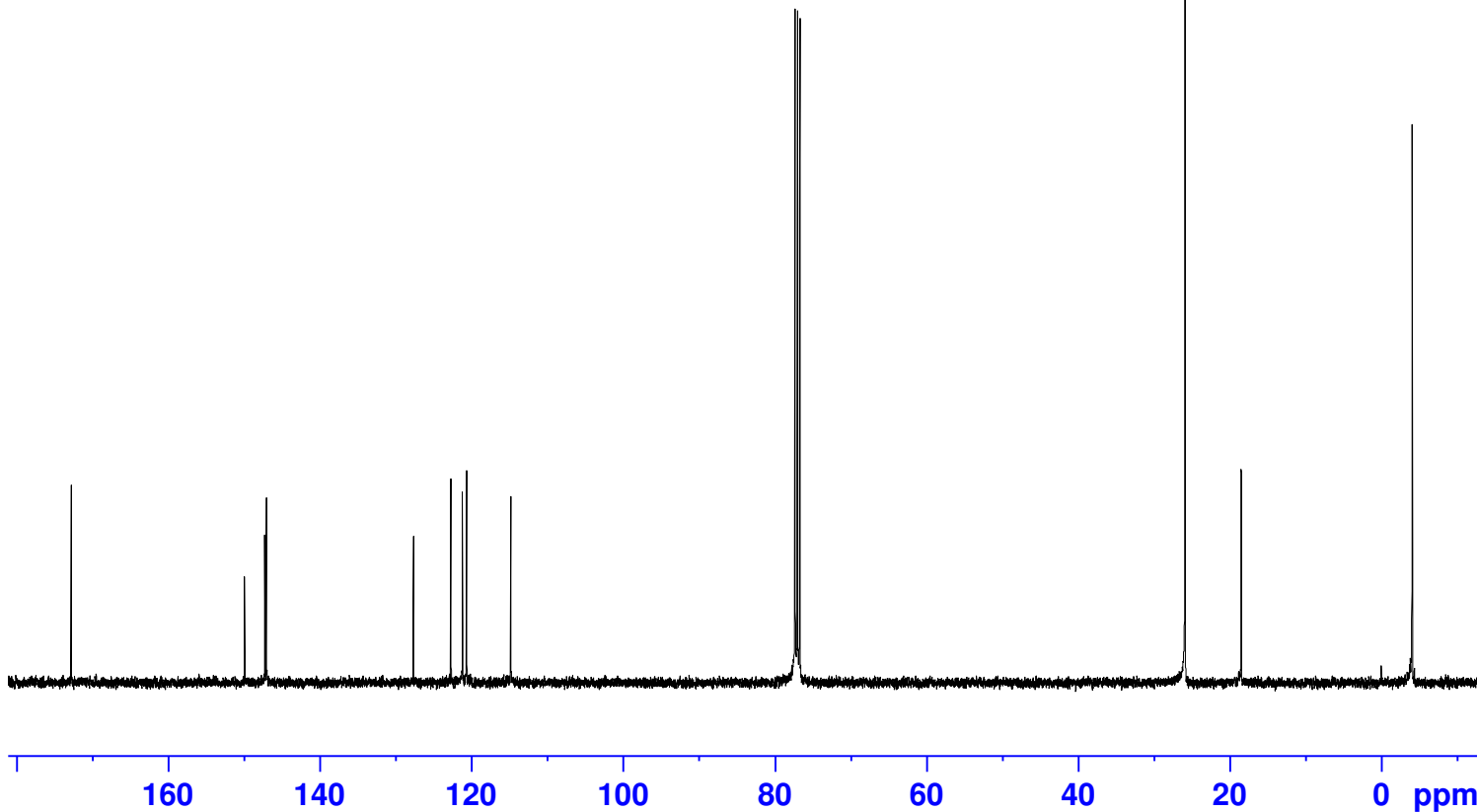
Current Data Parameters
NAME MBR17-13 1
EXPNO 2
PROCNO 1

F2 - Acquisition Parameters
Date_ 20170506
Time 17.05
INSTRUM spect
PROBHD 5 mm PABBO BB/
PULPROG zgpg30
TD 65536
SOLVENT CDC13
NS 1024
DS 4
SWH 24038.461 Hz
FIDRES 0.366798 Hz
AQ 1.3631488 sec
RG 200.88
DW 20.800 usec
DE 6.50 usec
TE 300.0 K
D1 2.00000000 sec
D11 0.03000000 sec
TD0 1

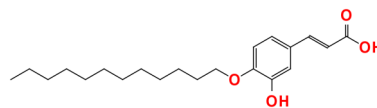
=====
SFO1 100.6228293 MHz
NUC1 13C
P1 8.40 usec
PLW1 88.19999695 W

=====
SFO2 400.1316005 MHz
NUC2 1H
CPDPRG[2] waltz16
PCPD2 90.00 usec
PLW2 18.10000038 W
PLW12 0.16527000 W
PLW13 0.13387001 W

F2 - Processing parameters
SI 32768
SF 100.6127685 MHz
WDW EM
SSB 0
LB 1.00 Hz
GB 0
PC 1.40



(9c)

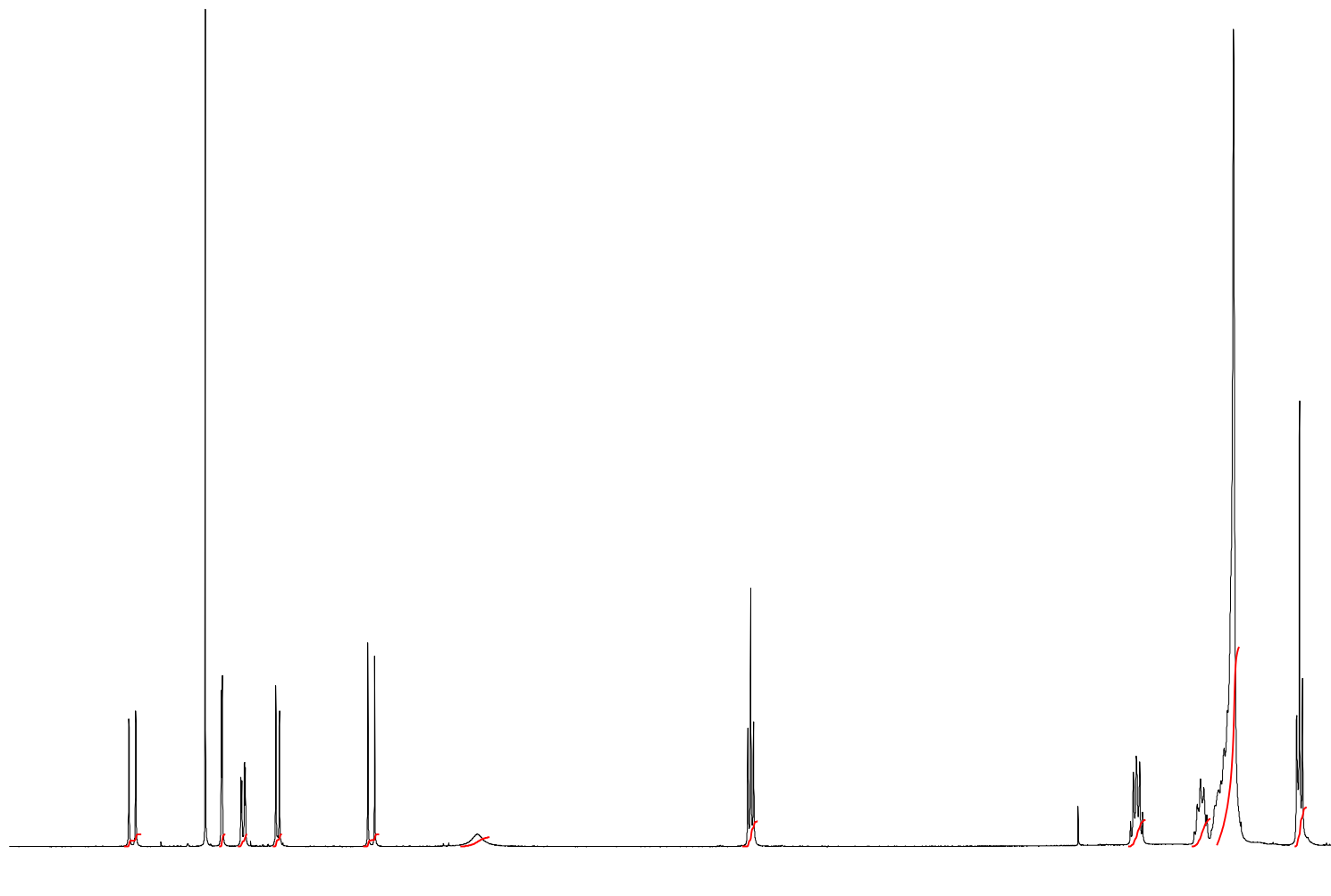


Current Data Parameters
NAME MBR17-54
EXPNO 1
PROCNO 1

F2 - Acquisition Parameters
Date_ 20170601
Time 0.52
INSTRUM spect
PROBHD 5 mm PABBO BB/
PULPROG zg30
TD 65536
SOLVENT CDC13
NS 16
DS 2
SWH 8012.820 Hz
FIDRES 0.122266 Hz
AQ 4.0894465 sec
RG 177.22
DW 62.400 usec
DE 6.50 usec
TE 300.0 K
D1 1.00000000 sec
TD0 1

==== CHANNEL f1 =====
SFO1 400.1324710 MHz
NUC1 1H
P1 8.60 usec
PLW1 18.10000038 W

F2 - Processing parameters
SI 65536
SF 400.1300100 MHz
WDW EM
SSB 0
LB 0.30 Hz
GB 0
PC 1.00



8.0 7.5 7.0 6.5 6.0 5.5 5.0 4.5 4.0 3.5 3.0 2.5 2.0 1.5 ppm

1.00 0.98 0.99 1.00 1.00 0.76 2.04 2.17 2.27 16.21 3.19

148.33
146.88
146.01

127.52

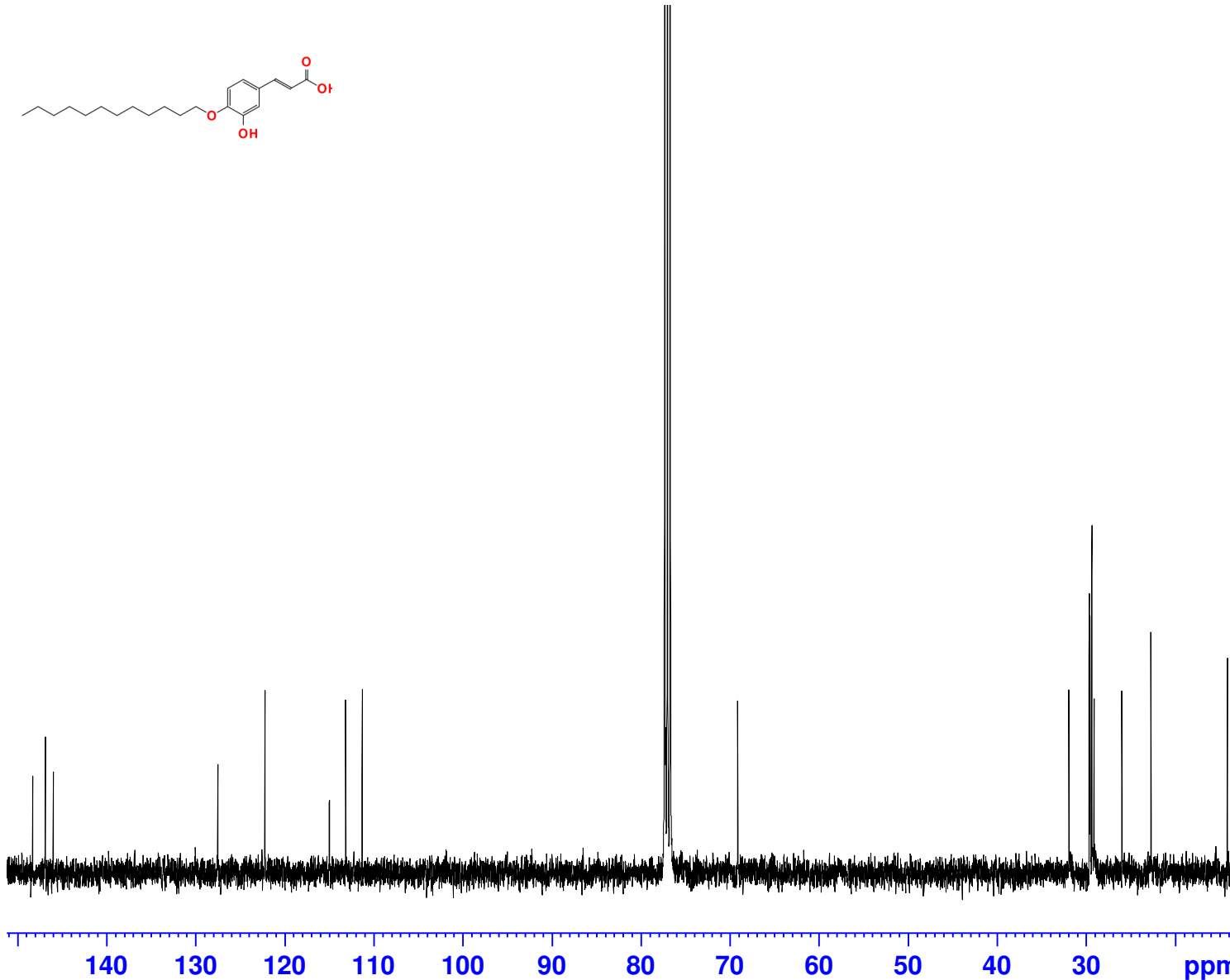
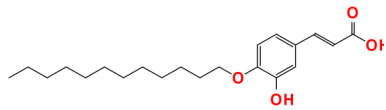
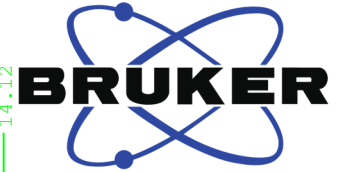
122.21

114.99
113.16
111.31

69.11

31.92
29.64
29.62
29.57
29.54
29.34
29.09
25.96
22.69

14.12



Current Data Parameters
NAME MBR17-54
EXPNO 2
PROCNO 1

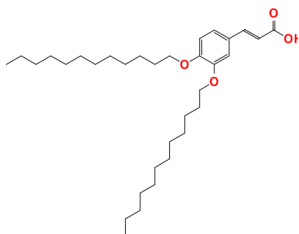
F2 - Acquisition Parameters
Date_ 20170601
Time 1.52
INSTRUM spect
PROBHD 5 mm PABBO BB/
PULPROG zgpg30
TD 65536
SOLVENT CDC13
NS 1024
DS 4
SWH 24038.461 Hz
FIDRES 0.366798 Hz
AQ 1.3631488 sec
RG 200.88
DW 20.800 usec
DE 6.50 usec
TE 300.0 K
D1 2.00000000 sec
D11 0.03000000 sec
TD0 1

=====
CHANNEL f1
SFO1 100.6228293 MHz
NUC1 13C
P1 8.40 usec
PLW1 88.19999695 W

=====
CHANNEL f2
SFO2 400.1316005 MHz
NUC2 1H
CPDPRG[2] waltz16
PCPD2 90.00 usec
PLW2 18.10000038 W
PLW12 0.16527000 W
PLW13 0.13387001 W

F2 - Processing parameters
SI 32768
SF 100.6127685 MHz
WDW EM
SSB 0
LB 1.00 Hz
GB 0
PC 1.40

(9d)

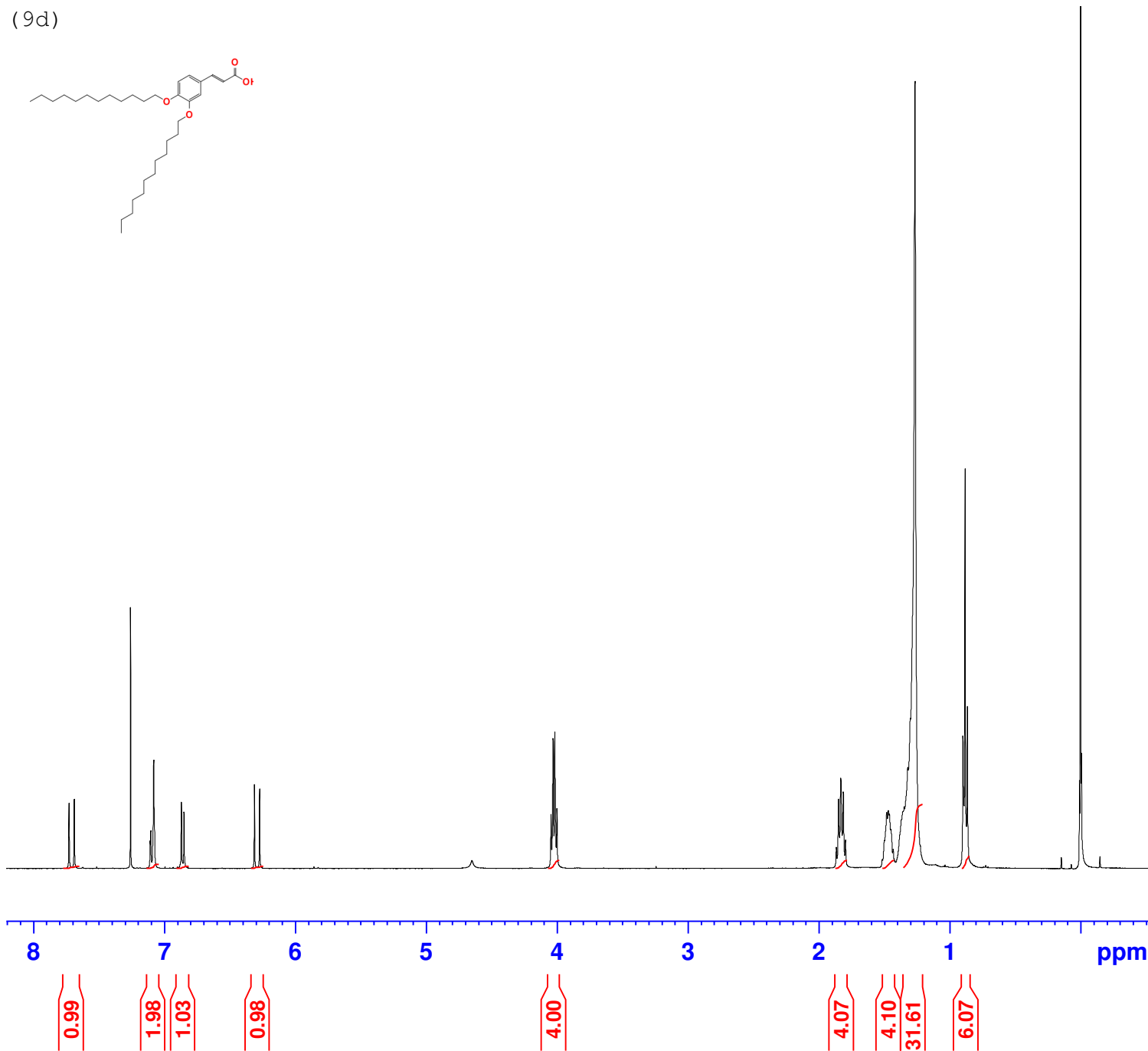


Current Data Parameters
NAME MBR17-67
EXPNO 1
PROCNO 1

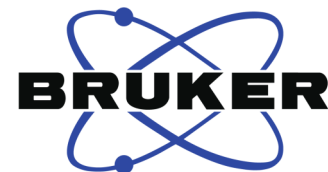
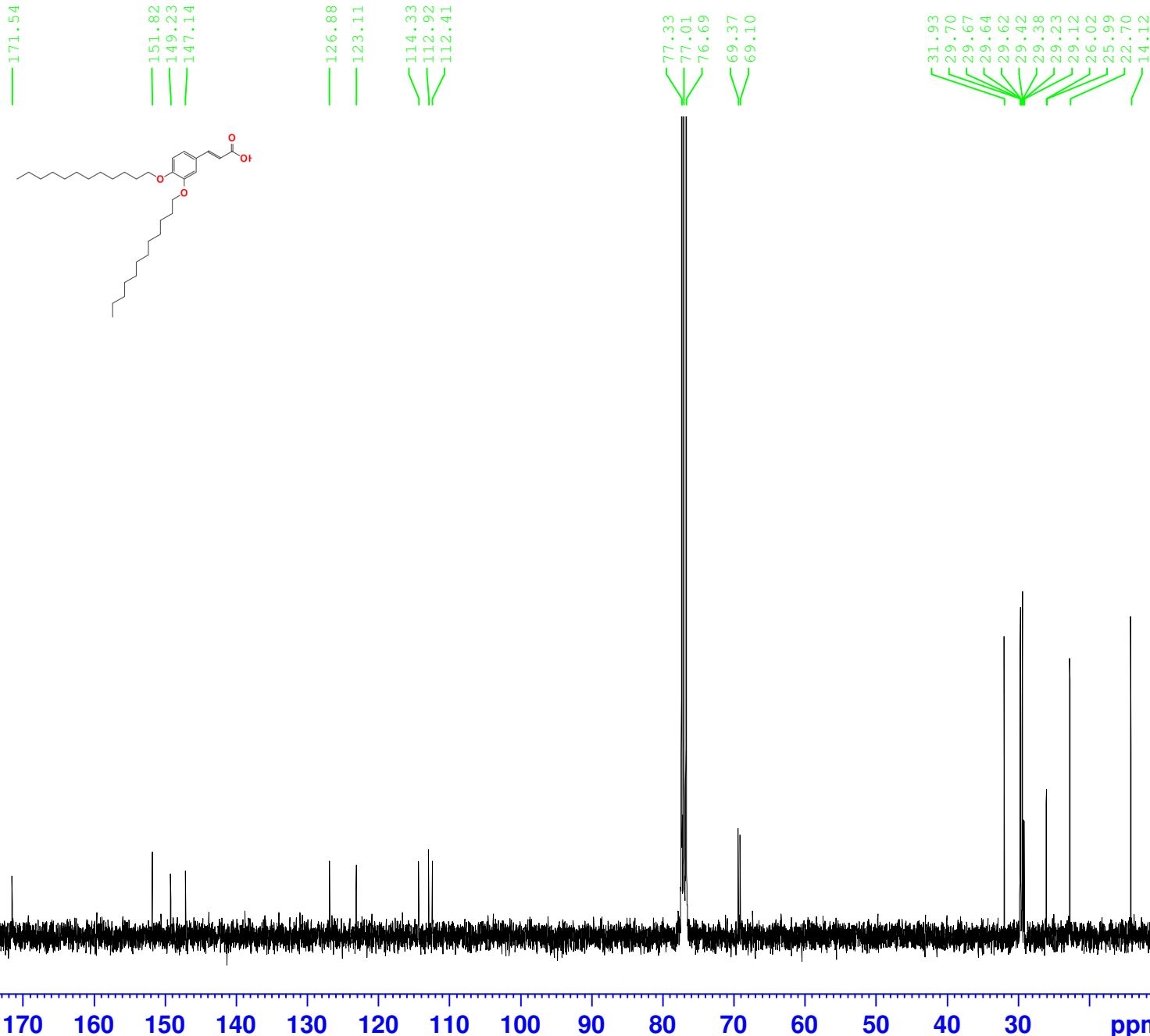
F2 - Acquisition Parameters
Date_ 20170703
Time 14.01
INSTRUM spect
PROBHD 5 mm PABBO BB/
PULPROG zg30
TD 65536
SOLVENT CDC13
NS 16
DS 2
SWH 8012.820 Hz
FIDRES 0.122266 Hz
AQ 4.0894465 sec
RG 128.29
DW 62.400 usec
DE 6.50 usec
TE 300.0 K
D1 1.00000000 sec
TD0 1

==== CHANNEL f1 =====
SFO1 400.1324710 MHz
NUC1 1H
P1 8.60 usec
PLW1 18.1000038 W

F2 - Processing parameters
SI 65536
SF 400.130098 MHz
WDW EM
SSB 0
LB 0.30 Hz
GB 0
PC 1.00



(9d)



Current Data Parameters
 NAME MBR17-67
 EXPNO 2
 PROCNO 1

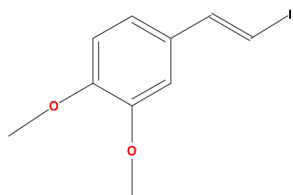
F2 - Acquisition Parameters
 Date_ 20170703
 Time 19.01
 INSTRUM spect
 PROBHD 5 mm PABBO BB/
 PULPROG zgpg30
 TD 65536
 SOLVENT CDC13
 NS 1024
 DS 4
 SWH 24038.461 Hz
 FIDRES 0.366798 Hz
 AQ 1.3631488 sec
 RG 200.88
 DW 20.800 usec
 DE 6.50 usec
 TE 300.0 K
 D1 2.00000000 sec
 D11 0.03000000 sec
 TD0 1

==== CHANNEL f1 =====
 SFO1 100.6228293 MHz
 NUC1 13C
 P1 8.40 usec
 PLW1 88.19999695 W

==== CHANNEL f2 =====
 SFO2 400.1316005 MHz
 NUC2 1H
 CPDPRG[2] waltz16
 PCPD2 90.00 usec
 PLW2 18.10000038 W
 PLW12 0.16527000 W
 PLW13 0.13387001 W

F2 - Processing parameters
 SI 32768
 SF 100.6127686 MHz
 WDW EM
 SSB 0
 LB 1.00 Hz
 GB 0
 PC 1.40

(11a)

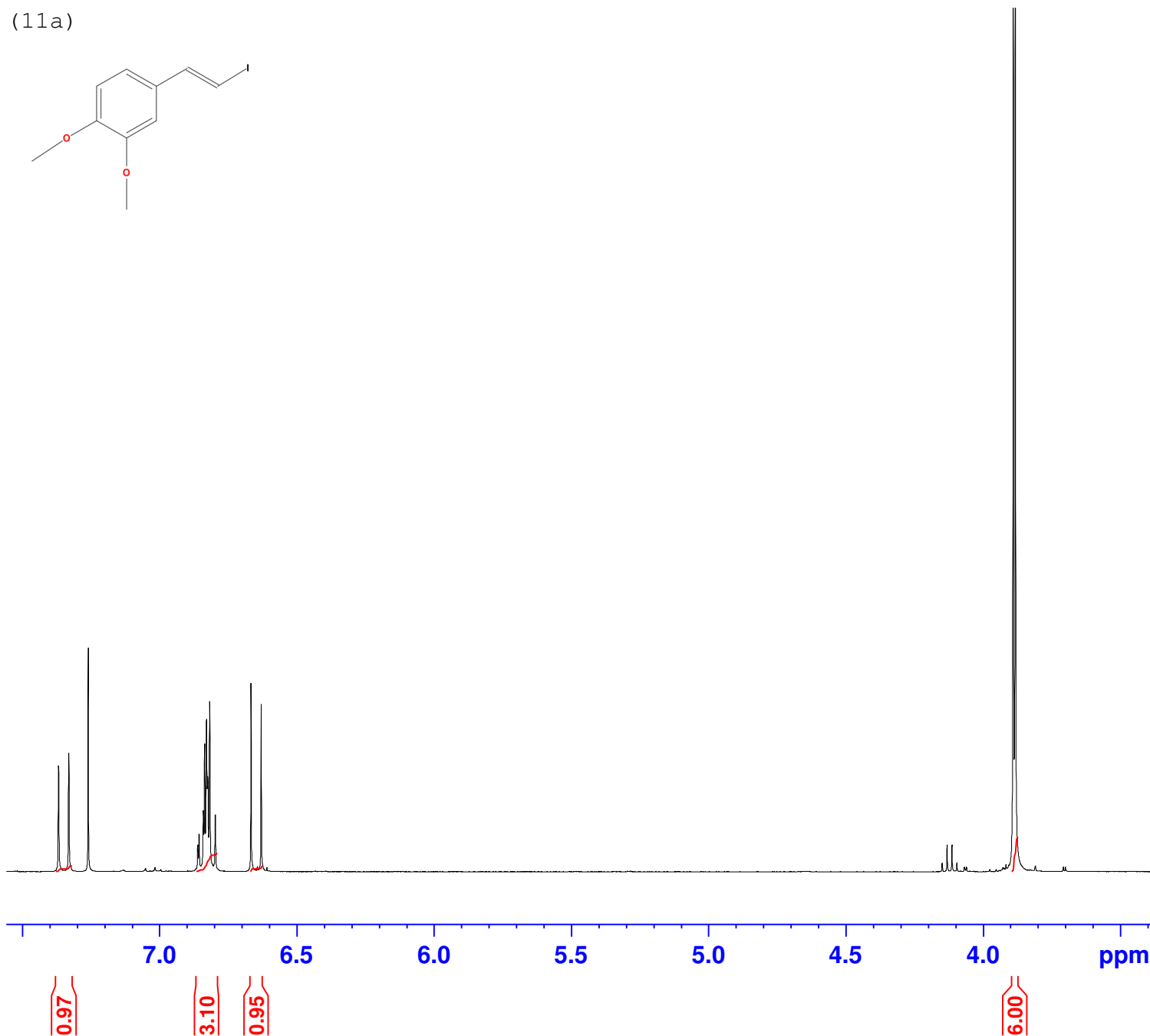


Current Data Parameters
NAME MBR17-21
EXPNO 1
PROCNO 1

F2 - Acquisition Parameters
Date_ 20170303
Time 11.19
INSTRUM spect
PROBHD 5 mm PABBO BB/
PULPROG zg30
TD 65536
SOLVENT CDC13
NS 16
DS 2
SWH 8012.820 Hz
FIDRES 0.122266 Hz
AQ 4.0894465 sec
RG 158.48
DW 62.400 usec
DE 6.50 usec
TE 300.0 K
D1 1.00000000 sec
TD0 1

==== CHANNEL f1 =====
SFO1 400.1324710 MHz
NUC1 1H
P1 8.60 usec
PLW1 18.10000038 W

F2 - Processing parameters
SI 65536
SF 400.1300094 MHz
WDW EM
SSB 0
LB 0.30 Hz
GB 0
PC 1.00





149.46
149.08
144.55

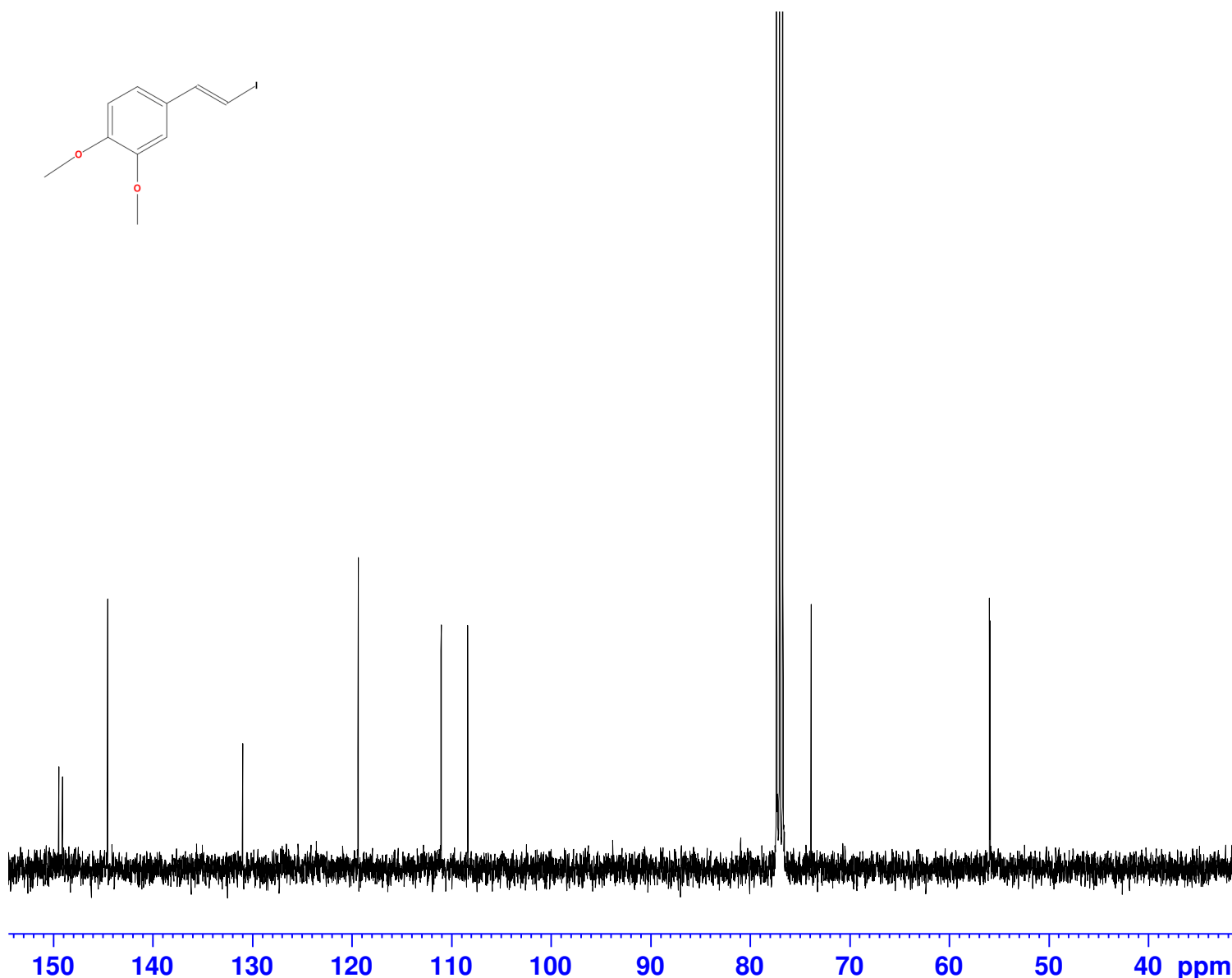
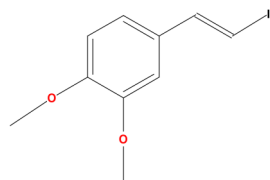
130.97

119.38

111.04
108.36

73.85

55.94
55.88



Current Data Parameters
NAME MBR17-21
EXPNO 2
PROCNO 1

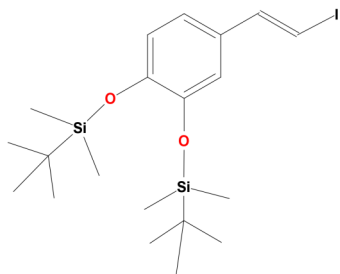
F2 - Acquisition Parameters
Date_ 20170303
Time 11.35
INSTRUM spect
PROBHD 5 mm PABBO BB/
PULPROG zgpg30
TD 65536
SOLVENT CDC13
NS 256
DS 2
SWH 24038.461 Hz
FIDRES 0.366798 Hz
AQ 1.3631488 sec
RG 200.88
DW 20.800 usec
DE 6.50 usec
TE 300.0 K
D1 2.00000000 sec
D11 0.03000000 sec
TD0 1

=====
CHANNEL f1
SFO1 100.6228298 MHz
NUC1 13C
P1 8.40 usec
PLW1 88.19999695 W

=====
CHANNEL f2
SFO2 400.1316005 MHz
NUC2 1H
CPDPRG[2] waltz16
PCPD2 90.00 usec
PLW2 18.10000038 W
PLW12 0.16527000 W
PLW13 0.13387001 W

F2 - Processing parameters
SI 32768
SF 100.6127685 MHz
WDW EM
SSB 0
LB 1.00 Hz
GB 0
PC 1.40

(11b)

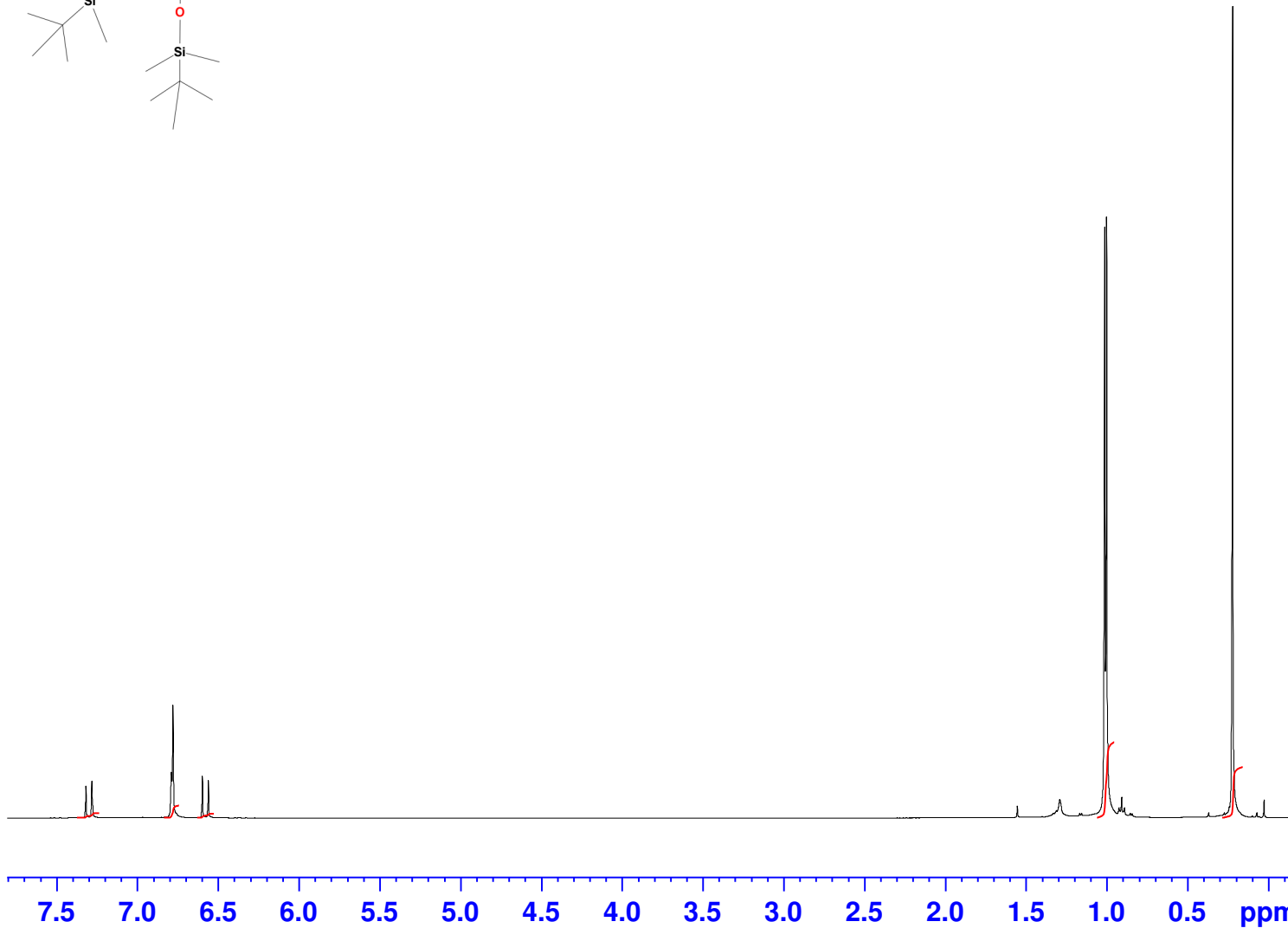


Current Data Parameters
NAME MBR17-48
EXPNO 1
PROCNO 1

F2 - Acquisition Parameters
Date_ 20170508
Time 13.26
INSTRUM spect
PROBHD 5 mm PABBO BB/
PULPROG zg30
TD 65536
SOLVENT CDC13
NS 16
DS 2
SWH 8012.820 Hz
FIDRES 0.122266 Hz
AQ 4.0894465 sec
RG 31.74
DW 62.400 usec
DE 6.50 usec
TE 300.0 K
D1 1.00000000 sec
TD0 1

==== CHANNEL f1 =====
SFO1 400.1324710 MHz
NUC1 1H
P1 8.60 usec
PLW1 18.10000038 W

F2 - Processing parameters
SI 65536
SF 400.1300024 MHz
WDW EM
SSB 0
LB 0.30 Hz
GB 0
PC 1.00



1.15

2.93

1.02

18.00

12.05

147.56
146.97
144.53

131.53

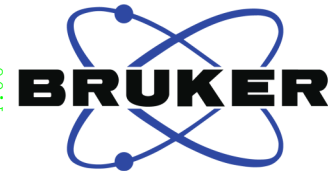
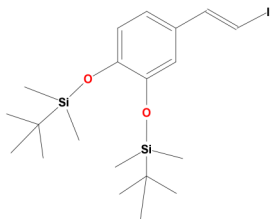
121.06
119.56
118.60

73.69

25.94

18.46

-4.06



Current Data Parameters
 NAME MBR17-48
 EXPNO 2
 PROCNO 1

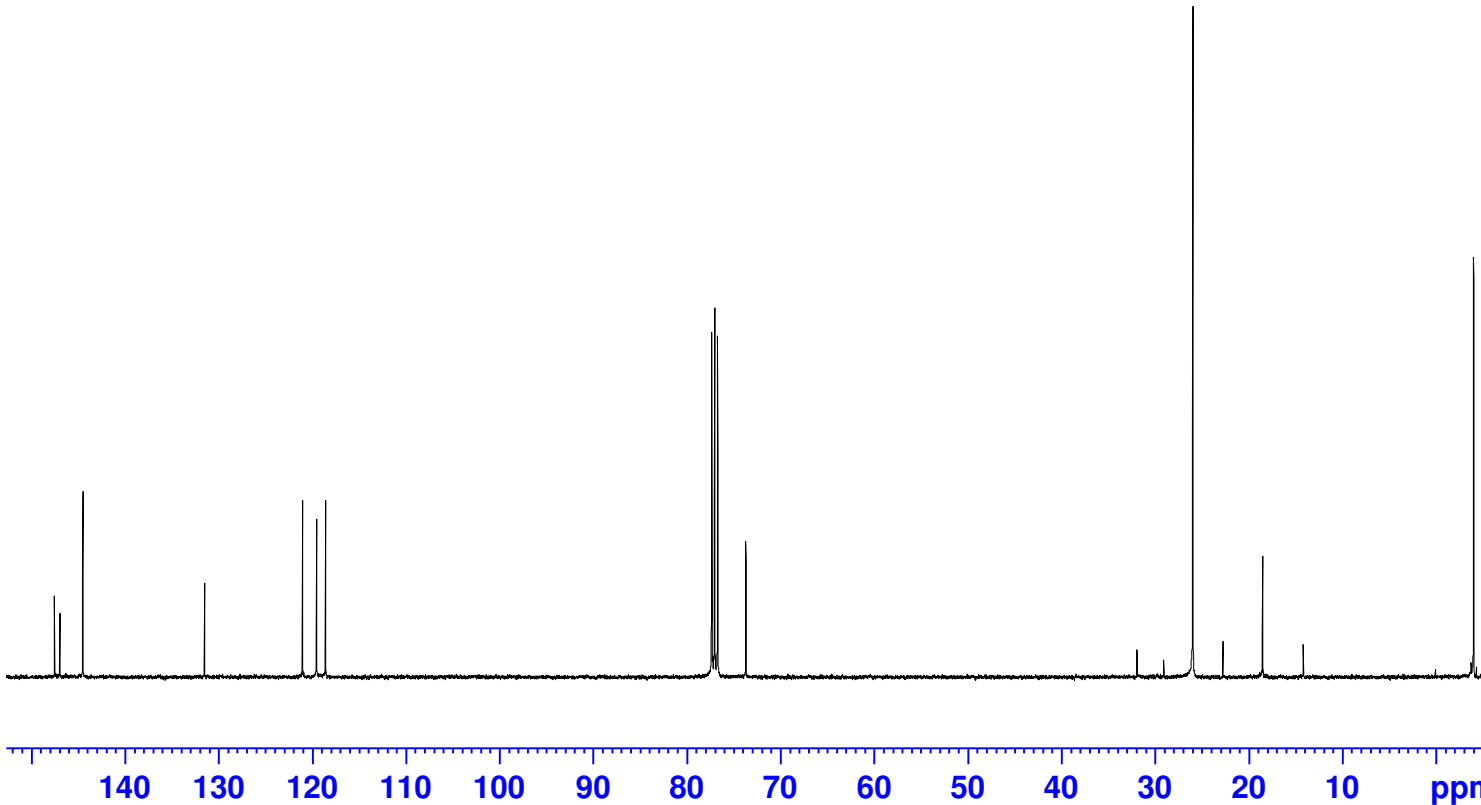
F2 - Acquisition Parameters

Date_ 20170509
 Time 3.10
 INSTRUM spect
 PROBHD 5 mm PABBO BB/
 PULPROG zgpg30
 TD 65536
 SOLVENT CDC13
 NS 1024
 DS 4
 SWH 24038.461 Hz
 FIDRES 0.366798 Hz
 AQ 1.3631488 sec
 RG 200.88
 DW 20.800 usec
 DE 6.50 usec
 TE 300.0 K
 D1 2.00000000 sec
 D11 0.03000000 sec
 TD0 1

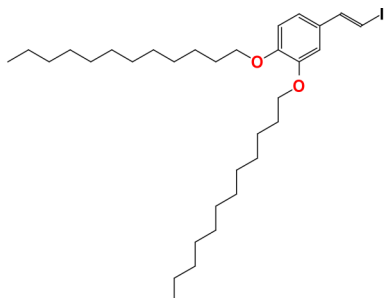
===== CHANNEL f1 =====
 SFO1 100.6228293 MHz
 NUC1 13C
 P1 8.40 usec
 PLW1 88.19999695 W

===== CHANNEL f2 =====
 SFO2 400.1316005 MHz
 NUC2 1H
 CPDPRG[2] waltz16
 PCPD2 90.00 usec
 PLW2 18.10000038 W
 PLW12 0.16527000 W
 PLW13 0.13387001 W

F2 - Processing parameters
 SI 32768
 SF 100.6127685 MHz
 WDW EM
 SSB 0
 LB 1.00 Hz
 GB 0
 PC 1.40



11c

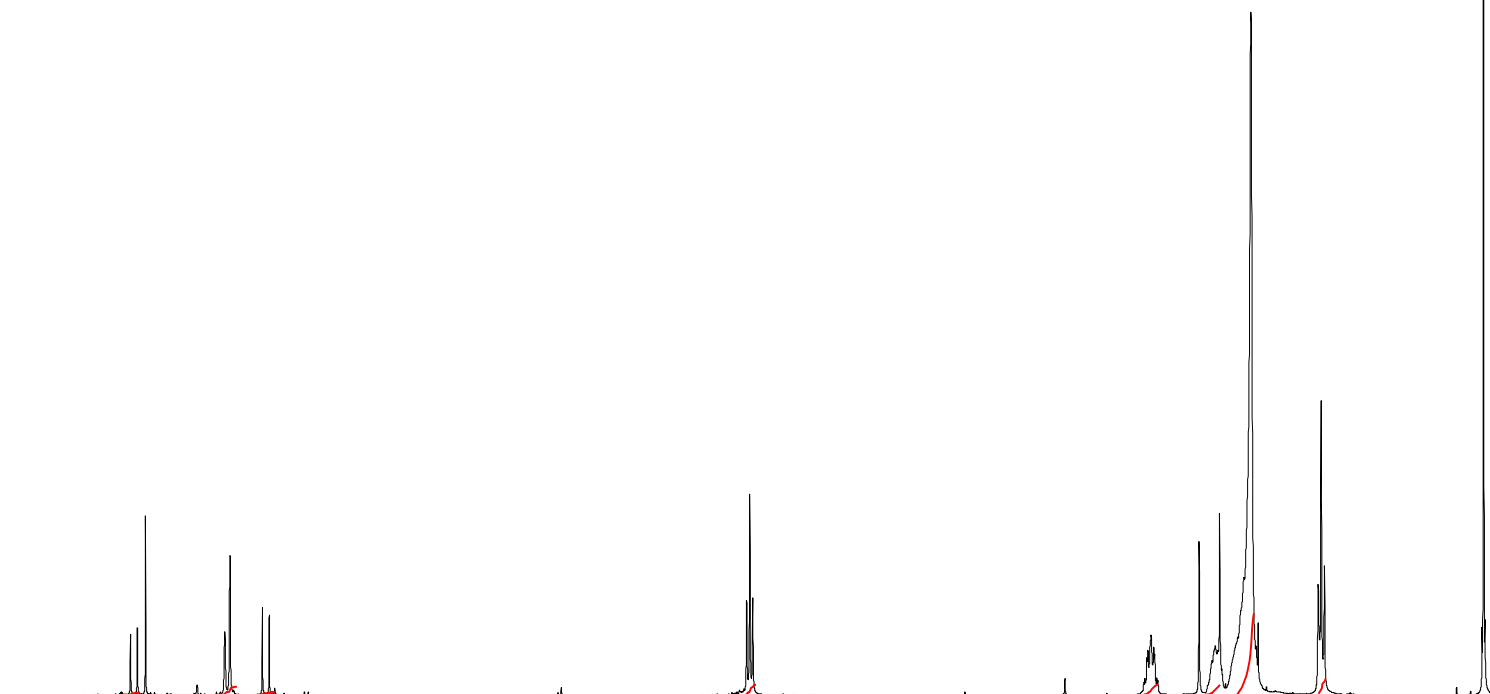


Current Data Parameters
NAME MBR17-68
EXPNO 1
PROCNO 1

F2 - Acquisition Parameters
Date_ 20170706
Time 12.25
INSTRUM spect
PROBHD 5 mm PABBO BB/
PULPROG zg30
TD 65536
SOLVENT CDC13
NS 16
DS 2
SWH 8012.820 Hz
FIDRES 0.122266 Hz
AQ 4.0894465 sec
RG 103.33
DW 62.400 usec
DE 6.50 usec
TE 300.0 K
D1 1.00000000 sec
TD0 1

==== CHANNEL f1 =====
SFO1 400.1324710 MHz
NUC1 1H
P1 8.60 usec
PLW1 18.10000038 W

F2 - Processing parameters
SI 65536
SF 400.1300102 MHz
WDW EM
SSB 0
LB 0.30 Hz
GB 0
PC 1.00



7.5 7.0 6.5 6.0 5.5 5.0 4.5 4.0 3.5 3.0 2.5 2.0 1.5 1.0 0.5 ppm

1.00

3.08

1.07

4.01

4.12

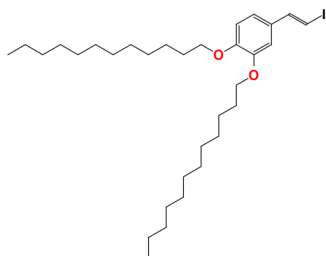
3.98

32.51

6.52

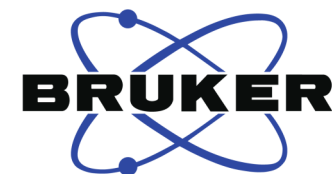
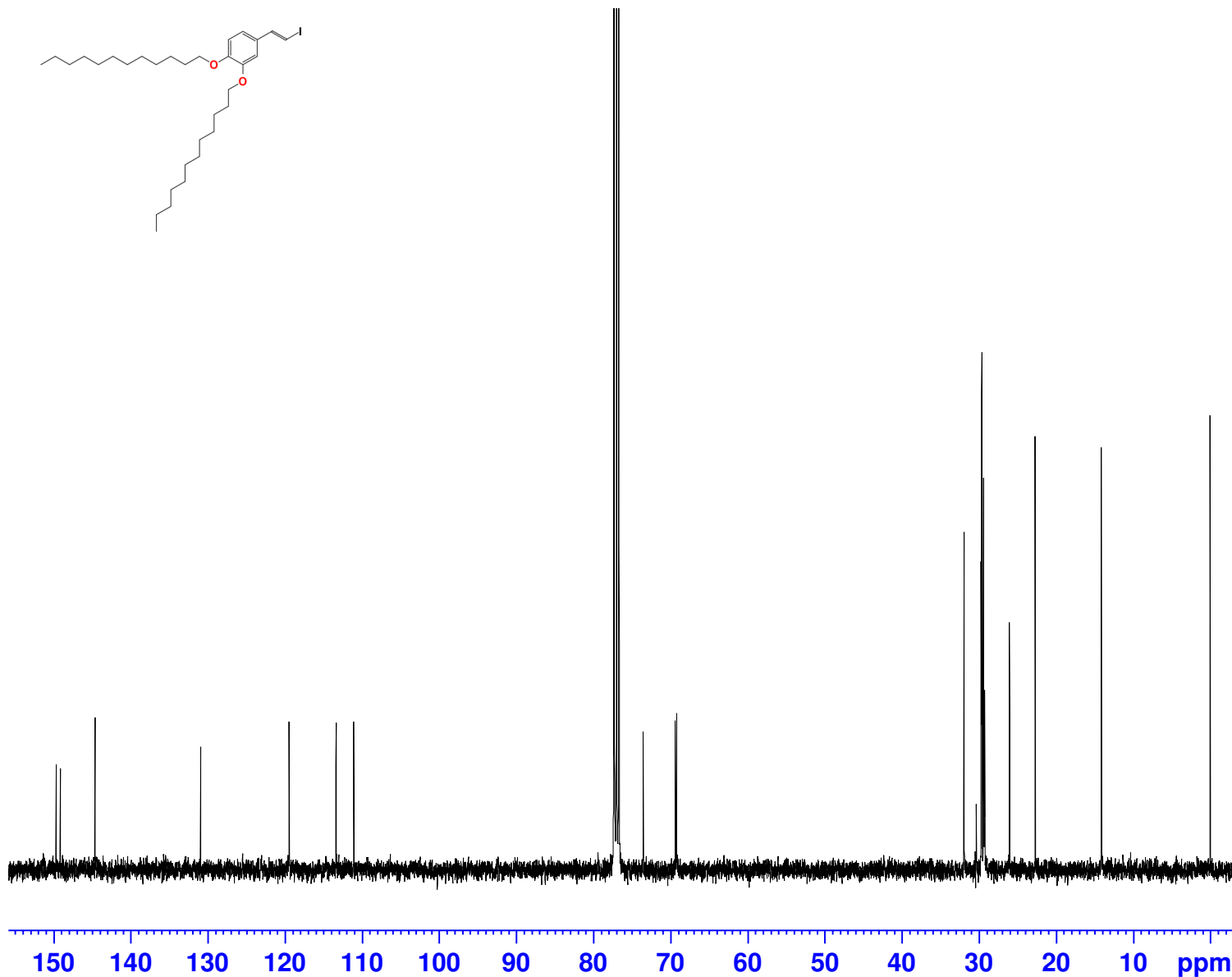
11c

149.71
149.17
144.66
130.95
119.49
113.39
111.09



73.55
69.38
69.21

31.94
29.63
29.42
29.37
29.28
29.24
26.02
22.70
14.12



Current Data Parameters
NAME MBR17-68
EXPNO 2
PROCNO 1

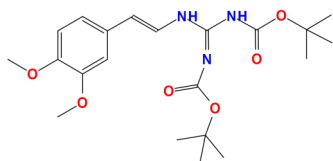
F2 - Acquisition Parameters
Date_ 20170707
Time 6.26
INSTRUM spect
PROBHD 5 mm PABBO BB/
PULPROG zgpg30
TD 65536
SOLVENT CDC13
NS 1024
DS 4
SWH 24038.461 Hz
FIDRES 0.366798 Hz
AQ 1.3631488 sec
RG 200.88
DW 20.800 usec
DE 6.50 usec
TE 300.0 K
D1 2.00000000 sec
D11 0.03000000 sec
TD0 1

==== CHANNEL f1 =====
SFO1 100.6228293 MHz
NUC1 13C
P1 8.40 usec
PLW1 88.19999695 W

==== CHANNEL f2 =====
SFO2 400.1316005 MHz
NUC2 1H
CPDPRG[2] waltz16
PCPD2 90.00 usec
PLW2 18.10000038 W
PLW12 0.16527000 W
PLW13 0.13387001 W

F2 - Processing parameters
SI 32768
SF 100.6127688 MHz
WDW EM
SSB 0
LB 1.00 Hz
GB 0
PC 1.40

12a

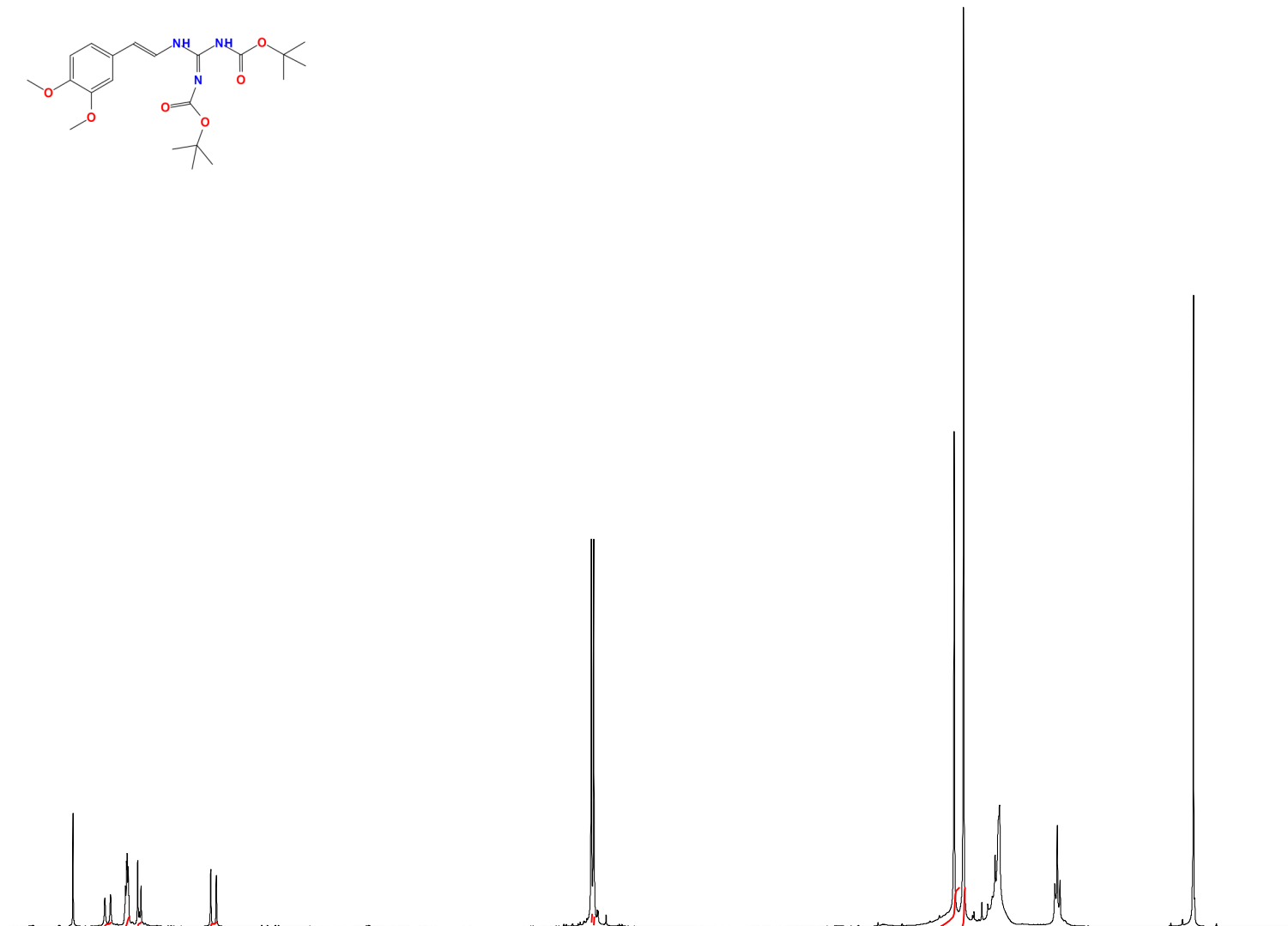


Current Data Parameters
NAME MBR17-66.12 22-25
EXPNO 1
PROCNO 1

F2 - Acquisition Parameters
Date_ 20170710
Time 17.33
INSTRUM spect
PROBHD 5 mm PABBO BB/
PULPROG zg30
TD 65536
SOLVENT CDC13
NS 128
DS 2
SWH 8012.820 Hz
FIDRES 0.122266 Hz
AQ 4.0894465 sec
RG 128.29
DW 62.400 usec
DE 6.50 usec
TE 300.0 K
D1 1.00000000 sec
TD0 1

==== CHANNEL f1 =====
SFO1 400.1324710 MHz
NUC1 1H
P1 8.60 usec
PLW1 18.10000038 W

F2 - Processing parameters
SI 65536
SF 400.1300088 MHz
WDW EM
SSB 0
LB 0.30 Hz
GB 0
PC 1.00

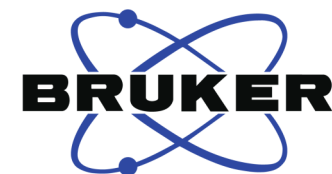


1.07
2.37
1.12
1.19

3.00
3.29

8.91
9.08

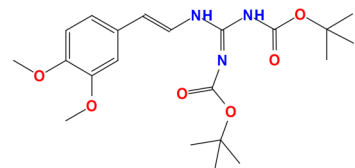
0 ppm



158.27
152.30
149.15
148.44

129.23
124.85
120.12
118.73

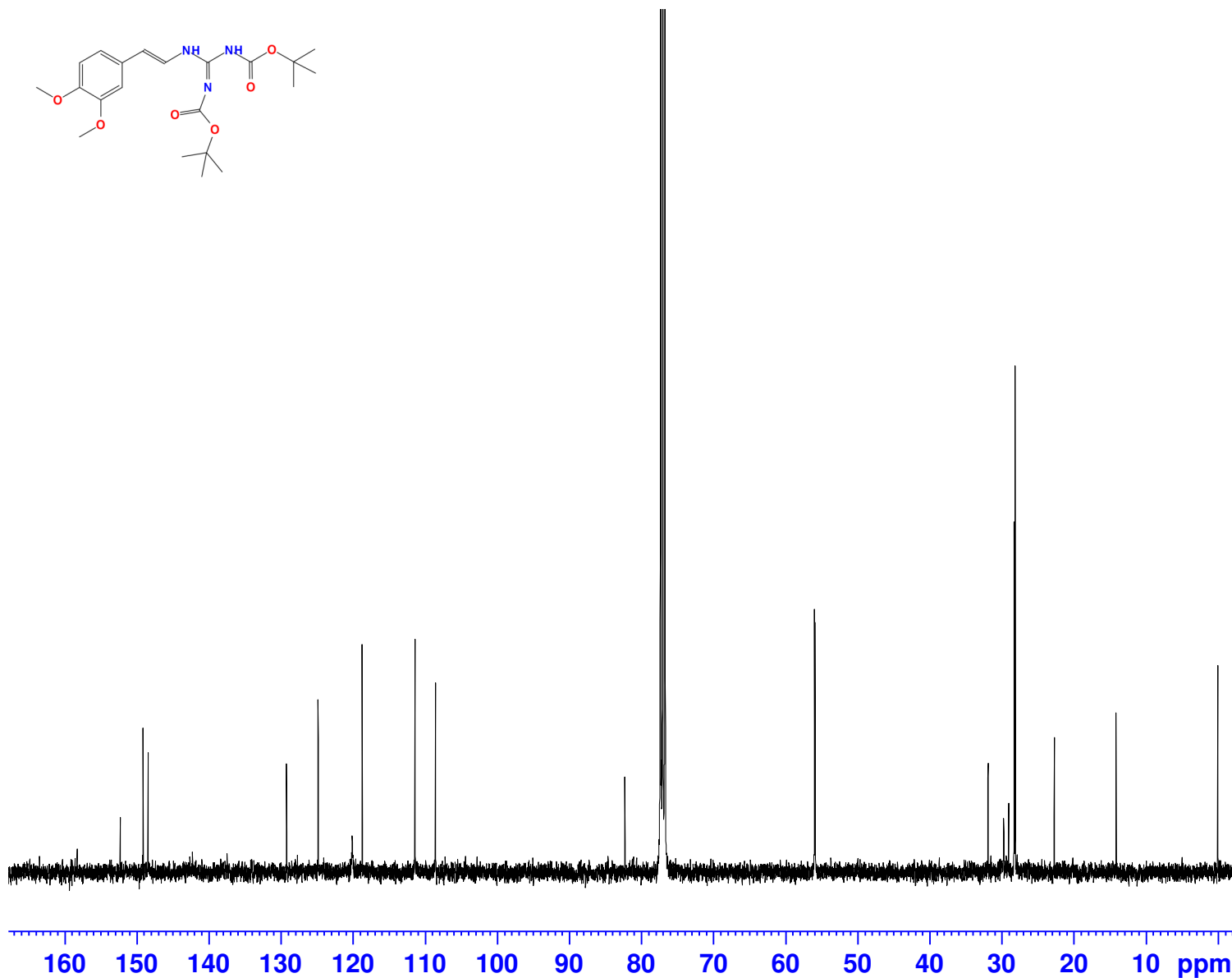
111.40
108.55



82.28

55.98
55.88

28.27
28.11



Current Data Parameters
NAME MBR17-66.12 22-25
EXPNO 2
PROCNO 1

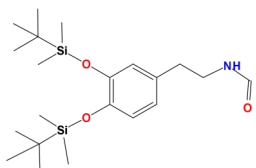
F2 - Acquisition Parameters
Date_ 20170710
Time 20.01
INSTRUM spect
PROBHD 5 mm PABBO BB/
PULPROG zgpg30
TD 65536
SOLVENT CDC13
NS 2048
DS 4
SWH 24038.461 Hz
FIDRES 0.366798 Hz
AQ 1.3631488 sec
RG 200.88
DW 20.800 usec
DE 6.50 usec
TE 300.0 K
D1 2.00000000 sec
D11 0.03000000 sec
TD0 1

===== CHANNEL f1 =====
SFO1 100.6228293 MHz
NUC1 13C
P1 8.40 usec
PLW1 88.19999695 W

===== CHANNEL f2 =====
SFO2 400.1316005 MHz
NUC2 1H
CPDPRG[2] waltz16
PCPD2 90.00 usec
PLW2 18.10000038 W
PLW12 0.16527000 W
PLW13 0.13387001 W

F2 - Processing parameters
SI 32768
SF 100.6127684 MHz
WDW EM
SSB 0
LB 1.00 Hz
GB 0
PC 1.40

Amide by-product from the synthesis of compound 14

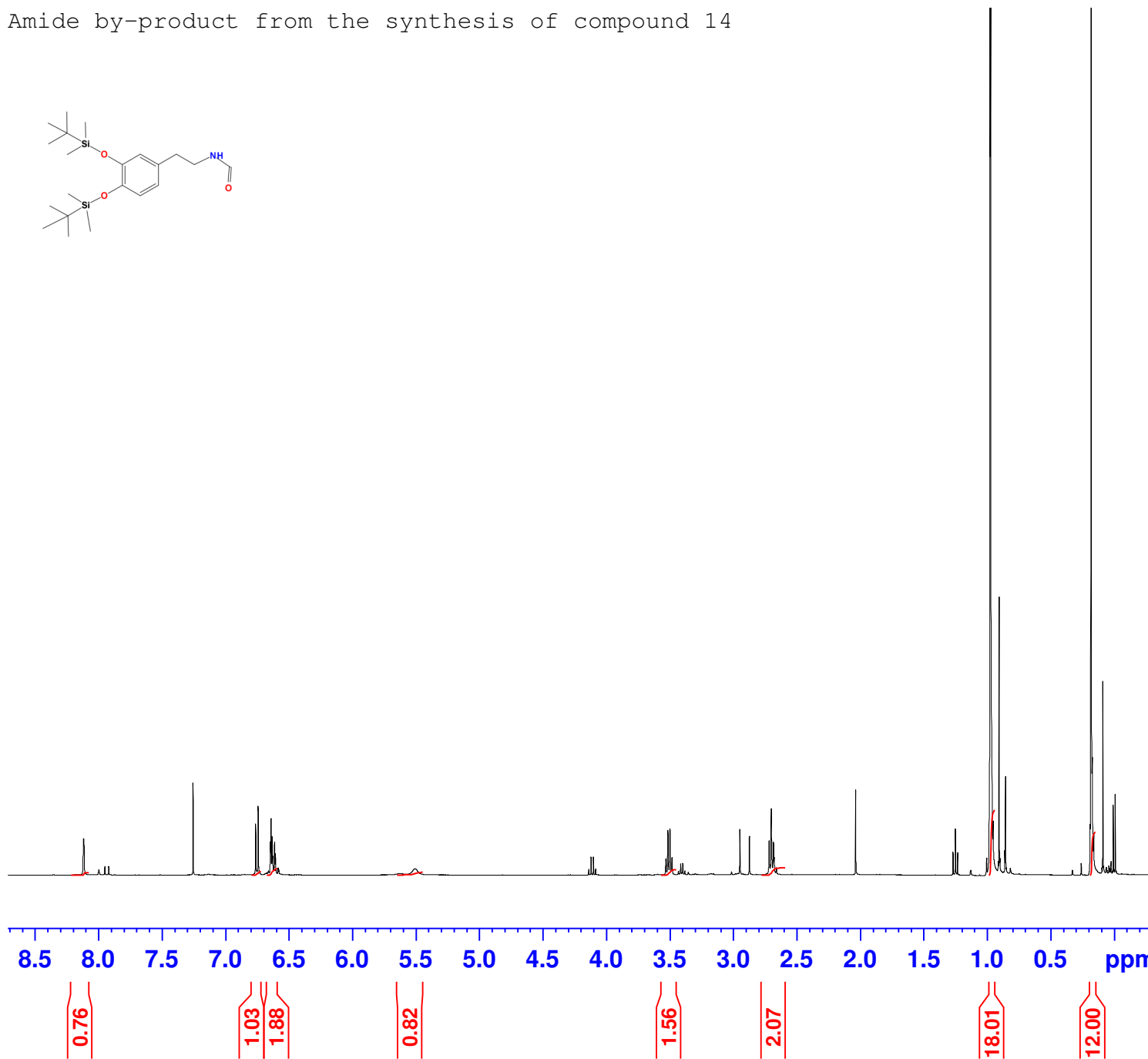


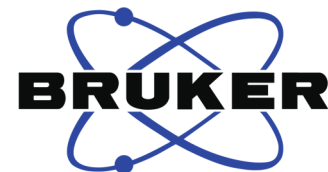
Current Data Parameters
NAME MBR17-35 oil
EXPNO 1
PROCNO 1

F2 - Acquisition Parameters
Date_ 20170604
Time 19.54
INSTRUM spect
PROBHD 5 mm PABBO BB/
PULPROG zg30
TD 65536
SOLVENT CDC13
NS 16
DS 2
SWH 8012.820 Hz
FIDRES 0.122266 Hz
AQ 4.0894465 sec
RG 71.31
DW 62.400 usec
DE 6.50 usec
TE 297.0 K
D1 1.00000000 sec
TD0 1

==== CHANNEL f1 =====
SFO1 400.1324710 MHz
NUC1 1H
P1 8.60 usec
PLW1 18.10000038 W

F2 - Processing parameters
SI 65536
SF 400.1300115 MHz
WDW EM
SSB 0
LB 0.30 Hz
GB 0
PC 1.00





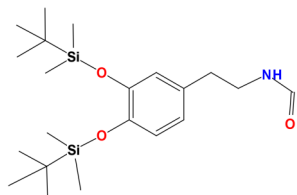
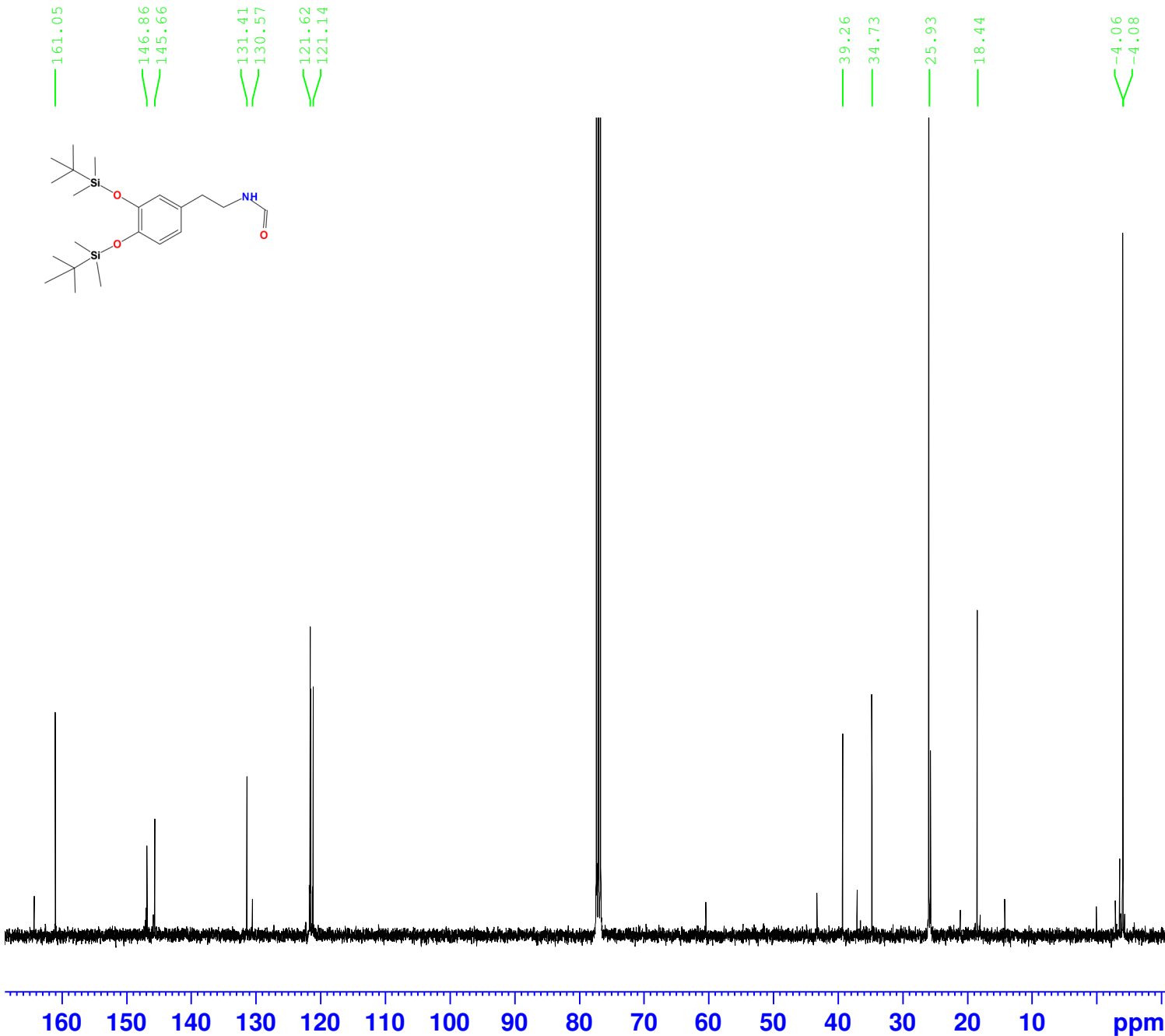
Current Data Parameters
NAME MBR17-35 oil
EXPNO 2
PROCNO 1

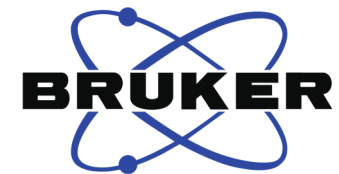
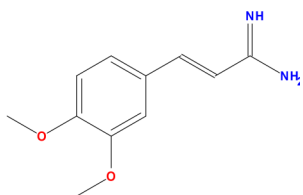
F2 - Acquisition Parameters
Date_ 20170604
Time 20.54
INSTRUM spect
PROBHD 5 mm PABBO BB/
PULPROG zgpg30
TD 65536
SOLVENT CDC13
NS 1024
DS 4
SWH 24038.461 Hz
FIDRES 0.366798 Hz
AQ 1.3631488 sec
RG 200.88
DW 20.800 usec
DE 6.50 usec
TE 297.9 K
D1 2.00000000 sec
D11 0.03000000 sec
TD0 1

=====
CHANNEL f1
SFO1 100.6228293 MHz
NUC1 13C
P1 8.40 usec
PLW1 88.19999695 W

=====
CHANNEL f2
SFO2 400.1316005 MHz
NUC2 1H
CPDPRG[2] waltz16
PCPD2 90.00 usec
PLW2 18.10000038 W
PLW12 0.16527000 W
PLW13 0.13387001 W

F2 - Processing parameters
SI 32768
SF 100.6127685 MHz
WDW EM
SSB 0
LB 1.00 Hz
GB 0
PC 1.40



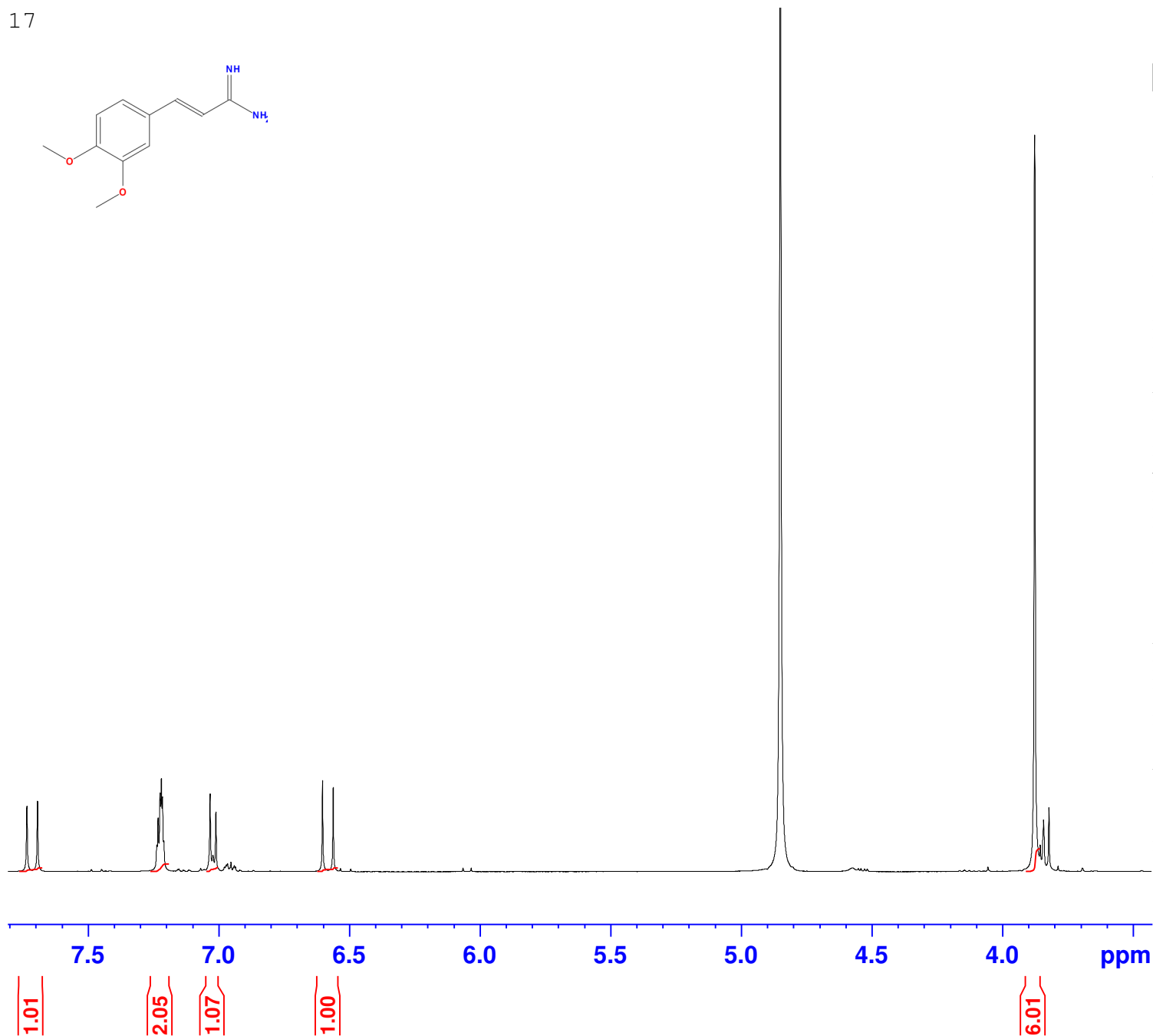


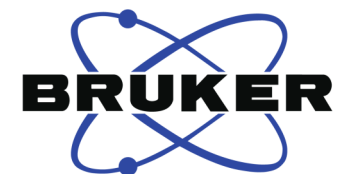
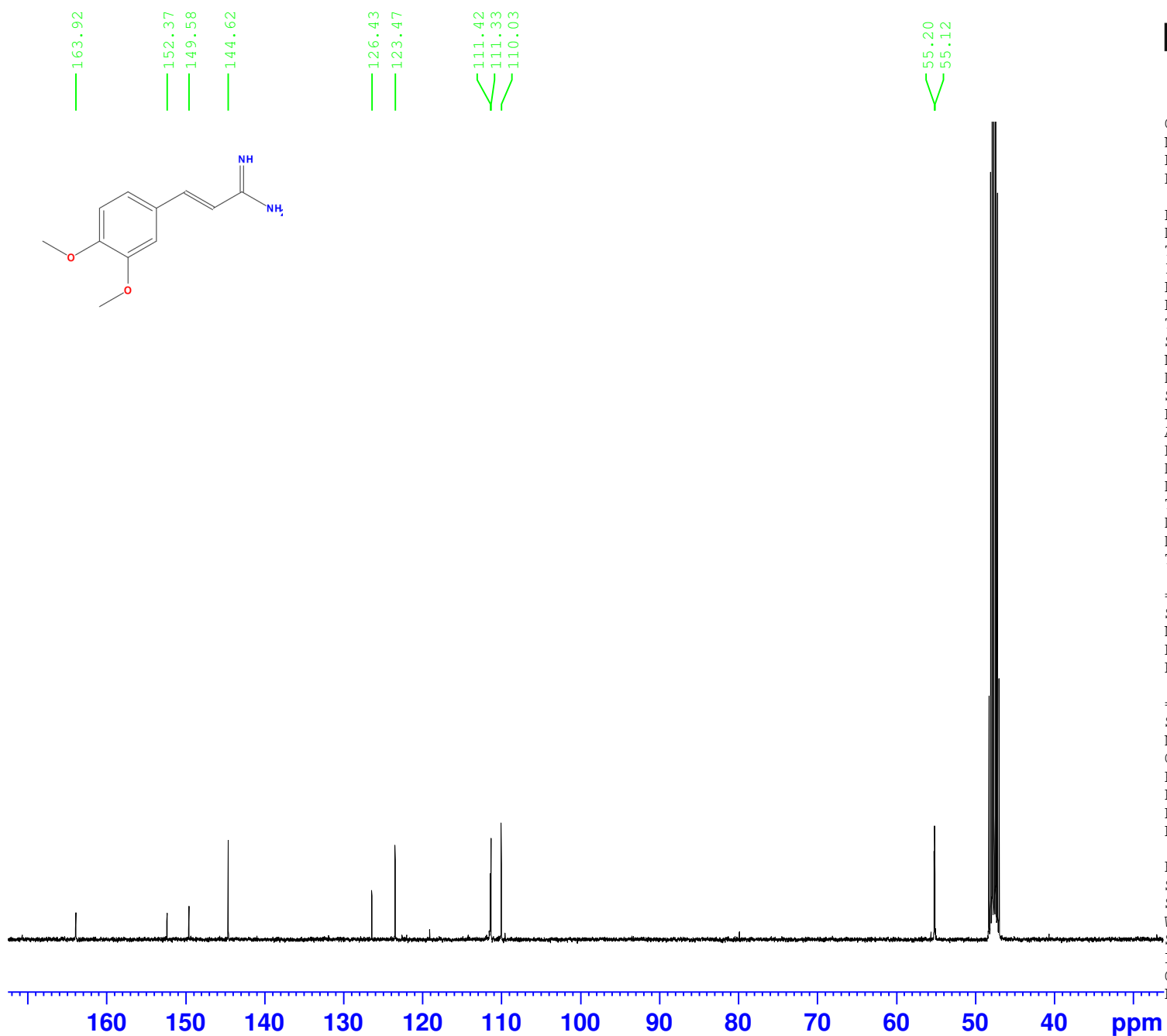
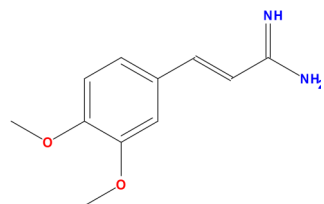
Current Data Parameters
 NAME MBR17-60 purified
 EXPNO 1
 PROCNO 1

F2 - Acquisition Parameters
 Date_ 20170627
 Time 16.16
 INSTRUM spect
 PROBHD 5 mm PABBO BB/
 PULPROG zg30
 TD 65536
 SOLVENT MeOD
 NS 16
 DS 2
 SWH 8012.820 Hz
 FIDRES 0.122266 Hz
 AQ 4.0894465 sec
 RG 128.29
 DW 62.400 usec
 DE 6.50 usec
 TE 296.8 K
 D1 1.00000000 sec
 TD0 1

===== CHANNEL f1 =====
 SFO1 400.1324710 MHz
 NUC1 1H
 P1 8.60 usec
 PLW1 18.10000038 W

F2 - Processing parameters
 SI 65536
 SF 400.1300142 MHz
 WDW EM
 SSB 0
 LB 0.30 Hz
 GB 0
 PC 1.00





Current Data Parameters
 NAME MBR17-60 purified 2
 EXPNO 4
 PROCNO 1

F2 - Acquisition Parameters
 Date_ 20170628
 Time 0.04
 INSTRUM spect
 PROBHD 5 mm PABBO BB/
 PULPROG zgpg30
 TD 65536
 SOLVENT MeOD
 NS 2048
 DS 4
 SWH 24038.461 Hz
 FIDRES 0.366798 Hz
 AQ 1.3631488 sec
 RG 200.88
 DW 20.800 usec
 DE 6.50 usec
 TE 297.8 K
 D1 2.00000000 sec
 D11 0.03000000 sec
 TD0 1

===== CHANNEL f1 =====
 SFO1 100.6228293 MHz
 NUC1 13C
 P1 8.40 usec
 PLW1 88.19999695 W

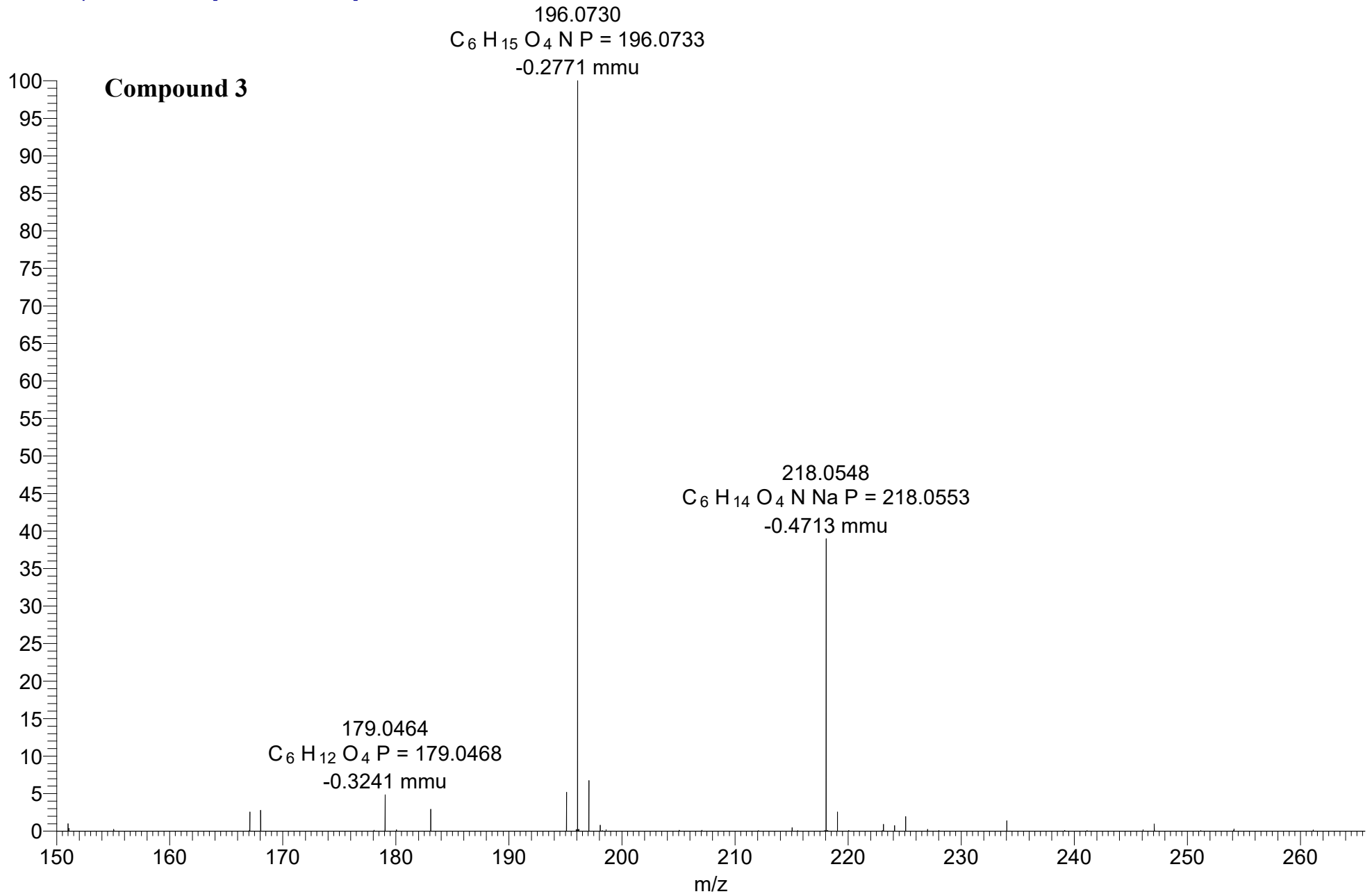
===== CHANNEL f2 =====
 SFO2 400.1316005 MHz
 NUC2 1H
 CPDPRG[2] waltz16
 PCPD2 90.00 usec
 PLW2 18.10000038 W
 PLW12 0.16527000 W
 PLW13 0.13387001 W

F2 - Processing parameters
 SI 32768
 SF 100.6127685 MHz
 WDW EM
 SSB 0
 LB 1.00 Hz
 GB 0
 PC 1.40

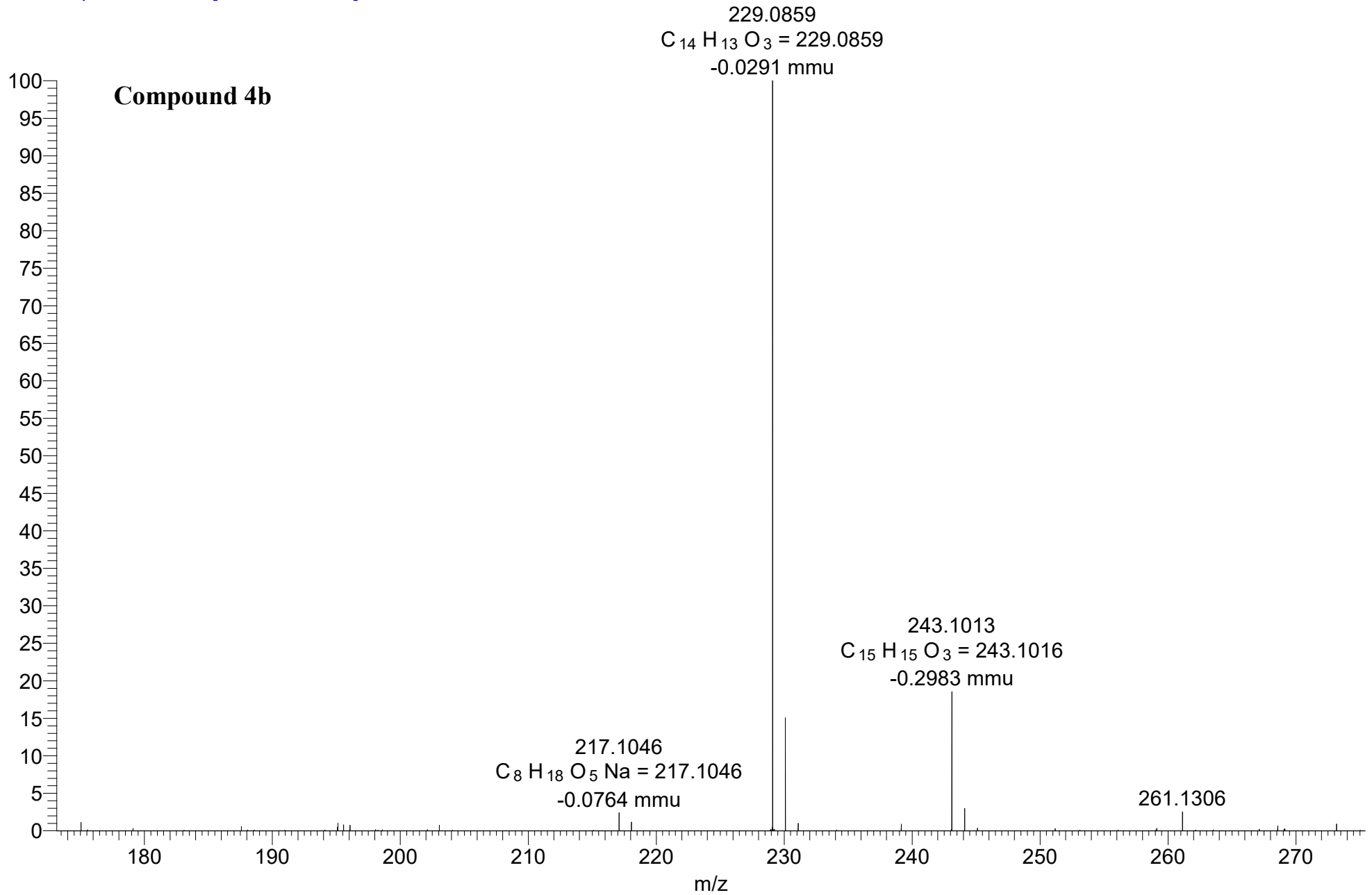
APPENDIX B

MS spectra

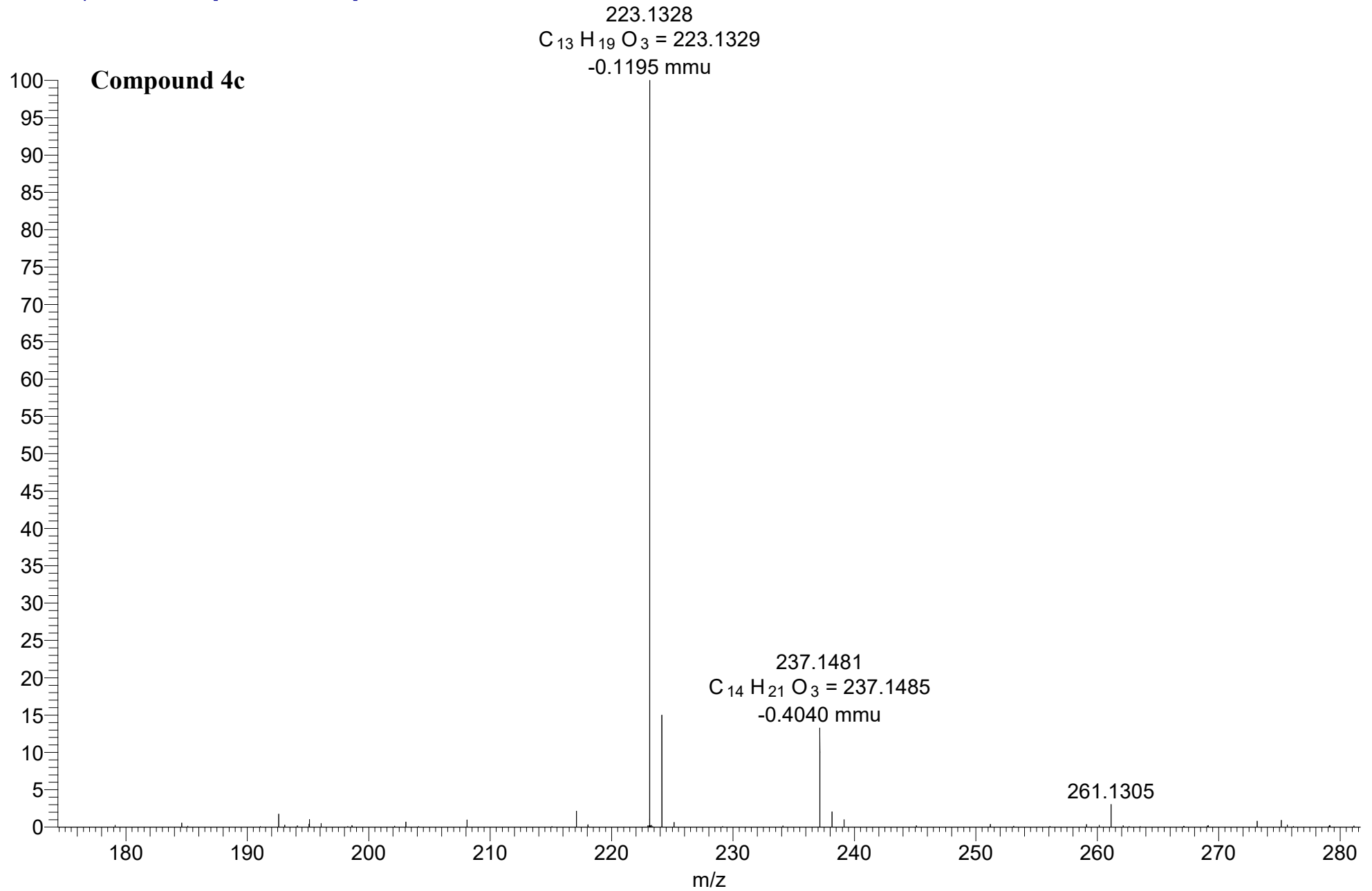
MBR17-05 #17 RT: 0.42 AV: 1 NL: 1.81E8
T: FTMS + p ESI Full ms [150.00-600.00]



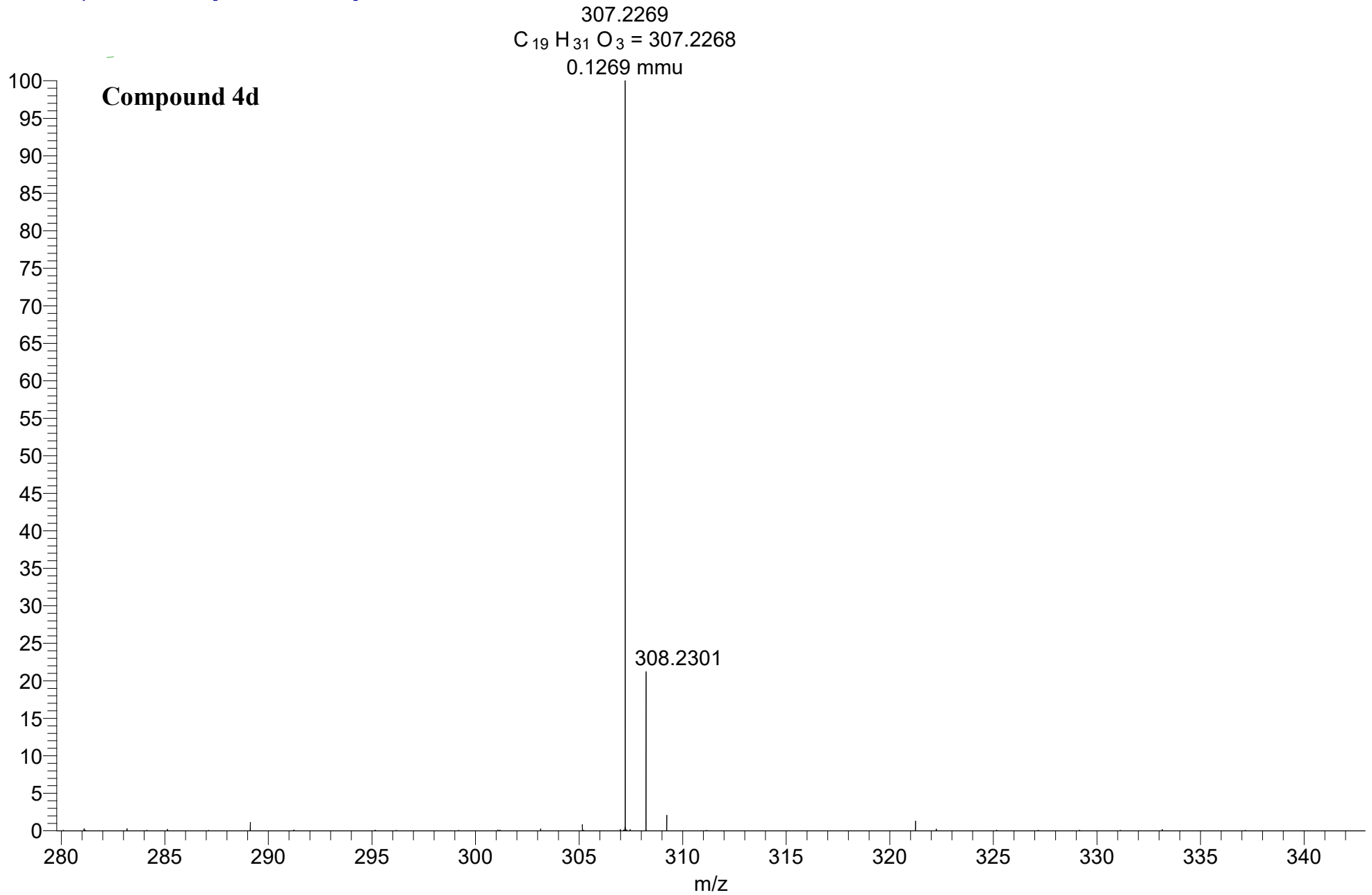
MBR17-29 #18 RT: 0.45 AV: 1 NL: 4.30E7
T: FTMS + p ESI Full ms [150.00-600.00]



MBR17-43 #18 RT: 0.45 AV: 1 NL: 3.75E7
T: FTMS + p ESI Full ms [150.00-600.00]

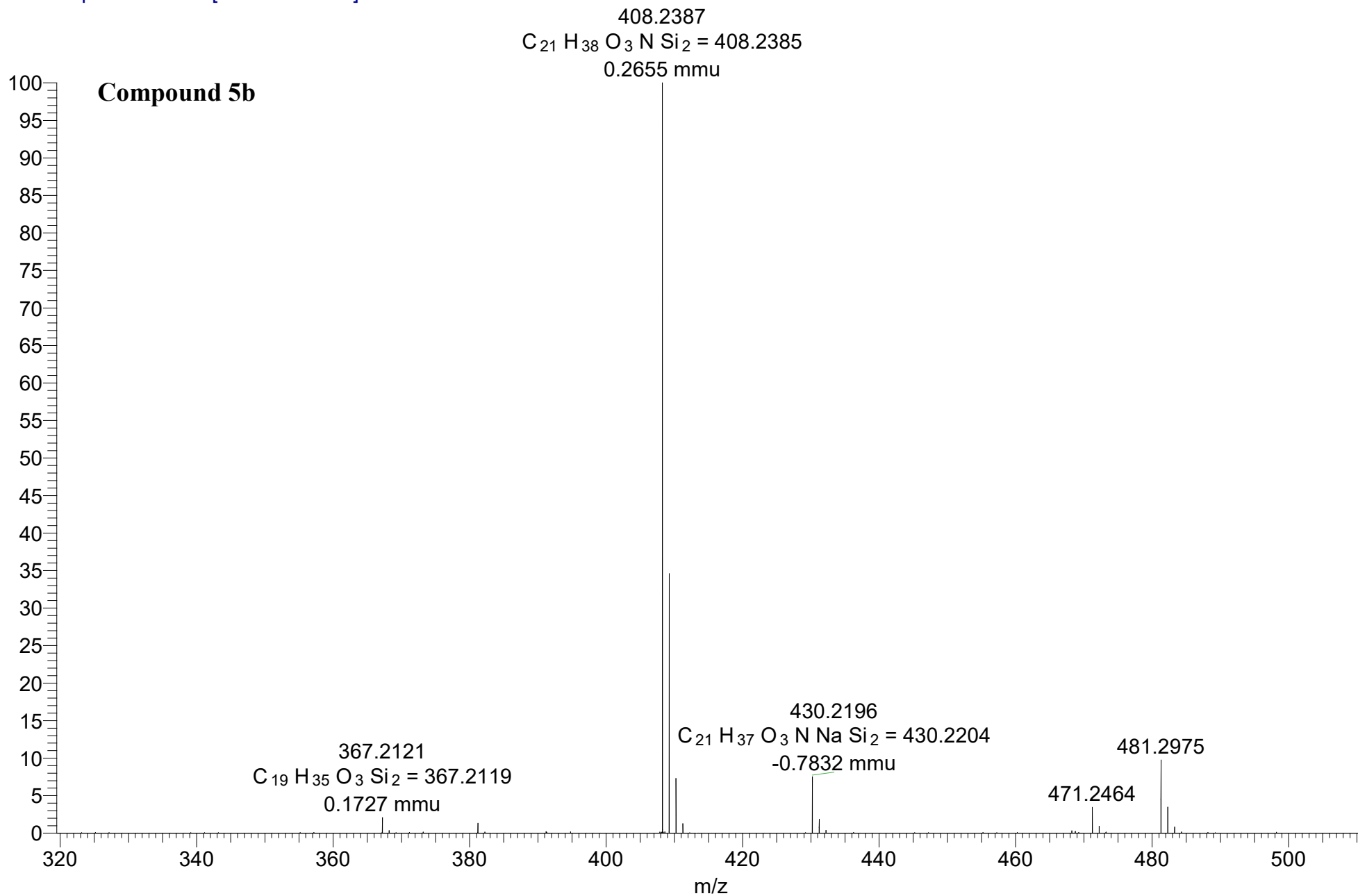


MBR17-45 #25 RT: 0.65 AV: 1 NL: 1.63E7
T: FTMS + p ESI Full ms [150.00-600.00]

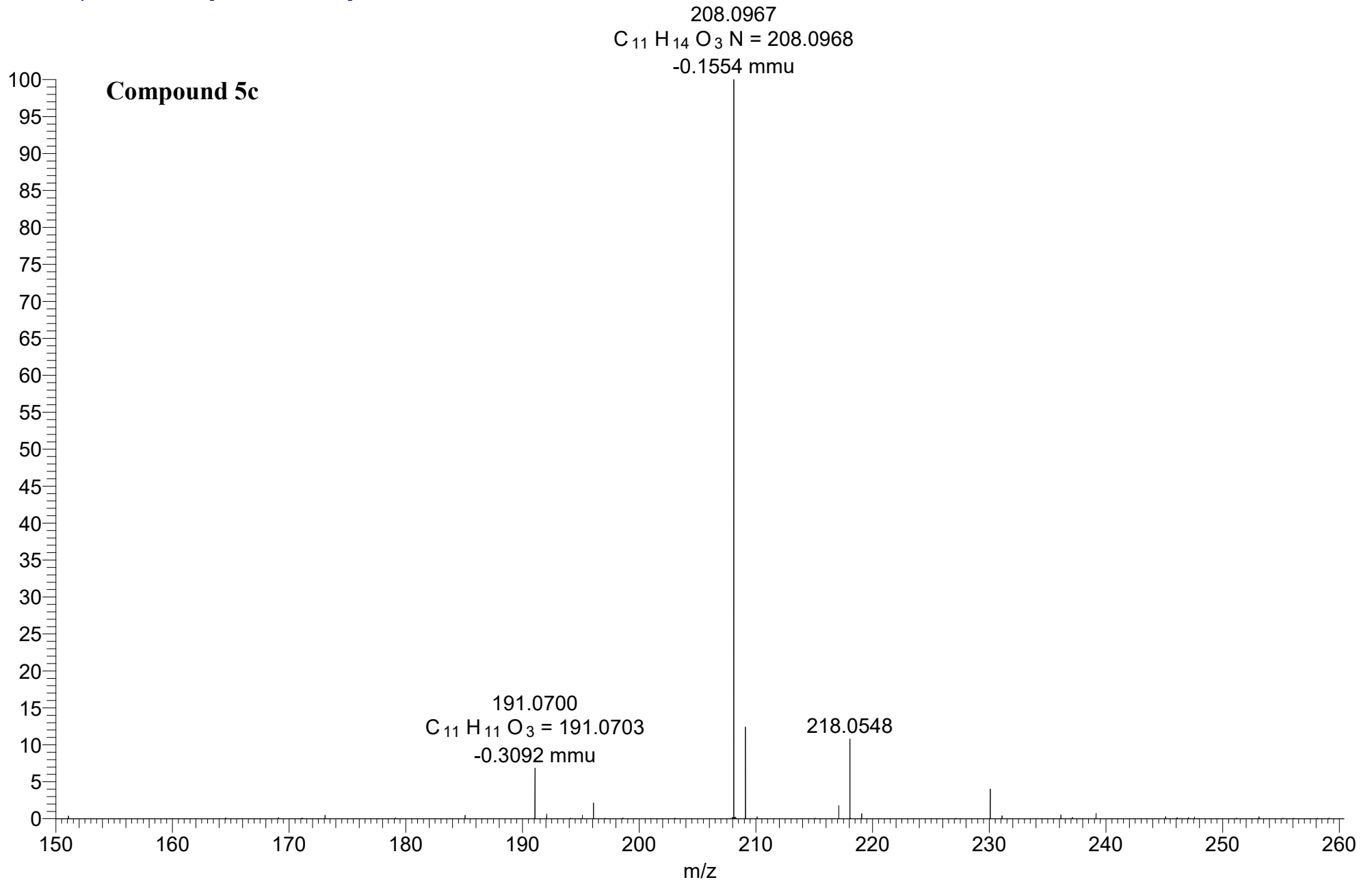


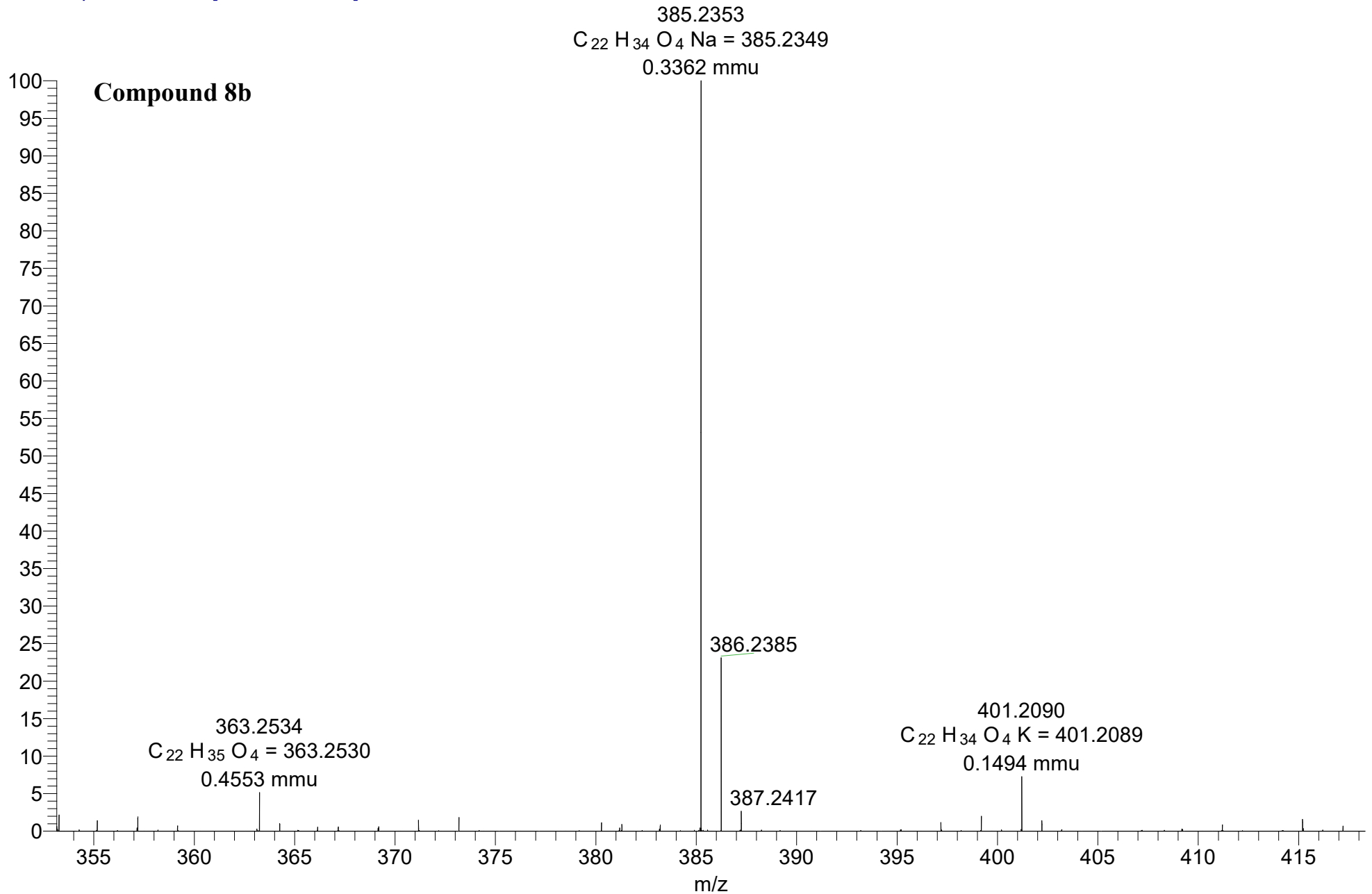
MBR17-22 #18 RT: 0.45 AV: 1 NL: 7.26E7

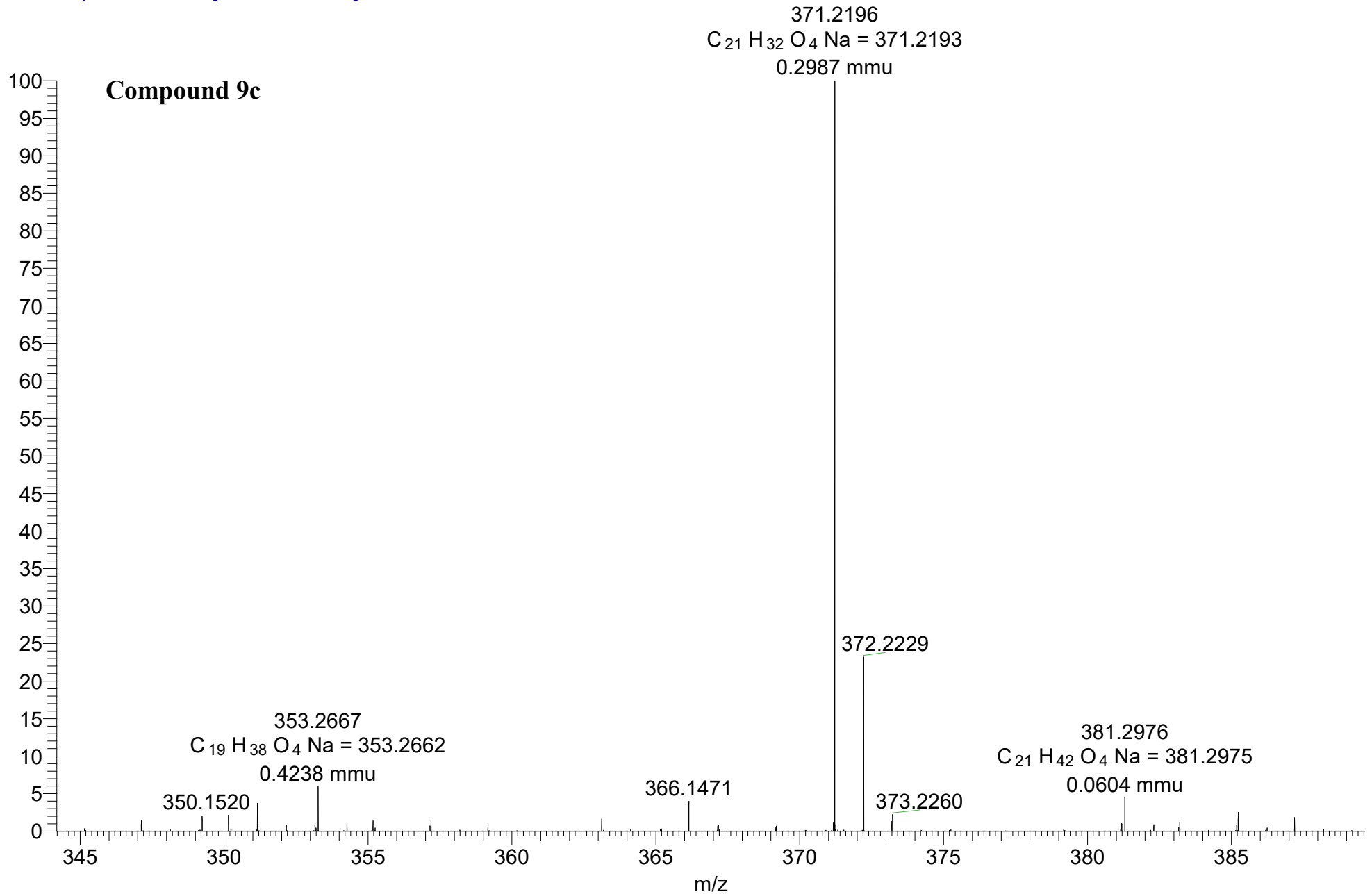
T: FTMS + p ESI Full ms [150.00-600.00]



MBR17-36 #16 RT: 0.40 AV: 1 NL: 6.01E7
T: FTMS + p ESI Full ms [150.00-600.00]



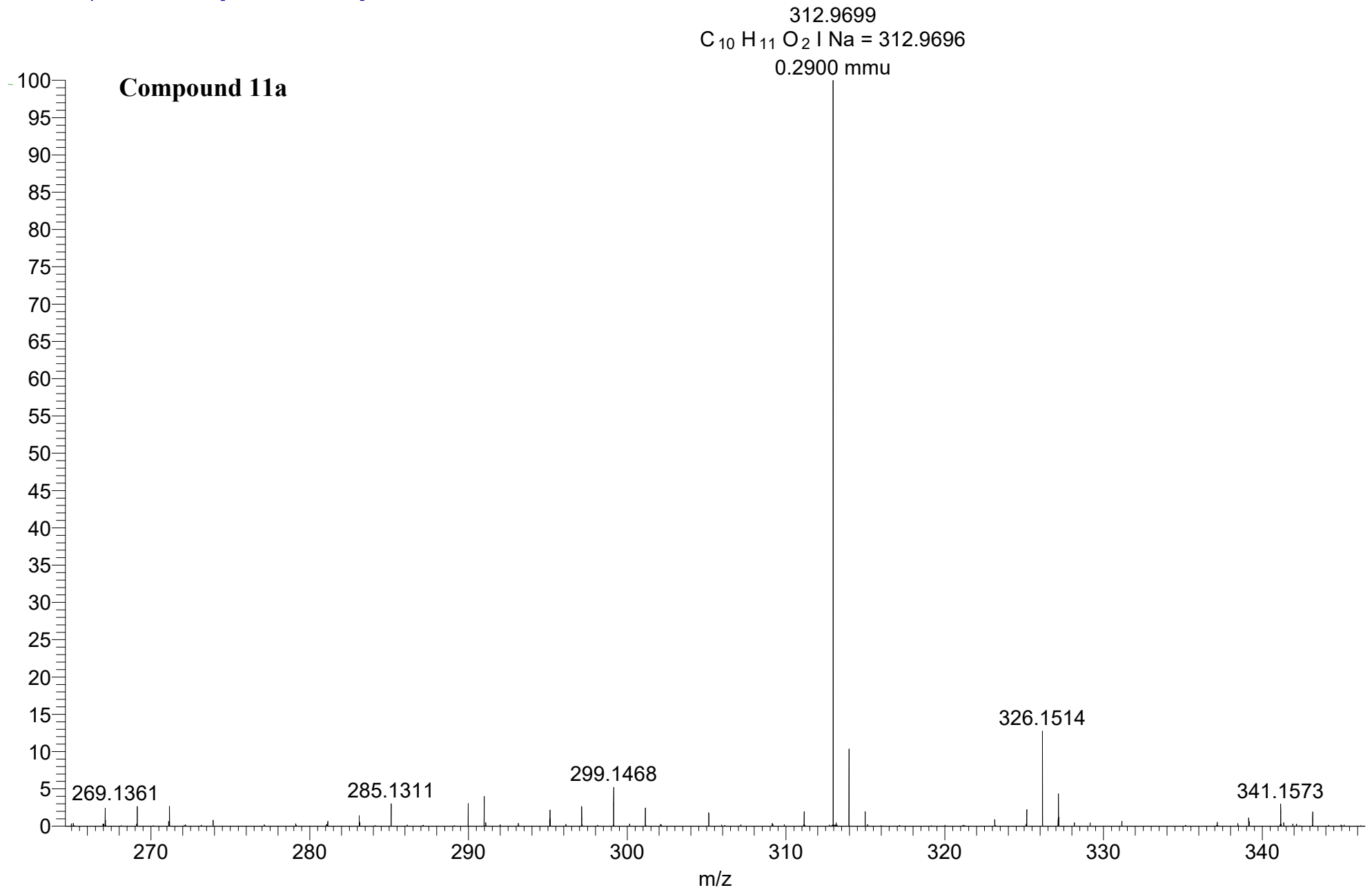




5 7 30

MBR17-21-SP #1-5 RT: 0.02-0.13 AV: 5 NL: 7.47E6

T: FTMS + p ESI Full ms [200.00-600.00]



MBR17-35 #26 RT: 0.67 AV: 1 NL: 8.53E7
T: FTMS + p ESI Full ms [150.00-600.00]

